UTILIZING –OMICS TECHNOLOGIES TO STUDY DROUGHT STRESS RELATED TO HOST RESISTANCE AGAINST *ASPERGILLUS FLAVUS* COLONIZATION AND AFLATOXIN PRODUCTION

by

JAKE CLAYTON FOUNTAIN

(Under the Direction of Robert C. Kemerait)

ABSTRACT

Aspergillus flavus is a pathogen of several important crop species including maize and peanut. During infection, *A. flavus* produces mycotoxins known as aflatoxins which pose a serious threat to global food safety and security. Host resistance to infection and aflatoxin contamination has been linked to drought stress with drought tolerant hosts tending to be more resistant. However, potential causes of this phenomenon have yet to be characterized. To better understand both the host and pathogen stress interactions, field and laboratory analyses, particularly biochemical and –omics analyses including metabolomics, proteomics, and transcriptomics were used. Drought sensitive, aflatoxin contamination susceptible maize lines were found to accumulate higher levels of reactive oxygen species (ROS) in their leaf and kernel tissues compared to tolerant and resistant lines. Drought sensitive lines also exhibited more rapid and vigorous physiological responses to stress including changes in antioxidant enzyme activity, photosynthesis, and stomatal conductance. Metabolomics analysis of developing kernels under drought also showed increased accumulation of free simple sugars, oxylipins, and polyunsaturated fatty acids in drought sensitive lines which may provide resources for aflatoxin

production during *A. flavus* infection. Examination of *A. flavus* responses *in vitro* using H_2O_2-derived oxidative stress as a mimic for drought stress found that these responses correlate with aflatoxin production capability with highly aflatoxigenic isolates exhibiting greater stress tolerance. Biological control isolates were also able to tolerate greater levels of stress than field isolated atoxigenic isolates suggesting this as a trait for biocontrol selection. Transcriptional and proteomic examination of isolate responses to oxidative stress suggest that isolate development, pathogenicity, and secondary metabolite production are regulated in response to oxidative stress. Secondary metabolite production, including aflatoxin, composed a large component of oxidative stress responses in *A. flavus* suggesting their possible roles in stress alleviation for the fungus under adverse environmental conditions. Together, these studies identified stress responsive mechanisms in both the host and pathogen which can be targeted and manipulated independently or in tandem including ROS signaling, sugar metabolism, and oxylipin signaling using biotechnologies such as genome editing. This will provide a novel avenue to search for and produce practical solutions to mitigate aflatoxin contamination.

INDEX WORDS: Drought stress, *Aspergillus flavus*, Aflatoxin, Oxidative stress, Hydrogen peroxide, Maize kernel development, Biological control, Metabolomics, Transcriptomics, Proteomics, Fungal development, Kojic acid, Germplasm evaluation, Topcross

UTILIZING –OMICS TECHNOLOGIES TO STUDY DROUGHT STRESS RELATED TO HOST RESISTANCE AGAINST *ASPERGILLUS FLAVUS* COLONIZATION AND AFLATOXIN PRODUCTION

by

JAKE CLAYTON FOUNTAIN

B.S., Georgia Southwestern State University, 2009

M.S., Louisiana State University, 2013

A Dissertation Submitted to the Graduate Faculty of The University of Georgia in Partial Fulfillment of the Requirements for the Degree

DOCTOR OF PHIOLOSPHY

ATHENS, GEORGIA

2017

UTILIZING –OMICS TECHNOLOGIES TO STUDY DROUGHT STRESS RELATED TO HOST RESISTANCE AGAINST *ASPERGILLUS FLAVUS* COLONIZATION AND AFLATOXIN PRODUCTION

by

JAKE CLAYTON FOUNTAIN

Major Professor: Robert C. Kemerait

Committee: Baozhu Guo
Anthony E. Glenn
Scott E. Gold
Shavannor M. Smith

Electronic Version Approved:

Suzanne Barbour
Dean of the Graduate School
The University of Georgia
August 2017

DEDICATION

To my mother and father.

ACKNOWLEDGEMENTS

First and foremost I would like to thank my major advisor, Robert Kemerait, and my co-advisor Baozhu Guo, without whom this work would not have been possible. Their careful guidance over the course of my studies has shaped me and helped me to mature both as a person and as a scientist. They have helped cultivated and grow in me a passion for plant pathology and science which will last a lifetime. I am forever in their debt.

I would also like to thank our collaborators at the International Crops Research Institute for the Semi-Arid Tropics (ICRISAT), Rajeev Varshney, Manish Pandey, Spurthi Nayak, Prasad Bajaj, Anu Chitikineni, Vinay Kumar, and Ashwin Jayale for their support and friendship. I celebrate all our work, and am thankful for their warm hospitality. Also Sixue Chen and Jin Koh at the University of Florida for their efforts in helping with the proteomics work included here. I would also like to thank Anthony Glenn, Scott Gold, and Shavannor Smith for their tireless service on my committee that has kept me grounded and focused in my development as a scientist.

Enough recognition cannot be given to the excellent technical support I have received from the staff at the USDA Crop Protection and Management Research Unit. Without help from Billy Wilson, our technician, none of this work would be possible. Special thanks to Shannon Giddens and Deborah Osborne at CPMRU for helping me with countless forms and to CPMRU research leaders Brian Scully and Theodore Webster for hosting me in your facility. Thanks as well to Christy Fletcher, Glenda Thomas, and Jodi Figgatt with the Department of Plant Pathology in Tifton who are the often unsung heroines of so many students. Thanks also to

Kippy Lewis for teaching me all I know about running a lab, and for all the support and advice over the years. The members of the Guo lab have been and continue to be my friends and family, and have been invaluable to me. Thanks to Hui Wang, Liming Yang, Gaurav Agarwal, Divya Choudhary, Pawan Khera, Xiangyun Ji, Xiaohong Guo, Joseph Harnage, Fanxu Lin, Keith Melcher, and Faith Spearman for your constant support. Finally, I would also like to thank the Department of Plant Pathology for the opportunity to study and be trained during my PhD. Special thanks to department heads Harald Scherm and John Sherwood, and graduate coordinator Ron Walcott for all that you have done for me and for the department.

"For the moment all discipline seems painful rather than pleasant, but later it yields the peaceful fruit of righteousness to those who have been trained by it."

- Hebrews 12:11 (ESV)

TABLE OF CONTENTS

LIST OF TABLES

Page

LIST OF FIGURES

Page

CHAPTER 1

LITERATURE REVIEW PART I:

ENVIRONMENTAL INFLUENCES ON MAIZE-*ASPERGILLUS FLAVUS* INTERACTIONS AND AFLATOXIN PRODUCTION

Fountain, J. C., Scully, B. T., Ni, X., Kemerait, R. C., Lee, R. D., Chen, Z. Y., & Guo, B. (2014). Environmental influences on maize-*Aspergillus flavus* interactions and aflatoxin production. *Frontiers in Microbiology* 5:40. doi: 10.3389/fmicb.2014.00040. Reprinted here with permission of the publisher.

Abstract

Since the early 1960s, the fungal pathogen *Aspergillus flavus* (Link ex Fr.) has been the focus of intensive research due to the production of carcinogenic and highly toxic secondary metabolites collectively known as aflatoxins following pre-harvest colonization of crops. Given this recurrent problem and the occurrence of a severe aflatoxin outbreak in maize (*Zea mays* L.), particularly in the Southeast U.S. in the 1977 growing season, a significant research effort has been put forth to determine the nature of the interaction occurring between aflatoxin production, *A. flavus*, environment and its various hosts before harvest. Many studies have investigated this interaction at the genetic, transcript, and protein levels, and in terms of fungal biology at either pre- or post-harvest time points. Later experiments have indicated that the interaction and overall resistance phenotype of the host is a quantitative trait with a relatively low heritability. In addition, a high degree of environmental interaction has been noted, particularly with sources of abiotic stress for either the host or the fungus such as drought or heat stresses. Here, we review the history of research into this complex interaction and propose future directions for elucidating the relationship between resistance and susceptibility to *A. flavus* colonization, abiotic stress, and its relationship to oxidative stress in which aflatoxin production may function as a form of antioxidant protection to the producing fungus.

Introduction

Aspergillus flavus (Link ex Fr.; Teleomorph: *Petromyces flavus*) is a facultative, plant parasitic pathogen, which has the ability to colonize a number of common crop species including cotton, maize, peanut, and rice (Diener et al., 1987). Economic losses due to the infection of grain crops such as maize (*Zea mays* L.) by *A. flavus* is not primarily due to the expression of symptoms known as *Aspergillus* ear rot but, rather, is due to the subsequent contamination of the grain with the fungal metabolite aflatoxin. Aflatoxins are a group of polyketide-derived furanocoumarin secondary metabolites produced by certain species of fungi, including the genus *Aspergillus* (Bennett and Klich, 2003; Chanda et al., 2009). Aflatoxins are highly carcinogenic and can be acutely toxic or fatal if ingested in sufficient quantities for both livestock and humans (Shephard, 2008).

Although this species was first described by Link in 1809 (Amaike and Keller, 2011), major research on the biology and pathogenicity of *A. flavus* did not commence until the mid-1960's with the incident of Turkey X disease which killed over 100,000 turkeys due to aflatoxin contaminated feed associated with *A. flavus* infected peanuts (Wogan, 1966). Shortly thereafter broad screening of feed and food was initiated, the chemical structures of the major aflatoxins (B1, B2, G1, and G2) were elucidated, and research was conducted on preventing post-harvest contamination of grain crops through the modulation of storage conditions (Asao et al., 1965; Trenk and Hartman, 1970). However, it was found during a particularly severe outbreak of aflatoxin contamination in maize in the late 1970's in the U.S. that it was possible for *A. flavus* to both colonize and produce aflatoxin on developing maize kernels prior to harvest (Diener et al., 1987).

Since that time, research efforts have focused on determining the source of host plant resistance to prevent *A. flavus* colonization and subsequent aflatoxin production pre-harvest and before transportation to storage. These efforts have employed numerous techniques and approaches including modern plant breeding and genetics tools such as proteomic, transcriptomic, and biochemical analyses in an effort to discover the underlying mechanism of host plant resistance and the interaction between the two organisms. To date, these efforts have revealed that resistance is quantitatively inherited with a strong genotype by environment component. It is a complex interaction with a high degree of environmentally induced variability with abiotic and biotic stress strongly influencing resistance or susceptibility. Here we review the results of research into the mechanism of host resistance to both *A. flavus* colonization and abiotic stress, and propose future research directions for determining the relationship between oxidative stress and aflatoxin contamination.

Host Resistance against *A. flavus*: Gene-for-Gene or Genotype x Environment Interaction?

From a gene-for-gene perspective, host resistance against *A. flavus* colonization and subsequent aflatoxin contamination has been approached as a single virulence factor produced by the invading pathogen that would be countered by a single avirulence or resistance protein in the host. This results in compatible or incompatible reactions based on specific recognition (Keen, 1990). The particular virulence mechanisms of these plant-microbe interactions are utilized to classify plant pathogens into groups such as biotrophic, necrotrophic, and hemibiotrophic pathogens (Glazebrook, 2005).

The classification of *A. flavus* into a particular class of plant pathogens has yet to be determined. A microscopy study of the growth of *A. flavus* in maize kernel tissue by Smart et al.

(1990) showed that cellular components such as cell walls were broken down in advance of mycelia. This has been interpreted as being indicative of necrotrophic pathogenicity in the literature (Mideros et al., 2009), however, not all research concurs with this conclusion. Recently, Magbanua et al. (2007) found that the colonization of kernel tissue from resistant maize lines exhibited increased levels of salicylic acid (SA) and unchanged levels of jasmonic acid (JA), traits commonly associated with resistance to biotrophic pathogens in various plant species (Glazebrook, 2005). As a facultative parasite, which naturally exists as a saprophyte, *A. flavus* may possess a unique pathogenicity mechanism that does not categorically fit into this classification scheme.

In keeping with the concept of gene-for-gene resistance, virulence factors produced by *A. flavus* during the colonization of maize tissues as well as maize kernel avirulence proteins have been the focus of multiple studies. These efforts have helped to better characterize the nature of this plant-pathogen interaction, and have sought to identify pathogen and host-derived proteins encoded by potential single-gene sources of host resistance or susceptibility. Proteomics-based techniques have identified several virulence proteins produced by *A. flavus*, most of which being hydrolytic enzymes. Examples of these enzymes are amylases, cellulases, chitinases, cutinases (e.g. phyto-cutinase), lipases, pectinases (P2c), proteases such as alkaline protease, and xylanases (Cleveland and Cotty, 1991; Guo et al., 1995; Chen et al., 1998; Chen et al., 1999; Fakhoury and Woloshuk, 1999; Mellon et al., 2000; Brown et al., 2001; Cleveland et al., 2004; Chen et al., 2009a; Pechanova et al., 2013). These enzymes are consistent with the biology and classification of *A. flavus* as a saprophyte since they typically catabolize decaying plant materials as a source of nutrition.

Several constitutively expressed and inducible proteins have been described in the literature which have been shown counter the function of other hydrolytic virulence proteins produced by *A. flavus*. For example, Chen et al. (1998) described a 14-kDa trypsin inhibitor (TI) which functions as an inhibitor of α-amylase, a protein utilized by *A. flavus* for the catabolism of complex carbohydrates. The same group also showed that silencing the expression of the TI gene in maize increases the susceptibility of maize kernel tissue to *A. flavus* infection and aflatoxin contamination (Chen et al., 2009b). In addition, β-1,3-glucanases, chitinases, pathogenesis-related proteins 10 and 10.1, ribosome inactivating proteins (RIPs), and zeamatin have also been shown to be involved in the resistance of maize against *A. flavus* (Lozovaya et al., 1998; Mauch et al., 1988; Walsh et al., 1991; Huynh et al., 1992; Guo et al., 1997; Chen et al., 2006; Chen et al., 2010; Xie et al., 2010). Liang et al. (2005) reported that the increase of β-1,3-glucanases in the resistant peanut lines was higher than in the susceptible lines after infection with *A. flavus*.

Accumulation of such antifungal and avirulence proteins has been shown to contribute to the resistance observed in several maize lines along with morphological characteristics of resistant kernels such as thickened wax cuticles (Guo et al., 1995). Various breeding techniques have been employed to develop varieties with enhanced resistance to *A. flavus* and aflatoxin contamination on the basis of utilizing phenotypic screenings and molecular markers associated with known avirulence genes to identify quantitative trait loci (QTL) for selection (Brown et al., 2013). These efforts have met with some success such as in the case of Willcox et al. (2013) which identified 20 QTL explaining 22 to 43% of phenotypic variation within a F_2 mapping population derived from Mp313E x Va35. This study along with others (Paul et al., 2003; Brooks et al., 2005; Kelley et al., 2012) illustrate two important challenges in breeding resistant maize varieties, including 1) that resistance to *A. flavus* is a quantitative trait involving multiple genes

rather than single-gene forms of gene-for-gene resistance, and 2) a large genotype x environment (G x E) interaction conditions the expression of this trait. For example Willcox et al. (2013) determined that only 11 of the 20 identified QTL were consistently expressed across different environments with these accounting for 2.4 to 9.5% of phenotypic variance.

Environmental factors can have a significant effect on maize resistance to *A. flavus*, particularly abiotic stresses such as drought and heat stress. This was clearly demonstrated as early as 1977 when widespread and intense drought conditions in the Midwestern and Southeastern United States resulted in a high degree of aflatoxin contamination of maize kernels pre-harvest (Zuber and Lillehoj, 1979; Diener et al., 1987). However, maize genotypes possessing drought tolerance tend to be less susceptible to aflatoxin contamination such as Lo964 and Tex6 (Guo et al., 2008; Luo et al., 2008; Jiang et al., 2012).

Relationship of Drought Tolerance and *A. flavus* Resistance

It has been hypothesized that there is an underlying relationship among various molecular mechanisms of drought stress adaptation and resistance to *A. flavus* infection and subsequent aflatoxin contamination. This connection has been demonstrated experimentally in a number of studies. For example, Chen et al. (2007) found a number of drought stress-related proteins that were induced in response to *A. flavus* colonization in maize endosperm tissue including late embryogenesis abundant proteins LEA 3, 14, peroxiredoxin (PER1), and a 17.9-kDa heat shock protein (HSP17.9). Pechanova et al. (2011) found that these proteins along with several antioxidant proteins, such as ascorbate peroxidase and superoxide dismutase, were up-regulated in resistant maize rachis tissue earlier in development and formed the basis, when combined with

increased expression of anti-fungal and pathogenesis-related proteins, for resistance to *A. flavus* colonization.

It has also been shown that global defense regulators have the potential modulate maize resistance to drought stress, oxidative stress, and possibly *A. flavus* resistance. For example, WRKY transcription factors, which have been shown to regulate the responses of multiple plant species to both biotic and abiotic stresses (Rushton et al., 2010). The transcription factor *Zm*WRKY33 was recently shown to enhance abscisic acid (ABA) signaling and enhance osmotic stress tolerance in maize seedlings (Li et al., 2013). *Zm*WRKY33 along with *Zm*WRKY19, whose homolog in *Arabidopsis thaliana* (*At*WRKY53) has been shown to be induced in response to oxidative stress and regulates the expression of antioxidant enzymes like catalase (Miao et al., 2004; Eulgem and Somssich, 2007; Miao et al., 2007; Rushton et al., 2010), were found to be up-regulated earlier in resistant maize varieties in response to *A. flavus* inoculation in whole kernel tissues (Fountain et al., 2013).

Oxidative Responses of Plants to Insect Herbivory

Oxidative responses of plants to feeding damage by both chewing and piercing-sucking insects have been described in recent years. Walling (2000) and Kaloshian and Walling (2005) described the piercing-sucking hemipteran insect feeding on crop plants as resembling plant pathogen infections that are often related to chitosan (oligogalacturonides produced by pectinases) and reactive oxygen species (ROS)-activated wound or defense signaling pathways in host plants. Kessler and Baldwin (2002) reviewed the molecular mechanisms underlying plant responses to insect herbivory and how they differ from pathogen infections. They concluded that insect herbivores are physiologically independent from their host plants, whereas pathogens are

physiologically dependent on their host plants for their growth and development (Kessler and Baldwin, 2002). Oxidative enzyme-mediated wounding responses also play a critical role in understanding plant responses to insect herbivory, although the insect-specific elicitors frequently modify the responses of their host plants, and allow the host plants to optimize their defenses against a specific insect pest (Kessler and Baldwin, 2002).

Bi and Felton (1995) reported that corn earworm, *Helicoverpa zea* (Boddie), herbivory caused significant increases in lipid peroxidation and hydroxyl radical formation in the soybean leaves. The activities of several oxidative enzymes (i.e., lipoxygenases, peroxidase, diamine oxidase, ascorbate oxidase, and NADH oxidase I) were also increased following *H. zea* herbivory on soybean leaves. They concluded that oxidative responses in the soybean plants may have led to a decrease in herbivory and an increase in oxidative damage to the plant. Ni et al. (2000) described the salivary enzyme profiles of the leaf-chlorosis-eliciting Russian wheat aphid, *Diuraphis noxia* (Mordvilko), and the non-leaf-chlorosis-eliciting bird cherry-oat aphid, *Rhopalosiphum padi* (L.), which differ in oxidative enzyme activities. While only peroxidase activity was detected in *R. padi*, catalase activity was only detected in *D. noxia*. The oxidative responses of four cereal plants (i.e., susceptible 'Arapahoe' and resistant 'Halt' wheat, susceptible 'Morex' barley, and resistant 'Border' oat) to the feeding of the two species of aphid differed (Ni et al., 2001a). The chlorosis-eliciting *D. noxia* feeding caused a three-fold increase in peroxidase activity in the resistant Halt wheat, and nine-fold increase in the susceptible Morex barley nine days after infestation when compared to the control leaves. In contrast, *R. padi* did not cause any changes in peroxidase activity in any of the cereal leaves. At the same time, *D. noxia* feeding did not elicit any change in either catalase or polyphenol oxidase activity in comparison with either the *R. padi*-infested or the control cereal leaves (Ni et al., 2001a).

Furthermore, oxidative bleaching in leaf chlorosis elicited by *D. noxia* was not detected, but Mg-dechelatase activity was increased in the *D. noxia*-elicited chlorosis in wheat leaves (Ni et al., 2001b).

Research on the leaf chlorosis-elicitation process has revealed the complex nature of the oxidative responses of plants against wounding and insect herbivory. Zavala et al. (2013) also proposed a cellular mechanism to decipher the influence of elevated CO_2 on insect herbivory. They highlighted that oxidative enzyme activities in the sub-cellular organelles, such as peroxisomes and chloroplasts, via the jasmonic signaling pathway are likely to be critical factors in dissecting the molecular mechanisms of plant defenses against both biotic and abiotic stresses. In general, the oxidative responses of plants to pathogen infection and insect herbivory under varying environmental conditions (e.g., drought and the elevated CO_2) are critical for the management of pest outbreaks and the reduction of mycotoxin contamination in agricultural crops.

The Role of Oxidative Stress in Aflatoxin Biosynthesis

The presence of increased expression of antioxidant mechanisms in resistant maize tissues leads to the hypothesis that increased resistance to ROS-induced oxidative stress may correlate to resistance to *A. flavus* and aflatoxin contamination. Although this conclusion seems credible due to the high degree of correlative evidence present in the literature, the exact mechanism of how this phenomenon functions has yet to be elucidated completely. However, more recent studies into the biology of *A. flavus* and the mechanisms regulating the production of aflatoxin may shed light on this issue.

Aflatoxin biosynthesis is a complex process involving multiple gene products and regulatory mechanisms coded for by an approximately 70-kb cluster of 25 genes (Yu et al., 2004). This pathway is responsible for the biosynthesis of five major mycotoxins: sterigmatocystin, B_1, B_2, G_1, and G_2 aflatoxins (Yu et al., 2004), and is the focus of intensive research into methods of negatively regulating its function. Although the structure and biochemical characteristics of aflatoxins have been known since the 1960's (Asao et al., 1965; Wogan, 1966), the specific purpose of their production by *A. flavus* or other aflatoxigenic fungi has remained a mystery. Prior research exploring the roles of oxidative stress in regulating aflatoxin biosynthesis as well as recent discoveries into the upstream regulation of major pathway regulatory factors, however, have given clues as to the biological function of aflatoxins (Roze et al., 2013). It has been shown that aflatoxin production by *A. flavus* is higher in maize kernel tissues containing higher levels of lipids, such as embryo tissues (Earle et al., 1946; Fabbri et al., 1980; Brodhagen and Keller, 2006). Given this information, the roles of lipids in regulating aflatoxin biosynthesis in *Aspergillus spp*. have been investigated, particularly oxylipins (Reviewed in Gao and Kolomiets, 2009). An earlier study by Fabbri et al. (1983) found that seeds of high-oil crops such as peanut support higher levels of aflatoxin production by *A. parasiticus* than seeds of graminaceous plants such as maize or wheat, which contain higher levels of starch. In addition, they found that culturing *A. parasiticus* amended with peroxidized lipids resulted in significantly elevated aflatoxin production with no significant effect on fungal biomass (Fabbri et al., 1983).

Lipid peroxidation is a byproduct of lipid metabolism in peroxisomes as well as the reaction of naturally produced free fatty acids with ROS (Reverberi et al., 2012). Therefore, it is possible that excessive peroxisome function in the fungal mycelia or oxidative stress may be a

causative factor in the production of aflatoxin. In-vitro, Jayashree and Subramanyam (2000) showed that toxigenic strains of *A. parasiticus* have increased oxygen requirements, which they postulate to be a potential source of ROS accumulation, in comparison to non-toxigenic strains. In addition, they showed that higher levels of glutathione and thiobarbituric acid-reactive substances (TBARS), as well as antioxidant enzyme activities, were present in toxigenic strains in comparison to non-toxigenic strains. This indicated that oxidative stress may be a pre-requisite for aflatoxin production (Jayashree and Subramanyam, 2000). Also, Reverberi et al. (2012) found that bezafibrate and transformation of the *Cymbidium ringspot virus* P33 gene into *A. flavus* induced peroxisome proliferation resulting in an increase in aflatoxin production both in-vitro and when cultured on maize kernel tissues in addition to increased levels of antioxidant enzyme gene expression, lipid metabolism, oxylipin biosynthesis, and ROS accumulation in the *A. flavus* mycelia. Recent studies have also found that cAMP and G-protein -mediated quorum sensing signaling pathways based on oxylipin perception can play a vital role in growth regulation and aflatoxin production in *A. nidulans* (Affeldt et al., 2012). Such G-protein mediated signaling has also been reported in other *Aspergillus spp*. including *A. fumigatus* (Grice et al., 2013). Therefore, it may be concluded that oxidative stress in *A. flavus* induced by ROS and/or oxylipins in the growth environment/medium will result in increased aflatoxin production from a biochemical perspective.

Recent studies have also shown that ROS can play a role in the transcriptional regulation of aflatoxin and sterigmatosystin biosynthesis pathway genes. Reverberi et al. (2008) found that a putative binding site for the Ap*yapA* gene, which regulates oxidative stress tolerance and conidiogenesis, was present in the promoter of the regulatory gene *AflR* in *A. parasiticus*, and that silencing Ap*yapA* results in an increase in aflatoxin biosyntheisis. It has also been shown

that the basic leucine zipper (bZIP) transcription factor AtfB regulates the aflatoxin biosynthesis genes *fas-1, ver-1,* and *omtA* as well as antioxidant genes encoding for catalase and superoxide dismutase (SOD) (Hong et al., 2013). They also found that the promoter regions associated with AtfB also contained cAMP-responsive elements implicating cAMP in the regulation of aflatoxin biosynthesis (Hong et al., 2013).

Potential Reactive Oxygen Species-Mediated Crosstalk between Maize and *A. flavus*

Given the apparent role of oxidative stress in the promotion of aflatoxin biosynthesis, the hypothesis has been proposed that aflatoxin may function as a form of antioxidant protection to Aspergilli (Reverberi et al., 2010). This would provide an explanation to the long standing question, rather the mystery, as to the biological significance of aflatoxin, although the potential antioxidant mechanism of action of aflatoxin has yet to be fully elucidated. In addition, this explanation also provides for the potential role of ROS and oxylipins cross-kingdom communication between maize and *A. flavus*.

Cross-kingdom communication between plants and various fungi through the use of oxylipins has been previously documented (Christensen and Kolomiets, 2011). Specifically, the role of oxylipins has been clearly illustrated in the specific interaction between maize and *A. flavus*. In a recent study, it was found that maize lipoxygenase-3 (LOX3) is required for resistance to *A. flavus* indicating that certain 9-oxylipins can play important roles in suppressing aflatoxin biosynthesis while other oxylipins may promote aflatoxin biosynthesis (Gao et al., 2009). The role of LOX-1 in resistance mechanisms against *A. flavus*, *A. nidulans* and *A. parasiticus* has also been implied in soybean (Doehlert et al., 1993; Burow et al., 1997), although there are contradicting reports on the subject in the literature. Mellon and Cotty (2002) found that

soybeans lacking LOX activity were just as resistant to *A. flavus* and aflatoxin contamination as those possessing LOX activity. This seems to imply some degree of specificity in the role of LOX enzymes or their products in resistance to certain *Aspergillus* species.

In addition to oxylipins, other host-derived compounds may influence oxidative stress including ROS and phytohormones. It was found that 2-chloroethyl phosphoric acid (CEPA), the metabolic precursor to ethylene, was capable of reducing the expression of *AflR* and *AflD*, reducing the accumulation of oxidative compounds, and regulating glutathione redox in *A. flavus* mycelia (Huang et al., 2009). Therefore, host-derived ethylene may result in the reduction of ROS accumulation in *A. flavus* mycelia and reduce aflatoxin biosynthesis. This hypothesis seems plausible since the expression of the maize Ethylene Responsive Factor 1 (*Zm*ERF1), a key transcription factor involved in ethylene and jasmonic acid signaling, was found to be higher in the immature kernel tissues of the resistant maize variety TZAR101 in comparison to the susceptible maize variety B73 following *A. flavus* inoculation (Fountain et al., 2013).

Previous research has shown that maize varieties resistant to *A. flavus* tend to accumulate antioxidant enzymes, such as peroxidase and superoxide dismutase, and tend to be more resistant to drought and heat stress than varieties susceptible to *A. flavus* (Guo et al., 2008; Pechanova et al., 2011). Given the reported role of oxidative stress in *Aspergillus spp*. biology, it may be possible for host-derived antioxidant proteins, phytohormones, and oxylipins to negatively regulate the production of aflatoxin in infecting *A. flavus* by reducing the level of oxidative stress endured by both the host and the fungus, particularly during drought or heat stress. Such an interaction may explain several observed phenomena in the literature. For example, Guo et al. (1996) observed that the pre-incubation of maize kernels in high-humidity conditions for three days prior to inoculation with *A. flavus* results in a significant reduction in aflatoxin

contamination in comparison kernels inoculated without pre-incubation. Given the fact that ROS such as hydrogen peroxide accumulates to maximum quantities two days post-imbibition (DPI) followed by increased catalase activity beginning at three DPI in maize kernels (Hite et al., 1999), a combination of host-derived resistance and antioxidant proteins and reduced ROS production at the time of inoculation may have contributed to the reduction in aflatoxin production (Guo et al., 1996).

Conclusions

Determining the role of oxidative stress in the regulation of aflatoxin biosynthesis as well as the role of host defenses against both *A. flavus* infection and mycotoxin biosynthesis are critical areas of research for the mitigation of aflatoxin contamination in maize. Maize resistance to *A. flavus* is a complex, quantitative trait which is the culmination of the interaction of numerous resistance-associated proteins and antioxidant enzymes which have been the subject of more than 50 years of rigorous research. Solutions to the problem of aflatoxin contamination of crops, particularly maize, have been elusive given the high level of environmental influence on the interaction and the lack of stable resistance in maize germplasm across multiple environments. By better understanding the role of oxidative stress and its remediation by the host and the pathogen, additional tools will be made available to counter the threat aflatoxin poses to food safety and security and further enhance the knowledge of cross-kingdom interactions which may be applied to other mycotoxin producing pathogens in various agricultural commodities.

Acknowledgements

This work is partially supported by the U.S. Department of Agriculture Agricultural Research Service (USDA-ARS), the Georgia Agricultural Commodity Commission for Corn, and AMCOE (Aflatoxin Mitigation Center of Excellence). Mention of trade names or commercial products in this publication is solely for the purpose of providing specific information and does not imply recommendation or endorsement by the USDA. The USDA is an equal opportunity provider and employer.

References

1. Affeldt, K.J., Brodhagen, M., and Keller, N.P. (2012). *Aspergillus* oxylipin signaling and quorum sensing pathways depend on G protein-coupled receptors. *Toxins* 4**,** 695-717.
2. Amaike, S., and Keller, N.P. (2011). *Aspergillus flavus*. *Ann. Rev. Phytopathol.* 49**,** 107-133.
3. Asao, T., Büchi, G., Abdel-Kader, M., Chang, S., Wick, E.L., and Wogan, G. (1965). The structures of aflatoxins B and G1. *J. Am. Chem. Soc.* 87**,** 882-886.
4. Bennett, J.W., and Klich, M. (2003). Mycotoxins. *Clin. Microbiol. Rev.* 16**,** 497-516.
5. Bi, J., and Felton, G. (1995). Foliar oxidative stress and insect herbivory: primary compounds, secondary metabolites, and reactive oxygen species as components of induced resistance. *J. Chem. Ecol.* 21**,** 1511-1530.
6. Brodhagen, M., and Keller, N.P. (2006). Signalling pathways connecting mycotoxin production and sporulation. *Mol. Plant Pathol.* 7**,** 285-301.
7. Brooks, T.D., Williams, W.P., Windham, G.L., Willcox, M.C., and Abbas, H.K. (2005). Quantitative trait loci contributing resistance to aflatoxin accumulation in the maize inbred Mp313E. *Crop Sci.* 45**,** 171-174.

8. Brown, R.L., Chen, Z.Y., Cleveland, T.E., Cotty, P.J., and Cary, J.W. (2001). Variation in in vitro alpha-amylase and protease activity is related to the virulence of *Aspergillus flavus* isolates. *J. Food Protect.* 64**,** 401-404.
9. Brown, R.L., Menkir, A., Chen, Z.-Y., Bhatnagar, D., Yu, J., Yao, H., and Cleveland, T.E. (2013). Breeding aflatoxin resistant maize lines using recent advances in technologies–a review. *Food Add. Contam.: Part A*.
10. Burow, G., Nesbitt, T., Dunlap, J., and Keller, N. (1997). Seed lipoxygenase products modulate *Aspergillus* mycotoxin biosynthesis. *Mol. Plant-Microbe Interact.* 10**,** 380-387.
11. Chanda, A., Roze, L.V., Kang, S., Artymovich, K.A., Hicks, G.R., Raikhel, N.V., Calvo, A.M., and Linz, J.E. (2009). A key role for vesicles in fungal secondary metabolism. *Proc. Nat. Acad. Sci. U.S.A.* 106**,** 19533-19538.
12. Chen, Z.-Y., Brown, R., Damann, K., and Cleveland, T. (2007). Identification of maize kernel endosperm proteins associated with resistance to aflatoxin contamination by *Aspergillus flavus*. *Phytopathology* 97**,** 1094-1103.
13. Chen, Z.-Y., Brown, R.L., Cary, J.W., Damann, K.E., and Cleveland, T.E. (2009a). Characterization of an *Aspergillus flavus* alkaline protease and its role in the infection of maize kernels. *Toxin Rev.* 28**,** 187-197.
14. Chen, Z.-Y., Brown, R.L., Damann, K.E., and Cleveland, T.E. (2010). PR10 expression in maize and its effect on host resistance against *Aspergillus flavus* infection and aflatoxin production. *Mol. Plant Pathol.* 11**,** 69-81.
15. Chen, Z.Y., Brown, R.L., Guo, B.Z., Menkir, A., and Cleveland, T.E. (2009b). Identifying aflatoxin resistance-related proteins/genes through proteomics and RNAi gene silencing. *Peanut Sci.* 36**,** 35-41.

16. Chen, Z.Y., Brown, R.L., Lax, A.R., Guo, B.Z., Cleveland, T.E., and Russin, J.S. (1998). Resistance to *Aspergillus flavus* in corn kernels is associated with a 14-kDa protein. *Phytopathology* 88**,** 276-281.

17. Chen, Z.Y., Brown, R.L., Rajasekaran, K., Damann, K.E., and Cleveland, T.E. (2006). Identification of a maize kernel pathogenesis-related protein and evidence for its involvement in resistance to *Aspergillus flavus* infection and aflatoxin production. *Phytopathology* 96**,** 87-95.

18. Chen, Z.Y., Brown, R.L., Russin, J.S., Lax, A.R., and Cleveland, T.E. (1999). A corn trypsin inhibitor with antifungal act inhibits *Aspergillus flavus* alpha-amylase. *Phytopathology* 89**,** 902-907.

19. Christensen, S.A., and Kolomiets, M.V. (2011). The lipid language of plant–fungal interactions. *Fungal Genet. Biol.* 48**,** 4-14.

20. Cleveland, T.E., and Cotty, P.J. (1991). Invasiveness of *Aspergillus flavus* isolates in wounded cotton bolls is associated with production of a specific fungal polygalacturonase. *Phytopathology* 81**,** 155-158.

21. Cleveland, T.E., Yu, J.J., Bhatnagar, D., Chen, Z.Y., Brown, R.L., Chang, P.K., and Cary, J.W. (2004). Progress in elucidating the molecular basis of the host plant - *Aspergillus flavus* interaction, a basis for devising strategies to reduce aflatoxin contamination in crops. *Toxin Rev.* 23**,** 345-380.

22. Diener, U.L., Cole, R.J., Sanders, T.H., Payne, G.A., Lee, L.S., and Klich, M.A. (1987). Epidemiology of aflatoxin formation by *Aspergillus flavus*. *Ann. Rev. Phytopathol.* 25**,** 249-270.

23. Doehlert, D.C., Wicklow, D.T., and Gardner, H.W. (1993). Evidence implicating the lipoxygenase pathway in providing resistance to soybeans against *Aspergillus flavus*. *Phytopathology* 83**,** 1473-1477.

24. Earle, F.R., Curtis, J.J., and Hubbard, J.E. (1946). Composition of the component parts of the corn kernel. *Cereal Chem.* 23**,** 504-511.

25. Eulgem, T., and Somssich, I.E. (2007). Networks of WRKY transcription factors in defense signaling. *Curr.Opin. Plant Biol.*10**,** 366-371.

26. Fabbri, A., Fanelli, C., Panfili, G., Passi, S., and Fasella, P. (1983). Lipoperoxidation and aflatoxin biosynthesis by *Aspergillus parasiticus* and *A. flavus*. *J. Gen. Microbiol.*129**,** 3447-3452.

27. Fabbri, A., Fanelli, C., and Serafini, M. (1980). Aflatoxin production on cereals, oil seeds and some organic fractions extracted from sunflower. *Rendiconti Accademia Nazionale delle Sciencze detta dei XL* 98**,** 219-228.

28. Fakhoury, A.M., and Woloshuk, C.P. (1999). Amy1, the alpha-amylase gene of *Aspergillus flavus*: Involvement in aflatoxin biosynthesis in maize kernels. *Phytopathology* 89**,** 908-914.

29. Fountain, J.C., Raruang, Y., Luo, M., Brown, R.L., and Chen, Z.Y. (2013). Maize WRKY transcription factors and their potential roles in regulating defense gene expression during *Aspergillus flavus* infection. *Phytopathology* 103(Suppl. 1)**,** S1.4.

30. Gao, X., Brodhagen, M., Isakeit, T., Brown, S.H., Göbel, C., Betran, J., Feussner, I., Keller, N.P., and Kolomiets, M.V. (2009). Inactivation of the lipoxygenase *Zm*LOX3 increases susceptibility of maize to *Aspergillus* spp. *Mol. Plant-Microbe Interact.* 22**,** 222-231.

31. Gao, X., and Kolomiets, M.V. (2009). Host-derived lipids and oxylipins are crucial signals in modulating mycotoxin production by fungi. *Toxin Revi.* 28**,** 79-88.

32. Glazebrook, J. (2005). Contrasting mechanisms of defense against biotrophic and necrotrophic pathogens. *Ann.Rev. Phytopathol.* 43, 205-227.

33. Grice, C., Bertuzzi, M., and Bignell, E. (2013). Receptor-mediated signaling in *Aspergillus fumigatus*. *Front. Microbiol.* 4.

34. Guo, B., Chen, Z.-Y., Lee, R.D., and Scully, B.T. (2008). Drought stress and preharvest aflatoxin contamination in agricultural commodity: Genetics, genomics and proteomics. *J. Int. Plant Biol.*50**,** 1281-1291.

35. Guo, B.Z., Chen, Z.Y., Brown, R.L., Lax, A.R., Cleveland, T.E., Russin, J.S., Mehta, A.D., Selitrennikoff, C.P., and Widstrom, N.W. (1997). Germination induces accumulation of specific proteins and antifungal activities in corn kernels. *Phytopathology* 87**,** 1174-1178.

36. Guo, B.Z., Russin, J.S., Brown, R.L., Cleveland, T.E., and Widstrom, N.W. (1996). Resistance to aflatoxin contamination in corn as influenced by relative humidity and kernel germination. *J. Food Protect.* 59**,** 276-281.

37. Guo, B.Z., Russin, J.S., Cleveland, T.E., Brown, R.L., and Widstrom, N.W. (1995). Wax and cutin layers in maize kernels associated with resistance to aflatoxin production by *Aspergillus flavus*. *J. Food Protect.* 58**,** 296-300.

38. Hite, D.R., Auh, C., and Scandalios, J.G. (1999). Catalase activity and hydrogen peroxide levels are inversely correlated in maize scutella during seed germination. *Redox Rep.* 4**,** 1-2.

39. Hong, S.Y., Roze, L.V., Wee, J., and Linz, J.E. (2013). Evidence that a transcription factor regulatory network coordinates oxidative stress response and secondary metabolism in Aspergilli. *MicrobiologyOpen* 2**,** 144-160.

40. Huang, J.-Q., Jiang, H.-F., Zhou, Y.-Q., Lei, Y., Wang, S.-Y., and Liao, B.-S. (2009). Ethylene inhibited aflatoxin biosynthesis is due to oxidative stress alleviation and related to glutathione redox state changes in *Aspergillus flavus*. *Int. J. Food Microbiol.*130**,** 17-21.

41. Huynh, Q.K., Hironaka, C.M., Levine, E.B., Smith, C.E., Borgmeyer, J.R., and Shah, D.M. (1992). Antifungal proteins from plants - purification, molecular cloning, and antifungal properties of chitinases from maize seed. *J. Biol.Chem.* 267**,** 6635-6640.

42. Jayashree, T., and Subramanyam, C. (2000). Oxidative stress as a prerequisite for aflatoxin production by *Aspergillus parasiticus*. *Free Rad. Biol. Med.*29**,** 981-985.

43. Jiang, T., Fountain, J., Davis, G., Kemerait, R., Scully, B., Lee, R.D., and Guo, B. (2012). Root morphology and gene expression analysis in response to drought stress in maize (*Zea mays*). *Plant Mol. Biol. Rep.* 30**,** 360-369.

44. Kaloshian, I., and Walling, L.L. (2005). Hemipterans as plant pathogens. *Annu. Rev. Phytopathol.* 43**,** 491-521.

45. Keen, N.T. (1990). Gene-for-gene complementarity in plant-pathogen interactions. *Ann. Rev. Genet.* 24**,** 447-463.

46. Kelley, R.Y., Williams, W.P., Mylroie, J.E., Boykin, D.L., Harper, J.W., Windham, G.L., Ankala, A., and Shan, X. (2012). Identification of maize genes associated with host plant resistance or susceptibility to *Aspergillus flavus* infection and aflatoxin accumulation. *PLoS One* 7**,** e36892.

47. Kessler, A., and Baldwin, I.T. (2002). Plant responses to insect herbivory: the emerging molecular analysis. *Ann. Rev. Plant Biol.* 53**,** 299-328.

48. Li, H., Gao, Y., Xu, H., Dai, Y., Deng, D., and Chen, J. (2013). *Zm*WRKY33, a WRKY maize transcription factor conferring enhanced salt stress tolerances in *Arabidopsis*. *Plant Growth Reg.* 70**,** 207-216.

49. Liang, X.Q., Holbrook, C.C., Lynch, R.E., and Guo, B.Z. (2005). β-1,3-Glucanase activity in peanut seed (*Arachis hypogaea*) is induced by inoculation with *Aspergillus flavus* and copurifies with a conglutin-like protein. *Phytopathology* 95, 506-511.

50. Lozovaya, V.V., Waranyuwat, A., and Widholm, J.M. (1998). β-l,3-glucanase and resistance to *Aspergillus flavus* infection in maize. *Crop Sci.* 38**,** 1255-1260.

51. Luo, M., Liu, J., Lee, R., and Guo, B. (2008). Characterization of gene expression profiles in developing kernels of maize (*Zea mays*) inbred Tex6. *Plant Breed.*127**,** 569-578.

52. Magbanua, Z.V., De Moraes, C.M., Brooks, T.D., Williams, W.P., and Luthe, D.S. (2007). Is catalase activity one of the factors associated with maize resistance to Aspergillus flavus? *Mol. Plant-Microbe Interact.* 20**,** 697-706.

53. Mauch, F., Mauchmani, B., and Boller, T. (1988). Antifungal hydrolases in pea tissue: 2. Inhibition of fungal growth by combinations of chitinase and beta-1,3-glucanase. *Plant Physiol.* 88**,** 936-942.

54. Mellon, J., and Cotty, P. (2002). No effect of soybean lipoxygenase on aflatoxin production in *Aspergillus flavus*-inoculated seeds. *J. Food Protect.* 65**,** 1984-1987.

55. Mellon, J.E., Cotty, P.J., and Dowd, M.K. (2000). Influence of lipids with and without other cottonseed reserve materials on aflatoxin B-1 production by *Aspergillus flavus*. *J. Ag. Food Chem.* 48**,** 3611-3615.

56. Miao, Y., Laun, T., Zimmermann, P., and Zentgraf, U. (2004). Targets of the WRKY53 transcription factor and its role during leaf senescence in *Arabidopsis*. *Plant Mol. Biol.* 55**,** 853-867.

57. Miao, Y., Laun, T.M., Smykowski, A., and Zentgraf, U. (2007). *Arabidopsis* MEKK1 can take a short cut: it can directly interact with senescence-related WRKY53 transcription factor on the protein level and can bind to its promoter. *Plant Mol. Biol.* 65**,** 63-76.

58. Mideros, S.X., Windham, G.L., Williams, W.P., and Nelson, R.J. (2009). *Aspergillus flavus* biomass in maize estimated by quantitative real-time polymerase chain reaction is strongly correlated with aflatoxin concentration. *Plant Dis.* 93**,** 1163-1170.

59. Ni, X., Quisenberry, S.S., Heng-Moss, T., Markwell, J., Sarath, G., Klucas, R., and Baxendale, F. (2001a). Oxidative responses of resistant and susceptible cereal leaves to symptomatic and nonsymptomatic cereal aphid (Hemiptera: Aphididae) feeding. *J. Econom. Entomol.* 94**,** 743-751.

60. Ni, X., Quisenberry, S.S., Markwell, J., Heng-Moss, T., Higley, L., Baxendale, F., Sarath, G., and Klucas, R. (2001b). In vitro enzymatic chlorophyll catabolism in wheat elicited by cereal aphid feeding. *Entomologia experimentalis et applicata* 101**,** 159-166.

61. Ni, X., Quisenberry, S.S., Pornkulwat, S., Figarola, J.L., Skoda, S.R., and Foster, J.E. (2000). Hydrolase and oxido-reductase activities in *Diuraphis noxia* and *Rhopalosiphum padi* (Hemiptera: Aphididae). *Ann. Entomol. Soc. Am.* 93**,** 595-601.

62. Paul, C., Naidoo, G., Forbes, A., Mikkilineni, V., White, D., and Rocheford, T. (2003). Quantitative trait loci for low aflatoxin production in two related maize populations. *Theor. Appl. Genet.* 107**,** 263-270.

63. Pechanova, O., Pechan, T., Rodriguez, J.M., Williams, W.P., and Brown, A.E. (2013). A two-dimensional proteome map of the aflatoxigenic fungus *Aspergillus flavus*. *Proteomics* 13**,** 1513-1518.

64. Pechanova, O., Pechan, T., Williams, W.P., and Luthe, D.S. (2011). Proteomic analysis of the maize rachis: Potential roles of constitutive and induced proteins in resistance to *Aspergillus flavus* infection and aflatoxin accumulation. *Proteomics* 11**,** 114-127.

65. Reverberi, M., Punelli, M., Smith, C.A., Zjalic, S., Scarpari, M., Scala, V., Cardinali, G., Aspite, N., Pinzari, F., and Payne, G.A. (2012). How peroxisomes affect aflatoxin biosynthesis in *Aspergillus flavus*. *PloS one* 7**,** e48097.

66. Reverberi, M., Ricelli, A., Zjalic, S., Fabbri, A.A., and Fanelli, C. (2010). Natural functions of mycotoxins and control of their biosynthesis in fungi. *App. Microbiol. Biotech.* 87**,** 899-911.

67. Reverberi, M., Zjalic, S., Ricelli, A., Punelli, F., Camera, E., Fabbri, C., Picardo, M., Fanelli, C., and Fabbri, A.A. (2008). Modulation of antioxidant defense in *Aspergillus parasiticus* is involved in aflatoxin biosynthesis: a role for the *ApyapA* gene. *Eukaryotic Cell* 7**,** 988-1000.

68. Roze, L.V., Hong, S.-Y., and Linz, J.E. (2013). Aflatoxin biosynthesis: current frontiers. *Ann. Rev. Food Sci. Tech.* 4**,** 293-311.

69. Rushton, P.J., Somssich, I.E., Ringler, P., and Shen, Q.J. (2010). WRKY transcription factors. *Trends in Plant Sci.* 15**,** 247-258.

70. Shephard, G.S. (2008). Impact of mycotoxins on human health in developing countries. *Food additives & contaminants. Part A, Chemistry, analysis, control, exposure & risk assessment* 25**,** 146-151.

71. Smart, M.G., Wicklow, D.T., and Caldwell, R.W. (1990). Pathogenesis in *Aspergillus* ear rot of maize - light microscopy of fungal spread from wounds. *Phytopathology* 80**,** 1287-1294.

72. Trenk, H.L., and Hartman, P.A. (1970). Effects of moisture content and temperature on aflatoxin production in corn. *Appl. Microbiol.* 19**,** 781-784.

73. Walling, L.L. (2000). The myriad plant responses to herbivores. *J. Plant Growth Reg.* 19**,** 195-216.

74. Walsh, T.A., Morgan, A.E., and Hey, T.D. (1991). Characterization and molecular cloning of a proenzyme form of a ribosome-inactivating protein from maize: Novel mechanism of proenzyme activation by proteolytic removal of a 2.8 kilodalton internal peptide segment. *J. Biol. Chem.* 266**,** 23422-23427.

75. Willcox, M.C., Davis, G.L., Warburton, M.L., Windham, G.L., Abbas, H.K., Betrán, J., Holland, J.B., and Williams, W.P. (2013). Confirming quantitative trait loci for aflatoxin resistance from Mp313E in different genetic backgrounds. *Mol. Breeding* 32**,** 15-26.

76. Wogan, G.N. (1966). Chemical nature and biological effects of the aflatoxins. *Bacteriol. Rev.* 30**,** 460.

77. Xie, Y.-R., Chen, Z.-Y., Brown, R.L., and Bhatnagar, D. (2010). Expression and functional characterization of two pathogenesis-related protein 10 genes from *Zea mays*. *J. Plant Physiol.*167**,** 121-130.

78. Yu, J., Chang, P.-K., Ehrlich, K.C., Cary, J.W., Bhatnagar, D., Cleveland, T.E., Payne, G.A., Linz, J.E., Woloshuk, C.P., and Bennett, J.W. (2004). Clustered pathway genes in aflatoxin biosynthesis. *App. Environ. Microbiol.*70**,** 1253-1262.

79. Zavala, J.A., Nabity, P.D., and Delucia, E.H. (2013). An emerging understanding of mechanisms governing insect herbivory under elevated CO_2. *Ann. Rev. Entomol.* 58**,** 79-97.

80. Zuber, M., and Lillehoj, E. (1979). Status of the aflatoxin problem in corn. *J. Environ. Qual.* 8**,** 1-5.

CHAPTER 2

LITERATURE REVIEW PART II:

RESISTANCE TO *ASPERGILLUS FLAVUS* IN MAIZE AND PEANUT: MOLECULAR BIOLOGY, BREEDING, ENVIRONMENTAL STRESS, AND FUTURE PERSPECTIVES

Fountain, J. C., Khera, P., Yang, L., Nayak, S. N., Scully, B. T., Lee, R. D., Chen, Z.Y., Kemerait, R.C., Varshney, R.K., & Guo, B. (2015). Resistance to *Aspergillus flavus* in maize and peanut: Molecular biology, breeding, environmental stress, and future perspectives. *The Crop Journal* 3:229-237. doi.org/10.1016/j.cj.2015.02.003. Reprinted here with permission of the publisher.

Abstract

The colonization of maize (*Zea mays* L.) and peanut (*Arachis hypogaea* L.) by the fungal pathogen *Aspergillus flavus* results in the contamination of kernels with carcinogenic mycotoxins known as aflatoxins leading to economic losses and potential health threats to humans. The regulation of aflatoxin biosynthesis in various *Aspergillus spp.* has been extensively studied, and has been shown to be related to oxidative stress responses. Given that environmental stresses such as drought and heat stress result in the accumulation of reactive oxygen species (ROS) within host plant tissues, host-derived ROS may play an important role in cross-kingdom communication between host plants and *A. flavus*. Recent technological advances in plant breeding have provided the tools necessary to study and apply knowledge derived from metabolomic, proteomic, and transcriptomic studies in the context of productive breeding populations. Here, we review the current understanding of the potential roles of environmental stress, ROS, and aflatoxin in the interaction between *A. flavus* and its host plants, and the current status in molecular breeding and marker discovery for resistance to *A. flavus* colonization and aflatoxin contamination in maize and peanut. We will also propose future directions and a working model for continuing research efforts linking environmental stress tolerance and aflatoxin contamination resistance in maize and peanut.

Introduction

The colonization of maize and peanut by *Aspergillus flavus* and *A. parasiticus* (Link ex Fr.; Teleomorph: *Petromyces flavus* and *P. parasiticus*) [1, 2] results in the contamination of their derived agricultural products with aflatoxins [3]. Aflatoxins are among the most potent mycotoxins, carcinogenic and teratogenic compounds, produced during infection and growth of fungi *A. flavus* and *A. parasiticus* on crops such as maize, peanut, cottonseed and tree nuts. Maize and peanuts are the most susceptible crops to aflatoxin contamination and serve as the main source of aflatoxin contamination for humans [4]. Aflatoxins not only have been associated with numerous diseases and disorders in humans and livestock, but also have a negative economic impact due to loss of crop value [5-7]. Resistance to *A. flavus* colonization and subsequent aflatoxin production is a complex phenomenon involving numerous genetic, physiological, and morphological factors and acts as a quantitative trait [8-10].

Examining the functional composition of the resistance mechanisms in maize and, to a lesser extent, in peanut using transcriptomic, proteomic, and metabolomic approaches have led to the elucidation of the roles of several specific genes, proteins, and signal molecules including pathogenesis-related proteins (PR-10, PR-10.1, 14-kDa trypsin inhibitor, chitinase, zeamatin, B1,3-glucanase, etc.), stress-responsive proteins (catalase, superoxide dismutase, glyoxalase I, glutathione-s-transferase, etc.), and reactive oxygen species (ROS) in regulating *A. flavus* resistance as well as their potential roles in cross-kingdom communication between host plants and *Aspergillus spp.* [11-20]. In addition, the link that exists between aflatoxin contamination and environmental stress, particularly drought stress, has also been a focal point of molecular research and applied breeding programs in recent years [5, 21-25]. Hence, the use of drought

tolerant germplasm with aflatoxin resistance has gained momentum for selection various genetic studies [21, 26].

Despite considerable advances in molecular research, a complete understanding of the details of the host-parasite interaction between *A. flavus* and its hosts including maize and peanut, namely the precise signaling mechanisms employed in this interaction, remains elusive and there is a need for continuing investigation. Therefore, in this review we focus on recent findings related to the biochemistry of defense regulation with regard to environmental stress, ROS, and inter-cellular communication between *A. flavus* and its host crops. In addition, recent advances in conventional and molecular breeding for aflatoxin resistance in maize and peanut, and the potential utilization of molecular markers for use in marker assisted selection (MAS) in breeding programs are highlighted.

Molecular biology of potential host-*A. flavus* interactions mediated by ROS

The molecular and biochemical bases of the interaction between the host crops and *A. flavus* has been the subject of numerous studies in recent years for identifying both the sources of resistance to *A. flavus* colonization, and the regulation of aflatoxin biosynthesis in *A. flavus* and other Aspergilli including *A. fumigatus* and *A. parasiticus*. Integration of the findings of these studies into a coherent model for explaining the subtleties of the interaction is lacking in the literature. In addition, the functional roles of the components/genes thought to be involved in the host-pathogen interactions were not well characterized. Hence, the potential components of the interaction and their implications for future research efforts are discussed.

Pathogen recognition and upstream resistance gene expression regulation

The plant-pathogen recognition is the first step in the interaction which causes rapid activation of appropriate defensive and infective mechanisms in the plant and the pathogen, respectively. Using maize as an example, the recognition of *A. flavus* by maize cells in contact with the pathogen and the subsequent transcriptional activation of the upstream defense signaling system constitute the first line of defense and response to infection. But the precise upstream recognition mechanisms employed by maize or peanut against *A. flavus* are not currently known. However, recent studies on WRKY transcription factors in maize [27] and model species such as *Arabidopsis thaliana* [28] may provide insight into this aspect of defense initiation.

WRKY transcription factors, which possess a rarely variable amino acid sequence of 'WRKY' at the amino terminus of their DNA binding domain, function in the upstream regulation of various cellular processes in plants and other organisms, including pathogen defense response coordination [28]. It has been demonstrated that two WRKY transcription factor-encoding genes, *ZmWRKY19* and *53*, were significantly up-regulated by *A. flavus* inoculation in the resistant maize line TZAR101, and may play an important role in regulating upstream defense responses in developing maize kernels in response to *A. flavus* inoculation [27]. The ortholog of *Zm*WRKY19 in *Arabiodpsis*, *At*WRKY53, in contrast, functions in oxidative stress responses by promoting the expression of catalase and other antioxidant genes, and has been shown to interact with calmodulins [29-30]. *Zm*WRKY53 has been shown to enhance abiotic stress tolerance, including drought and salt stress [31]. Similarly, the WRKY genes were found to be associated with conferring tolerance to salinity in interspecific derivatives of peanut [32]. The ortholog of *Zm*WRKY53 in *Arabidopsis*, *At*WRKY33, has also been demonstrated to function in necrotrophic pathogen defense responses and thermotolerance

while its orthologs in wheat (*Ta*WRKY53) and rice (*Os*WRKY53) have been shown to function in regulating chitinase and peroxidase gene expression [33].

Interestingly, the *Arabidopsis* orthologs of these WRKY transcription factors have been shown to be directly regulated by mitogen activated protein kinases (MAPK) pathways including MEKK1 and MPK3/6 in response to chitin perception by receptor kinases as a part of a pathogen associated molecular pattern (PAMP)-triggered immunity (PTI) mechanism [28-29, 34-37]. This prospect of chitin perception as a trigger for PTI seems plausible given that previous research has demonstrated that resistant maize lines accumulate chitinase which may provide a source for chitin monomers that can be percieved by receptor kinases [17]. Also, given the high level of expression of these orthologous WRKY genes in resistant maize, it is possible that such a signal transduction and receptor system may be present in maize and functional in the maize-*A. flavus* interaction [27]. In addition, appropriate studies need to be carried out in peanut to determine the role of WRKY genes in inititation of plant defence mechanism. Furthermore, the expression of the WRKY transcription factors in response to *A. flavus* inoculation might result in increased expression of antioxidant and pathogenesis-related genes in resistant maize lines providing enhanced oxidative stress tolerance and pathogen resistance (Figure 2.1A) [5, 27].

Calcium signaling and reactive oxygen species (ROS) in defense regulation

In addition to MAPK signaling to promote the expression of defense-related genes, calcium signaling and reactive oxygen species (ROS) play a role in regulating defense responses. Recently, Ma and Berkowitz [38] reviewed the Ca^{2+}-calmodulin signaling and its role in regulating defense activation and hypersensitive cell death. Briefly, as a part of PTI responses, receptor kinase-bound nucleotidyl cyclases activate cyclic nucleotide gated ion channels

(CNGCs) through cAMP or cGMP signal intermediates. This results in the influx of Ca^{2+} ions into the plant cell cytosol and the activation of calmodulins and calcium dependent protein kinases (CDPKs). These CDPKs then, in turn, activate the transmembrane protein complex NADPH oxidase which converts molecular O_2 to a superoxide anion (O_2^-). The superoxide anion is then detoxified by superoxide dismutase (SOD) to form H_2O_2 whose neutral charge allows it to pass through the plasma membrane and function in cytosolic defense signaling. In maize, Jiang and Zhang [39] demonstrated a similar mechanism functional in oxidative stress responses. Another study by Hu et al. [40] further demonstrated an interaction between Ca^{2+}/calmodulin signaling components and abscisic acid (ABA)-based ROS defense responses.

The presence of calcium/calmodulin signaling system in maize is interesting because of the role of calmodulin in the regulation of *At*WRKY53, the ortholog of *ZmWRKY19*, in order to stimulate antioxidant gene expression [29-30]. Also, free mobility of H_2O_2 across cell membranes and its role as a source of oxidative stress, as H_2O_2 as a mobile signaling molecule, involves in cross-kingdom communication between maize and *A. flavus* or other invading pathogens (Figure 2.1B). The role of cytosolic levels of Ca^{2+} ions in stimulating these responses may also be relevant to the interaction between maize resistance to *A. flavus* and drought stress since cytosolic levels of Ca^{2+} would be proportionally higher due to water loss under drought stress conditions that activate the associated signaling mechanisms. However, detailed studies are needed to validate the role of Ca^{2+} signaling in regulating resistance to *A. flavus* in maize and other crop species.

Potential role of ROS in aflatoxin biosynthesis and stress responsive gene regulation

As the defense signaling-derived ROS are generated extracellularly, it may stimulate the production of aflatoxin by *Aspergillus spp.* potentially as a part of an antioxidative defense mechanism [5]. A recent study by Roze et al. [41] demonstrated that aflatoxin biosynthesis and stress response are potentially linked in *A. parasiticus* by a transcription factor complex with the basic leucine zipper (bZIP) transcription factors AtfB and AP-1, in response to available carbohydrate or oxidative stress through a cAMP signaling mechanism. The protein complex directly promotes the expression of genes pertaining to secondary metabolism, particularly in aflatoxin biosynthesis. This study postulates that the protein complex or its components stimulate the expression of antioxidant defense genes and the promoters of the antioxidant genes are bound by bZIP transcription factors (Figure 2.1C). In addition, ROS cross-talk between the host plant cell and *Aspergillus spp*. may also result in the formation of oxylipins which have been shown to regulate the reproductive development of Aspergilli as well as aflatoxin production [5, 42-44] (Figure 2.1D,E).

Aflatoxin metabolism and potential effects on plant cell physiology

The connection between ROS-derived oxidative stress and aflatoxin production seems to indicate the antioxidant property of aflatoxin that may favor growth and function of *A. flavus* or other Aspergilli and would, therefore, be advantageous for fungal survivability. However, it is possible that the opposite is true, and this link may be useful to remediate oxidative stress caused by aflatoxin reacting with fungal cellular components. This seems plausible given two considerations.

First, the final stages of aflatoxin biosynthesis are confined to specialized, membrane-bound organelles termed aflatoxisomes [45-48]. This compartmentalization of aflatoxin biosynthesis followed by direct exocytosis lends itself to the possibility that mature aflatoxin compounds may be cytotoxic (Figure 2.1D). However, further experimentation will be required in order to examine the precise aflatoxin detoxification and damage remediation mechanisms employed by *Aspergillus spp*.

Second, aflatoxin may be metabolized by fungal or plant cells into toxic byproducts. Studies of the metabolism of aflatoxin B_1 (AFB_1) by human hepatocytes have revealed that cytochrome p450 monooxygenases are capable of oxidizing AFB_1, resulting in the bioactivation of the toxin [49]. Specifically, cytochrome p450-3A4 converts AFB_1 into an epoxidized form, AFB_1-exo-8,9-epoxide, which readily reacts with DNA structures resulting in mutation and oxidative damage to various macromolecules [50]. Conversely, cytochrome p450-1A2 converts AFB_1 into AFB_1-endo-8,9-epoxide which is non-reactive and rapidly detoxified [50]. Since p450 monooxygenases are universally abundant in eukaryotic organisms, including maize [51], it is possible that aflatoxin is metabolized in a similar fashion in maize or peanut, resulting in oxidative damage to cellular components potentially leading to localized cell death (Figure 2.1E). However, for such a reaction to occur, the ability of aflatoxin to be absorbed by plant cells and its subsequent metabolism remain fundamental issues to be addressed in future research endeavors.

If indeed aflatoxin causes oxidative damage to cellular components of both the pathogen and the host, a question quickly arises. What is the advantage provided by the biosynthesis of aflatoxin? It has been hypothesized in the literature that *A. flavus* functions as a facultative necrotroph during infection of maize kernel tissues [5, 52]. Aflatoxin could enhance

pathogenicity by causing localized death of host cells surrounding the invading mycelia of the fungus, while *A. flavus* is afforded protection by the co-expression of high levels of stress responsive genes [41]. In either case, detailed study of molecular mechanisms involved in aflatoxin biosynthesis in maize and peanut are needed to confirm these hypotheses.

Breeding for aflatoxin resistance in maize: Biomarkers, quantitative trait loci (QTL) discovery, and applications in conventional programs

Biomarkers

The preceding discussion on the biochemistry of the interaction between maize and *A. flavus* presents both challenges and opportunities for continuing research, particularly while considering their potential applications. It has been established that there exists a correlation between the drought tolerance of maize lines and their relative resistance to aflatoxin contamination under hot and dry conditions [5, 26]. These conditions are also known to result in the accumulation of ROS in plant tissues, and, given that recent reports demonstrate that ROS can regulate aflatoxin production in *Aspergillus spp.*, this provides a potential link existing between aflatoxin production and host-derived oxidative stress [19, 25, 41, 53]. Therefore, if host derived oxidative stress in response to abiotic stress can possibly exacerbate aflatoxin production, the selection of components involved in antioxidant mechanism such as metabolites, proteins, and gene expression levels may allow them to be utilized as molecular markers, "biomarkers," for use in selection in breeding applications.

For instance, Pechanova et al. [18] reported that resistant maize lines accumulate high levels of superoxide dismutase, peroxidases, chaperonins, etc. in rachis tissues. Such highly expressed proteins could be utilized for screening germplasm and populations for markers related

to both aflatoxin resistance, as well as abiotic stress tolerance. Fountain et al. [54] reported on the expression of the gene encoding the 14-kDa trypsin inhibitor, which is known to inhibit fungal amylases, was highly expressed in kernel tissues of resistant maize lines compared to susceptible lines when infected by *A. flavus* under drought stress conditions. In addition, detoxifying enzymes such as glutathione-S-transferase (GST) and pathogenesis-related proteins such as PR-10 can also be used to screen for pathogen resistance or abiotic stress tolerance based on their respective biological activities [15, 55-56]. Genomic and proteomic expression studies during the infection process have indicated that oxidative stress tolerance is vital to adaptive changes in fungal biology during infection [57]. Additional studies have also shown that maize lines with known resistance to drought and aflatoxin contamination are more recalcitrant to oxidative stress due to more stably expressed antioxidant components than susceptible lines [25]. Therefore, these oxidative stress tolerance mechanisms may serve as sources for selectable markers for use in breeding applications for aflatoxin contamination resistance and drought tolerance. By combining these and additional "biomarkers" in conjunction with traditional genetic markers such as insertion/deletions (indels), single nucleotide polymorphisms (SNPs), or simple sequence repeat/microsatellite (SSR) markers, the efficiency of selection for resistant germplasm will be enhanced. In addition, by selecting for "biomarkers" which afford both abiotic stress tolerance and aflatoxin resistance, some of the confounding effects of genotype × environment interactions may be avoided. Future studies should examine the utilization and feasibility of potential multi-purpose "biomarkers" for use in large scale marker assisted selection (MAS) applications.

QTL discovery

As previously stated, resistance to *A. flavus* colonization and aflatoxin contamination has been demonstrated to be quantitative in nature and is heavily influenced by environmental interactions [5, 9, 58]. Therefore, recent breeding studies focused on the discovery and characterization of quantitative trait loci (QTL) for aflatoxin resistance have been forced to consider the environment in obtaining phenotypic data, and have faced numerous challenges in identifying consistent QTL for aflatoxin resistance.

For example, Wilcox et al. [59] utilized a F_2 mapping population derived from Mp313E × Va35 (resistant x susceptible) to identify 20 QTLs with combined phenotypic variance explained (PVE) of 22 – 43%. However, when the mapping populations were grown in multiple environments, only 11 QTLs were found to be consistent with a combined PVE of 2.4 – 9.5%. An earlier study by Brooks et al. [60] also examined a population derived from Mp313E for the presence of QTL for aflatoxin resistance. A collection of 210 $F_{2:3}$ families derived from Mp313E × B73 (resistant x susceptible) was utilized for the study and a total of 85 polymorphic SSR markers for genotyping and map construction. By analyzing phenotypic data from three locations, they were able to identify two consistent QTLs, one with PVE of 7 – 18%, and a second with PVE of 8 – 18%, indicating a nominal degree of variation between the environments. In another study, a single consistent QTL (PVE 8.42%) was identified using a recombinant inbred line (RIL) population of 228 $F_{8:9}$ RILs derived from RA × M53 (resistant x susceptible) utilizing 916 SNP markers for linkage map construction, and phenotyping data was obtained from two locations with contrasting environments for phenotypic analysis [61].

These studies demonstrate that resistance to *A. flavus* is not derived from a single gene and is highly quantitative in nature. In addition, given the relatively low level of PVE provided

by each QTL, it is likely that many QTL with low PVE (< 10%) contribute to aflatoxin resistance and may be indicative of the polygenic nature of resistance and the involvement of multiple physiological and morphological traits in the overall resistance phenotype [5, 62]. Interestingly, similar difficulties are also faced when examining drought tolerance QTL in maize. For example, Almeida et al. [63] recently performed QTL analysis for drought tolerance in three populations: a RIL population derived from CML444 × MALAWI, a $F_{2:3}$ family set derived from CML440 × CML504, and a second $F_{2:3}$ family set derived from CML444 × CML441. They identified QTLs for grain yield under drought stress with PVE ranging from 2.6 – 17.8%, and for anthesis-silking interval under drought stress with PVE ranging from 1.7 – 17.8%. Genome wide association studies (GWAS), which rely on ancient recombination among diverse inbred for mapping QTL, are limited in their detection of QTL with low PVE, and may prevent the identification of aflatoxin resistance and drought tolerance QTL unless high numbers of individuals and markers are used to increase the power of the experiment [62, 64].

Once identified, QTL function and composition must be determined in order to elucidate the mechanism being employed to produce a particular phenotype, namely aflatoxin resistance. In conjunction with QTL discovery in traditional bi-parental populations, the integration of functional genomics technologies has been shown to enhance QTL validation by confirming the expression and identity of genes present in the QTL region. A recent study by Kelley et al. [9] utilized microarray to validate the expression of QTL associated genes involved in *A. flavus* resistance and/or susceptibility in the maize lines Mp313E and Va35. As this study illustrates, coupling functional genomics analysis with QTL discovery also allows the determination of the mechanism employed by maize in response to *A. flavus* infection by determining not only which genes within the QTL regions are regulated, but also whether they are up or down-regulated and

the amount of regulation. Coupling the expression and QTL studies with functional genetics, experiments conducted to determine the function of specific genes, such as pathogenesis-related defense genes through methods such as RNA interference-(RNAi) based gene silencing [14]. These studies will provide for the identification of the causal basis for a gene contribution to a QTL PVE and provide possible explanations for the influence of the environment on the detection and stability of the QTL.

Applications of biomarkers and QTL in conventional breeding programs

Conventional breeding for resistance has formed the basis of generating aflatoxin contamination resistant maize lines with recent efforts in this field resulting in the release of several lines with promising levels of aflatoxin contamination resistance [23, 65-67]. As recently reviewed by Williams et al. [68], several aflatoxin resistant lines including GT601, GT602, GT603, Mp715, Mp717, Mp718, and Mp719 have been derived from conventional breeding programs in the southeastern U.S. In addition, the incorporation of exotic lines with aflatoxin accumulation resistance and additional desirable traits into breeding programs to widen the genetic base of traditional temperate lines through cooperative efforts such as the Germplasm Enhancement of Maize (GEM) project will allow for further enhancement of previously identified resistant lines [68]. In addition to variety development, recent research has also focused on the evaluating the general and specific combining ability of aflatoxin resistant lines to enhance hybrid development. For example, Williams et al. [69] performed a diallel cross using ten inbred lines with varying levels of resistance to aflatoxin contamination including: CI66, GA209, NC408, Mo18W, Mp313E, Mp494, Mp715, Mp717, SC212m, and T173. They found that the resistant lines Mp313E, Mp494, Mp715, Mp717, Mo18W, and NC408 possessed significant general

combining ability (GCA) effects for resistance to aflatoxin and propose that utilizing GCA to plan crosses in resistance breeding will expedite progress in developing aflatoxin resistant hybrids.

This diallel study illustrates the potential utility of additional selection methodologies in enhancing aflatoxin resistance in maize. Currently, screening for aflatoxin resistance is carried out either in the field with direct inoculation which can produce variable results depending on environmental conditions and the method used, or in the laboratory with kernel screening assays (KSAs) for high throughput screening [70]. Given the potential for variability in these systems, the incorporation of molecular markers into breeding programs for use in MAS could provide for more consistent results. However, while many QTLs and associated polymorphic markers have been discovered in maize for resistance to aflatoxin contamination and *A. flavus* colonization, their utility in conventional breeding programs has been limited. This is likely due to the variable nature of the expression of these QTLs across multiple environments and conditions. Therefore, biomarkers selected based on their role in both aflatoxin resistance and abiotic stress responses may provide a method to account for environmental influences on aflatoxin resistance. When used in conjunction with traditional DNA-based marker systems and conventional resistance breeding, biomarkers may prove to valuable tools in the breeder's arsenal to enhance aflatoxin resistance and associated traits such as drought tolerance into novel germplasm.

Correlating environmental stress and aflatoxin resistance in peanut

Peanut (*Arachis hypogaea* L.) is an allotetraploid ($2n = 4x = 40$) crop grown in over 100 countries around the world. One of the major concerns about the import/export of peanut is aflatoxin contamination (AC) which may result in the rejection of seed lots if levels of aflatoxin

are above maximum permissible limits [71]. AC in peanut is caused by two fungal pathogens, *Aspergillus flavus* and *A. parasiticus* with *A. flavus* being the most prevalent in infected pods. A typical pattern of fungal infection includes the entry of the fungi through small cracks developed during process of pod maturation/drying in the ground resulting in colonization of the pod [72].

It has been demonstrated that pre-harvest aflatoxin contamination (PAC) is increased when abiotic stress such as drought stress is imposed on the crop. This may be due to reduced water activity during pod development which could lead to the creation of cracks in the pod wall. Hence, damaged pods tend to be more susceptible to PAC than undamaged pods [73-74]. Other studies point out that reduced kernel water content may decrease phytoalexin production thereby decreasing the plant's natural defense against infection leading to increased AC [75-76]. In addition to drought stress, heat stress has also been found to play an important role in PAC [75, 77]. Apart from genetic sources of resistance in peanut, PAC management practices such as proper irrigation, application of chemical fungicides, avoiding mechanical damage, biological control, crop rotation, harvest timing, and proper post-harvest storage conditions play critical roles in limiting AC in peanut [24, 58].

Drought stress seems to function as a predisposing factor for PAC in peanut [78-79]. Therefore, a common idea arises that developing drought tolerant cultivars would assist in alleviating PAC, indicating a direct or indirect selection for PAC through drought tolerance. In order to understand the molecular mechanisms of aflatoxin biosynthesis, some genomic and proteomic studies have been carried out [80-83]. A positive correlation was found between 20 drought tolerant lines and PAC resistance [84]. Further, the measures of several drought tolerance component traits such as SPAD (SPAD-502 meter: Minolta, Tokyo, Japan) chlorophyll meter reading (SCMR), and specific leaf area (SLA) were also found to show a positive

correlation with PAC resistance [73]. Conversely, the results of a recent study have pointed out that although drought tolerance increases PAC resistance in several lines, this is not universally true for all peanut genetic backgrounds. Hence, drought tolerance and resistance to PAC may possess different resistance mechanisms in peanut [85].

The lack of high levels of resistance for aflatoxin contamination in cultivated germplasm and a reliable phenotyping protocol, poses challenges in using conventional breeding methods to identify resistance to PAC in peanuts. Nevertheless, large scale screening efforts consisting of 831 accessions in the US peanut core collection has led to the identification of 19 accessions with low PAC and relatively high yield [86]. At the International Crops Research Institute for the Semi-Arid Tropics (ICRISAT) several resistant sources were identified for three types of resistance (i.e. PAC, resistance to *in vitro* seed colonization (IVSC) and aflatoxin production by *A. flavus*) after extensive screening of more than 2000 peanut accessions in a heavily inoculated field plot ("sick plot") for *A. flavus* seed infection under imposed drought [87].

Use of molecular markers for PAC resistance is very limited. For instance, a set of 6 amplified fragment length polymorphism (AFLP) markers with low PVE in *A. cardenasii* derived lines were identified [88] and in another study six QTLs for resistance to *A. flavus* infection with PVE up to 22.7% were identified [89]. Since resistance to PAC is a global problem, an international effort was recently undertaken under the ambit of the Peanut & Mycotoxin Innovation Lab (PMIL) and has been initiated with collaboration between ICRISAT, the University of Georgia (UGA), and Institut Sénégalais de Recherches Agricoles (ISRA). This effort utilizes RIL populations, association mapping panels, multiparent advanced generation intercross (MAGIC) populations, interspecific introgression lines, and genomic selection approaches in order to enhance our understanding of the genetic components of PAC.

In summary, resistance to PAC in peanut is a complex trait which possesses a high G × E interaction, low heritability, and a lack of reliable phenotyping protocols. These limitations pose challenges in identifying and developing genetic resistance. Unfortunately, there is no single, high PVE source of resistance which can be used to tackle this issue from a genetic perspective. Therefore, crop management in conjunction with enhancing genetic resistance should be the way forward for imparting PAC resistance in peanut.

Conclusions and future perspectives

Resistance to *A. flavus* infection and aflatoxin contamination in maize and peanut is a complex trait that is heavily influenced by environmental factors. Current efforts in determining the biochemical basis for this link as well as its potential utilization in breeding programs for the development of resistance germplasm has led to a greater understanding of elements of this plant-pathogen interaction. However, many questions remain to be answered as to the role of aflatoxin in the biology and ecology of *Aspergillus* fungi as well as its role in pathogenesis including the role of aflatoxin as a source of cellular oxidative stress. In addition, the potential role of host-derived ROS in stimulating aflatoxin production is also in need of further experimental examination. Future experiments should also address the potential use of identified proteins, metabolites, and candidate genes as selectable biomarkers for use in MAS. By utilizing such markers, breeding programs can be optimized to select not only for aflatoxin resistance but also for associated abiotic stress tolerance in an efficient manner.

Acknowledgements

This work is partially supported by the U.S. Department of Agriculture Agricultural Research Service (USDA-ARS), the Georgia Agricultural Commodity Commission for Corn, the Georgia Peanut Commission, Peanut Foundation and AMCOE (Aflatoxin Mitigation Center of Excellence). This work has been undertaken as part of the CGIAR Research Program on Grain Legumes. ICRISAT is a member of CGIAR Consortium. Mention of trade names or commercial products in this publication is solely for the purpose of providing specific information and does not imply recommendation or endorsement by the USDA. The USDA is an equal opportunity provider and employer.

References

1. B.W. Horn, G.G. Moore, I. Carbone, Sexual reproduction in *Aspergillus flavus*, *Mycologia* 101 (2009a) 423–429.
2. B.W. Horn, J.H. Ramirez-Prado, I. Carbone, The sexual state of *Aspergillus parasiticus*, *Mycologia* 101 (2009b) 275–280.
3. U.L. Diener, R.J. Cole, T.H. Sanders, G.A. Payne, S. Lee, M.A. Klich, Epidemiology of aflatoxin formation by *Aspergillus flavus*, Annu. Rev. Phytopathol. 25 (1987) 249-270.
4. F. Wu, P. Khlangwiset, Health economic impacts and cost-effectiveness of aflatoxin reduction strategies in Africa: Case studies in biocontrol and postharvest interventions, Food Addit. Contam. A, 27 (2010) 496-509.
5. J.C. Fountain, B.T. Scully, X. Ni, R.C. Kemerait, R.D. Lee, Z.Y. Chen, B.Z. Guo, Environmental influences on maize-*Aspergillus flavus* interactions and aflatoxin production, Front. Microbiol. 5 (2014) 1-7.

6. G.S. Shephard, Impact of mycotoxins on human health in developing countries. Food Addit. Contam. A, 25 (2008) 146–151.
7. C.P. Wild, Y.Y. Gong, Mycotoxins and human disease: a largely ignored global health issue. Carcinogenesis 31 (2010) 71-82.
8. S. Amaike, N.P. Keller, *Aspergillus flavus*, Annu. Rev. Phytopathol. 49 (2011) 107-133.
9. R.Y. Kelley, W.P. Williams, J.E. Mylroie, D.L. Boykin, J.W. Harper, G.L. Windham, A. Ankala, X. Shan, Identification of maize genes associated with host plant resistance or susceptibility to *Aspergillus flavus* infection and aflatoxin accumulation, PLoS One 7 (2012) 5.
10. X. Liang, M. Luo, B.Z. Guo, Resistance Mechanisms to *Aspergillus falvus* infection and aflatoxin contamination in peanut (*Arachis hypogaea*). Plant Pathol. J. 5 (2006) 115-124.
11. P. Chadha, R.H. Das, A pathogenesis related protein, AhPR10 from peanut: an insight of its mode of antifungal activity. Planta 225 (2006) 213–222.
12. Z.Y. Chen, R.L. Brown, K.E. Damann, T.E. Cleveland, Identification of a maize kernel stress-related protein and its effect on aflatoxin accumulation, Phytopathology 94 (2004) 938-945.
13. Z.Y. Chen, R.L. Brown, A.R. Lax, B.Z. Guo, T.E. Cleveland, J.S. Russin, Resistance to *Aspergillus flavus* in corn kernels is associated with a 14-kDa protein, Phytopathology 88 (1998) 276-281.
14. Z.Y. Chen, R.L. Brown, A. Menkir, T.E. Cleveland, Identification of resistance-associated proteins in closely-related maize lines varying in aflatoxin accumulation, Mol. Breed. 30 (2012) 53-68.

15. Z.Y. Chen, R.L. Brown, K. Rajasekaran, K.E. Damann, T.E. Cleveland, Identification of a maize kernel pathogenesis-related protein and evidence for its involvement in resistance to *Aspergillus flavus* infection and aflatoxin production, Phytopathology 96 (2006) 87-95.
16. Z.Y. Chen, Brown, R. L., Russin, J. S., Lax, A. R., and Cleveland, T. E., A corn trypsin inhibitor with antifungal activity inhibits *Aspergillus flavus* α-amylase. Phytopathology 89 (1999) 902-907.
17. K.G. Moore, M.S. Price, R.S. Boston, A.K. Weissinger, G.A. Payne, A chitinase from Tex6 maize kernels inhibits growth of *Aspergillus flavus*. Phytopathology 94 (2004) 82-87.
18. O. Pechanova, T. Pechan, W.P. Williams, D.S. Luthe, Proteomic analysis of the maize rachis: potential roles of constitutive and induced proteins in resistance to *Aspergillus flavus* infection and aflatoxin accumulation, Proteomics 11 (2011) 114-127.
19. L.V. Roze, S.Y. Hong, J.E. Linz, Aflatoxin biosynthesis: current frontiers, Ann. Rev. Food Sci. Tech. 4 (2013) 293-311.
20. T. Wang, X-P. Chen, H-F. Li, H-Y. Liu, Y-B. Hong, Q-L. Yang, X-Y. Chi, Z. Yang, S-L. Yu, L. Li, X-Q. Liang, Transcriptome identification of the resistance-associated genes (RAGs) to *Aspergillus flavus* infection in pre-harvested peanut (*Arachis hypogaea*). Funct. Plant Biol. 40 (2013) 292–303.
21. B.Z. Guo, Z.Y. Chen, R.D. Lee, B.T. Scully, Drought stress and preharvest aflatoxin contamination in agricultural commodity: Genetics, genomics and proteomics, J. Int. Plant Biol. 50 (2008) 1281-1291.
22. T. Jiang, J. Fountain, G. Davis, R. Kemerait, B. Scully, R.D. Lee, B. Guo, Root morphology and gene expression analysis in response to drought stress in maize (*Zea mays*), Plant Mol. Biol. Rep. 30 (2012) 360-369.

23. B.T. Scully, M.D. Krakowsky, X. Ni, J.P. Wilson, R.D. Lee, B.Z. Guo, Preharvest aflatoxin contamination of corn and other grain crops grown on the U.S. Southeastern Coastal Plain, Toxin Rev. 28 (2009) 169-179.

24. A.M. Torres, G.G. Barros, S.A. Palacios, S.N. Chulze, P. Battilani, Review on pre- and post-harvest management of peanuts to minimize aflatoxin contamination. Food Research International 62 (2014) 11–19.

25. L. Yang, J.C. Fountain, T. Jiang, B.T. Scully, R.D. Lee, R.C. Kemerait, S. Chen, B. Guo, Protein profiles reveal diverse drought-responsive signaling pathways in maize kernels, Int. J. Mol. Sci. 15 (2014) 18892-18918.

26. B.Z. Guo, J. Yu, X. Ni, R.D. Lee, R.C. Kemerait, B.T. Scully, Crop stress and aflatoxin contamination: perspectives and prevention strategies. In: B. Venkateswarlu, A.K. Shankerk, C. Shanker, M. Makeswari, editors. Crop Stress and its Management: Perspectives and Strategies, NY: Springer (2012a) p. 399-427.

27. J.C. Fountain, Y. Raruang, M. Luo, R.L. Brown, B.Z. Guo, Z.Y. Chen, Potential roles of WRKY transcription factors in regulating host defense responses during *Aspergillus flavus* infection of immature maize kernels, Physiol. Mol. Plant Pathol. 89 (2015) 31-40.

28. P.J. Rushton, I.E. Somssich, P. Ringler, Q.J. Shen, WRKY transcription factors, Trend. Plant Sci. 15 (2010) 247-258.

29. Y. Miao, T. Laun, P. Zimmermann, U. Zentgraf, Targets of the WRKY53 transcription factor and its role during leaf senescence in *Arabidopsis*, Plant Mol. Biol. 55 (2004) 853-867.

30. S.C. Popescu, G.V. Popescu, S. Bachan, Z. Zhang, M. Seay, M. Gerstein, M. Snyder, S.P Dinesh-Kumar, Differential binding of calmodulin-related proteins to their targets revealed through high-density *Arabidopsis* protein microarrays, Proc. Natl. Acad. Sci. 104 (2007) 4730-4735.

31. H. Li, Y. Gao, H. Xu, Y. Dai, D. Deng, J. Chen, *Zm*WRKY33, a WRKY maize transcription factor conferring enhanced salt stress tolerances in *Arabidopsis*, Plant Growth Regul. 70 (2013) 207-216.

32. S.K. Bera, B.C. Ajay, A.L. Singh, *WRKY* and Na+/H+ antiporter genes conferring tolerance to salinity in interspecific derivatives of peanut (*Arachis hypogaea* L.). Austral. J. Crop Sci. 7 (2013) 1173-1180.

33. S.S. Gill, N. Tuteja, Reactive oxygen species and antioxidant machinery in abiotic stress tolerance in crop plants, Plant Physiol. Biochem. 48 (2010) 909-930.

34. T. Eulgem, I.E. Somssich, Networks of WRKY transcription factors in defense signaling, Curr. Opin. Plant Biol. 10 (2007) 366-371.

35. Y. Miao, T.M. Laun, A. Smykowski, U. Zentgraf, Arabidopsis MEKK1 can take a short cut: it can directly interact with senescence-related WRKY53 transcription factor on the protein level and can bind to its promoter, Plant Mol. Biol. 65 (2007) 63-76.

36. J. Wan, S. Zhang, G. Stacey, Activation of a mitogen-activated protein kinase pathway in *Arabidopsis* by chitin, Mol. Plant Pathol. 5 (2004) 125-135.

37. B. Zhang, K. Ramonell, S. Somerville, G. Stacey, Characterization of early, chitin-induced gene expression in *Arabidopsis*, Mol. Plant-Microbe Interact. 15 (2002) 963-970.

38. W. Ma, G.A. Berkowitz, Ca^{2+} conduction by plant cyclic nucleotide gated channels and associated signaling components in pathogen defense signal transduction cascades, New Phytol. 190 (2011) 566-572.

39. M. Jiang, J. Zhang, Cross-talk between calcium and reactive oxygen species originated from NADPH oxidase in abscisic acid-induced antioxidant defence in leaves of maize seedlings, Plant Cell Environ. 26 (2003) 929-939.

40. X. Hu, M. Jiang, J. Zhang, A. Zhang, F. Lin, M. Tan, Calcium–calmodulin is required for abscisic acid-induced antioxidant defense and functions both upstream and downstream of H_2O_2 production in leaves of maize (*Zea mays*) plants, New Phytol. 173 (2007) 27-38.

41. L.V. Roze, A. Chanda, J. Wee, D. Awad, J.E. Linz, Stress-related transcription factor AtfB integrates secondary metabolism with oxidative stress response in aspergilla, J. Biol. Chem. 286 (2011a) 35137-35148.

42. K.J. Affeldt, M. Brodhagen, N.P. Keller, *Aspergillus* oxylipin signaling and quorum sensing pathways depend on G protein-coupled receptors, Toxins, 4 (2012) 695-717.

43. X. Gao, M.V. Kolomiets, Host-derived lipids and oxylipins are crucial signals in modulating mycotoxin production by fungi, Toxin Rev. 28 (2009) 79-88.

44. C.M. Grice, M. Bertuzzi, E.M. Bignell, Receptor-mediated signaling in *Aspergillus fumigatus*, Front. Microbiol. 4 (2013) 26.

45. A. Chanda, L.V. Roze, S. Kang, K.A. Artymovich, G.R. Hicks, N.V. Raikhel, A.M. Calvo, J.E. Linz, A key role for vesicles in fungal secondary metabolism, Proc. Natl. Acad. Sci. 106 (2009) 19533-19538.

46. A. Chanda, L.V. Roze, J.E. Linz, Aflatoxin export in *Aspergillus parasiticus*: a possible role for exocytosis. Eukaryot. Cell. 9 (2010) 1724-1727.

47. J.E. Linz, A. Chanda, S.Y. Hong, D.A. Whitten, C. Wilkerson, L.V. Roze, Proteomic and biochemical evidence support a role for transport vesicles and endosomes in stress response and secondary metabolism in *Aspergillus parasiticus*, J. Proteome Res. 11 (2011) 767-775.

48. L.V. Roze, A. Chanda, J.E. Linz, Compartmentalization and molecular traffic in secondary metabolism: a new understanding of established cellular processes, Fungal Genet. Bio. 48 (2011b) 35-48.

49. L.L. Bedard, T.E. Massey, Aflatoxin B_1-induced DNA damage and its repair. Cancer Letters, 241 (2006) 174-183.

50. F.P. Guengerich, W.W. Johnson, T. Shimada, Y.F. Ueng, H. Yamazaki, S. Langouët, Activation and detoxication of aflatoxin B1, Mutat. Res. 402 (1998) 121-128.

51. N. Jameson, N. Georgelis, E. Fouladbash, S. Martens, L.C. Hannah, S. Lal, Helitron mediated amplification of cytochrome P450 monooxygenase gene in maize, Plant Mol. Bio. 67 (2008) 295-304.

52. S.X. Mideros, G.L. Windham, W.P. Williams, R.J. Nelson, *Aspergillus flavus* biomass in maize estimated by quantitative real-time polymerase chain reaction is strongly correlated with aflatoxin concentration, 93 (2009) 1163-1170.

53. M. Farooq, A. Wahid, N. Kobayashi, D. Fujita, S.M.A. Basra, Plant drought: effects, mechanisms, and management. Agron. Sustain. Dev. 29 (2009) 185-212.

54. J.C. Fountain, Z.Y. Chen, B.T. Scully, R.C. Kemerait, R.D. Lee, B.Z. Guo, Pathogenesis-related gene expressions in different maize genotypes under drought stressed conditions, Afr. J. Plant Sci. 4 (2010) 433-440.

55. M. Hajheidari, A. Eivazi, B.B. Buchanan, J.H. Wong, I. Majidi, G.H. Salekdeh, Proteomics uncovers a role for redox in drought tolerance in wheat, J. Proteome Res. 6 (2007) 1451-1460.

56. A. Kakumanu, M.M. Ambavaram, C. Klumas, A. Krishnan, U. Batlang, E. Myers, R. Grene, A. Pereira, Effects of drought on gene expression in maize reproductive and leaf meristem tissue revealed by RNA-Seq, Plant Physiol. 160 (2012) 846-67.

57. M. Reverberi, M. Punelli, V. Scala, M. Scarpari, P. Uva, W.I. Mentzen, A.L. Dolezal, C. Woloshuk, F. Pinzari, A.A. Fabbri, C. Fanelli, G.A. Payne, Genotypic and phenotypic versatility of *Aspergillus flavus* during maize exploitation. PLoS ONE 8 (2013) e68735.

58. B.Z. Guo, N.W. Widstrom, R.D. Lee, D.M. Wilson, A.E. Coy, Prevention of preharvest aflatoxin contamination: integration of crop management and genetics in corn. In: H. Abbas (ed.) Aflatoxin and Food Safety. CRC Press, Boca Raton, FL (2005) pp. 437-457.

59. M.C. Willcox, G.L. Davis, M.L. Warburton, G.L. Windham, H.K. Abbas, J. Betrán, J.B. Holland, W.P. Williams, Confirming quantitative trait loci for aflatoxin resistance from Mp313E in different genetic backgrounds. Mol. Breed. 32 (2013) 15-26.

60. T.D. Brooks, W.P. Williams, G.L. Windham, M.C. Willcox, H.K. Abbas, Quantitative trait loci contributing resistance to aflatoxin accumulation in maize inbred Mp313E, Crop Sci. 45 (2005) 171-174.

61. Z. Yin, Y. Wang, F. Wu, X. Gu, Y. Bian, Y. Wang, D. Deng, Quantitative trait locus mapping of resistance to *Aspergillus flavus* infection using a recombinant inbred line population in maize. Mol. Breed. 33 (2014) 39-49.

62. M.L. Warburton, W.P. Williams, Aflatoxin resistance in maize: what have we learned lately?, Adv. Botany, 2014 (2014) 10.

63. G.D. Almeida, D. Makumbi, C. Magorokosho, S. Nair, A. Borém, J.M. Ribaut, M. Bänziger, B.M. Prasanna, J. Crossa, R. Babu, QTL mapping in three tropical maize populations reveals a set of constitutive and adaptive genomic regions for drought tolerance, Theor. Appl. Genet. 126 (2013) 583-600.

64. P.M. Visscher, D. Posthuma, Statistical power to detect genetic loci affecting environmental sensitivity, Behavior Genet. 40 (2010) 728-733.

65. B.Z. Guo, M.D. Krakowsky, X. Ni, B.T. Scully, R.D. Lee, A.E. Coy, N.W. Widstrom, Registration of maize inbred line GT603, J. Plant Regist. 5 (2011) 211-214.

66. B.Z. Guo, N.W. Widstrom, R.D. Lee, A.E. Coy, R.E. Lynch, Registration of maize germplasm GT601 (AM-1) and GT602 (AM-2), J. Plant Regist. 1 (2007) 153-154.

67. B.T. Scully, M.D. Krakowsky, X. Ni, P.J.Tapp, J.K. Knoll, R.D. Lee, B.Z. Guo, Registration of Maize Inbred Line 'GT888', J. Plant Regist. 9 (2015) (in press).

68. W.P. Williams, M.D. Krakowsky, B.T. Scully, R.L. Brown, A. Menkir, M.L. Warburton, G.L. Windham, Identifying and developing maize germplasm with resistance to accumulation of aflatoxins. World Mycotox. J. (2014) in press.

69. W.P. Williams, G.L. Windham, P.M. Buckley, Diallele analysis of aflatoxin accumulation in maize. Crop Sci. 48 (2008) 134-138.

70. R.L. Brown, A. Menkir, Z.Y. Chen, D. Bhatnagar, J. Yu, H. Yao, T.E. Cleveland, Breeding aflatoxin-resistant maize lines using recent advances in technologies – a review, Food Addit. Contam. A, 30 (2013) 1382-1391.

71. J.M. Wagacha, J.W. Muthomi, Mycotoxin problem in Africa: Current status, implications to food safety and health and possible management strategies, Int. J. Food Microbiol. 124 (2008) 1-12.

72. T.H. Sanders, P.D. Blankenship, R.J. Cole, R.A. Hill, Effect of soil temperature and drought on peanut pod and stem temperatures relative to *Aspergillus flavus* invasion and aflatoxin contamination, Mycopathologia 86 (1984) 51-54.

73. T. Girdthai, S. Jogloy, N. Vorasoot, C. Akkasaeng, S. Wongkaew, C.C. Holbrook, A. Patanothai, Associations between physiological traits for drought tolerance and aflatoxin contamination in peanut genotypes under terminal drought, Plant Breed. 129 (2010a) 693-699.

74. P. Sudhakar, P. Lathat, M. Babitha, P.V. Reddy, P.H. Naidu, Relationship of drought tolerance traits with aflatoxin contamination in groundnut, Indian J. Plant Physiol. 12 (2007) 261-265.

75. J. Dorner, R. Cole, T. Sanders, P. Blankenship, Interrelationship of kernel water activity, soil temperature, maturity, and phytoalexin production in pre-harvest aflatoxin contamination of drought-stressed peanuts, Mycopathologia 105 (1989)117-128.

76. J.I. Pitt, M.H. Taniwaki, M.B. Cole, Mycotoxin production in major crops as influenced by growing, harvesting, storage and processing, with emphasis on the achievement of Food Safety Objectives, Food Control 32 (2013) 205-215.

77. S.D. Golombek, C. Johasen, Effect of soil temperature on vegetative and reproductive growth and development in three Spanish genotypes of groundnut (*Arachis hypogaea* L), Peanut Sci. 24 (1997) 67-72.

78. A. Arunyanark, S. Jogloy, S. Wongkaew, C. Akkasaeng, N. Vorasoot, G.C. Wright, R.C.N. Rachaputi, A. Patanothai, Association between aflatoxin contamination and drought tolerance traits in peanut, Field Crops Res. 114 (2009) 14-22.

79. T. Girdthai, S. Jogloy, N. Vorasoot, C. Akkasaeng, S. Wongkaew, C.C. Holbrook, A. Patanothai, Heritability of, and genotypic correlations between, aflatoxin traits and physiological traits for drought tolerance under end of season drought in peanut (*Arachis hypogaea* L.), Field Crops Res. 118 (2010b) 169-176.

80. B.Z. Guo, J. Yu, C.C. Holbrook, T.E. Cleveland, W.C. Nierman, B.T. Scully, Strategies in prevention of preharvest aflatoxin contamination in peanuts: aflatoxin biosynthesis, genetics and genomics, Peanut Sci. 36 (2009)11-20.

81. B.Z. Guo, C.Y. Chen, Y. Chu, C.C. Holbrook, P. Ozias-Akins, H.T. Stalker, Advances in genetics and genomics for sustainable peanut production. In: N. Benkeblia, editor. Sustainable Agriculture and New Biotechnologies, Boca Raton, FL: CRC Press (2012b) p. 341-367.

82. T. Wang, E.H. Zhang, X.P. Chen, L. Li, X.Q. Liang, Identification of seed proteins associated with resistance to pre-harvested aflatoxin contamination in peanut (*Arachis hypogaea* L). BMC Plant Biol. 10 (2010) 267-278.

83. Z. Wang, S. Yan, C. Liu, F. Chen, T. Wang, Proteomic analysis reveals an aflatoxin-triggered immune response in cotyledons of *Arachis hypogaea* infected with *Aspergillus flavus*. J Proteome 11 (2012) 2739–2753.

84. C.C. Holbrook, C.K. Kvien, K.S. Rucker, D.W. Wilson, J.E. Hook, Preharvest aflatoxin contamination in drought tolerant and intolerant peanut genotypes, Peanut Sci. 27 (2000) 45-48.

85. F. Hamidou, A. Rathore, F. Waliyar, V. Vadez, Although drought intensity increases aflatoxin contamination, drought tolerance does not lead to less aflatoxin contamination, Field Crops Res. 156 (2014) 103-110.

86. C.C. Holbrook, B.Z. Guo, D.M. Wilson, P. Timper, The U.S. breeding program to develop peanut with drought tolerance and reduced aflatoxin contamination. Peanut Sci. 36 (2009) 50-53.

87. S.N. Nigam, F. Waliyar, R. Aruna, S.V. Reddy, P.L. Kumar, P.Q. Craufurd, A.T. Diallo, B.R. Ntare, H.D. Upadhyaya, Breeding peanut for resistance to aflatoxin contamination at ICRISAT, Peanut Sci. 36 (2009) 42-49.

88. S.R. Milla, T.G. Isleib, S.P. Tallury, Identification of AFLP markers linked to reduced aflatoxin accumulation in *A. cardenasii*-derived germplasm lines of peanut, Proc. Am. Peanut Res. Edu. Soc. 37 (2005) 90.

89. X. Liang, G. Zhou, Y. Hong, X. Chen, H. Liu, S. Li, Overview of research progress on peanut (*Arachis hypogaea* L.) host resistance to aflatoxin contamination and genomics at the Guangdong Academy of Agricultural Sciences, Peanut Sci. 36 (2009) 29-34.

Figure 2.1. Hypothetical biochemical pathways and reactions present in the maize-*A. flavus* interaction. (A) The perception of chitin by receptor kinases activates a MAPK cascade leading to the expression of maize WRKY transcription factors *Zm*WRKY19 and 53 which promote the expression of antioxidant and pathogenesis-related gene expression; (B) PAMP triggered immunity (PTI) reactions lead to the activation of calcium signaling pathways resulting in the production of extracellular superoxide anions which are detoxified to hydrogen peroxide by superoxide dismutase (SOD); (C) Extracellular hydrogen peroxide functions in cross-kingdom communication between maize and *A. flavus* resulting in the stimulation of cAMP signaling and subsequent expression of genes encoding for stress response proteins and aflatoxin biosynthetic components; (D) The final stages of aflatoxin biosynthesis are confined to specialized structures known as aflatoxisomes while aflatoxin-derived and environmental ROS are detoxified by various stress response proteins. Host derived oxylipins may also stimulate conidiation and inhibit aflatoxin biosynthesis; (E) Aflatoxin is secreted from *A. flavus* and absorbed into the maize cell resulting in oxidative damage to DNA and other cellular components leading to cell death. Solid lines represent characterized pathways from the literature. Dashed lines represent hypothetical junctures between the components of the interaction.

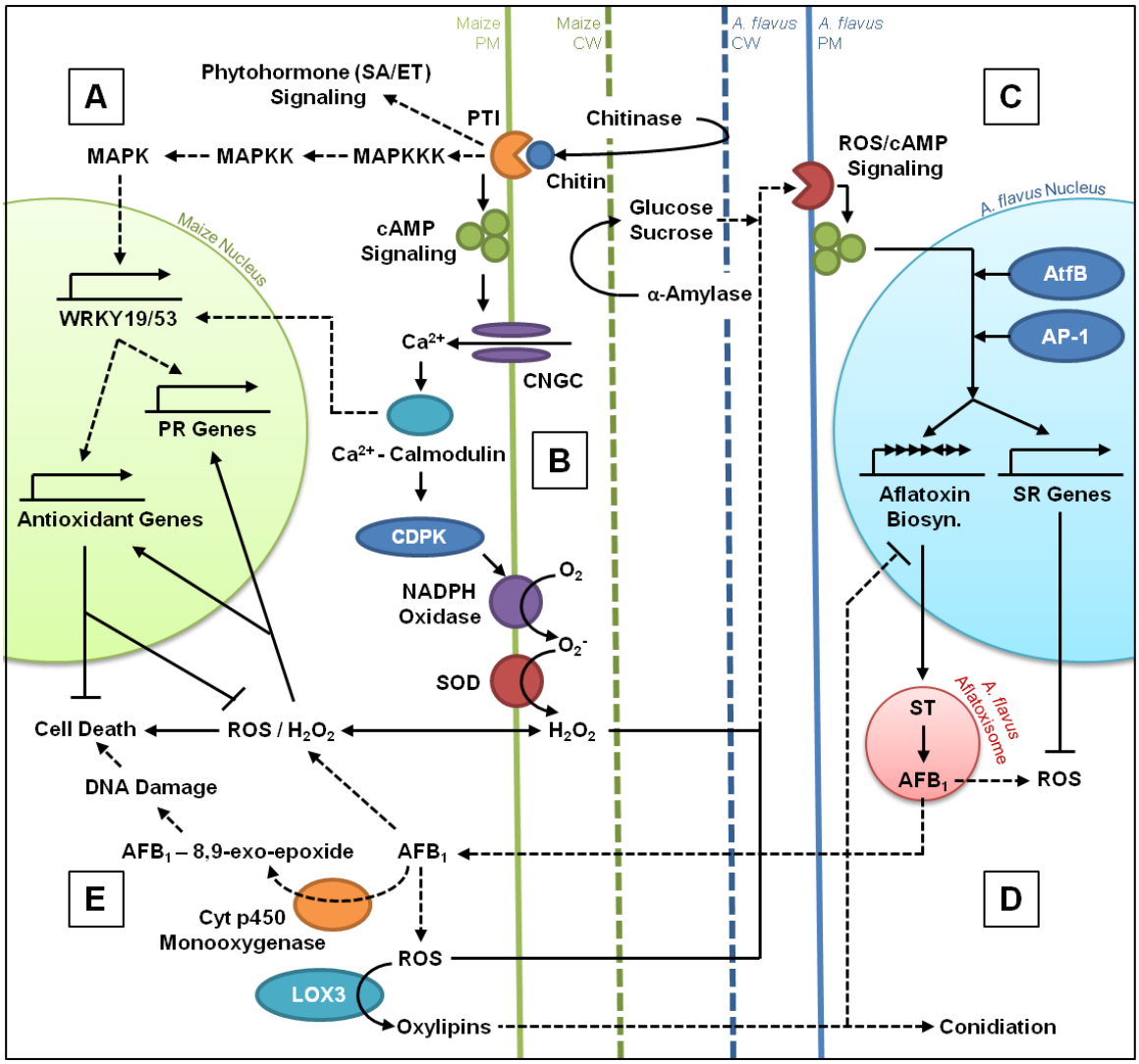
Maize PM
Maize CW
A. flavus CW
A. flavus PM
A
Phytohormone (SA/ET) Signaling
PTI
Chitinase
MAPK
MAPKK
MAPKKK
Chitin
C
ROS/cAMP Signaling
Maize Nucleus
cAMP Signaling
Glucose Sucrose
α-Amylase
A. flavus Nucleus
AtfB
AP-1
WRKY19/53
Ca2+
CNGC
PR Genes
Ca2+ - Calmodulin
B
Aflatoxin Biosyn.
SR Genes
Antioxidant Genes
CDPK
O2
NADPH Oxidase
O2-
SOD
ST
A. flavus Aflatoxisome
Cell Death
ROS / H2O2
H2O2
AFB1
ROS
DNA Damage
AFB1 – 8,9-exo-epoxide
AFB1
E
D
Cyt p450 Monooxygenase
ROS
LOX3
Oxylipins
Conidiation

CHAPTER 3

EVALUATION OF MAIZE INBRED LINES AND TOPCROSS PROGENY FOR RESISTANCE TO PRE-HARVEST AFLATOXIN CONTAMINATION

Fountain, J. C., Abbas, H. K., Scully, B. T., Lee, R. D., Kemerait, R.C., & Guo, B. (2017). Evaluation of maize inbred lines and topcross progeny for resistance to pre-harvest aflatoxin contamination. Prepared for submission to *Crop Science*.

Abstract

Pre-harvest aflatoxin contamination occurs in maize following colonization of kernel tissues by *Aspergillus flavus*. Resistance to aflatoxin contamination is a highly desired trait in the development of commercial varieties in breeding programs with the identification of novel sources of aflatoxin resistance being a major focus in germplasm screening efforts. Here, we performed a field evaluation of 64 inbred lines over two years for pre-harvest aflatoxin contamination resistance. Topcrosses were also performed with two testers, B73 and Mo17, to generate 128 F_1 hybrids which were also evaluated over two years. Hybrid performance was used to calculate both general combining ability (GCA) of the inbreds, and observed heterosis for aflatoxin resistance. Over both years of the study, concentrations of aflatoxin ranged from 80 ± 47 to 17,617 ± 8,816 µg kg^{-1} for the inbreds, and from 58 ± 39 to 2,771 ± 780 µg kg^{-1} for the hybrids with significant variation observed between years and lines. The inbred lines CML52, CML247, GT-603, Hi63, and M37W exhibited aflatoxin levels less than or comparable to the resistant control, Mp313E, and showed significant GCA with the testers in hybrid progeny. CML52, GT-603, and M37W also showed heterotic effects of -13.64%, -12.47%, and -24.50%, respectively, with B73 resulting in reduced aflatoxin contamination in their respective topcrosses. GT-603 also showed a similar heterotic effect for aflatoxin contamination, -13.11%, with Mo17 indicating that it may serve as a versatile source of aflatoxin contamination resistance in breeding programs.

Introduction

Aspergillus flavus is a facultative pathogen of maize and produces potent mycotoxins collectively known as aflatoxins (Amaike and Keller, 2011). These mycotoxins are highly carcinogenic and are also acutely toxic in sufficient quantities with long term low-level exposure resulting in an increased likelihood of developing hepatitis, cirrhosis, hepatocellular carcinoma, and birth defects (Kew, 2013; Williams et al. 2004). Due to the hazards associated with acute and chronic aflatoxin exposure, the US Food and Drug Administration (FDA) currently regulates aflatoxin content in maize products for human consumption at 20 μg kg^{-1} (FDA, 2000). It is estimated that aflatoxin contamination of maize results in over $225 million per year in the United States alone (Schmale and Munkvold, 2009), but has been modeled to potentially reach $1.68 billion in particularly susceptible years (Mitchell et al. 2016). Given the potential losses, both human and economic, the development of commercial varieties with aflatoxin contamination resistance is a major focus of breeding efforts.

Numerous breeding approaches have been applied since the mid 1970's following a severe outbreak of aflatoxin contamination reached the Midwestern US and stimulated interest in pre-harvest aflatoxin contamination resistance, an issue previously considered to primarily a post-harvest storage issue (Diener et al. 1987; Fountain et al. 2014; Trenk and Hartman, 1970). Traditional breeding approaches have focused on the identification of resistant germplasm using field evaluations and laboratory kernel assays in combination (Brown et al. 1993; Windham and Williams, 2002). These efforts have resulted in the identification of several aflatoxin resistant inbred lines including Mp420 and Mp313E (Windham and Williams, 1998), African and tropical germplasm such as TZAR101-TZAR106 developed by the International Institute of Tropical Agriculture (IITA) in collaboration with other institutions (Brown et al. 2016), and southern-

adapted inbred lines such as GT-601, GT-602, GT-603, Mp715, Mp717, Mp718, and Mp719 (Brown et al. 2013; Fountain et al. 2015; Williams et al. 2015).

Recent advances in DNA marker technologies and genotyping capabilities have also allowed for the application of molecular breeding techniques to this issue. Several quantitative trait loci (QTL) for aflatoxin resistance have been identified using both traditional bi-parental mapping populations and using diverse germplasm collections with a genome-wide association study (GWAS) method. For example, Dhakal et al. (2016) utilized an $F_{2:3}$ mapping population derived from Mp715 and B73 to identify seven QTL for aflatoxin contamination resistance explaining <10% phenotypic variance explained (PVE). Recent GWAS studies have also been used to identify QTL. For example, Farfan et al. (2015) used 346 inbred lines testcrossed to Tx714 for GWAS resulting in six minor QTL with PVE of approximately 5%, and Zhuang et al. (2016) used a combination of GWAS using 437 diverse lines and a recombinant inbred line (RIL) population with 228 individuals derived from RA x M53 to identify QTL and markers with 6.7 to 26.8% PVE.

These molecular studies and the relatively low PVEs obtained for detected QTL underscore the complicating nature of genotype x environment interactions which are major confounding factors for aflatoxin resistance breeding. To account for this and improve cultivar selection, multi-location germplasm selection trials such as the Southeast Regional Aflatoxin Test (SERAT) have been performed to examine germplasm performance across multiple environments (Wahl et al. 2017). Another confounding factor is the poor and/or inconsistent agronomic performance of inbred lines observed due to inbreeding depression. In order to compensate for this, F_1 topcross hybrids can be used to screen inbreds as potential sources of aflatoxin contamination resistance. This has been employed both in standard testcross designs,

and in diallel designs to examine both general and specific combining ability for aflatoxin resistance in addition to other relevant agronomic traits (Campbell and White, 1995; Henry et al. 2015; Naidoo et al. 2002, Williams and Windham, 2015).

Given the potential for more consistent agronomic performance in hybrids, and the possibility of heterotic effects on aflatoxin resistance, the objective of this study was to evaluate breeding germplasm available in our breeding program in Tifton, Georgia for aflatoxin contamination resistance in both inbreds and in F_1 topcross hybrids. The second objective was to investigate both GCA and heterotic effects on aflatoxin contamination observed in the generated hybrids. By identifying novel sources of resistance, these lines can be used in breeding commercial varieties with enhanced aflatoxin resistance.

Materials and Methods

Plant Materials

Sixty-four maize inbred lines were selected and cultivated as described by Guo et al. (2017). Briefly, these inbred lines were grown at the USDA-ARS Crop Protection and Management Research Unit (CPMRU) Belflower Research Farm, Tifton, GA, in 2014 and 2015. The inbreds were planted in a randomized complete block design with three replicates. Each inbred was planted in two row plots 3.0 m in length with 0.6 m row spacing, 1.0 m alleys between plots, and seed spacing of 15.2cm. Irrigation was applied as needed and recommended management practices were employed for all plots. F_1 hybrids were generated at the Belflower Farm, USDA-CPMRU, and the University of Georgia Gibbs Farm, Tifton, GA in 2014 and 2015. Two topcrosses/testcrosses were performed using the 64 inbred lines planted in crossing blocks in isolation from other maize plots which were open pollinated following inbred line emasculation

with a single tester line, B73 or Mo17 to generate the hybrid progeny used for screening. Each topcross was performed at a different location to avoid cross-contamination between testers. The 128 F_1 hybrids generated (64 inbreds x B73 and 64 inbreds x Mo17) were then grown in 2015 and 2016 at the Belflower Farm as previously described for the inbreds. Two commercial hybrids, Dekalb DKC69-43 and Dupont-Pioneer P-2023HR, were also included in 2016 as a commercial control.

Aspergillus flavus Inoculation

The *A. flavus* isolate NRRL3357 was used for all field inoculations. The isolate was cultured on V8 agar (20% V8 juice, 1% $CaCO_3$, 2% agar) at 37°C for 5-7 days. Conidia were then harvested into 0.01% (v/v) Tween 20 and quantified using a hemocytometer. Inoculum concentration was then adjusted to 4.0 x 10^6 conidia/mL and refrigerated at 4°C until use. Both the inbred and hybrid plants were inoculated using a side-needle inoculation method as previously described (Guo et al. 2017; Windham et al. 2003). Briefly, at 14 days after 50% plot silk emergence (DAS), an Idico tree-marking gun outfitted with a 14-guage hypodermic needle was used to inoculate maize ears by inserting the needle into the husk and injecting 3.0 mL of inoculum. Only the uppermost ear on each plant was inoculated. In total, five plants per row in each two row plot were inoculated, and bulk harvested at 45-50 days after inoculation (DAI). Ears from each bulk harvested row were dried, shelled, and ground together, and a 50.0 g subsample was taken for aflatoxin analyses.

Aflatoxin Quantification

Aflatoxin quantification was performed as previously described (Guo et al. 2017). Ground subsamples from both the inbred and hybrid lines were tested for total aflatoxin content using a Neogen Veratox for Aflatoxin ELISA kit (Neogen, Lansing, MI, USA) according to the manufacturer's instructions. Initially, 20.0 g of ground kernel tissue was placed into an 8.0 oz opaque container with a lid, and aflatoxin was extracted in 100 ml 70% (v/v) methanol with gentle shaking for three minutes. The mixture was then allowed to stand for several minutes before an aliquot of liquid extract was transferred to a 1.5 mL microcentrifuge tube and stored at 4°C until use in ELISA. Spectrometric analysis using a Veratox ELISA reader (Neogen) was then performed to quantify total aflatoxin content.

Statistical Analysis

All aflatoxin data for both inbred and hybrid samples were used for analysis of variance (ANOVA) using PROC GLM followed by Tukey's post-hoc analysis for pairwise comparisons within inbreds and hybrids using SAS 9.2 (SAS Institute, 2003) and R (v.3.3.0). General combining ability for each inbred was calculated using line x tester analysis using the Analysis of Genetic Designs with R for Windows (AGD-R, v.4.0) software package (Rodriguez et al. 2015). Hybrid vigor (heterosis) was calculated as described by Fehr (1987) using the equation heterosis (%) = $[(F_1 - MP) / (MP)] \times 100$ where F_1 is the average F_1 hybrid performance and MP is the average performance of the parent inbreds.

Results and Discussion

Over the course of two years of replicated analyses, 64 maize inbred lines and 128 F_1 hybrids generated from topcrosses of the inbreds with testers B73 and Mo17 were evaluated for aflatoxin contamination resistance. All of the field evaluated maize samples contained total aflatoxin in concentrations exceeding the FDA limit of 20.0 μg kg^{-1} (FDA, 2000). For the inbreds, an overall average of 2,275 ± 2,323 μg kg^{-1} ranging from 201 ± 186 to 5,000 ± 4,876 μg kg^{-1} in 2014 and from 80 ± 47 to 17,617 ± 8,816 μg kg^{-1} in 2015 were measured. For the hybrids, an overall average of 1,045 ± 784 μg kg^{-1} ranging from 58 ± 39 to 2,387 ± 430 μg kg^{-1} in 2015 and from 157 ± 135 to 2,771 ± 780 μg kg^{-1} in 2016 were measured. Overall, the hybrid progeny showed lower total aflatoxin content than the inbreds evaluated. The content of aflatoxin across the experiment was also found to not be normally distributed necessitating data transformation for further analyses. Therefore, aflatoxin content for both inbreds and hybrids was then $\log_2$ transformed for downstream analyses.

Analysis of variance (ANOVA) showed that there was a significant year effect and variety x year interaction for both the inbred and hybrid lines (Table 3.1). This interaction is representative of genotype x environment interactions classically reported for aflatoxin contamination resistance in maize (Warburton and Williams, 2014). The overall range of aflatoxin content observed in the hybrids, however, does suggest that the magnitude of this variation may indeed be reduced due to more consistent agronomic performance within and across environments compared to the inbred lines. Given this significant interaction, inbred line and hybrid effects were analyzed separately by year. Significant effects on aflatoxin content by both inbred and hybrid samples were detected in both years (Table 3.1).

Among the inbred lines examined, CML52, CML69, CML247, GT-603, GEMS-0005, Hi63, Hp301, and M37W showed consistently lower aflatoxin levels than those observed in the resistant control Mp313E (Table 3.2). This is consistent with previous reports on the observed resistance of these inbred lines in other environments. For example, Mideros et al. (2009) found that CML52, CML247, and M37W accumulated levels of aflatoxin and *A. flavus* mycelial growth comparable to Mp313E in Mississippi field conditions. CML69 was also found to be resistant to aflatoxin contamination in Mississippi and Texas field environments in previous evaluations (Warburton et al. 2013). GT-603 was derived from the GT-MAS:gk population, and has been shown to exhibit resistance in Georgia and other Southern US environments (Guo et al. 2011). GEMS-0005 was developed as a part of the Germplasm Enhancement of Maize (GEM) cooperative effort to enhance maize resistance to disease, and hybrids of GEMS-0005 have been shown to exhibit resistance to aflatoxin contamination across multiple environments in the Southern US (Wahl et al. 2017; Williams et al. 2015). Hi63 has no previously reported resistance to aflatoxin contamination, but has been reported to possess resistance to *Puccinia polysora* (Brewbaker et al. 2011). Hp301 has been found to possess an active *ZmLOX5* gene which has been linked to aflatoxin contamination resistance in previous QTL studies (De La Fuente et al. 2013). This indicates that these inbred lines may serve as novel sources of resistance for use in breeding programs.

Testcross hybrids generated also exhibited varying levels of resistance to aflatoxin contamination (Table 3.3). Interestingly, hybrids of several of the most resistant inbred lines including CML247, CML52, GT-603, and Hi63 showed among the lower levels of aflatoxin contamination observed when crossed with both B73 or Mo17 (Table 3.3). M37W x B73 was the most consistently resistant F_1 hybrid identified in the study with an average of 200 ± 180 µg kg^{-1}

across both years of the study. In contrast to these lines, the inbred lines used as testers in the topcrosses, B73 and Mo17, showed higher levels of aflatoxin contamination with an average of 1,824 ± 1,091 and 759 ± 654, respectively (Table 3.2). These hybrids between CML247, CML52, GT-603, Hi63, and M37W and the testers also exhibited lower aflatoxin contamination than observed in the two commercial hybrids included as checks in 2016, Dekalb DKC69-43 and Dupont-Pioneer P-2023HR, which accumulated an average of 764 ± 661 and 1,404 ± 962 μg kg^{-1}, respectively.

This reduction in aflatoxin content in the hybrids is consistent with the observed GCA (Table 3.2) and heterotic (Table 3.4) effects observed for these lines. General Combining Ability (GCA) describes the ability of a line to produce progeny with multiple testers, F_1 hybrids with B73 and Mo17 here, which have significantly improved performance (Sprague and Tatum, 1942). Hybrid vigor is a direct comparison between measureable traits of both the line and the average performance of a particular tester (Fefr, 1987). While no significant GCA effects were observed for the 2015 hybrid samples, in 2016, CML52, GT-603, and Hi63 showed significantly negative GCA effects ($p < 0.05$) toward reduced aflatoxin content in their hybrids with B73 and Mo17. When comparing across years, M37W also showed less significant negative GCA effects ($p < 0.10$) for reduced aflatoxin contamination. When examining mean parent heterosis, CML52 and M37W show heterotic effects across years on aflatoxin content of -24.50 and -13.64% when crossed with B73. In contrast, if crossed with Mo17, these lines show effects of 13.97 and -0.68%, respectively. This indicates that these lines show greater heterotic effects for aflatoxin contamination resistance with the stiff-stalk tester B73. For GT-603 and Hi63, negative heterotic effects across years were observed with both testers with -12.47 and -8.84%, respectively, with B73 and -13.11 and -9.90%, respectively, with Mo17. In addition, the greatest heterotic effect

was observed with Mo18W which showed a heterotic effect across years of -29.23% with B73 and -11.38% with Mo17. These results are consistent with previous observations of heterosis having an effect on aflatoxin contamination through unique genetic combinations, or through heterotic increases in hybrid yield and agronomic performance relative to the parental inbred lines (Campbell and White, 1995; Naidoo et al. 2002; Wahl et al. 2017; Warburton et al. 2013). Therefore, these inbred and hybrid combinations may be useful sources of aflatoxin resistance in breeding programs and potentially useful in commercial applications for the development of resistant germplasm.

Conclusions

Aflatoxin contamination of maize and other staple food crops is a serious threat to food safety and security, particularly in developing countries. Since the discovery of pre-harvest aflatoxin contamination, breeding efforts have been focused on the discovery of novel sources of resistance, and the investigation of the interactions of maize resistance and the environment toward the development of high yielding varieties with stable aflatoxin contamination resistance across multiple environments. Here, we evaluated the resistance of 64 maize inbred lines from our breeding program, and 128 topcross hybrids with two testers, B73 and Mo17 across two years in a field environment. Eight inbred lines: CML52, CML69, CML247, GT-603, GEMS-0005, Hi63, Hp301, and M37W were found to have aflatoxin contamination resistance comparable to Mp313E across the two years of the study. F_1 hybrids of these lines with inbreds and the testers also possessed reduced aflatoxin contamination, and significant combining ability and heterosis effects demonstrating their potential use in breeding programs for the development of resistant cultivars. The reduced overall range of aflatoxin levels detected in the hybrids also

suggests that this methodology of evaluating F_1 hybrids may provide more stable results for assessing potential sources of resistance.

Acknowledgements

We thank Billy Wilson and Hui Wang for technical assistance in the field. This work is partially supported by the U.S. Department of Agriculture Agricultural Research Service (USDA-ARS), the Georgia Agricultural Commodity Commission for Corn, and AMCOE (Aflatoxin Mitigation Center of Excellence, Chesterfield, MO, USA). Mention of trade names or commercial products in this publication is solely for the purpose of providing specific information and does not imply recommendation or endorsement by the USDA. The USDA is an equal opportunity provider and employer.

References

1. Amaike, S. & Keller, N. P. *Aspergillus flavus*. *Ann. Rev. Phytopathol*. 49, 107-133 (2011).
2. United States Food and Drug Administration (FDA). (2000) Available: https://www.fda.gov/food/guidanceregulation/guidancedocumentsregulatoryinformation/ucm077969.htm. Accessed on April 7, 2016.
3. Kew, M. C. Aflatoxins as a cause of hepatocellular carcinoma. *J. Gastrointestin. Liver Dis.* 22, 305-310 (2013).
4. Williams, J.H., Phillips, T.D., Jolly, P.E., Stiles, J.K., Jolly, C.M. & Aggarwal, D. Human aflatoxicosis in developing countries: a review of toxicology, exposure, potential consequences, and interventions. *Am. J. Clin. Nutr*. 80, 1106-1122 (2004).

5. Schmaile, D. G., & Munkvold, G. P. (2009). Mycotoxins in crops: a threat to human and domestic animal health. The Plant Health Instructor. DOI: 10.1094. PHI-I-2009-0715-01.
6. Mitchell, N. J., Bowers, E., Hurburgh, C., & Wu, F. (2016). Potential economic losses to the US corn industry from aflatoxin contamination. *Food Additives & Contaminants: Part A*, *33*(3), 540-550.
7. Diener, U. L., Cole, R. J., Sanders, T. H., Payne, G. A., Lee, L. S., & Klich, M. A. (1987). Epidemiology of aflatoxin formation by *Aspergillus flavus*. *Annual review of phytopathology*, *25*(1), 249-270.
8. Fountain, J., Scully, B., Ni, X., Kemerait, R., Lee, D., Chen, Z. Y., & GUO, B. (2014). Environmental influences on maize-*Aspergillus flavus* interactions and aflatoxin production. *Frontiers in Microbiology*, *5*, 40.
9. Trenk, H. L., & Hartman, P. A. (1970). Effects of moisture content and temperature on aflatoxin production in corn. *Applied microbiology*, *19*(5), 781-784.
10. Brown, R. L., Cotty, P. J., Cleveland, T. E., & Widstrom, N. W. (1993). Living maize embryo influences accumulation of aflatoxin in maize kernels. *Journal of Food Protection*, *56*(11), 967-971.
11. Windham, G. L., & Williams, W. P. (2002). Evaluation of corn inbreds and advanced breeding lines for resistance to aflatoxin contamination in the field. *Plant Disease*, *86*(3), 232-234.
12. Windham, G. L., & Williams, W. P. (1998). *Aspergillus flavus* infection and aflatoxin accumulation in resistant and susceptible maize hybrids. *Plant Disease*, *82*(3), 281-284.

13. Brown, R. L., Williams, W. P., Windham, G. L., Menkir, A., & Chen, Z. Y. (2016). Evaluation of African-bred maize germplasm lines for resistance to aflatoxin accumulation. *Agronomy*, *6*(2), 24.
14. Williams, W. P., Krakowsky, M. D., Scully, B. T., Brown, R. L., Menkir, A., Warburton, M. L., & Windham, G. L. (2014). Identifying and developing maize germplasm with resistance to accumulation of aflatoxins. *World Mycotoxin Journal*, *8*(2), 193-209.
15. Brown, R. L., Menkir, A., Chen, Z. Y., Bhatnagar, D., Yu, J., Yao, H., & Cleveland, T. E. (2013). Breeding aflatoxin-resistant maize lines using recent advances in technologies–a review. *Food Additives & Contaminants: Part A*, *30*(8), 1382-1391.
16. Fountain, J. C., Khera, P., Yang, L., Nayak, S. N., Scully, B. T., Lee, R. D., ... & Guo, B. (2015). Resistance to *Aspergillus flavus* in maize and peanut: Molecular biology, breeding, environmental stress, and future perspectives. *The Crop Journal*, *3*(3), 229-237.
17. Dhakal, R., Windham, G. L., Williams, W. P., & Subudhi, P. K. (2016). Quantitative trait loci (QTL) for reducing aflatoxin accumulation in corn. *Molecular Breeding*, *36*(12), 164.
18. Farfan, I. D. B., Gerald, N., Murray, S. C., Isakeit, T., Huang, P. C., Warburton, M., ... & Kolomiets, M. (2015). Genome wide association study for drought, aflatoxin resistance, and important agronomic traits of maize hybrids in the sub-tropics. *PloS one*, *10*(2), e0117737.
19. Zhang, Y., Cui, M., Zhang, J., Zhang, L., Li, C., Kan, X., ... & Yin, Z. (2016). Confirmation and Fine Mapping of a Major QTL for Aflatoxin Resistance in Maize Using a Combination of Linkage and Association Mapping. *Toxins*, *8*(9), 258.
20. Wahl, N., Murray, S. C., Isakeit, T., Krakowsky, M., Windham, G. L., Williams, W. P., ... & Scully, B. (2016). Identification of Resistance to Aflatoxin Accumulation and Yield Potential

in Maize Hybrids in the Southeast Regional Aflatoxin Trials (SERAT). *Crop Science*, 57(1), 202-215.

21. Williams, W. P., & Windham, G. L. (2015). Aflatoxin accumulation in a maize diallel cross. *Agriculture*, *5*(2), 344-352.
22. Henry, W. B., Blanco, M. H., Rowe, D. E., Windham, G. L., Murray, S. C., & Williams, W. P. (2014). Diallel analysis of diverse maize germplasm lines for agronomic characteristics. *Crop Science*, *54*(6), 2547-2556.
23. Campbell, K. W., & White, D. G. (1995). Evaluation of corn genotypes for resistance to Aspergillus ear rot: kernel infection, and aflatoxin production. *Plant Disease*, *79*(10), 1039-1045.
24. Naidoo, G., Forbes, A. M., Paul, C., White, D. G., & Rocheford, T. R. (2002). Resistance to Aspergillus Ear Rot and Aflatoxin Accumulation in Maize F Hybrids. *Crop Science*, *42*(2), 360-364.
25. Guo, B., Ji, X., Ni, X., Fountain, J. C., Li, H., Abbas, H. K., ... & Scully, B. T. (2017). Evaluation of maize inbred lines for resistance to pre-harvest aflatoxin and fumonisin contamination in the field. *The Crop Journal, in press*.
26. Windham, G. L., Williams, W. P., Buckley, P. M., & Abbas, H. K. (2003). Inoculation techniques used to quantify aflatoxin resistance in corn. *Journal of Toxicology: Toxin Reviews*, *22*(2-3), 313-325.
27. Fehr, W. R. (1987). *Principles of cultivar development. Volume 1. Theory and technique*. New York: Macmillan.
28. Warburton, M. L., & Williams, W. P. (2014). Aflatoxin resistance in maize: what have we learned lately?. *Advances in Botany*, *2014*.

29. Mideros, S. X., Windham, G. L., Williams, W. P., & Nelson, R. J. (2009). *Aspergillus flavus* biomass in maize estimated by quantitative real-time polymerase chain reaction is strongly correlated with aflatoxin concentration. *Plant Disease*, *93*(11), 1163-1170.

30. Warburton, M. L., Williams, W. P., Windham, G. L., Murray, S. C., Xu, W., Hawkins, L. K., & Duran, J. F. (2013). Phenotypic and genetic characterization of a maize association mapping panel developed for the identification of new sources of resistance to and aflatoxin accumulation. *Crop Science*, *53*(6), 2374-2383.

31. Guo, B. Z., Krakowsky, M. D., Ni, X., Scully, B. T., Lee, R. D., Coy, A. E., & Widstrom, N. W. (2011). Registration of maize inbred line GT603. *Journal of Plant Registrations*, *5*(2), 211-214.

32. Brewbaker, J. L., Kim, S. K., So, Y. S., Logroño, M., Moon, H. G., Ming, R., ... & Josue, A. D. (2011). General Resistance in Maize to Southern Rust (Underw.). *Crop science*, *51*(4), 1393-1409.

33. De La Fuente, G. N., Murray, S. C., Isakeit, T., Park, Y. S., Yan, Y., Warburton, M. L., & Kolomiets, M. V. (2013). Characterization of genetic diversity and linkage disequilibrium of ZmLOX4 and ZmLOX5 loci in maize. *PloS one*, *8*(1), e53973.

34. Sprague, G.F., & Tatum, L.A. (1942). General vs. specific combining ability in single crosses of corn. *Agronomy Journal, 34(10)*, 923-932.

Table 3.1. Analysis of Variance (ANOVA) for inbred and F_1 hybrid aflatoxin contamination levels [$\log_2(y+1)$].

Source	df	Mean Squares	F	*p*-value
Combined Inbred Lines				
Year	1	218.78	63.57	< 0.0001
Inbred	65	12.24	3.56	< 0.0001
Inbred x Year	62	6.01	1.75	0.0007
Inbred Lines by Year				
Inbred (2014)	63	11.79	2.87	< 0.0001
Inbred (2015)	64	8.03	4.41	< 0.0001
Combined F1 Hybrids				
Year	1	221.78	156.67	< 0.0001
Hybrid	124	4.00	2.83	< 0.0001
Hybrid x Year	86	3.15	2.23	< 0.0001
F1 Hybrids by Year				
Hybrid (2015)	87	3.98	1.93	0.0002
Hybrid (2016)	123	3.32	2.68	< 0.0001

y = Aflatoxin Contamination ($\mu g \times kg^{-1}$)

Table 3.2. Mean aflatoxin contamination (µg kg^{-1}) and general combining ability (GCA) for the inbred lines in 2014 and 2015.

	Total Aflatoxin		GCA [$log_2(y+1)$]	
Line	**2014**	**2015**	**2015**	**2016**
GT A661(SP)	5000 ± 4876 abc	1128 ± 1652 b-f	-0.02	-0.08
10 GEM06845-1B-1B	4489 ± 4687 abc	3240 ± 1234 a-e	0.11	0.17
GT A554	4446 ± 1991 a	1710 ± 442 a-f	-0.08	0.14
Coy 05 AT 709	4416 ± 2821 ab	8245 ± 3353 ab	0.11	0.36
GT A641(SP)	3905 ± 3027 abc	1479 ± 1114 a-f	-0.13	-0.08
I114H	3715 ± N/A	750 ± 779 b-f	0.39	0.35
GP 280	3074 ± 2795 abc	6267 ± 3286 abc	0.24	0.15
Grace E-5 (E-1)	2909 ± 1046 ab	17617 ± 8816 a	0.16	0.34
CY 5	2759 ± 3097 abc	3160 ± 1299 a-e	0.14	0.18
Coy 05 AT 805	2733 ± 1109 ab	4723 ± 2409 a-d	-0.01	-0.08
CY 3	2613 ± 1783 abc	3300 ± 2217 a-e	0.29	-0.08
GP 282	2588 ± 1383 abc	2700 ± 142 a-e	0.62	0.12
B97	2559 ± 860 ab	3137 ± 741 a-e	0.45	0.38
CML103-2	2525 ± 1071 ab	878 ± 531 a-f	-0.42	0.15
GT A638	2473 ± 949 ab	1660 ± 1912 b-f	-0.16	0.04
Tzi8	2428 ± 3138 abc	1820 ± 972 a-f	-0.23	-0.05
EP M6	2112 ± 1205 abc	1215 ± 1764 b-f	0.42	-0.25
CY 1	1930 ± 1104 abc	3957 ± 2340 a-e	0.21	0.48
Lo 964	1918 ± 1544 abc	3493 ± 1926 a-e	0.62	-0.06
LH 132	1901 ± 824 ab	4287 ± 871 a-d	-0.02	-0.03
Ky21	1857 ± 1970 abc	4287 ± 4641 a-e	0.25	0.29
B73	1824 ± 1091 abc	2170 ± 519 a-e	-0.41	0.00
Coy 05 AT 823	1823 ± 1378 abc	3490 ± 702 a-e	0.20	-0.42
F54	1687 ± 1364 abc	2450 ± 1387 a-e	0.22	0.14
Lo 1016	1632 ± 1648 abc	5578 ± 3823 a-d	0.37	-0.06
ZM 521 E-1	1576 ± 956 abc	2177 ± 1712 a-f	-0.01	0.38
TX 732	1530 ± 689 abc	1960 ± 166 a-e	-0.20	-0.17
Oh43	1429 ± 1535 abc	4345 ± 3923 a-e	0.19	-0.25
Syn AM 1 P43	1406 ± 1654 abc	731 ± 807 b-f	N/A	0.05
GT A2 R	1307 ± 1603 abc	4074 ± 4832 a-e	0.10	0.17
FAW 1430	1304 ± 1115 abc	3220 ± 1157 a-e	-0.30	0.28
Ki11	1303 ± 843 abc	743 ± 49 a-f	-0.43	-0.08
CY 2	1283 ± 1644 abc	301 ± 305 def	-0.16	-0.09
GT A1R TP Yellow E-1	1264 ± 1403 abc	N/A	0.07	-0.25
Coy 05 AT 819	1188 ± 1116 abc	3680 ± 632 a-e	-0.10	0.45
Tx303	1175 ± 1628 abc	5553 ± 1218 abc	0.52	0.33
GEM 0028-2-1-B-B-B-1B-1B	1156 ± 1207 abc	258 ± 92 c-f	-0.57	-0.11
B37	1129 ± 785 abc	6832 ± 3223 ab	N/A	-0.19
CML228	1116 ± 667 abc	1114 ± 1248 a-f	0.05	0.27
NC358	1015 ± 1202 abc	3213 ± 2913 a-e	-0.14	0.10
Tun 88-1B-B	969 ± 708 abc	2217 ± 1448 a-e	-0.05	-0.09
HBA-1-B	945 ± 800 abc	1359 ± 1055 a-f	0.10	0.37
CML333	937 ± 475 abc	3367 ± 1002 a-e	-0.13	0.24
NC290A-B	912 ± 1094 abc	1860 ± 1042 a-f	-0.03	-0.41
Hi31-1B-1B-1B	907 ± 738 abc	2300 ± 1814 a-f	0.01	-0.13
GT-888	880 ± 595 abc	231 ± 187 ef	-0.13	0.36
MS71	841 ± 751 abc	1326 ± 1301 b-f	-0.04	-0.21
A638/MP313E//MP313E/f_6-3_5-B_6	792 ± 1060 abc	1600 ± 737 a-f	0.00	0.26
LH 51	785 ± 981 abc	13513 ± 17716 ab	0.20	0.14

Table 3.2. Continued

	Total Aflatoxin				GCA [$log_2(y+1)$]	
Line	**2014**		**2015**		**2015**	**2016**
Mo17	759 ± 654	abc	2671 ± 713	a-e	0.41	0.00
CML69	758 ± 738	abc	180 ± 97	ef	-0.36	0.19
Hi 63-1B-1	714 ± 793	abc	282 ± 166	c-f	-0.38	-0.63 **
CY 4	665 ± 800	abc	3603 ± 1383	a-e	0.22	-0.02
GT 603	639 ± 616	abc	747 ± 240	a-f	-0.31	-1.04 **
M37W	547 ± 602	abc	967 ± 687	a-f	-0.58	-0.30
CML277	518 ± 520	abc	1430 ± 1679	a-f	-0.16	0.04
Tun 85-1B-B	516 ± 597	abc	2107 ± 900	a-e	0.23	0.47
CML322	503 ± 612	abc	3293 ± 1743	a-e	N/A	0.10
Va35	481 ± 740	bc	4197 ± 2962	a-e	0.09	0.07
Hp301	464 ± 638	abc	393 ± 346	def	N/A	-0.59
CML52	388 ± 423	abc	322 ± 87	b-f	-0.21	-0.86 **
Mo18W	381 ± 646	abc	4213 ± 2242	a-e	-0.36	-0.15
GEMS 0005-1-1-1-1B-1B	253 ± 189	abc	439 ± 128	b-f	-0.07	-0.05
CML247	245 ± 541	c	80 ± 47	f	-0.43	-0.38
NC350	201 ± 186	abc	6825 ± 2129	ab	-0.32	-0.42
MP313E	N/A		765 ± 420	a-f	N/A	0.04

Data are means of all replications within the indicated year. Concentrations of total aflatoxin (µg x kg^{-1}) are means ± SD.

Means with the same letters are not significantly different at $p < 0.05$ (Tukey's post-hoc analysis).

y = mean concentrations of aflatoxin (µg kg^{-1})

N/A - Not Available

*Significantly different from 0 at $p < 0.10$.

**Significantly different from 0 at $p < 0.05$.

Table 3.3. Mean aflatoxin contamination (µg kg^{-1}) for the F_1 topcross hybrids in 2015 and 2016.

	2015*		2016*	
Line	**x B73**	**x Mo17**	**x B73**	**x Mo17**
GP 282	2387 ± 430 ab	614 ± 195 abc	1647 ± 1265 a-e	1144 ± 816 a-f
Tx303	2277 ± 2082 abc	N/A	1289 ± 809 a-e	2121 ± 835 abc
Lo 964	2217 ± 2404 abc	1435 ± 1164 abc	1585 ± 1473 a-e	1030 ± 1169 a-f
Grace E-5 (E-1)	1870 ± 0 abc	551 ± 365 abc	1311 ± 872 a-e	2073 ± 743 abc
NC290A-B	1392 ± 2260 abc	N/A	913 ± 70 a-e	447 ± 333 c-f
F54	1075 ± 1208 abc	476 ± 177 abc	855 ± 518 a-f	1889 ± 564 a-d
B97	1047 ± 1435 abc	1790 ± 1001 abc	1737 ± 833 a-e	1808 ± 845 a-e
Ky21	874 ± 900 abc	913 ± 165 abc	1431 ± 949 a-e	1804 ± 1065 a-e
CML69	822 ± 1030 abc	166 ± 196 bc	1116 ± 710 a-e	1518 ± 458 a-e
Lo 1016	821 ± 814 abc	1027 ± 564 abc	799 ± 765 a-f	1816 ± 1278 a-e
HBA-1-B	651 ± 892 abc	782 ± 552 abc	2382 ± 1138 a-d	1409 ± 632 a-e
Tun 85-1B-B	611 ± 249 abc	N/A	2321 ± 895 abc	1596 ± 874 a-e
CML228	562 ± 433 abc	488 ± 170 abc	1374 ± 1022 a-e	1722 ± 722 a-e
Oh43	544 ± 218 abc	N/A	1086 ± 1250 a-f	1190 ± 695 a-e
MS71	467 ± 528 abc	N/A	1236 ± 916 a-f	668 ± 346 a-f
Va35	435 ± 312 abc	N/A	1319 ± 691 a-e	990 ± 585 a-f
GP 280	414 ± 227 abc	977 ± 250 abc	911 ± 519 a-f	1744 ± 869 a-e
GEM 0028-2-1-B-B-B-1B-1B	399 ± 511 abc	99 ± 72 bc	653 ± 475 a-f	1396 ± 800 a-e
CML52	398 ± 441 abc	713 ± 998 abc	293 ± 159 def	404 ± 302 b-f
GT A1R TP Yellow E-1	388 ± 283 abc	815 ± 716 abc	595 ± 217 a-f	961 ± 880 a-f
CY 5	388 ± 49 abc	657 ± 268 abc	620 ± 301 a-f	2238 ± 481 ab
Tun 88-1B-B	369 ± 354 abc	N/A	773 ± 362 a-f	989 ± 465 a-e
10 GEM06845-1B-1B	362 ± 299 bc	2190 ± N/A ab	1079 ± 715 a-f	1689 ± 511 a-e
CY 1	350 ± 108 abc	1100 ± 687 abc	2588 ± 1358 abc	1621 ± 923 a-e
Hi31-1B-1B-1B	298 ± 44 abc	N/A	841 ± 1039 a-f	1123 ± 383 a-e
GT A2 R	251 ± 135 abc	1642 ± 1318 abc	1842 ± 1132 a-e	1055 ± 615 a-e
GEMS 0005-1-1-1-1B-1B	246 ± 117 abc	N/A	898 ± 822 a-f	1290 ± 746 a-e
Hi 63-1B-1	245 ± 30 abc	151 ± 63 bc	715 ± 697 a-f	449 ± 280 b-f
Tzi8	245 ± 277 bc	N/A	1076 ± 848 a-f	1040 ± 763 a-f
GT A554	222 ± 29 abc	573 ± 562 abc	1789 ± 1051 a-e	1822 ± 1165 a-f
ZM 521 E-1	220 ± 116 bc	1065 ± 808 abc	2051 ± 1168 a-d	1365 ± 467 a-e
Mo18W	210 ± 130 bc	226 ± 50 abc	N/A	745 ± 473 a-f
CML103-2	207 ± 78 bc	493 ± 752 bc	1095 ± 980 a-f	1586 ± 591 a-e
GT 603	199 ± 237 bc	586 ± 662 abc	591 ± 596 a-f	157 ± 135 f
NC358	195 ± 52 bc	N/A	1073 ± 636 a-e	1269 ± 532 a-e
CML333	191 ± 96 bc	528 ± 133 abc	1622 ± 694 a-e	1194 ± 602 a-e
A638/MP313E//MP313E/f_6-3$_5$-B_6	187 ± 188 bc	1100 ± 257 abc	1670 ± 533 a-e	1260 ± 685 a-e
GT-888	169 ± 117 bc	853 ± 640 abc	2771 ± 780 a	1038 ± 589 a-e
NC350	152 ± 122 bc	N/A	520 ± 220 a-f	636 ± 324 a-f
CML247	117 ± 101 bc	344 ± 143 abc	944 ± 729 a-f	665 ± 513 a-f
Ki11	98 ± 62 bc	406 ± 219 abc	1210 ± 824 a-e	781 ± 567 a-f
M37W	58 ± 39 c	N/A	270 ± 182 ef	1812 ± 786 a-d
I114H	N/A	8400 ± 0 a	1439 ± 938 a-e	1908 ± 829 a-d
EP M6	N/A	2290 ± 1736 abc	1367 ± 1306 a-f	747 ± 162 a-f
Coy 05 AT 823	N/A	1801 ± 2425 abc	1031 ± 834 a-f	415 ± 117 a-f
CY 3	N/A	1437 ± 1084 abc	892 ± 626 a-f	901 ± 290 a-f
CY 4	N/A	1020 ± 410 abc	851 ± 389 a-f	1290 ± 1032 a-e
LH 51	N/A	1007 ± 543 abc	954 ± 452 a-f	1623 ± 1025 a-e
LH 132	N/A	941 ± 1232 abc	1552 ± 935 a-e	701 ± 450 a-f
Coy 05 AT 709	N/A	758 ± 409 abc	2104 ± 791 abc	1462 ± 1216 a-e
GT A661(SP)	N/A	626 ± 487 abc	N/A	912 ± 534 a-f
Coy 05 AT 819	N/A	516 ± 510 abc	2404 ± 1218 a-e	1925 ± 572 a-d

Table 3.3. Continued

	2015*			2016*				
Line	**x B73**	**x Mo17**		**x B73**		**x Mo17**		
TX 732	N/A	516 ± 417	abc	793 ± 220	a-f	987 ± 629	a-f	
Coy 05 AT 805	N/A	497 ± 116	abc	993 ± 510	a-e	1119 ± 950	a-f	
GT A641(SP)	N/A	433 ± 346	abc	1108 ± 702	a-e	980 ± 819	a-f	
CY 2	N/A	409 ± 291	abc	1370 ± 708	a-e	671 ± 513	a-f	
GT A638	N/A	382 ± 230	abc	1220 ± 810	a-e	1518 ± 947	a-e	
CML277	N/A	318 ± 59	abc	1351 ± 858	a-e	955 ± 506	a-f	
FAW 1430	N/A	222 ± 100	bc	1452 ± 799	a-e	1582 ± 796	a-e	
Syn AM 1 P43	N/A	N/A		1151 ± 502	a-e	888 ± 275	a-f	
CML322	N/A	N/A		1123 ± 552	a-e	1178 ± 504	a-e	
Hp301	N/A	N/A		N/A ± N/A		460 ± 325	def	
B37	N/A	N/A		531 ± 231	a-f	1089 ± 351	a-e	
MP313E	N/A	N/A		1210 ± 790	a-e	N/A		

Data are means of all replications within the indicated year. Concentrations of total aflatoxin (µg x kg^{-1}) are means ± SD.

Means with the same letters are not significantly different at $p < 0.05$ (Tukey's post-hoc analysis).

N/A - Not Available

Table 3.4. Heterosis effects observed for mean aflatoxin contamination in F_1 hybrids.

	Total Aflatoxin [$log_2(y+1)$]			Heterosis (%)	
Line	**Inbred**	**x B73**	**x Mo17**	**x B73**	**x Mo17**
Grace E-5 (E-1)	12.76	10.46	10.61	-11.35%	-4.93%
LH 51	12.61	9.90	10.47	-15.54%	-5.58%
Coy 05 AT 709	12.41	11.04	10.26	-5.03%	-6.64%
10 GEM06845-1B-1B	11.99	9.72	10.79	-14.87%	0.11%
GP 280	11.95	9.54	10.54	-16.21%	-2.02%
GT A661(SP)	11.95	N/A	9.67	N/A	-10.07%
GT A554	11.82	10.31	10.56	-9.02%	-1.27%
Coy 05 AT 805	11.70	9.96	9.83	-11.63%	-7.54%
GT A641(SP)	11.60	10.11	9.64	-9.82%	-8.90%
CY 5	11.49	9.03	10.68	-19.14%	1.46%
CY 3	11.46	9.80	10.08	-12.07%	-4.17%
Lo 1016	11.46	9.66	10.57	-13.37%	0.53%
Ky21	11.44	10.28	10.56	-7.64%	0.53%
B97	11.42	10.56	10.82	-5.10%	3.08%
CY 1	11.39	10.85	10.50	-2.39%	0.17%
B37	11.39	9.06	10.09	-18.51%	-3.72%
Tx303	11.36	10.66	11.05	-3.94%	5.58%
GP 282	11.36	10.89	9.92	-1.87%	-5.20%
LH 132	11.32	10.60	9.61	-4.29%	-7.97%
Oh43	11.30	9.82	10.22	-11.23%	-2.09%
Lo 964	11.22	10.81	10.21	-1.98%	-1.81%
GT A2 R	11.20	10.36	10.29	-5.96%	-0.90%
Coy 05 AT 823	11.18	10.01	9.78	-9.05%	-5.77%
Tzi8	11.13	9.64	10.02	-12.20%	-3.16%
GT A638	11.11	10.25	10.16	-6.52%	-1.76%
NC350	11.10	8.58	9.32	-21.74%	-9.85%
F54	11.01	9.86	10.47	-9.75%	1.73%
CML103-2	10.99	9.64	10.26	-11.62%	-0.23%
Mo18W	10.98	7.72	9.11	-29.23%	-11.38%
CY 4	10.91	9.73	10.23	-10.47%	-0.10%
Coy 05 AT 819	10.87	11.23	10.51	3.51%	2.83%
FAW 1430	10.84	10.50	10.14	-3.05%	-0.60%
EP M6	10.79	10.42	10.30	-3.67%	1.17%
ZM 521 E-1	10.77	10.49	10.29	-2.84%	1.22%
I114H	10.76	10.49	11.47	-2.84%	12.82%
NC358	10.71	9.61	10.31	-10.79%	1.68%
TX 732	10.71	9.63	9.70	-10.57%	-4.35%
CML333	10.64	10.16	9.93	-5.37%	-1.79%
Va35	10.55	10.00	9.95	-6.44%	-1.05%
Tun 88-1B-B	10.39	9.32	9.95	-12.18%	-0.29%
Hi31-1B-1B-1B	10.33	9.37	10.13	-11.47%	1.84%
GT A1R TP Yellow E-1	10.31	9.09	9.84	-14.02%	-1.03%
CML322	10.31	10.13	10.20	-4.12%	2.68%

Table 3.4. Continued.

	Total Aflatoxin [$log_2(y+1)$]			x B73	x Mo17
Line	**Inbred**	**x B73**	**x Mo17**	**%HV**	**%HV**
Syn AM 1 P43	10.26	10.17	9.80	-3.56%	-1.19%
Tun 85-1B-B	10.23	10.77	10.64	2.32%	7.50%
NC290A-B	10.23	10.07	8.81	-4.38%	-11.02%
Ki11	10.17	9.71	9.36	-7.49%	-5.16%
CML228	10.12	10.11	10.36	-3.53%	5.18%
HBA-1-B	10.05	10.82	10.20	3.61%	3.97%
CY 2	9.99	10.42	9.19	0.10%	-6.01%
A638/MP313E//MP313E/f_6-3_5-B_6	9.99	10.20	10.24	-2.01%	4.71%
CML277	9.93	10.40	9.54	0.19%	-2.17%
MS71	9.93	10.03	9.39	-3.40%	-3.72%
GEM 0028-2-1-B-B-B-1B-1B	9.83	9.15	9.91	-11.42%	2.19%
MP313E	9.58	10.24	N/A	0.34%	N/A
GT-888	9.46	10.81	9.93	6.55%	4.39%
M37W	9.43	7.65	10.82	-24.50%	13.97%
GT 603	9.39	8.85	8.24	-12.47%	-13.11%
Hi 63-1B-1	9.19	9.13	8.45	-8.84%	-9.90%
CML69	9.08	10.03	10.06	0.69%	7.88%
Hp301	8.78	N/A	8.85	N/A	-3.60%
CML52	8.53	8.36	8.99	-13.64%	-0.68%
GEMS 0005-1-1-1-1B-1B	8.28	9.41	10.33	-1.49%	15.82%
CML247	7.65	9.39	9.13	1.55%	6.00%

Data are means of 2014 and 2015 for inbreds, and 2015 and 2016 for hybrids.

y = mean concentrations of total aflatoxin (µg x kg^{-1})

HV is calculated as mid parent (MP) heterosis where MP = (P1 + P2)/2 and Heterosis = (F1 - MP)/MP x 100.

P1 is the average aflatoxin level in the female inbred and P2 is the same for either B73 or Lo964 with aflatoxin levels of 10.83 and 9.57 for each tester, respectively.

N/A - Not Available

CHAPTER 4

STRESS SENSITIVITY IS ASSOCIATED WITH DIFFERENTIAL ACCUMULATION OF REACTIVE OXYGEN AND NITROGEN SPECIES IN MAIZE GENOTYPES WITH CONTRASTING LEVELS OF DROUGHT TOLERANCE

Yang, L.*, Fountain, J.C.*, Wang, H., Ni, X., Ji, P., Lee, R.D., Kemerait, R.C., Scully, B.T., Guo, B. (2015). Stress sensitivity is associated with differential accumulation of reactive oxygen and nitrogen species in maize genotypes with contrasting levels of drought tolerance. *International Journal of Molecular Sciences* 16:24791-24819. doi:10.3390/ijms161024791.

 *Equal Contribution.

Abstract

Drought stress decreases crop growth, yield, and can further exacerbate pre-harvest aflatoxin contamination. Tolerance and adaptation to drought stress is an important trait of agricultural crops like maize. However, maize genotypes with contrasting drought tolerances have been shown to possess both common and genotype-specific adaptations to cope with drought stress. In this research, the physiological and metabolic response patterns in the leaves of maize seedlings subjected to drought stress were investigated using six maize genotypes including: A638, B73, Grace-E5, Lo964, Lo1016, and Va35. During drought treatments, drought-sensitive maize seedlings displayed more severe symptoms such as chlorosis and wilting, exhibited significant decreases in photosynthetic parameters, and accumulated significantly more reactive oxygen species (ROS) and reactive nitrogen species (RNS) than tolerant genotypes. Sensitive genotypes also showed rapid increases in enzyme activities involved in ROS and RNS metabolism. However, the measured antioxidant enzyme activities were higher in the tolerant genotypes than in the sensitive genotypes in which increased rapidly following drought stress. The results suggest that drought stress causes differential responses to oxidative and nitrosative stress in maize genotypes with tolerant genotypes with slower reaction and less ROS and RNS production than sensitive ones. These differential patterns may be utilized as potential biological markers for use in marker assisted breeding.

Introduction

Drought stress dramatically limits crop growth and development, and can trigger a significant decrease in crop yield and quality. This is especially evident for maize grown as a summer crop in the Southern U.S. as drought stress in combination with high temperatures aggravate stress severity, and exacerbate *Aspergillus flavus* colonization leading to pre-harvest aflatoxin contamination [1–3]. Therefore, tolerance and adaptation to drought stress is an important trait of crops, and a detailed understanding of maize responses to drought stress is of importance for crop breeding and sustainable agriculture.

Mild oxidative or nitrosative stress affects signal transduction pathways and induces gene expression [4]. More drought-related factors can disturb the normal metabolic homeostasis of crop plants producing visible foliar symptoms and impairing growth by altering the physiological, biochemical and molecular statuses of plants. Plants can adapt to drought stress by regulating the homeostasis of many biochemical pathways related to water transport, transpiration, osmotic balance, signal transduction, antioxidant mechanisms, and the protection or degradation of proteins [1,5–7]. One of the earliest events in plant drought responses is a burst of reactive oxygen species (ROS) production leading to the over-accumulation of superoxide radicals ($O_2 \cdot^-$) and hydrogen peroxide (H_2O_2) [8,9]. Despite the damaging potential of these molecules, ROS are continuously produced at a low level by some metabolic processes in plants [10]. These ROS also act as signaling molecules to regulate the expression of multiple genes and diverse stress-responsive pathways [11]. However, over-accumulation of these ROS can change the normal redox status in plants under stress conditions, and initiate oxidative damage to proteins, DNA, and lipids, ultimately leading to destruction of macromolecules and can induce the cell death in plant leaves [12–16]. Plant defense systems can provide enough protection

against ROS damage produced at normal growth conditions through enzymatic and non-enzymatic antioxidant systems [17]. Previous studies have shown that these antioxidant systems can be induced by water stress accompanied with increasing activities of superoxide dismutase (SOD) and catalase (CAT) [18,19]. However, the generation of higher levels of ROS may destroy or overwhelm the defensive capabilities of these systems resulting in oxidative stress, and further exacerbation of visible drought symptom severity [12,20].

Nitric oxide (NO) is an additional redox signal that can react with some ROS to form highly reactive molecules referred to as reactive nitrogen species (RNS). These RNS can trigger various physiological processes [21,22]. Recent studies have reported that environmental stress factors including cold, heavy metal, and salt stresses can promote NO production [23–25], and modulate the level of gene expression and enzyme activities of RNS metabolism components [22,26,27]. Nitric oxide can also enhance plant drought tolerance by regulating the leaf photosynthetic rates, relative water content, and antioxidant systems [28–30]. Moreover, Wang *et al*. [31] found that NO resulting from abscisic acid (ABA) signaling resulted in the *S*-nitrosylation of protein kinase SnRK2.6 that can further result in stomatal closure to reduce transpirational water loss.

As signal molecules, H_2O_2 and NO have a synergistic effect in response to drought stress. Liao *et al*. [32] reported that drought stress can be alleviated by dose-dependent NO and H_2O_2 in marigold explants and promote adventitious root development by improving photosynthetic performance and regulating carbohydrate and nitrogen accumulation. It has also been demonstrated that H_2O_2 can increase NO in antioxidant defense processes by activating mitogen-activated protein kinase (MAPK) cascades in maize [33]. Although stress conditions have the common effect of resulting in the accumulation of H_2O_2 and NO in plants, the biological response

employed in maize plants can be different depending on the genotype of plants, and the intensity and duration of drought stress. However, the detailed molecular mechanisms through which they work are only partly understood.

Previous research has demonstrated that maize drought tolerance is associated with different responsive patterns in the processes of redox homeostasis and ROS metabolism in kernels of maize lines possessing differing drought sensitivities. For example, moderate drought stress triggers increases in the expression of ROS-scavenging enzymes such as SOD, glutathione S-transferase (GST), and antioxidant enzymes such as thioredoxin and peroxiredoxin in kernels of the sensitive maize genotype B73 as compared to the tolerant genotype Lo964 [19]. Expression profiling of genes encoding the proteins mentioned above have also exhibited genotype-specific responses in drought tolerant and sensitive maize lines in previous studies [34–39]. In order to further characterize the impact of drought stress on maize, the time-dependent responsive patterns in physiological and photosynthetic indices, specifically ROS and RNS metabolism components, were monitored in the leaves of six genotypes displaying varying sensitivity to drought stress. It was found that drought stress induced differential patterns of oxidative and nitrosative stress in tolerant and sensitive maize genotypes (Table 4.1). Given these differential patterns, it is possible that these indices can be utilized as biological markers in marker-assisted breeding to enhance maize drought tolerance and its secondary impact on aflatoxin contamination.

Materials and Methods

Plant Materials and Growth Conditions

Six different maize inbred lines with differential sensitivity to drought stress were used for this study (Table 4.1). Kernels of the maize inbred lines were sown into pots (30 cm diameter, 25 cm depth, 10 kernels per pot) that were lined with a polyethylene liner, filled with locally collected field topsoil, placed in a natural lighted greenhouse, and sufficiently watered with tap water at the USDA-ARS, Crop Protection and Management Research Unit, Tifton, GA, USA. Ten days after planting (10 DAP; vegetative 2 (V2) growth stage), pots were thinned to five plants with uniform growth were left in each pot. At 30 DAP (V3/4 growth stage), pots were divided into two groups per inbred, one being normally watered (well-watered controls), while the other was subjected to progressive drought stress by withholding the water for 9 days, followed by a recovery period of normal irrigation for 3 days. During the drought treatment period, the temperature ranged from 35 to 42 °C during the day and from 22 to 28 °C at night inside the greenhouse. Soil water content was monitored to assess the stress level using the method described by Cellier *et al.* [85]. The maize seedlings were utilized for morphological, physiological and biochemical measurements from both treatments at 3, 6 and 9 DAI and 3 days of recovery (12 DAI). The experiments were conducted in two biological replicates with six and three technical replicates for each biological replicate, respectively.

Measurement of Plant Growth Rate and Leaf Relative Water Content

Plant growth was measured according to Chen *et al.* [41] with slight modification. At the initiation of drought treatment (0 DAI), initial plant height was measured (H_o, height from soil surface to the base of first mature leaf), and was measured again at each treatment time point (H_e).

Plant growth (post-treatment) was then calculated as (H_e–H_o). The effect of drought on plant growth was expressed as the ratio of drought treatment height increase [(H_{ed}–H_{od})/H_{od} × 100%] in comparison to the well-watered (WW) controls [(H_{ew}–H_{ow})/H_{ow} × 100%].

The changes in leaf relative water content (LRWC) under drought stressed conditions were examined at each time point also using the method reported by Chen *et al.* [41]. To measure LRWC, a leaf segment (4 cm) was sampled from the middle section of the upper, fully expanded leaves and placed into a pre-weighed and pre-labeled tube at the same time of day for each collection (9:00–10:00am), and the fresh weight was measured after excision. The fully turgid fresh weight was measured after immersing the tissues in deionized water at 4 °C for 6 h. Dry weight was measured after drying the samples at 105 °C for 24 h. The LRWC was then calculated as (fresh weight − dry weight)/(turgid weight − dry weight) × 100%. The tube was capped immediately and then stored in a refrigerator (~4 °C). A total of six leaves per replicate were collected from six different plants.

Photosynthesis Parameters Measurements and Determination of Chlorophyll

The P_n, G_s, C_i and T_r were measured from 9:00–11:00 in the morning for every collection time on the leaves of four to five plants per line and treatment combination using a LI-6400XT Portable Photosynthesis System (Li-Cor, Lincoln, NE, USA) with light source (6200-02B LED, Li-Cor). The [CO_2] in the leaf chamber was controlled by the LI-Cor CO_2 injection system with the following chamber settings: (i) photosynthetic photon flux density of 1500 μmol m^{-2} s^{-1}; (ii) sample chamber CO_2 held constant by the CO_2 mixer at 400 μmol·mol^{-1} air. Leaf chlorophyll content was then measured using a portable chlorophyll meter (SPAD-502, Minolta, Tokyo, Japan).

ABA and IAA Content Measurement in Leaves

The ABA and IAA content assays were carried out using an ELISA-based method with the Phytodetek ABA and IAA test kit (Agdia, Elkhart, IN, USA) according to the manufacturer's instructions and Jiang *et al*. [37]. Briefly, for the ABA assay, leaf tissues were ground in liquid nitrogen and extracted in 80% methanol with 10 mg/L butylated hydroxytoluene (BHT), and 50 mg/L citric acid in the dark for 16 h with shaking at 4 °C. The supernatant was collected after centrifugation at 4000 rpm for 20 min and diluted 10-fold with 50 mM Tris, 1 mM $MgCl_2$, 150 mM NaCl, pH 7.5) for use with the Phytodetek ABA test kit. For the IAA content assay, IAA from leaf tissues was extracted and methylated by 2 M trimethylsilyl-diazomethane in hexane, and incubating for 30 min. The samples were dried and re-suspended in 500 µL 10% methanol solution. The IAA content was determined using a plate reader (Titertek Multiskan photometer, Titertek Instruments Inc. Winooski, VT, USA).

Superoxide Radical Staining and Quantification

The *in situ* detection of superoxide radical was done using nitroblue tetrazolium (NBT) (BP108-1, Fisher Scientific Inc., Pittsburgh, PA, USA) as a substrate according to the method of Jabs *et al.* [86] and Rao *et al.* [87] with modification as follows. Leaves were immersed in 12 mL NBT staining solution (6.0 mM NBT in 10 mM potassium phosphate containing10 mM NaN_3) in a 15 mL falcon tube and sand infiltrated using a vacuum pump for 20 min (KNF Neuberger, Inc., Trenton, NJ, USA). The samples were then illuminated using a light box (Model No. 300, 60 Hz, Wolf X-Ray Corp., Valdosta, GA, USA) for 8 h. After infiltration and illumination, the stained leaves were bleached in a solution of acetic acid-glycerol-ethanol (1:1:3) (*v*/*v*/*v*) at 100 °C for 2 h, and then stored in a glycerol-ethanol (1:4) (*v*/*v*) solution. Leaves were photographed under

uniform lighting. Superoxide quantification was conducted according to previously described methods [88,89]. Briefly, the stained leaves were ground in liquid nitrogen and solubilized in 2 M KOH-DMSO (1/1.16) (*v*/*v*) for 4 h, and then centrifuged for 30 min at 20,000× *g*. The absorbance at 630 nm was measured using a plate reader (Titertek Multiskan photometer, Titertek Instruments Inc., Huntsville, AL, USA). Experiments were repeated three times on at least three leaves.

Hydrogen Peroxide Staining and Quantification

The *in situ* detection of hydrogen peroxide is conducted by staining with 3,3′-diaminobenzidine tetrahydrochloride hydrate (DAB) (AC11209-0050, ACROS Organics, Pittsburgh, PA, USA) using previously described methods with slight modification [90–92]. For staining, 3–5 leaves from each time point were sampled and immediately placed in 15 mL falcon tubes. DAB staining solutions were freshly prepared by adding 50 mg DAB to 47.5 mL H_2O in a tube covered with aluminum foil, and, with constant stirring, the pH was reduced to 3.0 with 0.2 M NaOH prior to adding 25 μL Tween 20 and 2.5 mL 200 mM Na_2HPO_4. The staining solution was applied to the leaves in the tubes, and the volumes were adjusted to ensure that the leaves were completely immersed. The leaves were gently infiltrated under a vacuum for 20 min. The tubes were then covered with aluminum foil, and incubated for 4 h with gentle shaking (80 rpm) at room temperature in the dark. Following incubation, the staining solution was replaced with bleaching solution (ethanol:acetic acid:glycerol [3:1:1]), and the tubes were placed in 100 °C water bath for about 2 h until the chlorophyll was bleached out, and then stored in a glycerol-ethanol (1:4) (*v*/*v*) solution. The leaves were then photographed on a plain white background under uniform lighting. The H_2O_2 content was measured using the method reported by Kotchoni *et al.* [93].

Briefly, the DAB-stained leaves were ground in liquid nitrogen, and was homogenized in 0.2 M $HClO_4$. The homogenate was then centrifuged for 10 min at 20,000× *g*. The absorbance of the supernatant at 450 nm was measured using a plate reader (Titertek Multiskan photometer, Titertek Instruments Inc., Huntsville, AL, USA).

Extraction and Activity Determination of SOD and CAT

Crude protein/enzyme extraction was performed in accordance with Ramel *et al.* [94] with slight modification. Leaf tissues were ground in liquid nitrogen and suspended in 5 mL of 50 mM phosphate buffer (pH 7.8) containing 0.5% (*w*/*v*) polyvinylpyrrolidone (PVP-40), 0.1% (*v*/*v*) TritonX-100, 1 mM EDTA (pH 7.4) and a mixture of protease inhibitors (1 mL per 30 g plant tissues) (P9599, Sigma-Aldrich, St. Louis, MO, USA) for 20 min at room temperature. Homogenates were centrifuged at 4000× *g* for 20 min at 4 °C. Supernatants obtained were used for enzyme activity determination. Concentrations of the protein extracts were determined using a Bradford protein assay kit (Bio-Rad, Hercules, CA, USA) with bovine serum albumin (BSA) as a standard. The SOD activity was measured using the method reported by Beauchamp and Fridovich [95]. Briefly, an enzyme extract was mixed with 50 mM potassium phosphate buffer (pH 7.5), 130 mM methionine, 750 µM NBT, 20 µM riboflavin, and 100 µM EDTA, and the reaction mixtures were illuminated under a Transilluminator (115V, 60 Hz, VWR TW-26, VWR Scientific, Valdosta, GA, USA) at room temperature for 20 min. The CAT activity was measured with Spectro UV-Vis Auto UV-2602 (Labomed Inc., Culver City, CA, USA) at 240 nm by measuring the digestion of H_2O_2 ($E = 39.4\ mM^{-1} \cdot cm^{-1}$) in 50 mM potassium phosphate buffer (pH 7.5) with protein extract as described by Aebi [96].

Detection and Quantification of NO

Nitric oxide (NO) was visualized using 4-amino-5-methylamino-2′,7′-difluorofluoroscein diacetate (DAF-FM diacetate; D-23844, Invitrogen, Carlsbad, CA, USA), based on the method used previously by Yang *et al.* [25]. Leaf segments were immersed and vacuum infiltrated with 10 µM DAF-FM DA in 50 mM Tris-HCl buffer (pH 7.4). Infiltrated leaf segments were then incubated for 2 h at 37 °C, then fluorescence was detected using a Zeiss SV epi-fluorescence stereomicroscope with a 480 ± 30 nm excitation filter and a 515 nm emission filter (Chroma Technology, Brattleboro, VT, USA) coupled with a Zeiss Axiocam digital camera. The relative quantification of NO in leaves was conducted using DAF-FM DA according to published protocols [97,98]. Leaf segments of approximately 12 mm^2 were incubated with 10 µm DAF-FM diacetate in 10 mM Tris-HCl (pH 7.5) in 96-well plates, and were then washed in the same buffer for 30 min. Fluorescence measurements were obtained on a fluorescent plate reader (Synergy HTX Multi-Mode Reader, Biotek, Winooski, VT, USA). Fluorescence intensity was calculated by subtracting the DAF fluorescence measured in leaves from wells with Tris-HCl buffer only. The staining procedure for each sample was conducted with three replicates.

Determination of the NOS and GSNOR Activities

The NOS activity was measured using a Nitric Oxide Synthase Assay Kit (EMD Millipore, Billerica, MA, USA) based on the manufacturer's instructions. Total protein was extracted with 100 mM HEPES-KOH (pH 7.4), 1 mM EDTA (pH 7.4), 10% glycerol (*v*/*v*), 5 mM DTT, 10 µM PMSF, 0.1% Triton X-100 (*v*/*v*), 1% polyvinylpyrrolidone (PVP-40) and 20 µM FAD. GSNOR activity was measured as described by Corpas *et al*. [27].

Statistical Analysis

Analysis of Variance (ANOVA), Pearson correlation and clustering were performed using in-house developed R-software (R Development Core Team, Vienna, Austria). Principal component analysis was performed by "bpca" algorithm from the pcaMethods package [99]. The ANOVA analysis was conducted using Genotype, Treatment, and Tolerance as factors. The *p*-values were corrected using the method reported by Bonferroni and Yekutieli [100].

To estimate the statistical significance between means, ANOVA was performed for the entire dataset using SPSS v.15.0 (SPSS Inc., Chicago, IL, USA). The means ($n = 6$) were separated using Fisher's Least Significant Difference (LSD) test with $\alpha = 0.05$. Means not significantly different ($p > 0.05$) share the same letter in graphical representations, provided by the GraphPAD software (v.5.01, GraphPad Software Inc., San Diego, CA, USA). The data were Box-Cox transformed prior to use in PCA using the NIA array analysis tool [101]. We used the default settings for the analysis except for the false discovery rate (FDR) threshold defined as 0.01. For the PCA analysis, the settings were as follows: covariance matrix type, principal components, one-fold change threshold for clusters, and 0.8 correlation threshold for clusters as used by Chen *et al.* [102].

Results

Seedling Morphological Responses to Drought in Selected Maize Genotypes

To examine the responses of selected maize genotypes to drought stress, the morphological responses of the tolerant lines A638, Grace-E5, Lo964, and Va35 along with the sensitive lines B73 and Lo1016 (Table 4.1) to drought stress were measured every 3 days after induction (DAI) until 12 DAI for the drought treated and irrigated control samples at the V3-V4 growth stage.

The drought stress was applied up to 9 DAI in the treated samples with a watered recovery period from 9 to 12 DAI. As expected, drought stress resulted in a visible loss of turgor with curling and wilting symptoms apparent in seedling leaves during the period of drought, and this phenotype gradually worsened with continuing decreases in soil water content (SWC) over time. The SWC was held consistent in the pots of all six maize lines at each time point throughout the drought treatments (Figure S4.1). The sensitive lines exhibited more visible symptoms in response to drought treatments with increased flaccidity in seedling leaves from 3 to 9 DAI with the most obvious symptoms observed by 9 DAI, and with some seedlings dying during the course of the study. The tolerant lines, however, exhibited wilting symptoms later than the sensitive lines during the drought treatment.

Following the irrigated recovery period from 9 to 12 DAI, the tolerant lines displayed relatively stronger growth recovery from drought stress with only about half of the sensitive line plants survived. The growth rates of the seedlings were also measured during the course of the experiment. The growth rates up to 3 DAI were higher than those observed at 6 DAI and 9 DAI under drought treatment conditions in all the lines (Figure S4.2). Although the growth rates of the six maize lines showed the same decreasing trend during the progressive water deficit treatment, the growth rates of sensitive lines B73 and Lo1016 reached 0 at 6 DAI, but the other lines stopped growing at 9 DAI (Figure S4.2). After 3 days of recovery from water deficit stress, the growth rate of all lines remained unchanged. Leaf relative water content (LRWC) was also examined in samples at 2 days prior to drought treatment (noted as "−2 DAI"). The LRWC decreased at 3 DAI, and continued to decrease at 6 and 9 DAI, with the LRWC of the tolerant lines Va35 and Grace E-5 being significantly higher than that of the sensitive lines B73 and Lo1016, especially at 9 DAI (Figure S4.3).

Changes of Chlorophyll Content and Photosynthesis Parameters in Response to Progressive Drought Stress and Recovery

To determine the influence of drought stress on photosynthetic capacity, leaf chlorophyll content and photosynthetic parameters were investigated. The chlorophyll content of B73 and Lo1016 was significantly lower than that observed in the other four lines under the non-stressed condition (Figure S4.4). Although chlorophyll content was decreased following the drought treatments for the six maize lines, the chlorophyll content of stressed B73 and Lo1016 leaves was significantly lower than that of moderately tolerant and tolerant lines at 3 and 6 DAI. The tolerant lines and A638 have higher chlorophyll content under drought stress than the susceptible lines under drought or irrigated conditions at 9 DAI, and stress recovery for 3 additional days did not result in an obvious increase in chlorophyll content (Figure S4.4).

Four maize lines, including sensitive lines B73 and Lo1016 and tolerant lines Lo964 and Va35, were selected to investigate their photosynthesis parameters in leaves, soil water deficit decreased the leaf photosynthesis rate (P_n) (Figure 4.1A). The influence of drought stress on P_n in B73 and Lo1016 was more rapid than that of Lo964 and Va35. In B73 and Lo1016, P_n decreased by 85.3% and 88.4%, respectively, by 9 DAI relative to the well-watered controls while P_n had decreased by 74.9% and 76.0% in Lo964 and Va35, respectively. After 3 days of stress recovery (12 DAI), P_n was restored to only 49.0% and 40.3% of the level of the non-stressed controls for B73 and Lo1016, respectively, compared to 69.4% and 65.2% in Lo964 and Va35.

A similar pattern occurred in the stomatal conductance (G_s) of the sensitive and tolerant lines in response to drought stress (Figure 4.1B). The P_n and G_s for Lo964 and Va35 were higher than those observed in B73 and Lo1016 throughout the water deficit treatment and stress

recovery periods. Intercellular CO_2 concentration (C_i) increased with drought treatment, and the highest C_i was observed for drought-treated Lo1016 and B73 at 9 DAI, which had a larger increase in C_i in the drought treatment in comparison to their respective well-watered controls in contrast to Lo964 and Va35 which showed a slight increase during the progressive drought treatment (Figure 4.1C). However, all the selected lines did not show a marked difference in C_i following stress recovery. In addition, the drought stress treatment significantly decreased the transpiration rate (T_r) in all the six lines during progressive water deficit stress (Figure 4.1D). However, B73 and Lo1016 showed a rapid initial decrease in T_r while Lo964 and Va35 showed a gradual, progressive decrease in T_r during the process of water deficit treatment.

Drought Responses of Abscisic Acid (ABA) and indole-3-acetic Acid (IAA) Contents

Abscisic acid (ABA) and indole-3-acetic acid (IAA) are important phytohormones in plant responses during drought stress and development [49,50], therefore, subsequent changes of ABA and IAA contents in maize seedling leaves under drought stress were determined. Drought-stressed maize leaves exhibited higher ABA content than ones under well-watered conditions. At 3 and 6 DAI, drought-stressed B73 and Lo1016 presented a sharp rise in ABA contents, then a significant decrease with ongoing stress compared to the well-watered controls (Figure 4.2A). However, the ABA contents displayed a progressively increasing trend for Lo964 and Va35 during continued drought induction, and recovery did not reduce ABA contents to the level of well-watered controls (Figure 4.2A). Drought stress induced an increase of IAA content in maize seedling leaves. IAA contents gradually increased at 3 to 9 DAI of drought stress, and drought recovery decreased the IAA contents close to the level of well-watered plants in the tolerant lines (Figure 4.2B). For B73 and Lo1016, IAA contents increased dramatically at 3 to 6 DAI, and then

decreased at 9 DAI, but IAA levels did not recover to the level of well-watered plants (Figure 4.2B).

Effect of Drought Stress on ROS Metabolism

Detection of $O_2^{\cdot-}$ through the use of Nitroblue Tetrazolium Chloride (NBT) staining indicated that B73 and Lo1016 accumulated much more $O_2^{\cdot-}$ than A638, Lo964, Va35, and Grace E-5 over time in response to drought stress (Figure 4.3A). Although recovery decreased the content of $O_2^{\cdot-}$ in the leaves of B73 and Lo1016, the $O_2^{\cdot-}$ quantities were still higher than that of A638, Lo964, Va35, and Grace E-5 (Figure S4.5A). Specifically, B73 and Lo1016 accumulated approximately 2.5 times more $O_2^{\cdot-}$ in their leaves in comparison to Lo964 and Va35 (Figure S4.5A). Time-course detection of H_2O_2 accumulation using 3,3′-diaminobenzadine (DAB) staining in the leaves revealed that no obvious changes in well-watered controls, whereas H_2O_2 content increased progressively in drought-induced leaves over time with B73 and Lo1016 accumulating more H_2O_2 than Lo964, Va35 and Grace E5 which is consistent with microscopy observations. Also, the moderately resistant line A638 showed more H_2O_2 accumulation than Lo964, Va35 and Grace E5, but less than B73 and Lo1016 (Figures 4.3B and S4.5B). These results showed that stress occurred in the leaves of maize seedlings under drought treatment conditions causing severer oxidative stress for sensitive and moderate lines than for tolerant ones.

The activities of two key antioxidant enzymes, superoxide dismutase (SOD) and catalase (CAT) were measured to determine their roles in defense during drought treatments. It was found that the antioxidant enzyme activities were enhanced in response to oxidative stress in the examined drought stressed maize lines (Figure 4.4A,B). Specifically, SOD activity in the leaves

of B73 and Lo1016 increased by 2-fold immediately after drought treatment for 3 days then decreased gradually at 6 and 9 DAI. However, SOD activity increased by 1.3, 1.6, and 1.6 folds in Lo964 and Va35 at 3, 6 and 9 DAI, respectively, displaying a progressive increasing trend. But, SOD activities in A638 and Grace E-5 were induced at a high level at 3 and 6 DAI, and then decreased at 9 DAI (Figure 4.4A). The CAT activities displayed a rapid increase and then a slight drop after drought treatment for 3, 6 and 9 DAI by 3.4, 3.6 and 2.7 folds in B73 and Lo1016. The remaining lines displayed a gradually increasing pattern in CAT activities (Figure 4.4B). Although drought recovery reduced the activities of SOD and CAT, they remained higher in the drought stressed plants than in the well-watered controls.

NO Production and RNS-Related Enzyme Activities during Drought Stress

An NO-specific fluorescent probe, 4-amino-5-methylamino-2',7'-difluorofluorescein diacetate (DAF-FM DA), was used to monitor the endogenous NO production in the leaves of the six maize lines. Significant changes in NO content were observed between lines with contrasting drought sensitivity at 3 and 9 DAI and 3-day recovery (Figure 4.5). Normal irrigated plants had the weak NO fluorescence during 12-day period, but drought stress resulted in an increase of NO fluorescence intensity. Significant increases in NO accumulation were observed at 3 and 6 DAI with the most significant NO accumulation observed at 6 DAI. Slight decreases were also observed at 9 DAI in the leaves of B73 and Lo1016 and moderately tolerant A638. However, drought stress induced a gradual increase in NO accumulation from 3 to 9 DAI in Lo964, Va35 and Grace E-5 (Figure 4.5).

Quantitative analyses showed that the intensity of NO accumulation in the leaves of well-watered control maize plants were relatively constant during the 12-day period. An early burst of

NO at 3 DAI was around 1.5-fold higher in the sensitive lines B73 and Lo1016 and moderately tolerant A638 than in the tolerant lines Lo964, Va35 and Grace E-5, and then reached to about 2.1-fold higher at 6 DAI. The NO content displayed a gradually increased trend in the tolerant lines Lo964, Va35 and Grace E-5 in response to drought, though not as much as determined in the sensitive lines B73 and Lo1016 and moderately tolerant A638 (Figure S4.6). This increasing trend of NO accumulation is consistent with that of $O_2^{\cdot-}$ and H_2O_2 in B73 and Lo1016 under drought stress. Lo964, Va35 and Grace E-5 illustrated the same response profiles in NO, $O_2^{\cdot-}$ and H_2O_2 accumulation under drought treatment conditions. For the moderately tolerant line A638, the response pattern of gradual increasing at 3–6 DAI and slight decreasing at 9 DAI for NO accumulation is different from the gradually increasing trend at 3–9 DAI for $O_2^{\cdot-}$ and H_2O_2 under drought stress conditions (Figures 4.3 and 4.5).

Nitric oxide synthase (NOS) serves as a key enzyme for NO biosynthesis [51,52]. To examine the contribution of NOS to the drought-induced NO burst previously observed in the maize seedling leaves, we measured NOS activity in the lines during drought stress. NOS activities were found to vary significantly among the lines under drought stress (Figure 4.6A). The lines B73 and Lo1016 had significantly higher NOS activities than Lo964, Va35 and Grace E-5 at 3 and 6 DAI. Drought treatment triggered significantly elevated NOS activity at 3 and 6 DAI in B73 and Lo1016, 1.5 and 2.0-fold, respectively, which then reduced to levels similar to the well-watered controls at 9 DAI. In contrast, the NOS activities in Lo964, Va35 and Grace E-5 exhibited a slight increasing trend after drought treatment. After stress recovery, NOS activities declined to levels similar to those of the well-watered controls (Figure 4.6A).

S-nitrosoglutathione reductase (GSNOR), as a RNS-scavenging enzyme, can control NO levels, regulate *S*-nitrosylation of proteins by modifying cysteine residues using NO, and reduce

the content of *S*-nitrosoglutathione (GSNO) [22,53]. The GSNOR activity in drought treated B73, Lo1016, and A638 increased rapidly up to 1.9, 1.5 and 1.3 folds higher than that of the well-watered controls at 3 DAI, respectively, then dropped to below the levels of the well-watered controls at 6 and 9 DAI. Three days after a recovery irrigation, GSNOR activities were not restored to normal levels found in the controls (Figure 4.6B). Conversely, GSNOR activities in Lo964, Va35, and Grace E-5 did not display significant changes at 3 DAI, then exhibited slight and gradual increasing profiles at 6–9 DAI compared to the controls, and 3-day recovery decreased the GSNOR activities to the same level as that of well-watered plants.

Physiological and Biochemical Patterns Allow Clear Separation of Drought Tolerance Characterization between Different Maize Lines

Subjecting the physiological and biochemical data to a principal component analysis (PCA) separated the lines relative to all indices, independent from genotype or treatment influences (Figure 4.7), indicating significant differences exist within the physiological and biochemical indices between the different lines. PC1 (73% variance) separates the different treatments (well-watered and drought stress conditions), and shows that drought-treated lines display obviously different stress response patterns in comparison to well-watered ones with the lines divided into two groups. The first group includes Lo964, Va35, and Grace E5; and the second group includes B73, Lo1016, and A638. PC2 (13% variance) separates the different reactions of all lines responding to drought stress, and shows that Lo964, Va35, and Grace E5 have contrasting drought tolerance levels in comparison with B73, Lo1016, and A638.

Under well-watered conditions, all the lines show very similar responsive patterns, while under drought-treatment conditions the lines exhibited more diverse physiological and

biochemical changes with regard to their genetic background (Figures 4.7 and S4.7). The PCA analysis also separated lines predicted to be drought-sensitive or tolerant, and indicated that the factor that influenced the measured traits most was stress treatment, followed by genotype. In addition, the separation due to drought treatment was most profound at 6 and 9 DAI compared to 3 DAI (Figure S4.7).

Correlation and Variance Analysis of All Tested Traits in All Lines

In this study, we sought to correlate the physiological responses of the maize lines during drought stress with hormone content and biochemical processes involved in ROS and RNS metabolism. Therefore, a correlation analysis of all the tested parameters was performed and as shown in Figure 4.8. From the correlation matrix heat map, a positive correlation between hormone accumulation and RNS metabolism and ROS-scavenging enzyme activities was observed (Figure 4.8A). A positive correlation between G_s, NO, and ROS was also observed. Photosynthesis parameters P_n, G_s, and T_r also positively correlated with chlorophyll content and LRWC. A strong negative correlation for the photosynthesis parameters P_n, G_s, and T_r with the ROS and RNS systems was observed, and GSNOR negatively correlated with the ROS components $O_2\cdot^-$ and H_2O_2 (Figure 4.8A). Analysis of the variance showed that drought treatment and variety significantly contributed to the variance observed in the physiological and biochemical traits (Figure 4.8B). The variation in ROS content and activities of ROS-scavenging enzymes were highly significant among maize genotypes under drought stress conditions and water recovery; however, less variation was recorded in chlorophyll content and GSNOR activity.

Time-series hierarchical clustering analysis of each tested trait separates all six lines into two main clusters which is consistent with the lines' corresponding sensitivity to drought stress. Cluster one includes drought-sensitive lines B73 and Lo1016, and moderate A638; the second cluster contains the drought-tolerant lines Lo964, Va35 and Grace E5, with the exception of chlorophyll content and LRWC (Figure S4.8). This result is supported by the PCA analysis as shown in Figure 4.7, and consistent with the analysis of variance shown in Figure 4.8B. As expected, NO and its synthetic enzyme NOS exhibit the same clustering patterns to all lines, showing their close correlation in NO metabolism.

Discussion

Morphological and Physiological Responses to Drought Stress

Continuous drought stress resulted in significant growth inhibition in all tested lines, with the effect being much more pronounced in B73, Lo1016 and A638, and the drought tolerance of these six lines is consistent with previous reports determined through the observation of morphological responses to drought stress (Table 4.1). Photosynthetic parameters were affected by drought treatment in all tested lines, decreases in P_n, G_s and T_r and increase in C_i values may imply that the plant is subjected to stress conditions [54,55], and it can be proposed that the inhibition of photosynthesis was caused by the hypersensitive early stomata closure, with more pronounced occurrence in sensitive genotypes [56]. In addition, higher C_i but lower photosynthetic rate may be caused by non-stomatal factor [55,57].

The morphological injury and growth inhibition caused by drought stress is transmitted by a hormone signals such as ABA and IAA which are induced during drought [37,58,59]. A rapid induction of ABA and IAA in leaves of maize seedlings was found under drought stress

conditions, with more rapid and higher increases observed in the sensitive genotypes in comparison to the tolerant ones, which was similar with the results in Lo1016 and Lo964 under PEG-induced stress [37]. Taken together, these results imply that hormone signaling functions during drought stress to regulate photosynthetic processes in order to cope with stress-related damage [60,61]. Plant adaptation to stress can also be regulated through ABA-based activation of ROS signaling [62]. These ROS molecules function as second messengers, and play a rate-limiting role in ABA signal transduction [63,64].

Drought Stress Induces an ROS Burst and Disturbs the Redox Homeostasis

ROS can be transient induced in the early events of plant response to stress, and can be considered to act as secondary message for induction of stress response [65,66]. But excess ROS accumulation can be induced following stress treatment to a certain extent, and damages the plant [67,68]. Drought stress can cause ROS accumulation in plant leaves, and the observed ROS patterns greatly depend on the time and severity of the stress [18,69]. Therefore, it is important to characterize the profiles of ROS accumulation associated with specific drought stress conditions. As expected, drought stress resulted in increases of ROS, specifically $O_2^{\cdot -}$ and H_2O_2, levels especially in sensitive lines, which accumulate ROS at the early stages of drought treatment, while tolerant lines progressively and gradually accumulate ROS. This indicates that this drought treatment resulted in severe oxidative stress to the sensitive lines and moderate one, but relatively mild stress for the tolerant lines. These observations are supported by the different phenotypic and morphological traits of these maize genotypes under the same drought treatments.

In order to avoid oxidative injury due to ROS accumulation; plants possess complex antioxidant systems to scavenge ROS. The well-known antioxidant enzymes SOD and CAT can catalyze the decomposition of O_2^- and H_2O_2; respectively; to prevent the over-accumulation of these ROS. Interestingly; drought treatments resulted in increased CAT and SOD activities in all the tested seedlings likely in response to the over-production of O_2^- and H_2O_2 in order to prevent the oxidative injury. It can be suggested that drought stress induced a rapid production of ROS leading to disruption of cellular redox homeostasis and activation of the antioxidative system and ROS-scavenging enzymes [15,66].

In this study, drought stress induced differential responsive profiles of SOD and CAT activities in sensitive and tolerant lines with higher activities and levels being rapidly induced in sensitive lines at the initial stage of drought treatments compared to tolerant ones which displayed gradually increased patterns. Similar phenomena were also found in kernels of B73 and Lo964 subjected to drought stress in our previous research [19]. In addition, drought stress-induced ROS over-production and scavenging enzyme activities were reduced by water recovery, especially in tolerant lines compared to sensitive lines. Similar ROS accumulation and induced increase activities of antioxidant enzymes have been described for other plants. For example, in *Lotus japonicus*, water deficit caused an increase in ROS production accompanied by an increase of antioxidant enzymes [18], and drought has been shown to induce a much stronger oxidative stress in leaves of drought-sensitive varieties of barley compared to tolerant ones [70]. Plant adaptation to drought stress may depend on different response and defense mechanisms to oxidative damage in different genotypes, including the ability to maintain high levels of antioxidant system activity [71].

Drought Stress Affects NO Homeostasis

Drought stress caused an increase in NO production in all tested maize genotypes and was more pronounced in sensitive genotypes. This result implies that NO participates as an important messenger in the defense processes of plants, specifically maize, in responding to drought stress [72]. Similar results relating increased NO content to drought stress responses have been described in leaves of *Poncirus trifoliata* and *Lotus japonicus* [18,28], and under other stress conditions [25,27,73]. It has also proposed that NO is a signaling intermediate in enhancing the tolerance of maize seedlings to drought stress [72]. The NO content response patterns in the leaves is also well correlated with the increase of NOS activities observed during drought treatments in this study. This suggests that NOS activity, as one of the sources of NO, may be up-regulated to generate more NO in response to drought stress. Additionally, increased GSNOR activities were also found in the leaves of all six lines under drought stress. The GSNOR enzyme is a key regulator of NO synthesis and homeostasis [74,75]. Frungillo *et al*. [76] reported that mutation and silencing of *GSNOR*1 caused NO accumulation in *Arabidopsis thaliana*. Hence, it is proposed RNS scavenging systems such as GSNOR are produced in response to over-accumulation of NO in plants, which may result in nitrosative stress, in response to stress conditions.

Drought Stress Responses Involve Interconnections between ROS and RNS

Plants possess effective and fine-tuned mechanisms to regulate the metabolic balance, and to control the levels of all kinds of molecules, including ROS and RNS levels [30]. The results obtained here indicate that drought stress resulted in an imbalance in ROS and RNS metabolism and homeostasis, especially in drought sensitive genotypes. This suggests that drought treatments

induce oxidative and nitrosative stress in maize seedlings to different degrees in sensitive and tolerant genotypes. It is known that ROS and RNS metabolism are closely connected and cross-reacted, and that ROS and NO can directly interact to form peroxynitrite ($ONOO^-$), nitrous oxide (NO_2), and other RNS species [30,77,78]. In this study, drought stress disturbed the redox state homeostasis of ROS and RNS. Wang *et al.* [79] reported that ROS can trigger NO synthesis in roots of *Arabidopsis*, and it was also reported that NO also influenced ROS production and promoted the increases of ROS-scavenging enzymes in plants
under stress conditions [25,80].

Drought stress-induced ROS and RNS production may be involved in pathogen infection and aflatoxin production. It has been proposed that ROS may stimulate aflatoxin production in maize and other crops [3,81], and NO may function in response to infection of *Fusarium verticillioides* in maize [82,83]. From these reports, it was implied that a complex feed-back regulation exists between ROS and RNS metabolism in plants under drought stress. In this work, ROS and RNS bursts were induced simultaneously in the tested maize genotypes, and over-accumulation of ROS and RNS caused severe oxidative and nitrosative stress on maize seedlings, which further exacerbated the visible symptoms such as wilting and necrosis. Subsequently, plants may be more susceptible to pathogen infection due to weakened defensive capabilities.Drought stress induced a differential change of physiological and biochemical parameters in maize lines with different tolerance levels, this provides a potential link between drought stress and intensity of physiological and biochemical changes. The selection of parameters involved in these physiological and biochemical processes such as metabolites, proteins, or gene expression levels may allow them to be utilized as biomarkers for use in breeding applications [81,84].

Conclusion

The results in this study showed that drought stress resulted in obvious morphological and physiological changes, and induced a rapid accumulation of ROS and NO. This resulted in oxidative and nitrosative stress and activated the antioxidant defense system, primarily characterized by increases of SOD and CAT activities in all tested lines. The metabolic alterations of ROS and RNS levels were more pronounced in the sensitive lines as compared to the tolerant ones with the same being true for the activities of ROS and RNS scavenging enzymes. This implies that a much more vigorous metabolic response was likely triggered in the sensitive lines than in the tolerant lines. Taken together, these observations suggest that maize lines with contrasting drought sensitivity possess different defensive and responsive processes counteracting oxidative and nitrosative damage. However, possible synergistic effects and homeostasis of ROS and RNS in this system under drought stress conditions have yet to be elucidated and warrant further study.

Acknowledgments

We would like to thank Billy Wilson, Frank Lin, and Joseph Harnage for technical assistance in the greenhouse and laboratory. This work is partially supported by the U.S. Department of Agriculture Agricultural Research Service (USDA-ARS), the Georgia Agricultural Commodity Commission for Corn, AMCOE (Aflatoxin Mitigation Center of Excellence), and Qinglan Project of Jiangsu Province. Mention of trade names or commercial products in this publication is solely for the purpose of providing specific information and does not imply recommendation or endorsement by the USDA. The USDA is an equal opportunity provider and employer.

Supplemental Information

Links to supplemental datasets, figures, and tables can be found in Appendix A.

References

1. Guo, B.Z.; Chen, Z.Y.; Lee, R.D.; Scully, B.T. Drought stress and preharvest aflatoxin contamination in agricultural commodity: Genetics, genomics and proteomics. *J. Integr. Plant Biol.* **2008**, *50*, 1281–1291.
2. Scully, B.T.; Krakowsky, M.D.; Ni, X.Z.; Wilson, J.P.; Lee, R.D.; Guo, B.Z. Preharvest aflatoxincontamination of corn and other grain crops grown on the U.S. Southeastern Coastal Plain. *Toxin Rev.* **2009**, *28*, 169–179.
3. Fountain, J.C.; Scully, B.T.; Ni, X.; Kemerait, R.C.; Lee, R.D.; Chen, Z.Y.; Guo, B. Environmental influences on maize-*Aspergillus flavus* interactions and aflatoxin production. *Front. Microbiol.* **2014**, *5*, 40.
4. Fink, G. *Encyclopedia of Stress*; Academic Press: San Diego, CA, USA, 2000; Volume 3, p. 1341.
5. Farooq, M.; Wahid, A.; Kobayashi, N.; Fujita, D.; Basra, S.M.A. Plant drought stress: Effects, mechanisms and management. *Agron. Sustain. Dev.* **2009**, *29*, 185–212.
6. Luo, M.; Liu, J.; Lee, R.D.; Scully, B.T.; Guo, B.Z. Monitoring the expression of maize genes in developing kernels under drought stress using oligo-microarray. *J. Integr. Plant Biol.* **2010**, *52*, 1059–1074.
7. Alvarez, S.; Roy Choudhury, S.; Pandey, S. Comparative quantitative proteomics analysis of the ABA response of roots of drought-sensitive and drought-tolerant wheat varieties

identifies proteomic signatures of drought adaptability. *J. Proteome Res*. **2014**, *13*, 1688–1701.

8. Ashraf, M. Inducing drought tolerance in plants: Recent advances. *Biotechnol. Adv.* **2010**, *28*, 169–183.
9. Song, Y.; Miao, Y.; Song, C. Behind the scenes: The roles of reactive oxygen species in guard cells. *New Phytol.* **2014**, *201*, 1121–1140.
10. Dat, J.F.; Vandenabeele, E.; Vranova, M.; Mantagu, V.; Inze, D.; Breusegem, F.V. Dual action of the active oxygen species during plant stress responses. *Cell. Mol. Life Sci.* **2000**, *57*, 779–795.
11. Dalton, T.D.; Shertzer, H.G.; Puga, A. Regulation of gene expression by reactive oxygen. *Annu. Rev. Pharmaco. Toxicol.* **1999**, *39*, 67–101.
12. Mittler, R. Oxidative stress, antioxidants and stress tolerance. *Trends Plant Sci.* **2002**, *7*, 405–410.
13. Mittler, R.; Vanderauwera, S.; Gollery, M.; van Breusegem, F. Reactive oxygen gene network of plants. *Trends Plant Sci.* **2004**, *9*, 490–498.
14. Kerchev, P.; Mühlenbock, P.; Denecker, J.; Morreel, K.; Hoeberichts, F.A.; van Der Kelen, K.; Vandorpe, M.; Nguyen, L.; Audenaert, D.; van Breusegem, F. Activation of auxin signalling counteracts photorespiratory H_2O_2-dependent cell death. *Plant Cell Environ.* **2015**, *38*, 253–265.
15. Wan, X.Y.; Liu, J.Y. Comparative proteomics analysis reveals an intimate protein network provoked by hydrogen peroxide stress in rice seedling leaves. *Mol. Cell Proteomics* **2008**, *7*, 1469–1488.

16. Wang, Y.; Lin, A.; Loake, G.J.; Chu, C. H_2O_2-induced leaf cell death and the crosstalk of reactive nitric/oxygen species. *J. Integr. Plant Biol.* **2013**, *55*, 202–208.

17. Hasanuzzaman, M.; Hossain, M.A.; Silva, J.A.T.; Fujita, F. Plant response and tolerance to abiotic oxidative stress: Antioxidant defense is a key factor. In *Crop Stress and its Management: Perspectives and Strategies*; Venkateswarlu, B., Shanker, A.K., Shanker, C., Maheswari, M., Eds.; Springer: Dordrecht, The Netherlands, 2012; pp. 261–315.

18. Signorelli, S.; Corpas, F.J.; Borsani, O.; Barroso, J.B.; Monza, J. Water stress induces a differential and spatially distributed nitro-oxidative stress response in roots and leaves of *Lotus japonicus*. *Plant Sci.* **2013**, 137–146.

19. Yang, L.; Jiang, T.; Fountain, J.C.; Scully, B.T.; Lee, R.D.; Kemerait, R.C.; Chen, S.; Guo, B. Protein profiles reveal diverse responsive signaling pathways in kernels of two maize inbred lines with contrasting drought sensitivity. *Int. J. Mol. Sci.* **2014**, *15*, 18892–18918.

20. Valderrama, R.; Corpas, F.J.; Carreras, A.; Gómez-Rodríguez, M.V.; Chaki, M.; Pedrajas, J.R.; Fernández-Ocaña, A.; del Río, L.A.; Barroso, J.B. The dehydrogenase-mediated recycling of NADPH is a key antioxidant system against salt-induced oxidative stress in olive plants. *Plant Cell Environ.* **2006**, *29*, 1449–1459.

21. Hill, B.G.; Dranka, B.P.; Bailey, S.M.; Lancaster, J.R.; Darley-Usmar, V.M. What part of NO don't you understand? Some answers to the cardinal questions in nitric oxide biology. *J. Biol. Chem.* **2010**, *285*, 19699–19704.

22. Groß, F.; Durner, J.; Gaupels, F. Nitric oxide, antioxidants and pro-oxidants in plant defense responses. *Front. Plant Sci*. **2013**, *4*, 419.

23. Airaki, M.; Leterrier, M.; Mateos, R.M.; Valderrama, R.; Chaki, M.; Barroso, J.B.; Del Río, L.A.; Palma, J.M.; Corpas, F.J. Metabolism of reactive oxygen species and reactive

nitrogen species in pepper (*Capsicum annuum* L.) plants under low temperature stress. *Plant Cell Environ.* **2012**, *35*, 281–295.

24. Bai, X.; Yang, L.; Yang, Y.; Ahmad, P.; Yang, Y.; Hu, X. Deciphering the protective role of nitric oxide against salt stress at the physiological and proteomic levels in maize. *J. Proteome Res.* **2011**, *10*, 4349–4364.
25. Yang, L.M.; Tian, D.G.; Todd, C.D.; Luo, Y.M.; Hu, X.Y. Comparative proteome analyses reveal that nitric oxide is an important signal molecule in the response of rice to aluminum toxicity. *J. Proteome Res.* **2013**, *12*, 1316–1330.
26. Díaz, M.; Achkor, H.; Titarenko, E.; Martínez, M.C. The gene encoding glutathione-dependent formaldehyde dehydrogenase/GSNO reductase is responsive to wounding, jasmonic acid and salicylic acid. *FEBS Lett.* **2003**, *543*, 136–139.
27. Corpas, F.J.; Chaki, M.; Fernández-Ocaña, A.; Valderrama, R.; Palma, J.M.; Carreras, A.; Airaki, M.; Begara-Morales, J.C.; del Río, L.A.; Barroso, J.B. Metabolism of reactive nitrogen species in pea plants under abiotic stress conditions. *Plant Cell Physiol.* **2008**, *49*, 1711–1722.
28. Fan, Q.; Liu, J. Nitric oxide is involved in dehydration/drought tolerance in *Poncirus trifoliata* seedlings through regulation of antioxidant systems and stomatal response. *Plant Cell Rep.* **2012**, *31*, 145–154.
29. Shan, C.; Zhou, Y.; Liu, M. Nitric oxide participates in the regulation of the ascorbate-glutathione cycle by exogenous jasmonic acid in the leaves of wheat seedlings under drought stress. *Protoplasma* **2015**, *252*, 1397–1405.

30. Yang, Y.; Yang, X.; Zhang, C.; Fu, G.; Chen, T.; Tao, L. Effects of nitric oxide on drought stress induced physiological characteristics in leaves of nipponbare (*Oryza sativa* L.). *Chin. J. Rice Sci.* **2015**, *29*, 65–72.

31. Wang, P.; Du, Y.; Hou, Y.J.; Zhao, Y.; Hsu, C.C.; Yuan, F.; Zhu, X.; Tao, W.A.; Song, C.P.; Zhu, J.K. Nitric oxide negatively regulates abscisic acid signaling in guard cells by *S*-nitrosylation of OST1. *Proc. Natl. Acad. Sci. USA* **2015**, *112*, 613–618.

32. Liao, W.B.; Huang, G.B.; Yu, J.H.; Zhang, M.L. Nitric oxide and hydrogen peroxide alleviate drought stress in marigold explants and promote its adventitious root development.
Plant Physiol. Biochem. **2012**, *58*, 6–15.

33. Zhang, A.; Jiang, M.; Zhang, J.; Ding, H.; Xu, S.; Hu, X.; Tan, M. Nitric oxide induced by hydrogen peroxide mediates abscisic acid-induced activation of the mitogen-activated protein kinase cascade involved in antioxidant defense in maize leaves. *New Phytol*. **2007**, *175*, 36–50.

34. Hayano-Kanashiro, C.; Calderón-Vázquez, C.; Ibarra-Laclette, E.; Herrera-Estrella, L.; Simpson, J. Analysis of gene expression and physiological responses in three Mexican maize landraces under drought stress and recovery irrigation. *PLoS ONE* **2009**, doi:10.1371/journal.pone.0007531.

35. Fountain, J.C.; Chen, Z.Y.; Scully, B.T.; Kemerait, R.C.; Lee, R.D.; Guo, B.Z. Pathogenesis-related gene expressions in different maize genotypes under drought stressed conditions. *Afr. J. Plant Sci.* **2010**, *4*, 433–440.

36. Jiang, T.B.; Zhou, B.R.; Luo, M.; Abbas, H.K.; Kemerait, R.; Lee, R.D.; Scully, B.T.; Guo, B.Z. Expression analysis of stress-related genes in kernels of different maize (*Zea mays* L.) inbred lines with different resistance to aflatoxin contamination. *Toxins* **2011**, *3*, 538–550.

37. Jiang, T.B.; Fountain, J.; Davis, G.; Kemerait, R.; Scully, B.T.; Lee, R.D.; Guo, B.Z. Root morphology and gene expression analysis in response to drought stress in maize (*Zea mays*). *Plant Mol. Biol. Rep.* **2012**, *30*, 360–369.

38. Krishnan, A.; Batlang, U.; Myers, E.; Grene, R.; Pereira, A. Effects of drought on gene expression in maize reproductive and leaf meristem tissue revealed by RNA-Seq. *Plant Physiol.* **2012**, *160*, 846–867.

39. Humbert, S.; Subedi, S.; Cohn, J.; Zeng, B.; Bi, Y.M.; Chen, X.; Zhu, T.; McNicholas, P.D.; Rothstein, S.J. Genome-wide expression profiling of maize in response to individual and combined water and nitrogen stresses. *BMC Genomics* **2013**, doi:10.1186/1471-2164-14-3.

40. Russell, W.A. Registration of B70 and B73 parental lines of maize. *Crop Sci.* **1972**, *12*, 721.

41. Chen, J.; Xu, W.; Velten, J.; Xin, Z.; Stout, J. Characterization of maize inbred lines for drought and heat tolerance. *J. Soil Water Conserv.* **2012**, *67*, 354–364.

42. Xu, J.; Yuan, Y.; Xu, Y.; Zhang, G.; Guo, X.; Wu, F.; Wang, Q.; Rong, T.; Pan, G.; Cao, M.; *et al*. Identification of candidate genes for drought tolerance by whole-genome resequencing in maize. *BMC Plant Biol.* **2014**, *14*, 83.

43. Sanguineti, M.C.; Giuliani, M.M.; Govi, G.; Tuberosa, R.; Landi, P. Root and shoot traits of maize inbred lines grown in the field and in hydroponic culture and their relationship with root lodging. *Maydica* **1998**, *43*, 211–216.

44. Losa, A.; Hartings, H.; Verderio, A.; Motto, M. Assessment of genetic diversity and relationships among maize inbred lines developed in Italy. *Maydica* **2010**, *56*, 95–104.

45. Aslam, M.; Khan, I.A.; Saleem, M.; Ali, Z. Assessment of water stress tolerance in different maize accessions at germination and early growth stage. *Pakistan J. Bot.* **2006**, *38*, 1571–1579.

46. Marković, K.; Anđelković, V.; Šukalović, H.T.V.; Vuletić, M. The Influence of Osmotic Stress on the Superoxide Dismutase and Peroxidase Isozymes in Roots of Two Maize Genotypes. In Genetics, Plant Breeding and Seed Production. Proceedings of 51th Croatian and 11th International Symposium on Agriculture. Opatija, Croatia. February 15-18, 2015. Agriculturae Conspectus Scientificus: Faculty of Agriculture, University of Zagreb, Zagreb, Croatia, 2010; pp. 461–465.

47. Vuletić, M.; Hadži-TaškovićŠukalović, V.; Marković, K.; DragišićMaksimović, J. Antioxidative system in maize roots as affected by osmotic stress and different nitrogen sources. *Biol. Plantarum* **2010**, *54*, 530–534.

48. Ramugondo, R.; McDonald, A. New maize offers better livelihoods for poor farmers. Available online: http://repository.cimmyt.org/xmLui/bitstream/handle/10883/3679/74981.pdf (13 March 2014).

49. Harris, M.J.; Outlaw, W.H.; Mertens, R.; Weiler, E.W. Water-stress-induced changes in the abscisic acid content of guard cells and other cells of *Vicia faba* L. leaves as determined by enzyme-amplified immunoassay. *Proc. Natl. Acad. Sci. USA* **1988**, *85*, 2584–2588.

50. Zhao, Y. Auxin biosynthesis and its role in plant development. *Annu. Rev. Plant Biol.* **2010**, *61*, 49–64.

51. Guo, F.Q.; Okamoto, M.; Crawford, N.M. Identification of a plant nitric oxide synthase gene involved in hormonal signaling. *Science* **2003**, *302*, 100–103.

52. Gas, E.; Flores-Pérez, U.; Sauret-Güeto, S.; Rodríguez-Concepción, M. Hunting for plant nitric oxide synthase provides new evidence of a central role for plastids in nitric oxide metabolism. *Plant Cell* **2009**, *21*, 18–23.

53. Ozawa, K.; Tsumoto, H.; Wei, W.; Tang, C.H.; Komatsubara, A.T.; Kawafune, H.; Shimizu, K.; Liu, L.; Tsujimoto, G. Proteomic analysis of the role of *S*-nitrosoglutathione reductase in lipopolysaccharide-challenged mice. *Proteomics* **2012**, *12*, 2024–2035.

54. Xu, Z.; Zhou, G.; Wang, Y.; Han, G.; Li, Y. Changes in chlorophyll fluorescence in maize plants with imposed rapid dehydration at different leaf ages. *J. Plant Growth Regul.* **2008**, *27*, 83–92.

55. De Souza, T.C.; Magalhaes, P.C.; de Castro, E.M.; de Albuquerque, P.E.P.; Marabesi, M.A.

The influence of ABA on water relation, photosynthesis parameters, and chlorophyll fluorescence under drought conditions in two maize hybrids with contrasting drought resistance. *Acta Physiologiae Plantarum* **2013**, *35*, 515–527.

56. Benešová, M.; Holá, D.; Fischer, L.; Jedelský, P.L.; Hnilička, F.; Wilhelmová, N.; Rothová, O.; Kočová, M.; Procházková, D.; Honnerová, J.; *et al*. The physiology and proteomics of drought tolerance in maize: Early stomatal closure as a cause of lower tolerance to short-term dehydration? *PLoS ONE* **2012**, 7, e38017.

57. Lopes, M.S.; Araus, J.L.; van Heerden, P.D.; Foyer, C.H. Enhancing drought tolerance in C4 crops. *J. Exp. Bot*. **2011**, *62*, 3135–3153.

58. De Micco, V.; Aronne, G. Morpho-anatomical traits for plant adaptation to drought. In *Plant Responses to Drought Stress: From Morphological to Molecular Features*; Ricardo, A., Ed.; Springer: New York, NY, USA, 2012; pp. 37–61.

59. Wilkinson, S.; Davies, W.J. Drought, ozone, ABA and ethylene: New insights from cell to plant to community. *Plant Cell Environ.* **2010**, *33*, 510–525.

60. Harb, A.; Krishnan, A.; Ambavaram, M.M.; Pereira, A. Molecular and physiological analysis of drought stress in *Arabidopsis* reveals early responses leading to acclimation in plant growth. *Plant Physiol.* **2010**, *154*, 1254–1271.

61. Aimar, D.; Calafat, M.; Andrade, A.M.; Carassay, L.; Abdala, G.; Molas, M.L. Drought tolerance and stress hormones: From model organisms to forage crops. In *Plants and Environment*; Vasanthaiah, H.K.N., Kambiranda, D., Eds.; InTech: Rijeka, Croatia, 2011; pp. 137–164.

62. Bai, L.; Wang, P.; Song, C. Reactive Oxygen Species (ROS) and ABA Signalling. In *Abscisic Acid: Metabolism, Transport and Signaling*; Zhang, D.P., Ed.; Springer: Dordrecht, The Netherlands, 2014; pp. 191–223.

63. Kwak, J.M.; Mori, I.C.; Pei, Z.M.; Leonhardt, N.; Torres, M.A.; Dangl, J.L.; Bloom, R.E.; Bodde, S.; Jones, J.D.G.; Schroeder, J.I. NADPH oxidase *AtrbohD* and *AtrbohF* genes function in ROS-dependent ABA signaling in *Arabidopsis*. *EMBO J.* **2003**, *22*, 2623–2633.

64. Zhang, H.; Liu, Y.; Wen, F.; Yao, D.; Wang, L.; Guo, J.; Ni, L.; Zhang, A.; Tan, M.; Jiang, M. A novel rice C_2H_2-type zinc finger protein, ZFP36, is a key player involved in abscisic acid-induced antioxidant defence and oxidative stress tolerance in rice. *J. Exp. Bot.* **2014**, *65*, 5795–5809.

65. Xiong, L.; Schumaker, K.S.; Zhu, J.K. Cell signaling during cold, drought, and salt stress. *Plant Cell.* **2002**, *14*, S165–S183.

66. Cruz de Carvalho, M.H. Drought stress and reactive oxygen species: Production, scavenging and signaling. *Plant Signal Behav.* **2008**, *3*, 156–165.

67. Filippou, P.; Antoniou, C.; Fotopoulos, V. Effect of drought and rewatering on the cellular status and antioxidant response of *Medicago truncatula* plants. *Plant Signal Behav*. **2011**, *6*, 270–277.

68. Sofo, A.; Scopa, A.; Nuzzaci, M.; Vitti, A. Ascorbate peroxidase and catalase activities and their genetic regulation in plants subjected to drought and salinity stresses. *Int. J. Mol. Sci.* **2015**, *16*, 13561–13578.

69. Laloi, C.; Przybyla, D.; Apel, K. A genetic approach towrds elucidating the biological activity of different reactive oxygen species in *Arabidopsis thalliana*. *J Exp. Bot*. **2006**, *57*, 1719–1724.

70. Marok, M.A.; Tarrago, L.; Ksas, B.; Henri, P.; Abrous-Belbachir, O.; Havaux, M.; Rey, P. A drought-sensitive barley variety displays oxidative stress and strongly increased contents in low-molecular weight antioxidant compounds during water deficit compared to a tolerant variety. *J. Plant Physiol.* **2013**, *170*, 633–645.

71. Loggini, B.; Scartazza, A.; Brugnoli, E.; Navari-Izzo, F. Antioxidative defense system, pigment composition, and photosynthetic efficiency in two wheat cultivars subjected to drought. *Plant Physiol.* **1999**, *119*, 1091–1100.

72. Hao, G.P.; Xing, Y.; Zhang, J.H. Role of nitric oxide dependence on nitric oxide synthase-like activity in the water stress signaling of maize seedling. *J. Integr. Plant Biol.* **2008**, *50*, 435–442.

73. Chaki, M.; Valderrama, R.; Fernández-Ocaña, A.M.; Carreras, A.; Gómez-Rodríguez, M.V.; Pedrajas, J.R.; Begara-Morales, J.C.; Sánchez-Calvo, B.; Luque, F.; Leterrier, M.; *et al*. Mechanical wounding induces a nitrosative stress by down-regulation of GSNO reductase and an increase in *S*-nitrosothiols in sunflower (*Helianthus annuus*) seedlings. *J. Exp. Bot.* **2011**, *62*, 1803–1813.

74. Benhar, M.; Forrester, M.T.; StamLer, J.S. Protein denitrosylation: Enzymatic mechanisms and cellular functions. *Nat. Rev. Mol. Cell Biol*. **2009**, *10*, 721–732.

75. Malik, S.I.; Hussain, A.; Yun, B.W.; Spoel, S.H.; Loake, G.J. GSNOR-mediated de-nitrosylation in the plant defence response. *Plant Sci.* **2011**, *181*, 540–544.

76. Frungillo, L.; Skelly, M.J.; Loake, G.J.; Spoel, S.H.; Salgado, I. *S*-nitrosothiols regulate nitric oxide production and storage in plants through the nitrogen assimilation pathway. *Nat. Commun.* **2014**, *5*, 1–10.

77. Delledonne, M.; Zeier, J.; Marocco, A.; Lamb, C. Signal interactions between nitric oxide and reactive oxygen intermediates in the plant hypersensitive disease resistance response. *Proc. Natl. Acad. Sci. USA* **2001**, *98*, 13454–13459.

78. Lindermayr, C.; Durner, J. Interplay of reactive oxygen species and nitric oxide: Nitric oxide coordinates reactive oxygen species homeostasis. *Plant Physiol.* **2015**, *167*, 1209–1210.

79. Wang, Y.; Ries, A.; Wu, K; Yang, A.; Crawford, N.M. The *Arabidopsis* prohibitin gene PHB3 functions in nitric oxide-mediated responses and in hydrogen peroxide-induced nitric oxide accumulation. *Plant Cell* **2010**, *22*, 249–259.

80. Yun, B.W.; Feechan, A.; Yin, M.; Saidi, N.B.; Le Bihan, T.; Yu, M.; Moore, J.W.; Kang, J.G.; Kwon, E.; Spoel, S.H.; *et al*. *S*-Nitrosylation of NADPH oxidase regulates cell death in plant immunity. *Nature* **2011**, *478*, 264–268.

81. Fountain, J.C.; Khera, P.; Yang, L.; Nayak, S.N.; Scully, B.T.; Lee, R.D.; Chen, Z.Y.; Kemerait, R.C.; Varshney, R.K.; Guo, B. Resistance to *Aspergillus flavus* in maize and peanut: Molecular biology, breeding, environmental stress, and future perspectives. *Crop J.* **2015**, *3*, 229–237.

82. Baldwin, T.T.; Glenn, A.E. Evaluation of nitric oxide detoxifying flavohaemoglobin in the *Fusarium verticillioides*–maize interaction. *Phytopathology* **2010**, *100*, S10–S11.

83. Baldwin, T.T. Maize Seedling Blight Caused by *Fusarium verticillioides* Involves Fumonisin B1 Mobility and Modulation of Nitric Oxide by the Denitrification Pathway. Doctor's Thesis, University of Georgia, Athens, GA, USA, 2013.

84. Ghanem, M.E.; Marrou, H.; Sinclair, T.R. Physiological phenotyping of plants for crop improvement. *Trends Plant Sci.* **2015**, *20*, 139–144.

85. Cellier, F.; Conéjéro, G.; Breitler, J.C.; Casse, F. Molecular and physiological responses to water deficit in drought-tolerant and drought-sensitive lines of sunflower. Accumulation of dehydrin transcripts correlates with tolerance. *Plant Physiol.* **1998**, *116*, 319–328.

86. Jabs, T.; Dietrich, R.A.; Dangl, J.L. Initiation of runaway cell death in an *Arabidopsis* mutant by extracellular superoxide. *Science* **1996**, *273*, 1853–1856.

87. Rao, M.; Kumar, M.M.; Rao, M.A. *In vitro* and *in vivo* effects of phenolic antioxidants against cisplatin-induced nephrotoxicity. *J. Biochem.* **1999**, *125*, 383–390.

88. Rook, G.A.; Steele, J.; Umar, S.; Dockrell, H.M. A simple method for the solubilization of reduced NBT, and its use as a colorimetric assay for activation of human macrophages by γ-interferon. *J. Immunol. Methods* **1985**, *82*, 161–167.

89. Mookerjee, A.; Basu, J.M.; Majumder, S.; Chatterjee, S.; Panda, G.S.; Dutta, P.; Pal, S; Mukherjee, P.; Efferth, T.; Roy, S. A novel copper complex induces ROS generation in doxorubicin resistant *Ehrlich ascites* carcinoma cells and increases activity of antioxidant enzymes in vital organs *in vivo*. *BMC Cancer* **2006**, *6*, 267.

90. Thordal-Christensen, H.; Zhang, Z.; Wei, Y.; Collinge, D.B. Subcellular localization of H_2O_2 in plants. H_2O_2 accumulation in papillae and hypersensitive response during the barley-powdery mildew interaction. *Plant J.* **1997**, *11*, 1187–1194.

91. Bindschedler, L.V.; Dewdney, J.; Blee, K.A.; Stone, J.M.; Asai, T.; Plotnikov, J.; Denoux, C.; Hayes, T.; Gerrish, C.; Davies, D.R.; *et al.* Peroxidase-dependent apoplastic oxidative burst in *Arabidopsis* required for pathogen resistance. *Plant J.* **2006**, *47*, 851–863.

92. Daudi, A.; Cheng, Z.; O'Brien, J.A.; Mammarella, N.; Khan, S.; Ausubel, F.M.; Bolwell, G.P. The apoplastic oxidative burst peroxidase in *Arabidopsis* is a major component of pattern-triggered immunity. *Plant Cell* **2012**, *24*, 275–287.

93. Kotchoni, S.O.; Kuhns, C.; Ditzer, A.; Kirch, H.H.; Bartels, D. Overexpression of different aldehyde dehydrogenase genes in *Arabidopsis thaliana* confers tolerance to abiotic stress and protects plants against lipid peroxidation and oxidative stress. *Plant Cell Environ.* **2006**, *29*, 1033–1048.

94. Ramel, F.; Sulmon, C.; Bogard, M.; Couée, I.; Gouesbet, G. Differential patterns of reactive oxygen species and antioxidative mechanisms during atrazine injury and sucrose-induced tolerance in *Arabidopsis thaliana* plantlets. *BMC Plant Biol.* **2009**, *9*, 28.

95. Beauchamp, C.; Fridovich, I. Superoxide dismutase: Improved assays and an assay applicable to acrylamide gels. *Anal. Biochem.* **1971**, *44*, 276–287.

96. Aebi, H. Catalase *in vitro*. *Meth. Enzymol.* **1984**, *105*, 121–126.

97. Mur, L.A.; Mandon, J.; Cristescu, S.M.; Harren, F.J.; Prats, E. Methods of nitric oxide detection in plants: A commentary. *Plant Sci.* **2011**, *181*, 509–519.

98. Zielonka, J.; Zielonka, M.; Sikora, A.; Adamus, J.; Joseph, J.; Hardy, M.; Ouari, O.; Dranka, B.P.; Kalyanaraman, B. Global profiling of reactive oxygen and nitrogen species in biological systems: High-throughput real-time analyses. *J Biol. Chem.* **2012**, *287*, 2984–2995.

99. Stacklies, W.; Redestig, H.; Scholz, M.; Walther, D.; Selbig, J. pcaMethods—A bioconductor package providing PCA methods for incomplete data. *Bioinformatics* **2007**, *23*, 1164–1167.

100. Benjamini, Y.; Yekutieli, D. The control of the false discovery rate in multiple testing under dependency. *Ann. Stat.* **2001**, *29*, 1165–1188.

101. Sharov, A.A.; Dudekula, D.B.; Ko, M.S.H. A web-based tool for principal component and significance analysis of microarray data. *Bioinformatics* **2005**, *21*, 2548–2549.

102. Chen, J.; Cheng, T.; Wang, P.; Liu, W.; Xiao, J.; Yang, Y.; Shi, J. Salinity-induced changes in protein expression in the halophytic plant Nitraria sphaerocarpa. *J. Proteom.* **2012**, *75*, 5226–5243.

Table 4.1. Maize genotypes selected in this study.

Genotypes	Pedigree	Origin	Tolerance to Drought	Reference
B73	Recurrent selection population (C5) of Iowa Stiff Stalk Synthetic	Iowa, USA	Susceptible	[40–42]
Lo1016	P3369A × Lo876o2	Italy	Susceptible	[37,43,44]
A638	(V3 × Wf9) × Wf9	Minnesota, USA	Moderate	[45]
Lo964	P3183	Italy	Tolerant	[37,43,44]
Va35	(C103 × T8) × T8	Virginia, USA	Tolerant	[46,47]
Grace-E5	/	CIMMYT, Mexico	Tolerant	[48]

CIMMYT, International Maize and Wheat Improvement Center.,

Figure 4.1. Photosynthetic parameters of seedling leaves from the sensitive genotypes, B73 and Lo1016, and the tolerant ones, Lo964 and Va35, under well-watered (WW) and drought stressed (D) conditions. Photosynthetic metrics were measured in sensitive and tolerant genotypes during drought stress and post-recovery including Pn (A), Gs (B), Ci (C), and Tr (D) measured from 9:00 to 11:00 in the morning for every collection time, at day zero (0), 3, 6, 9 or 12, on young leaves. Different letters indicate significant differences ($p < 0.05$) based on Tukey's test between control and treatments and between different treatment times. Data represent the mean ± SD of three or more replicates.

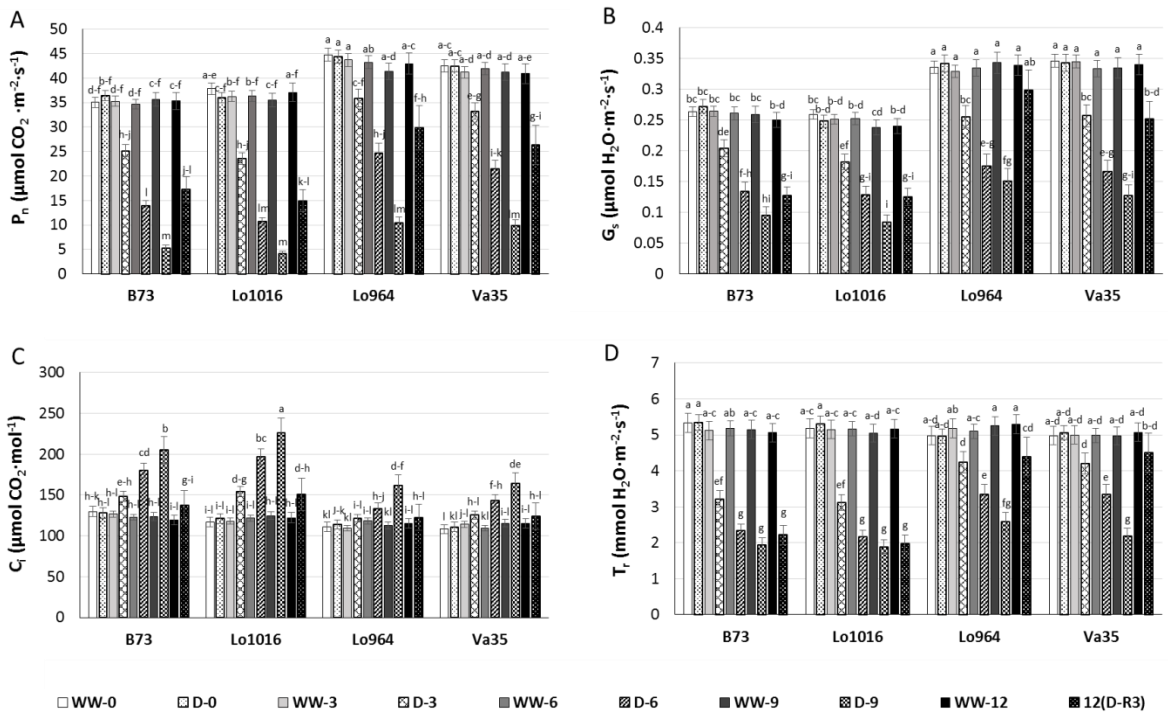
A
P_n (µmol $CO_2 \cdot m^{-2} \cdot s^{-1}$)
B
G_s (µmol $H_2O \cdot m^{-2} \cdot s^{-1}$)
C
C_i (µmol $CO_2 \cdot mol^{-1}$)
D
T_r (mmol $H_2O \cdot m^{-2} \cdot s^{-1}$)
B73
Lo1016
Lo964
Va35
WW-0
D-0
WW-3
D-3
WW-6
D-6
WW-9
D-9
WW-12
12(D-R3)

Figure 4.2. ABA and IAA content in maize seedling leaves under well-watered (WW) and drought (D) conditions. Phytohormone levels were measured in sensitive and tolerant genotypes over drought stress and recovery including ABA (A), and IAA (B). Different letters indicate significant differences ($p<0.05$) based on Tukey's test between control and treatments and between different treatment times. Data represent the mean ± SD of three or more replicates.

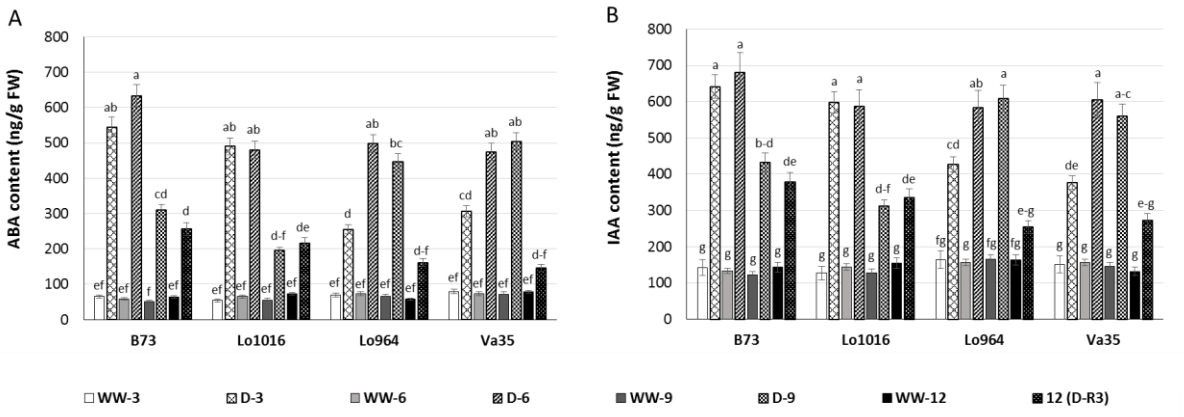
A
ABA content (ng/g FW)
800
700
600
500
400
300
200
100
0
B73
Lo1016
Lo964
Va35
WW-3
D-3
WW-6
D-6
B
IAA content (ng/g FW)
WW-9
D-9
WW-12
12 (D-R3)

Figure 4.3. Visualization of superoxide radical and hydrogen peroxide in the leaves of maize plants under well-watered (WW) and drought stressed (DT) conditions. Endogenous $O_2^{\cdot -}$ levels were monitored by staining $O_2^{\cdot -}$ using a Nitro blue tetrazolium (NBT) staining method (A), and the endogenous H_2O_2 level was monitored by staining H_2O_2 using 3,3′-diaminobenzidine tetrahydrochloride hydrate (DAB) (B).

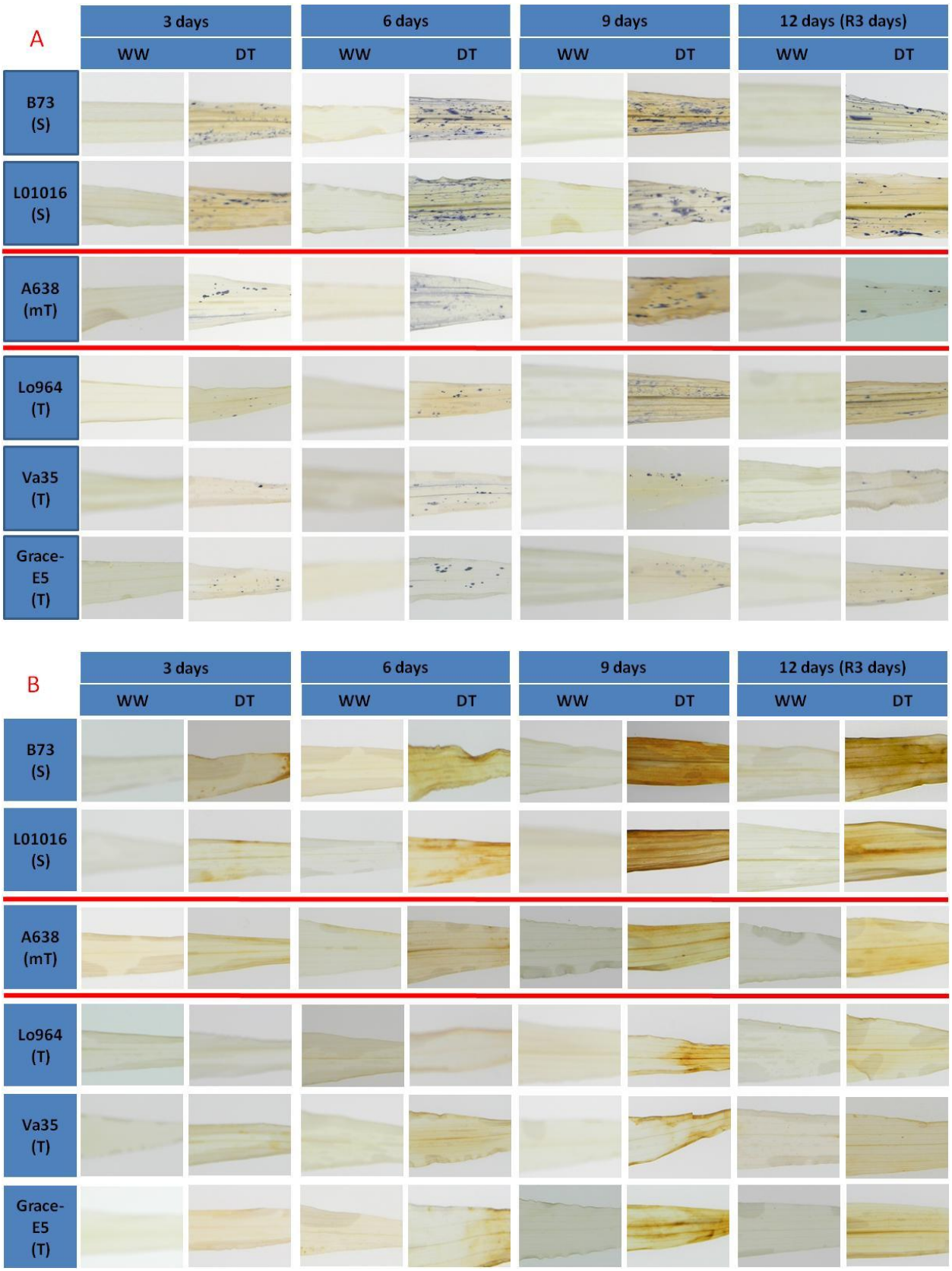
A
3 days
6 days
9 days
12 days (R3 days)
WW
DT
B73 (S)
L01016 (S)
A638 (mT)
Lo964 (T)
Va35 (T)
Grace-E5 (T)
B
3 days
6 days
9 days
12 days (R3 days)
WW
DT
B73 (S)
L01016 (S)
A638 (mT)
Lo964 (T)
Va35 (T)
Grace-E5 (T)

Figure 4.4. Effects of drought treatments on SOD and CAT activities in maize seedling leaves. The activities of ROS-remediating enzymes were measured in sensitive and tolerant genotypes over drought stress and recovery including SOD (A) and CAT (B). Different letters indicate significant differences ($p < 0.05$) based on Tukey's test between control and treatments and between different treatment times. Data represent the mean ± SD of three or more replicates.

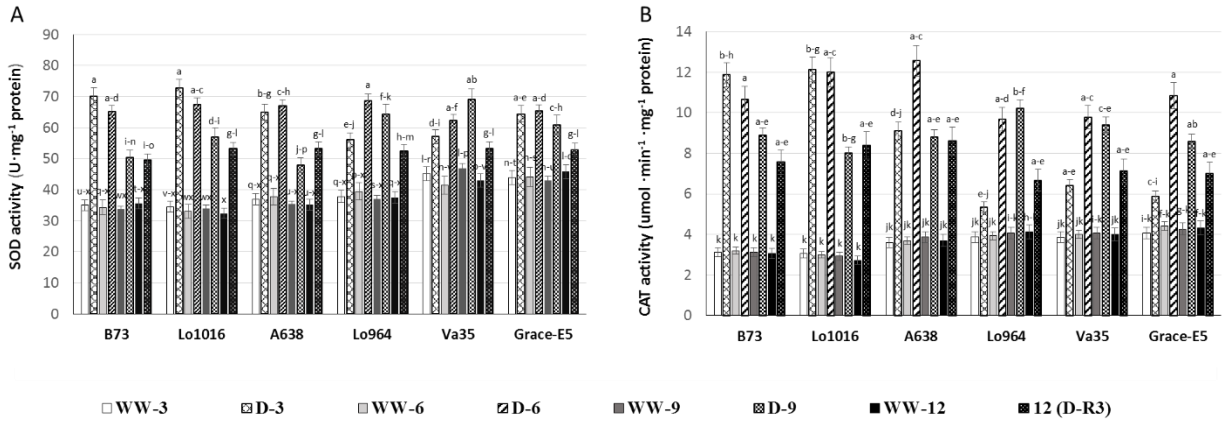
A
SOD activity (U·mg-1 protein)
B
CAT activity (umol ·min-1 ·mg-1 protein)
B73
Lo1016
A638
Lo964
Va35
Grace-E5
WW-3
D-3
WW-6
D-6
WW-9
D-9
WW-12
12 (D-R3)

Figure 4.5. Visualization of nitric oxide (NO) in maize leaf tissues subjected to drought stress. Endogenous NO levels was monitored in maize leaves by staining NO using DAF-FM diacetate, and displayed by green fluorescence; the red fluorescence represents the chlorophyll intensity. WW refers to well-watered leaves; DT refers to drought treated leaves of all tested maize genotypes.

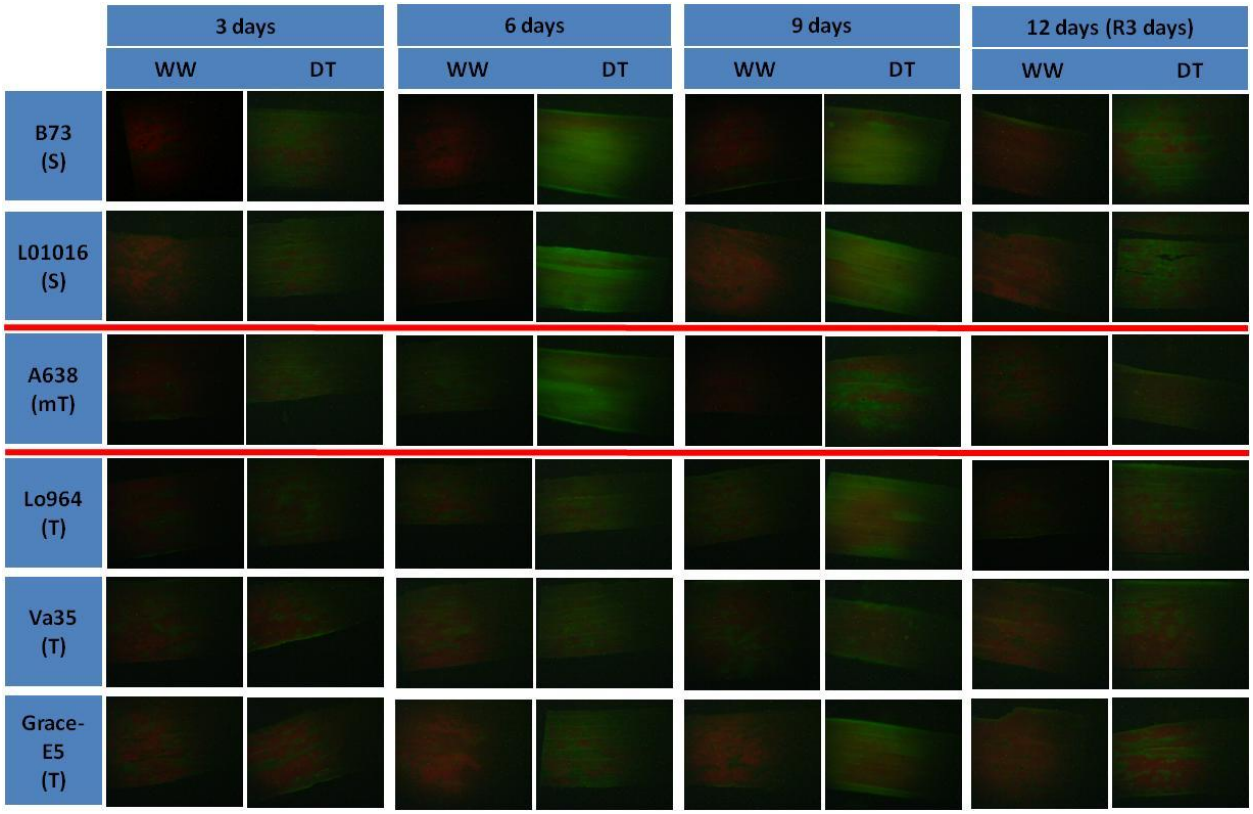
3 days
6 days
9 days
12 days (R3 days)
WW
DT
WW
DT
WW
DT
WW
DT
B73 (S)
L01016 (S)
A638 (mT)
Lo964 (T)
Va35 (T)
Grace-E5 (T)

Figure 4.6. The NOS and GSNOR activities in maize seedling leaves under well-watered (WW) and drought (D) conditions. Nitrosative stress-related enzyme activities were measured in sensitive and tolerant genotypes over drought stress and recovery including NOS (A), and GSNOR (B). Different letters indicate significant differences ($p<0.05$) based on Tukey's test between control and treatments and between different treatment times. Data represent the mean ± SD of three or more replicates.

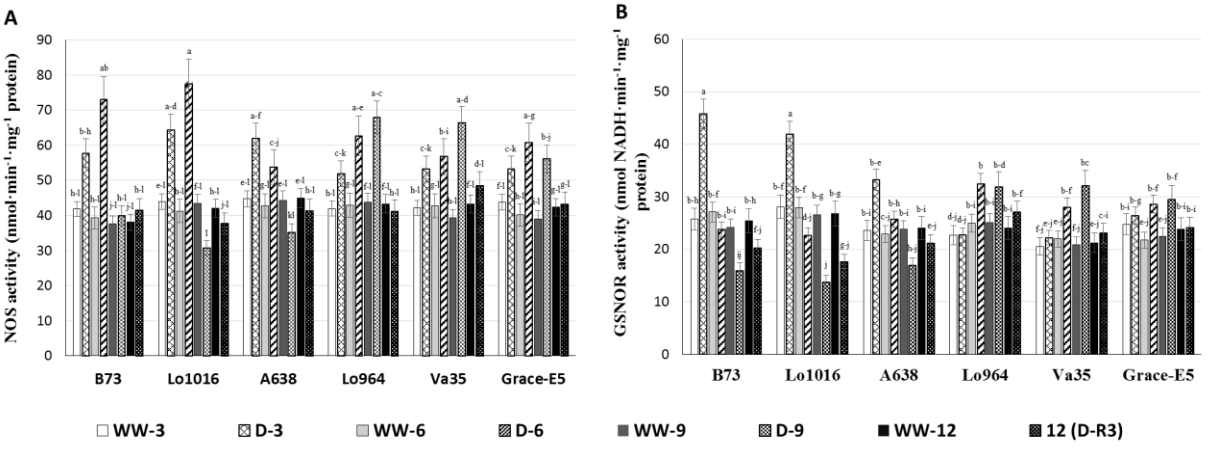
A
NOS activity (nmol·min-1·mg-1 protein)
B
GSNOR activity (nmol NADH·min-1·mg-1 protein)
B73
Lo1016
A638
Lo964
Va35
Grace-E5
WW-3
D-3
WW-6
D-6
WW-9
D-9
WW-12
12 (D-R3)

Figure 4.7. Principal component analysis (PCA) of all physiological and biochemical data in six different lines under well-watered and drought treated conditions. The blue points represent the well-watered (W) plants, while the red points represent the drought-stressed (D) plants.

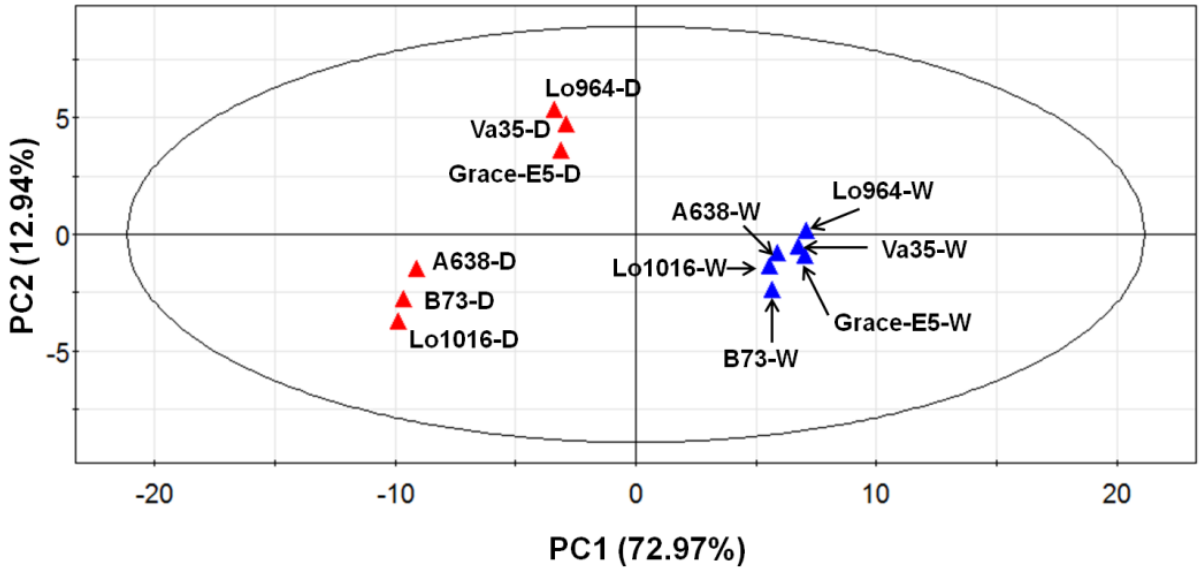
Lo964-D
Va35-D
Grace-E5-D
A638-D
B73-D
Lo1016-D
Lo964-W
A638-W
Va35-W
Lo1016-W
Grace-E5-W
B73-W
PC2 (12.94%)
PC1 (72.97%)
5
0
-5
-20
-10
0
10
20

Figure 4.8. Correlation and variance analysis of all tested dataset in six tested lines under well-watered and drought treated conditions. (A) shows the correlation among each parameter determined; and (B) shows the variance among each trait and each sample during the period of drought treatments.

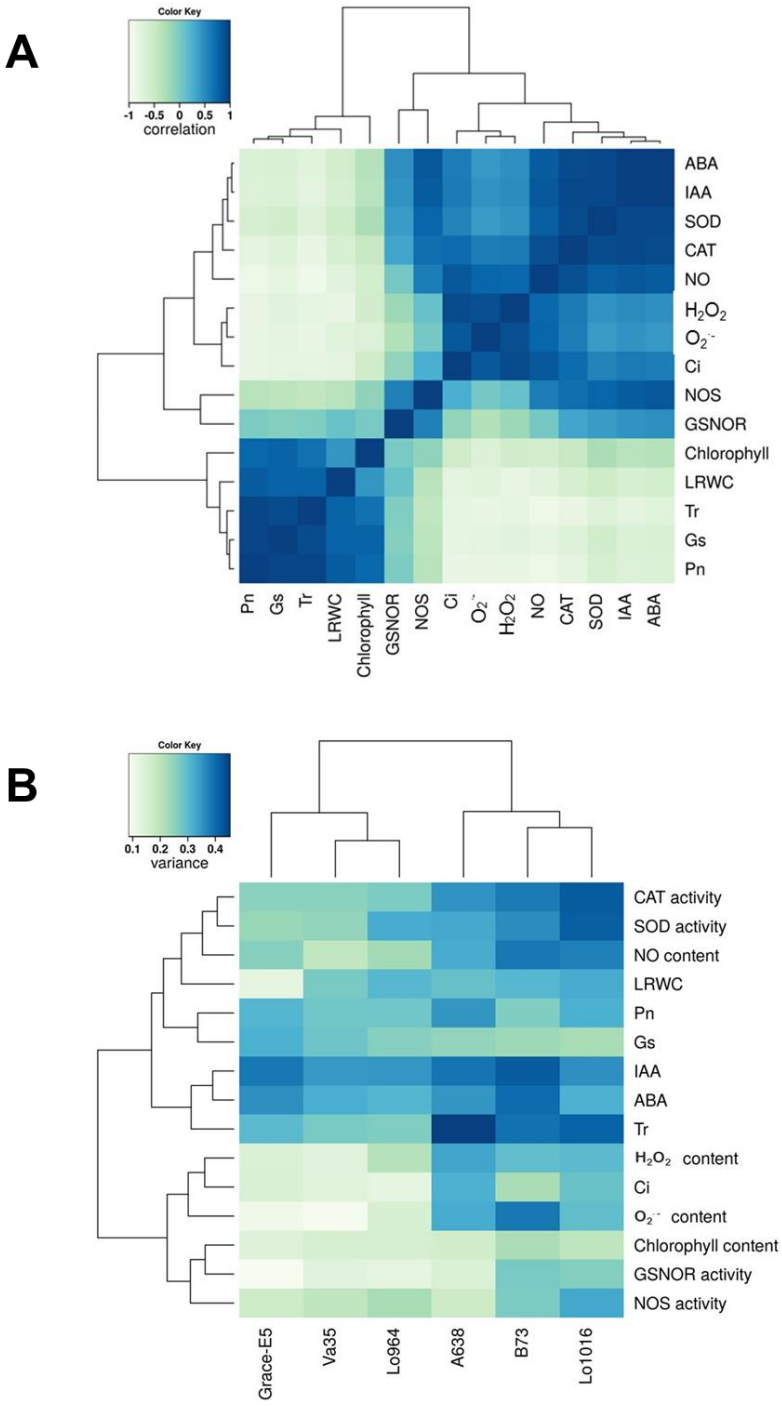
A
Color Key
-1 -0.5 0 0.5 1
correlation
ABA
IAA
SOD
CAT
NO
H2O2
O2-
Ci
NOS
GSNOR
Chlorophyll
LRWC
Tr
Gs
Pn
Pn Gs Tr LRWC Chlorophyll GSNOR NOS Ci O2- H2O2 NO CAT SOD IAA ABA
B
Color Key
0.1 0.2 0.3 0.4
variance
CAT activity
SOD activity
NO content
LRWC
Pn
Gs
IAA
ABA
Tr
H2O2 content
Ci
O2- content
Chlorophyll content
GSNOR activity
NOS activity
Grace-E5 Va35 Lo964 A638 B73 Lo1016

CHAPTER 5

DECIPHERING DROUGHT-INDUCED METABOLIC RESPONSES AND REGULATION IN DEVELOPING MAIZE KERNELS

Fountain, J.C.*, Yang, L.*, Ji, P., Ni, X., Chen, S., Lee, R.D., Kemerait, R.C., Guo, B. (2017). Deciphering drought-induced metabolic responses and regulation in developing maize kernels. Prepared for submission to *Plant Biotechnology Journal*. *Equal Contribution.

Abstract

Drought stress conditions decrease maize growth and yield, and aggravate pre-harvest aflatoxin contamination in kernels. While several studies have been performed on mature kernel tissues in response to drought, the metabolic profiles of developing kernels under drought are not as well characterized, particularly in breeding germplasm with contrasting resistance to drought and mycotoxin contamination. In this study, following screening of inbred lines for drought tolerance, a drought-sensitive line, B73, and a drought-tolerant line, Lo964, were selected and drought stressed beginning 14 days after pollination. Developing kernels were sampled 7 and 14 days after drought induction (DAI) from both stressed and irrigated plants. Comparative biochemical and metabolomic analyses profiled 409 differentially accumulated metabolites. Multivariate statistics and pathway analyses showed that drought stress induced an accumulation of simple sugars and polyunsaturated fatty acids and a decrease in amines, and polyamines, and dipeptides in B73. Conversely, sphingolipid, sterol, phenylpropanoid, and dipeptide metabolites accumulated in Lo964 under drought stress. Drought stress also resulted in the greater accumulation of reactive oxygen species (ROS) and aflatoxin in kernels of B73 in comparison to Lo964. Overall, field drought treatments disordered a cascade of normal metabolic programming during development of maize kernels and subsequently caused oxidative stress. The accumulation of simple sugars and ROS may compromise both grain filling and quality, and host plant resistance to aflatoxin contamination. These results also provide novel targets to enhance host drought tolerance and disease resistance through the use of biotechnologies such as genome editing.

Introduction

The impact of drought on crop production and quality is a continuously increasing issue as the world struggles to increase food production for meeting human population and societal needs, particularly in light of continuing global climate changes (Godfray et al. 2010; Schmidhuber and Tubiello 2007). Drought stress, which frequently occurs and is accompanied by high temperatures in the Southern U.S., is also associated with increased pre-harvest *Aspergillus flavus* colonization and aflatoxin contamination of maize (Fountain et al. 2014; Guo et al. 2008; Payne, 1998; Scully et al. 2009). Interestingly, drought tolerant maize and peanut lines tend to be aflatoxin resistant, though this resistance can still be partially compromised under drought conditions (Fountain et al. 2014; Guo et al. 2008). Therefore, deciphering which responses are critical and adaptive for maintaining maize production is essential for developing breeding strategies that increase drought tolerance and potentially decrease aflatoxin accumulation.

Crops have evolved complex strategies to cope with drought stress for survival with their differential drought tolerance mainly attributed to differences in stress perception, signaling, and metabolic pathways (Bartels and Sunkar, 2005). Much of what is currently known about crop drought adaptation at the molecular level comes from studies involving the genes and proteins that underlie the regulatory processes and mechanisms of drought tolerance. Previous reports have shown that plants respond to drought stress by initiation of early signal transduction (Shinozaki and Yamaguchi-Shinozaki 2007; Zhu, 2002), and the most common drought-responsive signaling pathways contain abscisic acid (ABA)-dependent and ABA-independent mechanisms (Zhu, 2002). Some key genes in these pathways include DRE-binding protein (DREB)/C-repeat-binding factor (CBF), ABA-binding factor (ABF), MYB, MYC, and ABA-responsive element (ABRE) and dehydration-responsive element (DRE) genes. These genes are

induced under drought conditions to reestablish cellular homeostasis for plant adaptation to stress (Golldack et al. 2011). At the metabolite level, those induced by drought stress can regulate the turgidity and rigidity of cells and tissues, and regulate ion transport, redox homeostasis, and enzyme biosynthesis and activity (Rai, 2002; Rodziewicz et al. 2014; Seki et al. 2007). Significant differences in metabolite accumulation have also been observed when comparing different maize hybrids (Harrigan et al. 2007).

These metabolites play essential roles in plant growth, development, and stress responses (Wen et al. 2014), and metabolite patterns, viewed as the metabolic phenotype or metabotype, can provide a link between genotypes and visible phenotypes (Fiehn et al. 2000; Suhre and Gieger 2012). Previous studies using comparative transcriptomic and proteomic approaches have shown that drought stress triggers some common and genotype-specific responses in the developing kernels of maize lines possessing differing drought sensitivities (Luo et al. 2010; Yang et al. 2014). These studies and biochemical examination of seedling-stage drought responses have also shown that genotype-specific responses are also associated with drought derived oxidative stress with drought sensitive genotypes accumulating higher levels of reactive oxygen species (ROS) in their tissues, and more vigorous overall responses to stress than their tolerant counterparts (Yang et al. 2014, 2015).

Maize kernels are particularly susceptible to the negative effects of drought stress during grain-filling (Bruce et al. 2002), a period also of interest from a disease resistance perspective. Kernel tissues become susceptible to *A. flavus* colonization and pre-harvest aflatoxin contamination beginning at the initiation of grain filling at the R2 – R3 growth stage, 7 to 14 days after pollination (Dolezal et al. 2014). This period is also used in field-based resistance screening for germplasm resistance to aflatoxin contamination for artificial *A. flavus* inoculation

(Scully et al. 2009). In screenings performed in our lab, we have identified germplasm with resistance to pre-harvest aflatoxin contamination and drought stress, and have observed a correlation between these two traits (Guo et al. 2008; Scully et al. 2009). In addition, ROS, which accumulate in maize tissues under drought stress, have been shown to stimulate the production of aflatoxin by *A. flavus in vitro* and is hypothesized to do so *in vivo* during colonization of stressed host tissues (Fountain et al. 2014, 2015; Yang et al. 2015). Maize kernel metabolites including starch, simple sugars, and polyunsaturated fatty acids also serve as the targets of hydrolytic enzymes secreted by *A. flavus* during host colonization, and are conducive substrates for aflatoxin production (Fountain et al. 2014; 2016a; Davis et al. 1966; Calvo et al. 1999; Priyadarshini and Tulpule, 1980).

Given the importance of kernel composition for grain quality, yield, and disease resistance during early phases of kernel development, we examined the metabolite accumulation patterns in developing kernels using an untargeted global metabolomics analysis to compare the metabolomic responses of two maize inbred lines with contrasting drought tolerance and aflatoxin contamination resistance to drought stress. By characterizing the metabolite profiles of these two lines, a better understanding of the influences of drought stress on kernel development can be obtained. In addition, compounds potentially contributing to pre-harvest aflatoxin contamination resistance can also be identified. Together, these results can be used in molecular breeding and biotechnological applications to improve maize disease resistance, quality, and yield under drought stress.

Materials and Methods

Plant materials

Six maize inbred lines with contrasting levels of drought tolerance were used for this study: the drought tolerant lines Grace E-5, Lo964, and Va35; the moderately tolerant line A638; and the sensitive lines B73 and Lo1016 (Yang et al. 2015). The lines were cultivated in four rain-out shelters in the field at the USDA Crop Protection and Management Research Unit in Tifton, GA. The shelters were divided into two groups, one well-watered control and one drought stressed. At flowering, each plant was self-pollinated using Lawson pollination bags (Lawson Bag Co., Northfield, IL, USA) as previously described (Yang et al. 2014). At 14 days after pollination (DAP), the plants in the well-watered control shelters were watered normally, whereas the plants in the drought stress treatment were subjected to drought simulation by completely stopping irrigation. Kernels were collected from both treatments at 21 DAP and 28 DAP corresponding to 7 and 14 days after drought induction (DAI), and were immediately frozen in liquid nitrogen and stored at −80°C prior to metabolomics analysis. A total of five ears representing 5 biological replicates were sampled for each treatment and line. At 28 DAP, the plants were recovered with irrigation at a rate 50% of that applied in the well-watered control until maturity (60 DAP). Environmental conditions in the shelters were recorded using a Watchdog weather station (Spectrum Technologies, Aurora, IL, USA). The detailed experimental design is shown in Figure S5.6.

Measurement of ear and kernel agronomic traits

At 28 DAP, ear length and the number of kernels per row from the six examined lines with and without drought stress treatments were measured. At physiological maturity, kernels from both

treatments were hand-harvested and weighed, and then were dried at 90 °C to constant weight for determining water content, dry weight, and 500-kernel weight. Five randomly selected ears were used for the agronomic trait investigation for each inbred line.

Aspergillus flavus inoculation and aflatoxin quantification

To evaluate the pre-harvest aflatoxin contamination resistance of the selected lines, we inoculated them with the *A. flavus* isolate NRRL3357 (Norton, 1999; Scarpari et al. 2014). Briefly, the isolate was cultured on V8 agar (20% V8 juice, 2% agar, 0.5% $CaCO_3$) in the dark at 37°C (Guo et al. 1996; Fountain et al. 2015). After five days, the spores were harvested in sterile 0.1% Tween 20. Conidial concentration of the suspension was determined using a hemocytometer, and the concentration was adjusted to 4.0×10^6 conidia/mL. The resulting spore suspension (3 mL) was used to inoculate ears at 14 DAP using the side injection method with a modified tree marking gun fitted with a needle (Guo et al. 2017; Windham et al. 2003). Inoculated ears with or without drought treatments were collected at 60 DAP for use in aflatoxin analysis and quantification. Aflatoxin extraction and analysis was conducted according to Guo et al. (1996) using thin-layer chromatography (TLC) (Park et al. 1994; Robertson et al. 1967; Trucksess et al. 1984). The aflatoxin standards were purchased from Sigma-Aldrich (St. Louis, MO, USA), and consisted of a total of 5 ml (B_1: 2.02, B_2: 0.50, G_1: 2.03 and G_2: 0.54 μg ml^{-1}). All the samples were analyzed in three replicates.

Metabolomic profiling analysis

Collected immature kernels were ground into fine powders in liquid nitrogen for use in global unbiased metabolomics by Metabolon (Morrisville, NC, USA). Briefly, 50 mg powder per

sample was extracted using an automated MicroLab STAR system (Hamilton, Reno, NV, USA), with several recovery standards added prior to extraction. The resulting extract was divided into five fractions: two for analysis by two separate reverse phase/ultrahigh performance liquid chromatography-tandem mass spectroscopy (RP/UPLC-MS/MS) methods (Evans et al. 2009) with positive ion mode electrospray ionization (ESI); one for analysis by RP/UPLC-MS/MS with negative ion mode ESI; one for analysis by HILIC/UPLC-MS/MS with negative ion mode ESI; and one reserved as a backup. Detailed methods and procedures including instrument parameters, data acquisition and processing, metabolite identification and quantification, data normalization, and statistical analyses can be found in Supplemental File 1.

Statistical and bioinformatics analysis

In order to determine the effect of the drought treatments on metabolite abundance, the identified metabolites were used for partial least squares-discriminant analysis (PLS-DA) using the chemometrics software Solo (Eigenvector Research, Wenatchee, WA, USA) as previously described (Chang et al. 2012). Metabolite functional annotation was performed using Blast2GO (Conesa et al. 2005), and metabolic pathways of identified metabolites were mapped by KEGG software (Kyoto Encyclopedia of Genes and Genomes). Metabolite-metabolite correlation analysis was conducted using Pearson's product-moment correlation using R (version 3.3.0), and mapping of the metabolite-metabolite correlations was constructed using Cytoscape (version 2.8.3).

Histochemical staining of hydrogen peroxide and hydroxyl radical

In order to observe and quantify ROS accumulation in immature kernel tissues (7 and 14 DAI), fluorescent histochemical staining with confocal microscopy was used to quantify two select ROS. An Amplex Red Hydrogen Peroxide/Peroxidase Assay Kit (A22188, Molecular Probes, Eugene, OR, USA) was used to detect hydrogen peroxide (Mohanty et al. 1997), and Aminophenyl fluorescein (A36003, Molecular Probe. Inc., Eugene, OR, USA) was used to detect hydroxyl radical (Setsukinai et al. 2003), according to the manufacturer's instructions. Briefly, the collected kernels were immersed in above-mentioned fluorescent dyes, and infiltrated in the dark using a vacuum oven (VWR Scientific, Neobits, Inc., Sunnyvale, CA) for 2 hours and kept in vacuum overnight. Afterward, the kernels were rinsed in 50 μM PBS buffer twice, and fluorescence was then detected using an Olympus BX41 spectrofluorometer (Olympus, Waltham, MA, USA) coupled with a camera as previously described by Yang et al. (2015).

Results

Effects of drought on phenotypes and kernel development.

In order to characterize the impact of drought on kernel development, six different maize lines with contrasting drought sensitivity were tested in the field in response to drought stress compared to well-watered treatments. Field drought treatments resulted in a visible loss of turgor in maize plants beginning at 7 DAI with visible drought symptoms gradually worsening with continuing stress (Figure S5.1). The sensitive lines B73 and Lo1016, and moderate line A638 exhibited more pronounced symptoms than that of the tolerant lines Lo964, Va35 and Grace E-5 (Jiang et al. 2011). Drought stress also had an obvious influence on the morphology and development of maize kernels (Figure 5.1A). Relative to the normal irrigated environments, at 14

DAI significantly reduced ear length, especially in the sensitive lines was observed. In B73, Lo1016 and A638, ear length decreased by 62.33%, 41.88% and 40.38%, respectively, relative to the irrigated control. Conversely, ear length only decreased by 23.89%, 24.30% and 27.70% in Lo964, Va35, and Grace E-5, respectively (Table 5.1). This was also accompanied with similar degrees of reduction in the number of kernels per ear row and in 500 kernel weight from ears of the sensitive and tolerant lines (Table 5.1).

Impact of drought on ROS generation and aflatoxin accumulation in maize kernels.

The ROS hydrogen peroxide (H_2O_2) and hydroxyl radical ($OH^{\cdot-}$) are the natural byproducts of the normal metabolism of plants whose over-production can be induced under stressful environmental conditions resulting in oxidative damage to cellular components. Fluorescent staining of H_2O_2 and $\cdot OH^{\cdot-}$ detected a higher intensity on drought stress-treated kernels compared to the irrigated control at 7 DAI with more prominent staining observed in B73 compared to Lo964. At 14 DAI the fluorescent intensity did not show an obvious increase in response to continuing drought stress compared to 7 DAI (Figure 5.2).

In addition to ROS accumulation in developing kernels, at maturity we also examined the accumulation of aflatoxin following *A. flavus* inoculation under drought stress. Comparing drought stressed and irrigated plants at maturity it was found that drought stress resulted in elevated levels of aflatoxin contamination in kernels of all tested maize lines after harvest (Figure 5.1B; Table 5.1). This was particularly true for B73 which exhibited a 7.1-fold increase in aflatoxin contamination under drought stress compared to the irrigated control (Figure 5.1B; Table 5.1).

Metabolome patterns of maize developing kernels under drought stress

Based on the obviously contrasting phenotypic changes observed in maize lines under drought stress, and supported by our previous studies (Yang et al. 2014; 2015), kernels from B73 and Lo964 were selected for metabolomics analysis. To comprehensively understand drought-induced changes and metabolomic responses of developing kernels, we performed non-biased, global metabolic profiling of kernels based on UPLC-MS/MS platforms from five different ears sampled at 7 DAI and 14 DAI for both B73 and Lo964 as biological replicates (Oliver et al. 2011). A total of 445 metabolites were identified (Table S5.1) representing the broadest metabolome of maize kernels examined compared to previous studies (Frank et al. 2012; Rao et al. 2014; Skogerson et al. 2010; Yang et al. 2013). The identified 445 metabolites were mapped to 9 super pathways and further 45 sub pathways, including 141 amino acids and metabolites, 62 carbohydrates, 133 lipids, 53 nucleotides, 21 CPGECs (Cofactors, Prosthetic Groups, Electron Carriers), 17 peptides, 11 secondary metabolism, 4 hormone metabolism, and 3 xenobiotics, based on the Kyoto Encyclopedia of Genes and Genomes (KEGG) and Plant Metabolic Network (PMN) databases (Table S5.1).

Most of the identified metabolites belonged to four super pathways: amino acids, carbohydrates, lipids, and nucleotides. In the amino acid super pathway group, there were eight sub pathways including the serine family (phosphoglycerate derived), aromatic amino acid metabolism (PEP derived), aspartate family (OAA derived), glutamate family (alpha-ketoglutarate derived), branched Chain Amino Acids (OAA derived), branched chain amino acids (pyruvate derived), amines and polyamines, and glutathione metabolism. In the carbohydrate super pathway, eight sub pathways were identified including glycolysis, TCA cycle, amino sugar and nucleotide sugar, and sucrose, glucose, fructose metabolism were

identified. The identified lipid metabolites were categorized into 12 sub-pathways, mainly consisting of phospholipids, free fatty acids, and glycerolipids. The nucleotide metabolites were involved into two sub-pathways of purine and pyrimidine metabolism (Table S5.2).

Metabolome differences in drought-sensitive and drought-tolerant maize lines

In order to investigate the metabolite abundance changes of all the tested samples associated with drought treatment, genotype background, and developmental stage, partial least squares-discriminant analysis (PLS-DA) was performed to build a comparative model of drought treatment and well-watered condition between B73 and Lo964 at 7 DAI and 14 DAI. Metabolites missing from three or more of the five replicate values in experimental samples were excluded resulting in a total of 409 metabolites for further statistical comparisons. The first three components of PLS-DA explained 52.3% of the variation, and highlighted the distinct clustering between B73 and Lo964 with or without drought stress suggesting that differential metabolite accumulation patterns account for the variation observed in the model (Figure 5.3).

B73 and Lo964 exhibited significantly different response patterns in their metabolite profiles in response to drought stress. In response to drought stress in B73 at 7 DAI and 14 DAI, 184 and 63 metabolites with significantly altered abundance ($p < 0.05$) were identified, respectively, including 80 increased and 104 decreased in abundance at 7 DAI, and 50 increased and 13 decreased at 14 DAI. In Lo964, 201 and 200 metabolites were identified under drought stress treatments at 7 DAI and 14 DAI, respectively, including 118 increased and 83 decreased in abundance at 7 DAI, and 125 increased and 75 decreased at 14 DAI (Figure 5.4; Figure S5.2).

Significant developmental effects on metabolite accumulation were also observed when comparing 7 and 14 DAI in each treatment. There were 177 and 113 metabolites showing an

altered abundance over time in B73 and Lo964, respectively, under well-watered conditions while 21 and 87 metabolites showed differences over time in B73 and Lo964, respectively, under drought treatment (Figure S5.3A). In addition, genotype effects also exist between B73 and Lo964. Overall, 192 and 120 metabolites showed a differential pattern between B73 and Lo964, respectively, at all time points under irrigation while 242 and 221 metabolites exhibited differential abundance between B73 and Lo964, respectively, at all time points under drought stress (Figure S5.3B).

Drought induced biochemical regulation in metabolites from carbohydrate and amino acid metabolic pathways

Carbohydrate and amino acid metabolism was strongly affected by drought stress. Of the 62 carbohydrate-related metabolites detected, 55 exhibited accumulation alteration in at least one of the lines following drought treatment. Similarly, 132 out of 141 amino acid metabolites detected were significantly altered by drought stress treatments (Table S5.1). Overall, drought stress resulted in a complex response in maize kernels from interconnected metabolic pathways including glycolysis, the tricarboxylic acid (TCA) cycle, glutathione metabolism, urea cycle, methionine (Met) salvage pathway, and primary amino acid metabolism (Figure 5.5). These metabolites detected in the above-mentioned pathways showed some common and distinct responsive patterns between B73 and Lo964 in response to drought stress treatments. Many glycolysis intermediates (e.g. 3-phosphoglycerate, 2-phosphoglycerate, phosphoenolpyruvate and pyruvate) were significantly less abundant in B73 mainly at 7 DAI, whereas they showed increasing trends in Lo964 at 7 and 14 DAI. Five TCA cycle intermediates (e.g. citrate, α-ketoglutarate, succinate and fumarate) were significantly down-regulated in Lo964 at 7 DAI or

14 DAI. However, two (e.g. citrate and isocitrate) were significantly up-regulated in B73 at 7 DAI. In addition, sucrose, in combination with other sugars such as fructose, glucose, raffinose, galactinol and kestose, exhibited increased abundance in B73, but in Lo964 they showed contrasting patterns under drought. Changes associated with glutathione metabolism were observed with a number of γ-glutamyl peptides. These γ-glutamyl peptides are synthesized through reactions between glutamate and other amino acids, including isoleucine, leucine, threonine, valine, tyrosine, and glycine, of which most showed an increase in abundance in Lo964 in response to drought stress. Conversely, other metabolites in glutathione metabolism (e.g. glutamate, proline, and 5-oxoproline) showed a decrease in abundance in B73 under drought stress treatments.

Glutathione metabolism is also conjugated with the urea cycle through N-acetyl glutamate. Four urea cycle metabolites, ornithine, citrulline, arginosuccinate and arginine, were detected, and were down-regulated in B73 under drought stress at 7 DAI, but showed diverse response patterns in Lo964. For example, citrulline abundance was down-regulated at 7 and 14 DAI, while ornithine and arginosuccinate abundance was up-regulated at 14 DAI. The abundance of arginosuccinate at 14 DAI increased when aspartate entered the urea cycle in Lo964 while the reaction chain from asparagine, aspartate, threonine to isoleucine showed an increasing pattern in B73 and Lo964 under drought stress at 7 and 14 DAI (Figure 5.5). In addition, three metabolites in the Met salvage pathway, conjugated with the TCA cycle through aspartate, were differentially accumulated under drought stress. Methy-thioadenosine and methyl-thio-2-oxobutanoate were down-regulated in Lo964 at 7 and 14 DAI, while in B73 S-adenosyl-methionine and methy-thioadenosine decreased only at 7 DAI.

Drought effects are characterized by regulation of lipid-derived metabolites

Lipids are another major class of metabolites that were regulated in response to drought stress, including free fatty acids, oxylipins, glycerolipids, phospholipids, sphingolipids, and galactolipids (Figure 5.6). In particular, unsaturated fatty acids and oxylipins, synthesized from oleate by a combination of elongation and desaturation reactions, showed obviously different patterns in B73 and Lo964 in response to drought stress treatments at 7 or 14 DAI. Two examples of this include chain reactions for unsaturated fatty acid synthesis from oleate/vaccinate and linoleate to 1-linoleoylglycerol (18:2) and 2-linoleoylglycerol (18:2); and another from oleate/vaccinate and linoleate to linolenate, 1-linolenoylglycerol (18:3), or arachidate. These two pathways showed significant increases in B73 under drought stress at 7 DAI, but decreased in Lo964 under drought stress at 14 DAI (Figure 5.6). A series of derivatives of linoleoyl-glycerol and linolenoylglycerol were also detected, and showed increases in B73 and Lo964 under drought stress at 7 and 14 DAI. Several metabolites belonging to the oxylipin sub-pathway showed diverse changes in abundance between lines and treatments. Increasing trends were observed for 13-HODE, 9-HODE, and 12, 13-DiHOME in B73 under drought stress; but in Lo964, 13-HODE and 9-HODE increased in abundance at 7 DAI, while 12, 13-DiHOME decreased at 7 and 14 DAI. In Lo964, 9(10)-EpOME also decreased at 14 DAI.

Four sphingolipid metabolites including sphinganine, N-palmitoyl-sphinganine, sphingosine, and phytosphingosine were significantly more abundant in Lo964 in both drought treatment stages (Figure 5.6). However, two of them, sphingosine and phytosphingosine, decreased in B73 (Figure 5.6). Meanwhile, metabolites in the ethanolamine/choline cycle were found to exhibit reduced abundance in B73 and Lo964 in response to drought stress treatments

with the exception of choline which showed an increasing trend in both lines at 14 DAI (Figure 5.6).

Analysis of metabolite-metabolite correlations and comprehensive metabolic networks under drought stress

To investigate the interactive responses in developing kernels to drought stress, metabolite-metabolite correlations were analyzed for the identified metabolites (Toubiana et al. 2012). Pearson pair-wise correlations across all samples were calculated (Table S5.3). The correlations were then visualized as a heat-map (Figure S5.4), which showed a total of 197,581 correlations, ranging from -0.859 for N-acetylalanine and succinimide to 0.989 for 1-linoleoylglycerol (18:2) and 2-linoleoylglycerol (18:2). Further screening found that there were 340 significant correlations with $r^2 \geq 0.9$ and a false discovery rate (FDR) ≤ 0.05 among the detected metabolites altered in abundance under drought stress treatments. Notably, lipids dominated the significant metabolite-metabolite correlation with 33 lipids being highly correlated with each other, or with other non-lipid metabolites. Another significant metabolite correlation was represented by amino acids, which constructed a complex interactive network among them and also with carbohydrate (e.g. 2-ketogluconate and gluconate), purine (e.g. adenosine 2'-monophosphate), and lipid (e.g. sphingosine) metabolism. These positive correlations were used to construct the metabolite networks (Table S5.4; Figure 5.7). Metabolic networks were constructed based on the KEGG and PMN information of differentially accumulating metabolites in B73 and Lo964 at 7 and 14 DAI. The results of metabolic networks constructed by the differentially accumulated metabolites showed that drought stress treatments caused some common and unique metabolic alterations in each line.

Firstly, changes in metabolite interactions over time during drought stress treatments were analyzed. Drought stress caused the regulation of common metabolic pathways involved in biosynthesis of amino acids, protein digestion and absorption, and ABC transporters in B73. But, 7 DAI of drought stress also resulted in changes to five other metabolic pathways including glycolysis/gluconeogenesis, citrate cycle (TCA cycle), biosynthesis of plant secondary metabolites, phosphotransferase system, two-component system, and zeatin biosynthesis. At 14 DAI drought stress caused changes in 4 different metabolic pathways including pyrimidine metabolism, lysine biosynthesis and degradation, taurine and hypotaurine metabolism, and carbon fixation in photosynthetic organisms in B73. In Lo964, five common metabolism pathways including biosynthesis of amino acids, biosynthesis of plant hormones, biosynthesis of plant secondary metabolites, ABC transporters, and citrate cycle (TCA cycle), were commonly regulated by drought stress. But, drought stress at 7 DAI showed changes in three pathways in Lo964 involved in protein digestion and absorption, biosynthesis of alkaloids, vitamin digestion and absorption; compared to 14 DAI which resulted in the changes of additional 3 metabolism pathways, including purine metabolism, zeatin biosynthesis, and antothenate and CoA biosynthesis.

Secondly, network changes between the lines were examined in response to drought stress treatments. Drought stress at 7 DAI caused the alteration of five common metabolic pathways between the lines including: biosynthesis of amino acids, biosynthesis of plant secondary metabolites, ABC transporters and citrate cycle (TCA cycle), and protein digestion and absorption. At 7 DAI, four other metabolic pathways, including glycolysis/gluconeogenesis, phosphotransferase system, two-component system, and zeatin biosynthesis, were regulated uniquely in B73. At the same point in Lo964, biosynthesis of plant hormone, biosynthesis of

alkaloids, vitamin digestion and absorption were uniquely regulated. At 14 DAI, obvious differences between the lines two different genotypes were observed with only two common metabolic pathways, biosynthesis of amino acids and ABC transporters, expressed in both B73 and Lo964. These results indicated that drought stress resulted in continuously increasing differences in metabolite levels in the kernels of both lines, and to a greater extent in B73 than in Lo964.

Discussion

Differential impact of drought stress on kernel development

Plant responses to environmental stress factors involve both physiological behavior and a complex and coordinated metabolic network. It has been previously demonstrated that maize depends on metabolic alteration and re-equilibrium to prevent large changes in physiological and growth status for adaptation to drought stress, which in turn determine its tolerance to stressed environments (Luo et al. 2010; Yang et al. 2014, 2015). Moreover, drought stress severely influences the plant tolerance and immunity, and subsequently the pathogen exploitation of the host, and plants adapt to drought stress by re-modulating the metabolome and specifically changing the metabolite patterns and metabolic pathways. Here, we utilized biochemical and large-scale metabolomics profiling of developing kernels of two maize inbred lines with contrasting drought sensitivity and aflatoxin contamination resistance to examine their responses to prolonged drought stress

The kernel filling period is closely related to maize yield potential, and drought stress during this filling period can result in kernel abortion, yield reduction, and aggravated *A. flavus* infection (Guo et al. 2008; Scully et al. 2009). In particular, the 20 DAP time frame is the critical

period of kernel development accompanied with important development events, such as endosperm cell division, cell expansion and starch accumulation (Consonni et al. 2005; Grimanelli et al. 2005). It is also a sensitive period to drought stress (Andjelkovic and Thompson, 2006; Luo et al. 2010). In the present study, 14 DAI of drought stress caused more severe foliar symptoms in sensitive lines than that of tolerant ones, which was similar with what was observed for the selected genotypes at the seedling stage (V1 – V2) under drought stress (Yang et al. 2015). Developmental inhibition of ears and kernels was caused by 14 DAI of drought treatments, with more significant decreases in 500-kernel weight and ear length observed in the sensitive lines compared to the tolerant ones. It may be proposed that drought stress treatments decreased photosynthetic rates thereby inhibiting metabolism in leaves, or delaying photosynthate influx into the developing kernels, with more pronounced occurrence in the sensitive genotypes (Boyer and Westgate, 2004; Gebeyehu, 2006).

Drought stress induced remodeling in carbohydrate and energy metabolism

Carbohydrates are a major class of metabolites that were altered in response to drought (Alpert and Oliver, 2002). Glycolysis, an important metabolic pathway that converts glucose into pyruvate and provides intermediates for conversion between sugars and amino acids, was also regulated by drought. Lo964 accumulated several intermediate metabolites of the glycolytic pathway in greater abundance than B73. This may indicate that a relatively higher level of glycolytic intermediates in Lo964 may provide a reservoir of intermediates for amino acid metabolism in kernels. The TCA cycle, as a central position in metabolic networks of most macromolecules, is a sequence of catabolic reactions which functions in and is utilized for the generation of reduced cofactors for use in ATP synthesis (Araujo et al. 2012). Under drought

stress conditions, B73 accumulated several TCA cycle metabolites in greater abundance than Lo964 (Figure 5.5). This may suggest that this decrease in the metabolite levels of TCA cycle may serve as an energy conservation strategy for Lo964 while B73 may require more energy to deal with drought stress (Yobi et al. 2012).

Soluble sugars can function in osmoregulation and prevention of membrane fusion in response to drought stress (Hoekstra et al. 2001; Morgan, 1984; Sakurai et al. 2008). In particular sucrose, 1-kestose, fructose, mannitol/sorbitol, and raffinose were observed to accumulate at significantly higher levels in B73 under drought. These metabolites are associated with membrane protection from oxidative stress in response to drought, and to limit or slow water loss, and subsequently alleviate oxidative stress, through osmoregulation (Bogdanović et al. 2008; Farrant et al. 2009; Oliver et al. 2011). For example, mannitol/sorbitol, raffinose, and galactinol may contribute to protecting against oxidative damage by scavenging hydroxyl radicals and other ROS, and regulating redox homeostasis (Chan et al. 2011; Farrant et al. 2009; Nishizawa et al. 2008a, 2008b; Sanchez et al. 2008; Yang et al. 2015; Yobi et al. 2012;). The lack of differential accumulation of protective sugar alcohols like sorbitol/mannitol in Lo964 may also be indicative of reduced physiological stress experienced by this line due to the accumulation of other antioxidant compounds and enzymes such as those involved in glutathione metabolism. This is consistent with the reduced levels of ROS observed to accumulate in the kernel tissues of Lo964 compared to B73 under drought stress (Figure 5.2). The other obvious difference in carbohydrate metabolism between the two lines was in polyol metabolism. Specifically, arabitol/xylitol exhibited the greater abundance in Lo964 compared with B73 which is consistent with their potential role in protein stabilization during drought stress (Yobi et al. 2012).

Drought stress induced responses in amino acid metabolism

Kernel development is accompanied by distinct and dynamic metabolic switches, and primary metabolites including sugars and amino acids are major components in kernel development and drought stress responses (Angelovici et al. 2010; Fait et al. 2006). Monitoring and coordinating cellular C/N balance is important for kernel development with some C/N metabolic pathways being genetically regulated during kernel filling (Cañas et al. 2001; Zheng, 2009). With the exception of carbohydrates, metabolites involved in amino acid metabolism comprised a greater proportion of the identified metabolites that exhibited differential accumulation patterns in the two examined lines under drought stress. These metabolite alterations and the flow of carbon and nitrogen between carbohydrates and amino acids contribute to maintaining C/N homeostasis for kernel development under drought stress conditions.

Drought stress was found to have significant effects on several biochemical pathways associated with the biosynthesis or degradation of amino acids. The γ-glutamyl amino acids, derived from transferring γ-glutamine to an amino acid, accumulated at a higher level in Lo964 than B73 suggesting that this may protect the tissues from oxidative stress through the glutathione recycling pathway (Farrant et al. 2007; Oliver et al. 2011; Yobi et al. 2012). Most nitrogen-rich amino acids, including asparagine, aspartate, ornithine, and arginosuccinate which are associated with the urea cycle showed increased abundance in Lo964 than in B73 under drought stress, and have been previously reported to be up-regulated in desiccation-tolerant *Selaginella* species (Oliver et al. 2011). In addition, drought stress decreased the abundance of Met salvage pathway components, an important pathway linked with sulfur, ethylene, and polyamine biosynthesis which function in plant stress responses (Miyazaki and Yang, 1987; Sauter et al. 2013). Also, betaine, a well-known osmoprotectant in plants and a target for

improving abiotic stress tolerance, showed an increase in abundance in Lo964 and a decrease in B73 under drought stress which may result in enhanced drought tolerance (Chen and Murata, 2011; Yobi et al. 2012).

Crucial role of lipid metabolism in relationship to drought tolerance

Drought stress in plants can result in damage to cellular components, and disorders in metabolic homeostasis due to enzyme denaturation and disruption of membrane integrity (Hoekstra et al., 2001; Sahsah et al., 1998). Under drought stress, lipid composition can be altered to maintain membrane stabilization and transmit cell signaling for plant adaptation to stress (Munnik and Vermeer, 2010; Webb and Green, 1991). Gasulla et al. (2013) found more significant changes in lipid profiling in drought-tolerant *Craterostigma plantagineum* than in drought sensitive ones. In the present study, lipids involved in glycerolipid, phospholipid, sphingolipid, and galactolipid metabolism were significantly altered in abundance in both of the examined lines. These lipids and lipid-derived signaling compounds have been shown possess regulatory roles in the metabolic reprogramming of plant tissues to cope with drought stress (Okazaki and Saito, 2014; Sahsah et al., 1998). An alternative explanation for the increase in accumulation of sphingoid bases and sphingolipid precursers observed in Lo964 (Figure 5.6) may be related to *Fusarium verticillioides* infection. Fumonisin B_1 produced by *F. verticillioides* inhibits ceramide synthease and the resulting accumulation of precursor sphingoid bases has been proposed as a biomarker for fumonisin contamination and *F. verticillioides* infection (Baldwin et al. 2011). Given that the plants used here were cultivated in the field, it is possible that *F. verticillioides* infection occurred. While asymptomatic infection is possible (Murillo-Williams and Munkvold, 2008), no visible signs or symptoms were observed in the samples collected for metabolomics analysis

suggesting that the changes may be indeed due to drought-related responses. In addition, an increase in polyunsaturated fatty acids such as oleic acid, linoleic acid, and linolenic acid was observed in B73 while a decreasing trend was observed in Lo964 under drought stress. Similar changes in the levels of these polyunsaturated fatty acids was also reported in maize under drought stress while applying exogenous proline (Ali et al. 2013). Also, oxylipins, important products of polyunsaturated fatty acids, have been shown to be modulated by drought to regulate stomatal aperture (Savchenko and Dehesh, 2014; Savchenko et al. 2014).

Drought-induced metabolic alterations and oxidative stress are potentially associated with pathogen susceptibility and aflatoxin accumulation

It is well-known that environmental factors, either biotic or nutritional, can affect aflatoxin production in toxigenic *Aspergillus spp.* during host plant colonization (Fountain et al. 2014; 2015; Guo et al. 2008; Payne, 1998). Drought stress, often occurring during the growing season of maize results in poor kernel development, and increased susceptibility *A. flavus* colonization and subsequent aflatoxin production (Cole et al. 1985; Guo et al. 2008; Payne, 1998). Sensitivity to drought stress has also been previously shown to be correlated with aflatoxin resistance in maize and other commodity crops such as peanut (Fountain et al. 2014). Here, this trend was also observed with increased aflatoxin accumulation at maturity occuring in drought-sensitive inbred lines, particularly B73, following *A. flavus* inoculation and drought stress exposure. While this phenomenon has been previously observed in other studies, the underlying factors involved in the promotion of aflatoxin production under drought stress have yet to be identified.

Nutritional components including carbohydrates, amino acids, and lipids, are also important factors affecting aflatoxin production (Brodhagen and Keller, 2006; Maggio-Hall et al.

2005; Payne, 1998; Wilkinson et al. 2007). Therefore, drought-induced alterations to kernel metabolite composition may influence the production of aflatoxin by *A. flavus* during infection. For example, sugars and their derivatives have been shown to function in plant immunity signaling (Moghaddam and Van den Ende, 2012), and can be used as carbon sources by fungal pathogens. These simple sugars have been reported to be required for the production of aflatoxin by *A. flavus* and *A. parasiticus in vitro* (Abdollahi and Buchanan, 1981; Buchanan and Stahl, 1984; Fountain et al. 2016a; Guo et al. 2008). Drought-induced increases in free simple sugars such as sucrose, glucose, and fructose in developing kernels as observed in B73 may provide additional carbon to support aflatoxin production. The above-mentioned increase in abundance of soluble sugars indirectly supports the observed increase in aflatoxin content in maize kernels under drought stress (Figure 5.1B; Table 5.1).

It has also been reported that polyunsaturated fatty acids have an obvious effect on aflatoxin production given that the addition of oleic, linoleic, and linolenic acids *in vitro* can further stimulate production (Gao and Kolomiets, 2009; Tiwari et al. 1986). In addition, the above-mentioned polyunsaturated fatty acids can be catabolized and oxidized into oxylipins by enzymes including lipoxygenase (LOX) and hydroperoxidase (Belitz et al. 2004). These oxylipins, including 9(10)-EpOME, 13-HODE, and 9-HODE, are produced in abundance in fungi or maize tissues infected by fungi (Fischer et al. 2016; Scarpari et al. 2014), and have been shown to stimulate aflatoxin production both *in vitro* and *in vivo* (Gao et al. 2007; Gao and Kolomiets, 2009). Interestingly, there appears to be a degree of specificity in this response. Gao et al. (2009) also reported that the inactivation of the maize 9-lipoxygenase *ZmLOX3* resulted in increased susceptibility of maize to *A. flavus* and subsequent aflatoxin contamination. The same group also showed that disruption of the same gene resulted in increased resistance to fumonisin

contamination following inoculation with *Fusarium verticilliodes* (Gao et al. 2007). Therefore, host lipid profile alterations by drought stress may have significant effects on resistance to mycotoxin contamination, and manipulation of the expression of oxylipin biosynthetic components using biotechnology may be a valid approach to enhance host resistance.

Oxidative stress caused by excessive ROS generation is another direct event that occurs in plants under drought stress. These same compounds, at lower concentrations, can also function as signal molecules to stimulate metabolic reprogramming for stress adaptation through regulating cellular redox status (Carvalho, 2008; Hasanuzzaman et al. 2013). Specifically, oxidative stress has also been shown to regulate metabolite accumulation including carbohydrates, amino acids, and lipids (Couée et al. 2006; Harding et al. 2003; Keunen et al. 2013; Sofo et al. 2015). Moreover, under oxidative stress caused by drought, hydroperoxidation of polyunsaturated fatty acids caused by lipoxygenase (LOX) can further stimulate oxylipin production both in maize kernel tissue and in invading *A. flavus* mycelia (Das and Roychoudhury, 2014; Reverberi et al. 2008). The ROS and oxylipins have been found to promote and to be required for the production of aflatoxin by *A. flavus* and other *Aspergillus spp*. (Fountain et al. 2014; Gao and Kolomiets, 2009; Jayashree and Subramanyam 2000; Narasaiah et al. 2006; Roze et al. 2013). The specific ROS observed accumulating in B73 compared to Lo964 such as H_2O_2 (Figure 5.2) have been shown to promote aflatoxin production, and to stimulate the expression of aflatoxin biosynthetic genes and host pathogenicity genes in field isolates of *A. flavus* (Fountain et al. 2016a, 2016b). Therefore, these ROS and oxylipin compounds may serve as important signals in the interaction between maize and *A. flavus*, and contribute to exacerbated aflatoxin contamination under drought stress (Fountain et al. 2014).

Conclusions

Our global metabolomic analysis in combining with agronomic traits and biochemical results has provided novel insights toward understanding the metabolic responses in developing maize kernels to drought stress conditions. Many metabolites from various metabolic pathways such as glycolysis, TCA, urea cycle, fatty acid biosynthesis, and sphingolipid metabolism exhibited common and differential regulation between tolerant and sensitive lines in efforts to adapt to drought environments. Comparison of the metabolomes of the lines examined here under drought stress indicated that metabolic reprogramming that contributes to drought tolerance or sensitivity is a complex process that is required to retain important metabolites, particularly carbon and nitrogen sources for kernel development, and remediate oxidative damage due to drought stress-induced ROS accumulation. These findings provide an understanding of the mechanisms utilized by maize in drought responses which may be used as selectable traits in breeding programs such as specific sugar content, amino acid content, lipid profiles, or antioxidant capacity for enhanced drought tolerance, grain quality, and yield. Moreover, the metabolites detected here in correlation with exacerbated aflatoxin contamination under drought stress in maize such as simple sugars, oxylipins, and ROS provide potential targets for enhancing maize resistance through both breeding program selection and the application of biotechnologies such as genome editing. This may be accomplished by selection of lines based on kernel composition, or manipulation of this composition by gene expression alteration.

Acknowledgements

We would like to thank Billy Wilson, Frank Lin, and Joseph Harnage for technical assistance in the field and laboratory. This work is partially supported by the U.S. Department of Agriculture

Agricultural Research Service (USDA-ARS), the Georgia Agricultural Commodity Commission for Corn, AMCOE (Aflatoxin Mitigation Center of Excellence). Mention of trade names or commercial products in this publication is solely for the purpose of providing specific information and does not imply recommendation or endorsement by the USDA. The USDA is an equal opportunity provider and employer.

Supplemental Information

Supplemental datasets, figures, and tables can be found in Appendix B.

References

1. Abdollahi, A. and Buchanan, R.L., 1981. Regulation of aflatoxin biosynthesis: induction of aflatoxin production by various carbohydrates. Journal of Food Science, 46(2), pp.633-635.
2. Ali, Q., Anwar, F., Ashraf, M., Saari, N. and Perveen, R., 2013. Ameliorating effects of exogenously applied proline on seed composition, seed oil quality and oil antioxidant activity of maize (Zea mays L.) under drought stress. International journal of molecular sciences, 14(1), pp.818-835.
3. Alpert, P. and Oliver, M.J., 2002. 1 Drying Without Dying. Desiccation and survival in plants: Drying without dying, p.3.
4. Andjelkovic, V. and Thompson, R., 2006. Changes in gene expression in maize kernel in response to water and salt stress. Plant cell reports, 25(1), pp.71-79.
5. Angelovici, R., Galili, G., Fernie, A.R. and Fait, A., 2010. Seed desiccation: a bridge between maturation and germination. Trends in plant science, 15(4), pp.211-218.

6. Araujo, W.L., NUNES-NESI, A.D.R.I.A.N.O., Nikoloski, Z., Sweetlove, L.J. and Fernie, A.R., 2012. Metabolic control and regulation of the tricarboxylic acid cycle in photosynthetic and heterotrophic plant tissues. Plant, Cell & Environment, 35(1), pp.1-21.
7. Baldwin, T.T., Riley, R.T., Zitomer, N.C., Voss, K.A., Coulombe Jr., R.A., Pastka, J.J., Williams, D.E., Glenn, A.E. 2011. The current state of mycotoxin biomarker development in humans and animals and the potential for application to plant systems. World Mycotoxin J. 4(3): 257-270.
8. Bartels D, Sunkar R. Drought and salt tolerance in plants. Critical reviews in plant sciences. 2005, 24(1):23-58.
9. Belitz, H.-D., Grosch, W., and Schieverle, P. 2004. Cereals and cereal products. In Food Chemistry. Springer, Berlin, pp. 670–745.
10. Bogdanović, J., Mojović, M., Milosavić, N., Mitrović, A., Vučinić, Ž. and Spasojević, I., 2008. Role of fructose in the adaptation of plants to cold-induced oxidative stress. European Biophysics Journal, 37(7), pp.1241-1246.
11. Boyer, J.S. and Westgate, M.E., 2004. Grain yields with limited water. Journal of experimental Botany, 55(407), pp.2385-2394.
12. Brodhagen, M. and Keller, N.P., 2006. Signalling pathways connecting mycotoxin production and sporulation. Molecular Plant Pathology, 7(4), pp.285-301.
13. Bruce WB, Edmeades GO, Barker TC. Molecular and physiological approaches to maize improvement for drought tolerance. J Exp Bot. 2002, 53(366):13-25.
14. Buchanan, R.L. and Stahl, H.G., 1984. Ability of various carbon sources to induce and support aflatoxin synthesis by Aspergillus parasiticus. Journal of Food Safety, 6(4), pp.271-279.

15. Calvo, A. M., Hinze, L. L., Gardner, H. W., & Keller, N. P. (1999). Sporogenic effect of polyunsaturated fatty acids on development of Aspergillus spp. *Applied and Environmental Microbiology*, *65*(8), 3668-3673.
16. Cañas, R.A., Amiour, N., Quilleré, I. and Hirel, B., 2011. An integrated statistical analysis of the genetic variability of nitrogen metabolism in the ear of three maize inbred lines (Zea mays L.). Journal of experimental botany, 62(7), pp.2309-2318.
17. Carvalho, M.D., 2008. Drought stress and reactive oxygen species. Plant Signal Behav, 3, pp.156-165.
18. Chan, Z., Grumet, R. and Loescher, W., 2011. Global gene expression analysis of transgenic, mannitol-producing, and salt-tolerant Arabidopsis thaliana indicates widespread changes in abiotic and biotic stress-related genes. Journal of experimental botany, 62(14), pp.4787-4803.
19. Chang, Y., Zhao, C., Zhu, Z., Wu, Z., Zhou, J., Zhao, Y., Lu, X. and Xu, G., 2012. Metabolic profiling based on LC/MS to evaluate unintended effects of transgenic rice with cry1Ac and sck genes. Plant Molecular Biology, 78(4-5), pp.477-487.
20. Chen, T.H. and Murata, N., 2011. Glycinebetaine protects plants against abiotic stress: mechanisms and biotechnological applications. Plant, cell & environment, 34(1), 1-20.
21. Cole, R.J., Sanders, T.H., Hill, R.A. and Blankenship, P.D., 1985. Mean geocarposphere temperatures that induce preharvest aflatoxin contamination of peanuts under drought stress. Mycopathologia, 91(1), pp.41-46.
22. Conesa, A., Götz, S., García-Gómez, J.M., Terol, J., Talón, M. and Robles, M., 2005. Blast2GO: a universal tool for annotation, visualization and analysis in functional genomics research. Bioinformatics, 21(18), pp.3674-3676.

23. Consonni, G., Gavazzi, G. and Dolfini, S., 2005. Genetic analysis as a tool to investigate the molecular mechanisms underlying seed development in maize. Annals of botany, 96(3), pp.353-362.
24. Couée, I., Sulmon, C., Gouesbet, G. and El Amrani, A., 2006. Involvement of soluble sugars in reactive oxygen species balance and responses to oxidative stress in plants. Journal of experimental botany, 57(3), pp.449-459.
25. Das, K. and Roychoudhury, A., 2014. Reactive oxygen species (ROS) and response of antioxidants as ROS-scavengers during environmental stress in plants. Frontiers in Environmental Science, 2, p.53.
26. Davis, N. D., Diener, U. L., & Eldridge, D. W. (1966). Production of aflatoxins B1 and G1 by Aspergillus flavus in a semisynthetic medium. *Applied microbiology*, *14*(3), 378-380.
27. De Luna-López, M.C; Valdivia-Flores, A.G; Jaramillo-Juárez, F.; Reyes, J.L.; Ortiz-Martínez, R.; Quezada-Tristán, T. Association between Aspergillus flavus Colonization and Aflatoxins Production in Immature Grains of Maize Genotypes. Journal of Food Science and Engineering 2013, 3, 688-698.
28. Dolezal, A. L., Shu, X., OBrian, G. R., Nielsen, D. M., Woloshuk, C. P., Boston, R. S., & Payne, G. A. (2014). Aspergillus flavus infection induces transcriptional and physical changes in developing maize kernels. *Frontiers in Microbiology*, *5*, 384.
29. Evans, A.M., DeHaven, C.D., Barrett, T., Mitchell, M. and Milgram, E., 2009. Integrated, nontargeted ultrahigh performance liquid chromatography/electrospray ionization tandem mass spectrometry platform for the identification and relative quantification of the small-molecule complement of biological systems. Analytical chemistry, 81(16), pp.6656-6667.

30. Fait, A., Angelovici, R., Less, H., Ohad, I., Urbanczyk-Wochniak, E., Fernie, A.R. and Galili, G., 2006. Arabidopsis seed development and germination is associated with temporally distinct metabolic switches. Plant physiology, 142(3), pp.839-854.

31. Farrant, J. M., Brandt, W., & Lindsey, G. G. An Overview of Mechanisms of Desiccation Tolerance in Selected Angiosperm Resurrection Plants. *Plant Stress*, *1*(1), 72-84.

32. Farrant, J.M., Lehner, A., Cooper, K. and Wiswedel, S., 2009. Desiccation tolerance in the vegetative tissues of the fern Mohria caffrorum is seasonally regulated. The Plant Journal, 57(1), pp.65-79.

33. Fiehn O, Kopka J, Dörmann P, Altmann T, Trethewey RN, Willmitzer L. Metabolite profiling for plant functional genomics. Nat Biotechnol. 2000, 18(11):1157-61.

34. Fischer, G.J. and Keller, N.P., 2016. Production of cross-kingdom oxylipins by pathogenic fungi: An update on their role in development and pathogenicity. Journal of Microbiology, 54(3), pp.254-264.

35. Fountain, J. C., Bajaj, P., Pandey, M., Nayak, S. N., Yang, L., Kumar, V., ... & Lee, R. D. (2016a). Oxidative stress and carbon metabolism influence Aspergillus flavus transcriptome composition and secondary metabolite production. *Scientific Reports*, *6*.

36. Fountain, J. C., Bajaj, P., Nayak, S. N., Yang, L., Pandey, M. K., Kumar, V., ... & Varshney, R. K. (2016b). Responses of Aspergillus flavus to Oxidative Stress Are Related to Fungal Development Regulator, Antioxidant Enzyme, and Secondary Metabolite Biosynthetic Gene Expression. *Frontiers in Microbiology*, *7*.

37. Fountain, J.C., Scully, B.T., Chen, Z.Y., Gold, S.E., Glenn, A.E., Abbas, H.K., Lee, R.D., Kemerait, R.C. and Guo, B., 2015. Effects of hydrogen peroxide on different toxigenic and atoxigenic isolates of Aspergillus flavus. Toxins, 7(8), pp.2985-2999.

38. Fountain, J.C.; Scully, B.T.; Ni, X.; Kemerait, R.C.; Lee, R.D.; Chen, Z.Y.; Guo, B. 2014. Environmental influences on maize-Aspergillus flavus interactions and aflatoxin production. Front. Microbiol. 2014, 5, 40.

39. Frank T, Röhlig RM, Davies HV, Barros E, Engel KH. Metabolite profiling of maize kernels--genetic modification versus environmental influence. J Agric Food Chem. 2012, 60(12):3005-12.

40. Furlan, A.L., Bianucci, E. and Castro, S., 2016. Signaling Role of ROS in Modulating Drought Stress Tolerance. In Drought Stress Tolerance in Plants, Vol 1 (pp. 309-330). Springer International Publishing.

41. Gao, X., Brodhagen, M., Isakeit, T., Brown, S. H., Göbel, C., Betran, J., ... & Kolomiets, M. V. (2009). Inactivation of the lipoxygenase ZmLOX3 increases susceptibility of maize to Aspergillus spp. *Molecular plant-microbe interactions*, *22*(2), 222-231.

42. Gao, X. and Kolomiets, M.V., 2009. Host-derived lipids and oxylipins are crucial signals in modulating mycotoxin production by fungi. Toxin Reviews, 28(2-3), pp.79-88.

43. Gao, X., Shim, W.B., Göbel, C., Kunze, S., Feussner, I., Meeley, R., Balint-Kurti, P. and Kolomiets, M., 2007. Disruption of a maize 9-lipoxygenase results in increased resistance to fungal pathogens and reduced levels of contamination with mycotoxin fumonisin. Molecular plant-microbe interactions, 20(8), pp.922-933.

44. Gasulla, F., Dorp, K., Dombrink, I., Zähringer, U., Gisch, N., Dörmann, P. and Bartels, D., 2013. The role of lipid metabolism in the acquisition of desiccation tolerance in Craterostigma plantagineum: a comparative approach. The Plant Journal, 75(5), pp.726-741.

45. Gebeyehu S. Physiological Response to Drought Stress of Common Bean (Phaseolus vulgaris L.) Genotypes Differing in Drought Resistance. PhD Dissertation, Justus-Liebig University of Giessen, Germany.
46. Godfray HC, Beddington JR, Crute IR, Haddad L, Lawrence D, Muir JF, Pretty J, Robinson S, Thomas SM, Toulmin C. Food security: the challenge of feeding 9 billion people. Science. 2010, 327(5967):812-8.
47. Golldack D, Lüking I, Yang O. Plant tolerance to drought and salinity: stress regulating transcription factors and their functional significance in the cellular transcriptional network. Plant Cell Rep. 2011, 30(8):1383-91.
48. Grimanelli, D., Perotti, E., Ramirez, J. and Leblanc, O., 2005. Timing of the maternal-to-zygotic transition during early seed development in maize. The Plant Cell, 17(4), pp.1061-1072.
49. Guo, B.Z.; Chen, Z.Y.; Lee, R.D.; Scully, B.T. Drought stress and preharvest aflatoxin contamination in agricultural commodity: Genetics, genomics and proteomics. J. Integr. Plant Biol. 2008, 50, 1281-1291.
50. Guo, B., Ji, X., Ni, X., Fountain, J. C., Li, H., Abbas, H. K., ... & Scully, B. T. (2017). Evaluation of maize inbred lines for resistance to pre-harvest aflatoxin and fumonisin contamination in the field. The Crop Journal, in press.
51. Guo, B.Z.; Russin, J.S.; Brown, R.L.; Cleveland, T.E.; Widstrom, N.W. Resistance to aflatoxin contamination in corn as influenced by relative humidity and kernel germination. J Food Prot. 1996, 59, 276-81.

52. Harding HP, Zhang Y, Zeng H, Novoa I, Lu PD, Calfon M, Sadri N, Yun C, Popko B, Paules R: An integrated stress response regulates amino acid metabolism and resistance to oxidative stress. Mol Cell. 2003, 11 (3): 619-633. 10.1016/S1097-2765(03)00105-9.

53. Harrigan GG, Stork LG, Riordan SG, Ridley WP, Macisaac S, Halls SC, Orth R, Rau D, Smith RG, Wen L, Brown WE, Riley R, Sun D, Modiano S, Pester T, Lund A, Nelson D. Metabolite analyses of grain from maize hybrids grown in the United States under drought and watered conditions during the 2002 field season. J Agric Food Chem. 2007, 55(15):6169-76.

54. Hasanuzzaman, M., Nahar, K., Gill, S.S. and Fujita, M., 2013. Drought stress responses in plants, oxidative stress, and antioxidant defense. Climate Change and Plant Abiotic Stress Tolerance, pp.209-250.

55. Hoekstra, F.A., Golovina, E.A. and Buitink, J. (2001) Mechanisms of plant desiccation tolerance. Trends Plant Sci. 6, 431–438.

56. Jayashree, T., & Subramanyam, C. (2000). Oxidative stress as a prerequisite for aflatoxin production by Aspergillus parasiticus. *Free Radical Biology and Medicine*, *29*(10), 981-985.

57. Jiang, T.; Zhou, B.; Luo, M.; Abbas, H.K.; Kemerait, R.; Lee, R.D.; Scully, B.T.; Guo, B. Expression analysis of stress-related genes in kernels of different maize (Zea mays L.) inbred lines with different resistance to aflatoxin contamination. Toxins (Basel) 2011, 3, 538-550.

58. Keunen, E.L.S., Peshev, D., Vangronsveld, J., Van Den Ende, W.I.M. and Cuypers, A.N.N., 2013. Plant sugars are crucial players in the oxidative challenge during abiotic stress: extending the traditional concept. Plant, cell & environment, 36(7), pp.1242-1255.

59. Luo, M., Liu, J., Lee, R.D., Scully, B.T. and Guo, B., 2010. Monitoring the Expression of Maize Genes in Developing Kernels under Drought Stress using Oligo-microarray. Journal of integrative plant biology, 52(12), pp.1059-1074.

60. Maggio-Hall, L.A., Wilson, R.A. and Keller, N.P., 2005. Fundamental contribution of β-oxidation to polyketide mycotoxin production in planta. Molecular plant-microbe interactions, 18(8), pp.783-793.
61. Miyazaki, J.H. and Yang, S.F., 1987. The methionine salvage pathway in relation to ethylene and polyamine biosynthesis. Physiologia Plantarum, 69(2), pp.366-370.
62. Moghaddam, M.R.B. and Van den Ende, W., 2012. Sugars and plant innate immunity. Journal of experimental botany, p.ers129.
63. Mohanty, J.G., Jaffe, J.S., Schulman, E.S. and Raible, D.G., 1997. A highly sensitive fluorescent micro-assay of H2O2 release from activated human leukocytes using a dihydroxyphenoxazine derivative. Journal of immunological methods, 202(2), pp.133-141.
64. Morgan, J.M., 1984. Osmoregulation and water stress in higher plants. Annual review of plant physiology, 35(1), pp.299-319.
65. Munnik, T. and Vermeer, J.E.M. (2010) Osmotic stress-induced phosphoinositide and inositolphosphate signalling in plants. Plant, Cell Environ. 33, 655–669.
66. Murillo-Williams, A., Munkvold, G.P. 2008. Systemic infection by *Fusarium verticillioides* in maize plants grown under three temperature regimes. Plant Dis. 92:1695-1700.
67. Narasaiah, K. V., Sashidhar, R. B., & Subramanyam, C. (2006). Biochemical analysis of oxidative stress in the production of aflatoxin and its precursor intermediates. *Mycopathologia*, *162*(3), 179-189.
68. Nishizawa, A., Yabuta, Y. and Shigeoka, S., 2008. Galactinol and raffinose constitute a novel function to protect plants from oxidative damage. Plant physiology, 147(3), pp.1251-1263.

69. Nishizawa-Yokoi, A., Yabuta, Y. and Shigeoka, S., 2008. The contribution of carbohydrates including raffinose family oligosaccharides and sugar alcohols to protection of plant cells from oxidative damage. Plant signaling & behavior, 3(11), pp.1016-1018.

70. Norton, R.A. Inhibition of aflatoxin B1 biosynthesis in Aspergillus flavus by anthocyanidins and related flavonoids. J. Agric. Food Chem. 1999, 47, 1230-1235.

71. Okazaki, Y. and Saito, K., 2014. Roles of lipids as signaling molecules and mitigators during stress response in plants. The Plant Journal, 79(4), pp.584-596.

72. Oliver MJ, Guo L, Alexander DC, Ryals JA, Wone BW, Cushman JC. A sister group contrast using untargeted global metabolomic analysis delineates the biochemical regulation underlying desiccation tolerance in Sporobolus stapfianus. Plant Cell. 2011, 23(4):1231-48.

73. Park, D.L.; Trucksess, M.W.; Nesheim, S.; Stack, M.; Newell, R.F. Solvent-efficient thin-layer chromatographic method for the determination of aflatoxins B1, B2, G1, and G2 in corn and peanut products: collaborative study. Journal of AOAC International 1994, 77, 637–646.

74. Payne, G.A. Process of contamination by aflatoxin-producing fungi and their impact on crops; In Mycotoxins in Agriculture and Food Safety; Sinha, K.K., Bhatnagar, D., Eds.; Marcel Dekker: New York, NY, USA, 1998; pp. 279-306.

75. Priyadarshini, E., & Tulpule, P. G. (1980). Effect of free fatty acids on aflatoxin production in a synthetic medium. Food and cosmetics toxicology, 18(4), 367-369.

76. Rai V. Role of amino acids in plants responses to stresses. Biol. Plant. 2002, 45:481-487.

77. Rao J, Cheng F, Hu C, Quan S, Lin H, Wang J, Chen G, Zhao X, Alexander D, Guo L, Wang G. Metabolic map of mature maize kernels. Metabolomics. 2014, 10(5):775-87.

78. Robertson, J.A.; Pons, W.A.; Goldblatt, L.A. Preparation of aflatoxins and determination of their ultraviolet and fluorescent characteristics. J. Agr. Food Chem. 1967, 15, 798-801.

79. Rodziewicz P, Swarcewicz B, Chmielewska K, Wojakowska A, Stobiechi M. Influence of abiotic stresses on plant hormone and metabolome changes. Acta Physiol. Plant. 2014, 36:1-19.

80. Roze, L. V., Hong, S. Y., & Linz, J. E. (2013). Aflatoxin biosynthesis: current frontiers. *Annual review of food science and technology*, *4*, 293-311.

81. Sahsah, Y., Campos, P., Gareil, M., Zuily-Fodil, Y. and Pham-Thi, A.T. (1998) Enzymatic degradation of polar lipids in *Vigna unguiculata* leaves and influence of drought stress. Physiol. Plant. 104, 577–586.

82. Sakurai, M., Furuki, T., Akao, K.I., Tanaka, D., Nakahara, Y., Kikawada, T., Watanabe, M. and Okuda, T., 2008. Vitrification is essential for anhydrobiosis in an African chironomid, Polypedilum vanderplanki. Proceedings of the National Academy of Sciences, 105(13), pp.5093-5098.

83. Sanchez, D.H., Siahpoosh, M.R., Roessner, U., Udvardi, M. and Kopka, J., 2008. Plant metabolomics reveals conserved and divergent metabolic responses to salinity. Physiologia Plantarum, 132(2), pp.209-219.

84. Sauter, M., Moffatt, B., Saechao, M.C., Hell, R. and Wirtz, M., 2013. Methionine salvage and S-adenosylmethionine: essential links between sulfur, ethylene and polyamine biosynthesis. Biochemical Journal, 451(2), pp.145-154.

85. Savchenko, T. and Dehesh, K., 2014. Drought stress modulates oxylipin signature by eliciting 12-OPDA as a potent regulator of stomatal aperture. Plant signaling & behavior, 9(4), pp.1151-60.

86. Savchenko, T., Kolla, V.A., Wang, C.Q., Nasafi, Z., Hicks, D.R., Phadungchob, B., Chehab, W.E., Brandizzi, F., Froehlich, J. and Dehesh, K., 2014. Functional convergence of oxylipin

and abscisic acid pathways controls stomatal closure in response to drought. Plant Physiology, 164(3), pp.1151-1160.

87. Scarpari M, Punelli M1, Scala V, Zaccaria M, Nobili C, Ludovici M, Camera E, Fabbri AA, Reverberi M, Fanelli C. Lipids in Aspergillus flavus-maize interaction. Front Microbiol. 2014, 5:74. doi: 10.3389/fmicb.2014.00074.
88. Schmidhuber J, Tubiello FN. Global food security under climate change. Proc Natl Acad Sci USA. 2007, 104(50):19703-8.
89. Scully, B.T.; Krakowsky, M.D.; Ni, X.Z.; Wilson, J.P.; Lee, R.D.; Guo, B.Z. Preharvest aflatoxin contamination of corn and other grain crops grown on the U.S. Southeastern Coastal Plain. Toxin Rev. 2009, 28, 169-179.
90. Seki M, Umezawa T, Urano K, Shinozaki K, Regulatory metabolic networks in drought stress responses. Curr. Opin. Plant Biol. 2007, 10:296-302.
91. Setsukinai, K.I., Urano, Y., Kakinuma, K., Majima, H.J. and Nagano, T., 2003. Development of novel fluorescence probes that can reliably detect reactive oxygen species and distinguish specific species. Journal of Biological Chemistry, 278(5), pp.3170-3175.
92. Shinozaki K, Yamaguchi-Shinozaki K. Gene networks involved in drought stress response and tolerance. J Exp Bot. 2007, 58(2):221-7.
93. Skogerson K, Harrigan GG, Reynolds TL, Halls SC, Ruebelt M, Iandolino A, Pandravada A, Glenn KC, Fiehn O. Impact of genetics and environment on the metabolite composition of maize grain. J Agric Food Chem. 2010, 58(6):3600-10.
94. Sofo, A., Scopa, A., Hashem, A. and Abd-Allah, E.F., 2015. Lipid metabolism and oxidation in plants subjected to abiotic stresses. Plant-Environment Interaction: Responses and Approaches to Mitigate Stress, p.205.

95. Suhre K, Gieger C. Genetic variation in metabolic phenotypes: study designs and applications. Nat Rev Genet. 2012, 13(11):759-69.

96. Tiwari, R.P., Mittal, V., Singh, G., Bhalla, T.C., Saini, S.S. and Vadehra, D.V., 1986. Effect of fatty acids on aflatoxin production byAspergillus parasiticus. Folia microbiologica, 31(2), pp.120-123.

97. Trucksess, M.; Brumley, W.; Nesheim, S. Rapid quantitation and confirmation of aflatoxins in corn and peanut butter, using a disposable silica gel column, thin layer chromatography, and gas chromatography/mass spectrometry. Journal of the Association of Official Analytical Chemists 1984, 67, 973–975.

98. Webb, M.S. and Green, B.R. (1991) Biochemical and biophysical properties of thylakoid acyl lipids. Biochim. Biophys. Acta, 1060, 133–158.

99. Wen W, Li D, Li X, Gao Y, Li W, Li H, Liu J, Liu H, Chen W, Luo J, Yan J. Metabolome-based genome-wide association study of maize kernel leads to novel biochemical insights. Nat Commun. 2014, 5:3438.

100. Wilkinson, J.R., Yu, J., Bland, J.M., Nierman, W.C., Bhatnagar, D. and Cleveland, T.E., 2007. Amino acid supplementation reveals differential regulation of aflatoxin biosynthesis in Aspergillus flavus NRRL 3357 and Aspergillus parasiticus SRRC 143. Applied microbiology and biotechnology, 74(6), pp.1308-1319.

101. Windham, G. L., Williams, W. P., Buckley, P. M., & Abbas, H. K. (2003). Inoculation techniques used to quantify aflatoxin resistance in corn. Journal of Toxicology: Toxin Reviews, 22(2-3), 313-325.

103. Yang L, Jiang T, Fountain JC, Scully BT, Lee RD, Kemerait RC, Chen S, Guo B. Protein profiles reveal diverse responsive signaling pathways in kernels of two maize inbred lines with contrasting drought sensitivity. Int J Mol Sci. 2014, 15(10):18892-918.

104. Yang XS, Staub JM, Pandravada A, Riordan SG, Yan Y, Bannon GA, Martino-Catt SJ. Omics technologies reveal abundant natural variation in metabolites and transcripts among conventional maize hybrids. Food and Nutrition Sciences. 2013, 4(03):335-341.

105. Yang, L., Fountain, J.C., Wang, H., Ni, X., Ji, P., Lee, R.D., Kemerait, R.C., Scully, B.T. and Guo, B., 2015. Stress sensitivity is associated with differential accumulation of reactive oxygen and nitrogen species in maize genotypes with contrasting levels of drought tolerance. International journal of molecular sciences, 16(10), pp.24791-24819.

106. Yobi, A., Wone, B.W., Xu, W., Alexander, D.C., Guo, L., Ryals, J.A., Oliver, M.J. and Cushman, J.C., 2012. Comparative metabolic profiling between desiccation-sensitive and desiccation-tolerant species of Selaginella reveals insights into the resurrection trait. The Plant Journal, 72(6), pp.983-999.

107. Zheng, Z.L., 2009. Carbon and nitrogen nutrient balance signaling in plants. Plant Signaling & Behavior, 4(7), pp.584-591.

108. Zhu JK. Salt and drought stress signal transduction in plants. Annu Rev Plant Biol. 2002, 53:247-73.

Table 5.1. Agronomic traits and aflatoxin contents of ears and kernels from six maize lines under normal irrigated conditions and drought stress conditions.

Inbred Lines	Ear length (cm)		Kernels per Row		500 kernel weight (g)		Aflatoxin content ($ng \cdot g^{-1}$)	
	W	D	W	D	W	D	W	D
B73	16.32±0.54	6.10±0.28	34.00±2.58	12.50±3.11	133.56±2.03	91.84±1.76	978.75+150.60	6901.96+388.22
Lo1016	18.33±0.64	10.65±0.60	37.25±2.99	16.00±1.83	129.75±0.91	96.99±1.22	917.33+54.28	1654.13+135.16
A638	11.95±0.44	7.13±0.30	22.50±2.65	11.75±2.50	103.69±1.13	76.39±2.67	856.40+15.83	932.27+8.17
Lo964	21.45±0.66	16.33±0.36	40.00±3.16	31.25±2.22	165.36±0.89	153.29±1.54	523.38+54.05	1510.62+248.15
Va35	18.83±0.51	14.25±0.55	31.50±2.08	23.00±1.83	127.39±1.07	117.97±3.19	738.71+23.83	1235.73+147.60
Grace-E5	10.20±0.72	7.38±0.35	19.75±1.71	13.00±2.58	143.90±1.28	132.46±1.77	1878.93+282.71	2256.48+213.49

Figure 5.1. Effects of drought on phenotypes of maize ears and aflatoxin accumulation in kernels. (A) Representative images of ears from six different maize lines collected at 14 DAI; left ears in each sub-image: without drought treatments, right ears in each sub-image: with drought treatment. (B) Thin layer chromatography (TLC) showing aflatoxin accumulation in mature kernels of six different maize lines; left spot in each column: without drought treatments; right spot in each column: with drought treatment. Aflatoxin standard with both B and G toxins are included on the outermost columns.

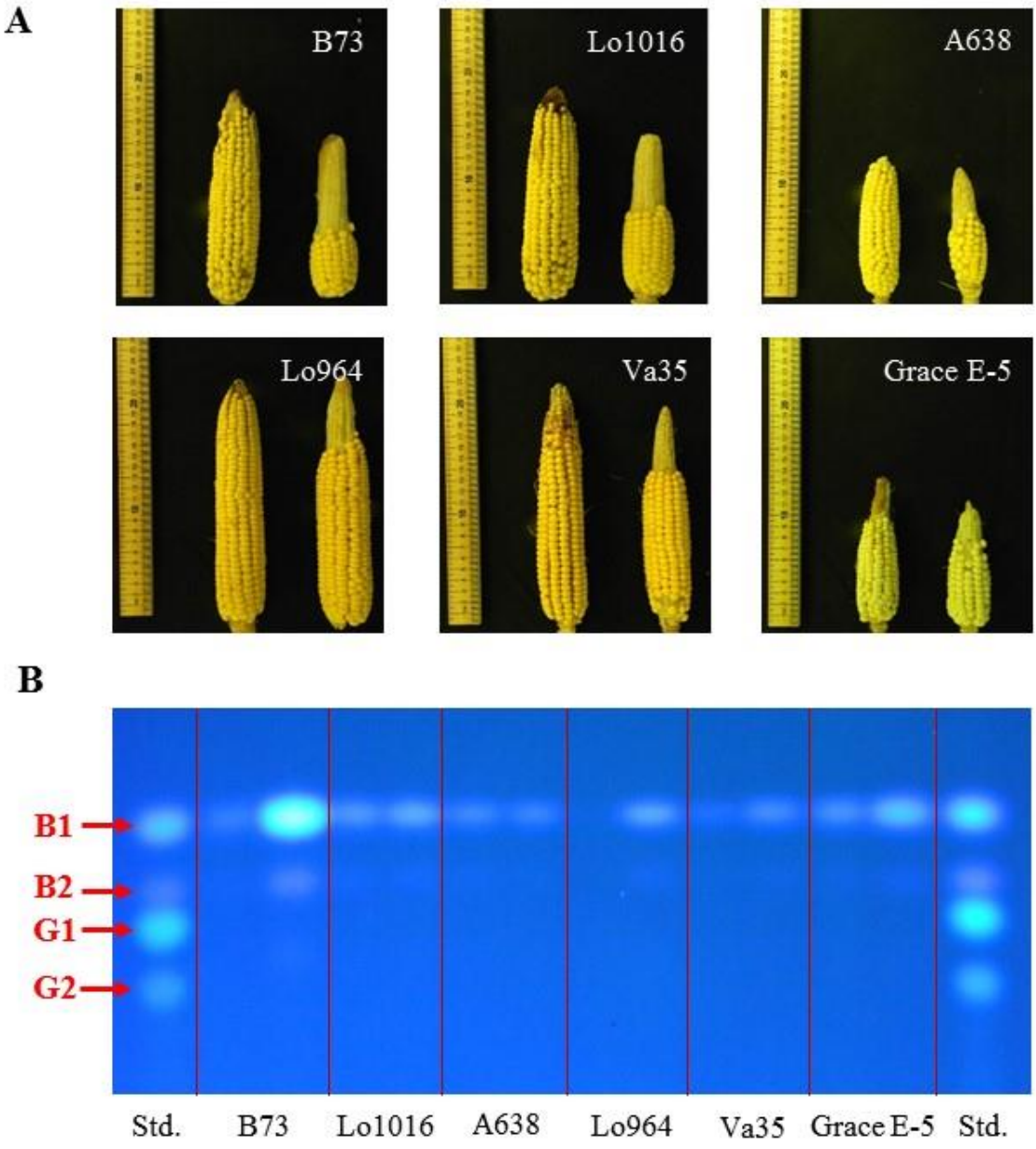
A
B73
Lo1016
A638
Lo964
Va35
Grace E-5
B
B1
B2
G1
G2
Std.
B73
Lo1016
A638
Lo964
Va35
Grace E-5
Std.

Figure 5.2. Fluorescent detection of H_2O_2 and $OH^{\cdot -}$ radicals in maize kernels at 7 DAI and 14 DAI. H_2O_2 is visualized in the top set of panels by fluorescence of Amplex Red (red fluorescence) staining while in the lower panels $OH^{\cdot -}$ radicals were visualized using Aminophenyl fluorescein staining (green fluorescence). Irrigated control and drought stressed kernels from both 7 and 14DAI are shown. Increasing levels of fluorescence for both ROS over time under drought stress can be observed to a greater extent in B73 than Lo964.

	B73		Lo964	
H2O2	7 DAI	7-day control	7 DAI	7-day control
			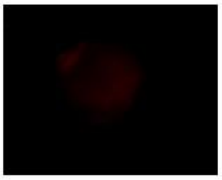	
	14 DAI	14-day control	14 DAI	14-day control
	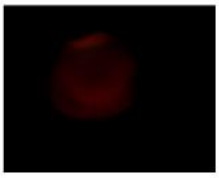			
·HO	7 DAI	7-day control	7 DAI	7-day control
	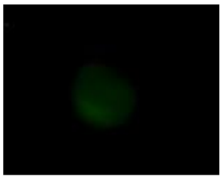			
	14 DAI	14-day control	14 DAI	14-day control
	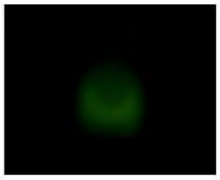	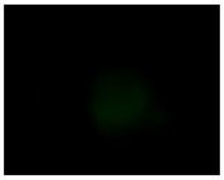	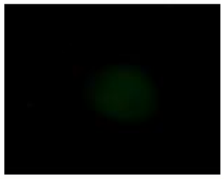	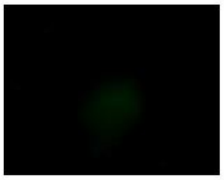

Figure 5.3. Metabolite distribution in maize kernels from B73 and Lo964 with or without drought stress treatments, as defined by partial least-squares discriminant analysis (PLS-DA). S7D, S14D, S7W and S14W refers to the metabolites from B73 with and without drought treatments for 7 and 14 DAI; R7D, R14D, R7W and R14W refers to the metabolites from Lo964 with and without drought treatments for 7 and 14 DAI. A clear distinction can be observed between both the treatments applied and the lines used in the study indicative of significant differences in metabolome content between treatments. The five points in each group are representative of the biological replicates performed for the study.

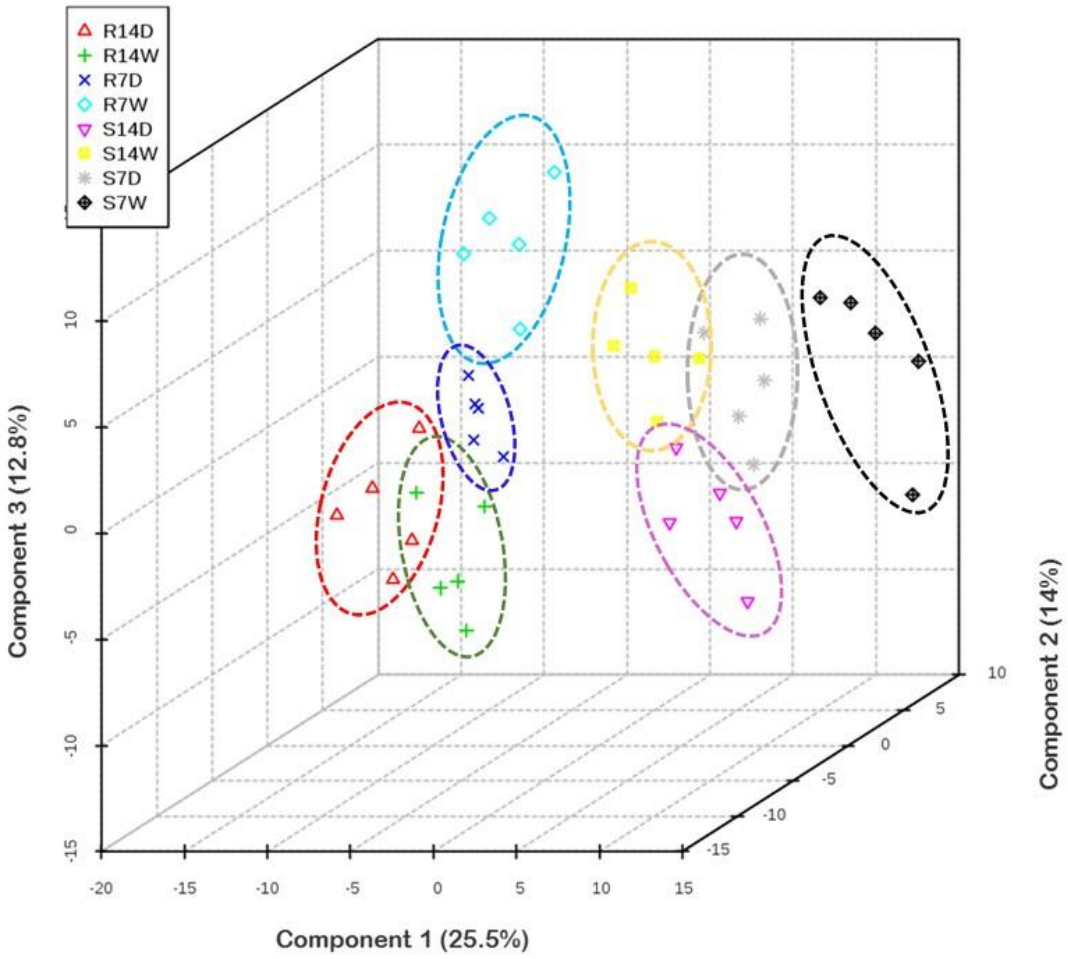
R14D
R14W
R7D
R7W
S14D
S14W
S7D
S7W
Component 3 (12.8%)
Component 1 (25.5%)
Component 2 (14%)

Figure 5.4. Venn diagram showing the overlap of differentially expressed metabolites in kernels of B73 and Lo964 responding to drought treatments compared to well-watered controls. S7D, S14D, S7W and S14W refers to the metabolites from B73 with and without drought treatments for 7 and 14 DAI; R7D, R14D, R7W and R14W refers to the metabolites from Lo964 with and without drought treatments for 7 and 14 DAI. The number in each sub-collection refers to quantity of metabolites in intersection, and the number in brackets refers to the quantity of metabolites with more than 2-fold change.

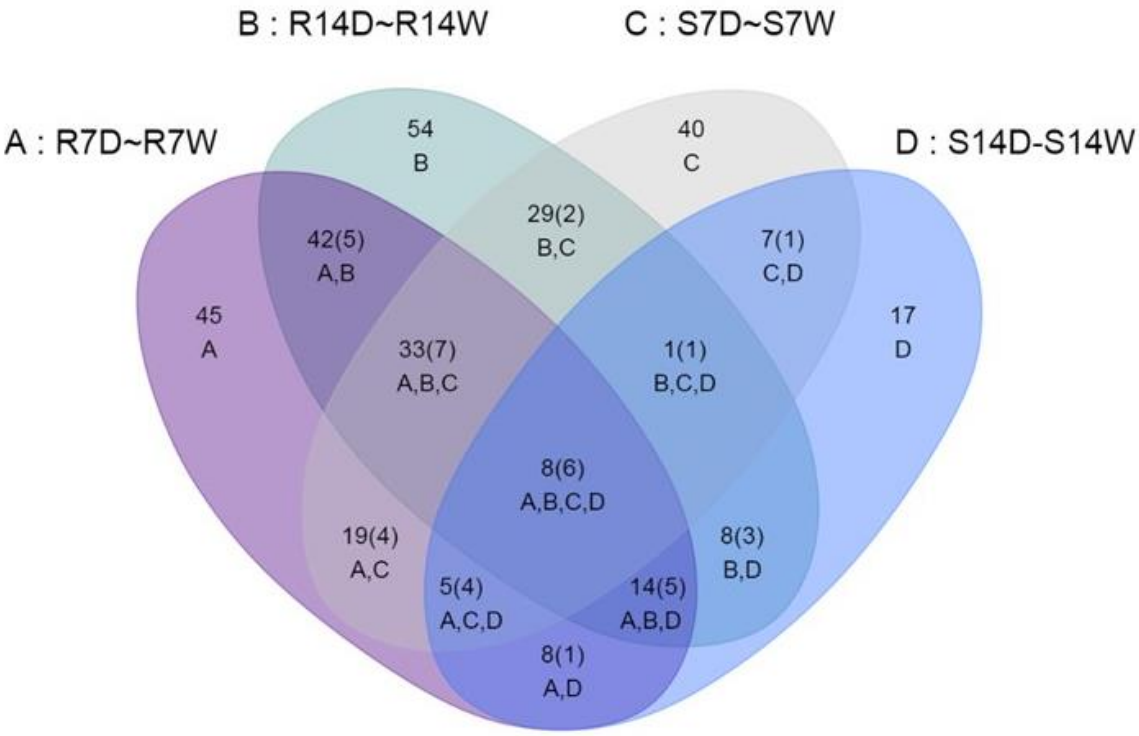
B : R14D~R14W
C : S7D~S7W
A : R7D~R7W
D : S14D-S14W
54
B
40
C
29(2)
B,C
42(5)
A,B
7(1)
C,D
45
A
17
D
33(7)
A,B,C
1(1)
B,C,D
8(6)
A,B,C,D
19(4)
A,C
8(3)
B,D
5(4)
A,C,D
14(5)
A,B,D
8(1)
A,D

Figure 5.5. Differences in the metabolites involved in carbohydrate and amino acid metabolism between B73 and Lo964 at 7 DAI and 14 DAI. Grids located beside each metabolite represent their respective accumulation in B73 or Lo964 at each time point when comparing the drought stressed and irrigated samples. Colors correspond to the significance of the change in accumulation. Red: up-abundance with $p < 0.05$; Light Red: up-abundance with $0.1 < p < 0.05$; Green: down-abundance with $p < 0.05$; Light Green: down-abundance with $0.1 < p < 0.05$; Gray: no significant difference. B73 showed increases in simple sugar content while Lo964 displayed increases in glycolytic intermediates and amino acids in response to drought.

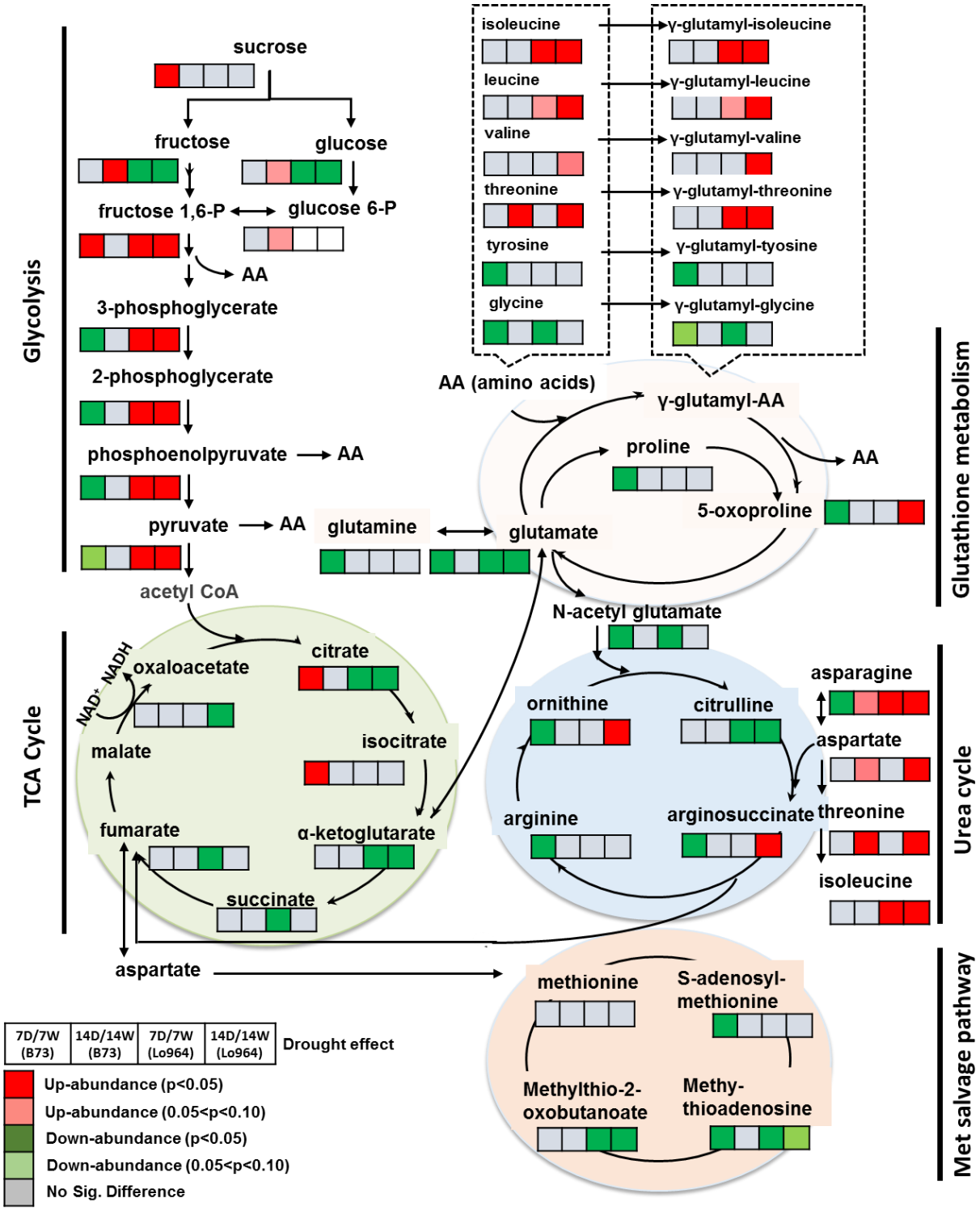
Glycolysis
sucrose
fructose
glucose
fructose 1,6-P
glucose 6-P
AA
3-phosphoglycerate
2-phosphoglycerate
phosphoenolpyruvate
AA
pyruvate
AA
acetyl CoA
isoleucine
leucine
valine
threonine
tyrosine
glycine
γ-glutamyl-isoleucine
γ-glutamyl-leucine
γ-glutamyl-valine
γ-glutamyl-threonine
γ-glutamyl-tyosine
γ-glutamyl-glycine
AA (amino acids)
γ-glutamyl-AA
proline
AA
5-oxoproline
glutamine
glutamate
N-acetyl glutamate
Glutathione metabolism
TCA Cycle
citrate
oxaloacetate
NAD+
NADH
isocitrate
malate
fumarate
α-ketoglutarate
succinate
aspartate
ornithine
citrulline
arginine
arginosuccinate
asparagine
aspartate
threonine
isoleucine
Urea cycle
methionine
S-adenosyl-methionine
Methylthio-2-oxobutanoate
Methy-thioadenosine
Met salvage pathway
7D/7W (B73)
14D/14W (B73)
7D/7W (Lo964)
14D/14W (Lo964)
Drought effect
Up-abundance (p<0.05)
Up-abundance (0.05<p<0.10)
Down-abundance (p<0.05)
Down-abundance (0.05<p<0.10)
No Sig. Difference

Figure 5.6. Differences in the metabolites involved in lipid metabolism between B73 and Lo964 at 7 DAI and 14 DAI. Grids located beside each metabolite represent their respective accumulation in B73 or Lo964 at each time point when comparing the drought stressed and irrigated samples. Colors correspond to the significance of the change in accumulation. Red: up-abundance with $p < 0.05$; Light Red: up-abundance with $0.1 < p < 0.05$; Green: down-abundance with $p < 0.05$; Light Green: down-abundance with $0.1 < p < 0.05$; Gray: no significant difference. B73 displayed increases in unsaturated fatty acid and oxylipin content while Lo964 displayed increases in sphingolipids and linoleate derivatives in response to drought.

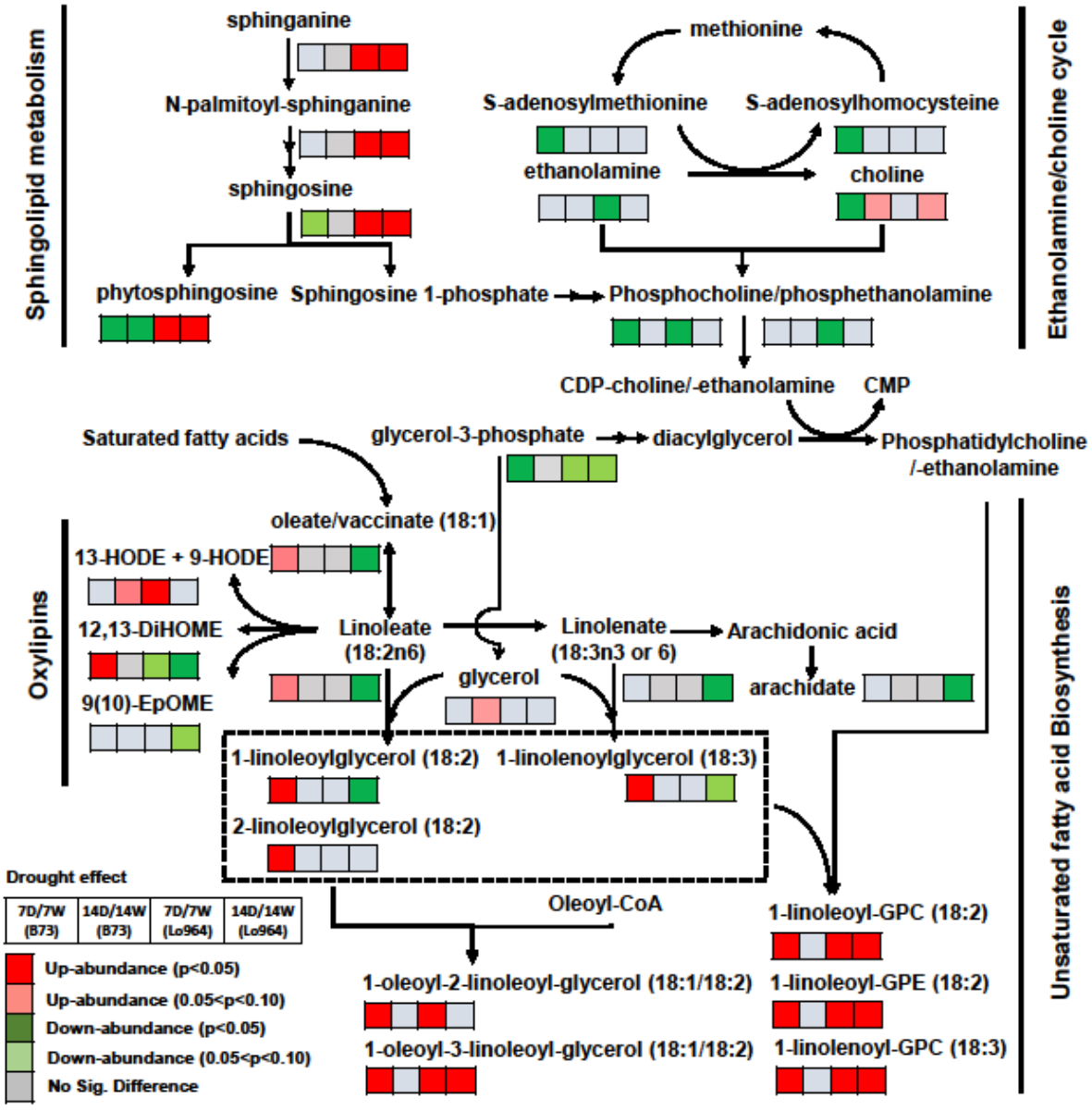
Sphingolipid metabolism
sphinganine
N-palmitoyl-sphinganine
sphingosine
phytosphingosine
Sphingosine 1-phosphate
methionine
S-adenosylmethionine
S-adenosylhomocysteine
ethanolamine
choline
Phosphocholine/phosphethanolamine
Ethanolamine/choline cycle
CDP-choline/-ethanolamine
CMP
Saturated fatty acids
glycerol-3-phosphate
diacylglycerol
Phosphatidylcholine
/-ethanolamine
oleate/vaccinate (18:1)
Oxylipins
13-HODE + 9-HODE
12,13-DiHOME
9(10)-EpOME
Linoleate
(18:2n6)
Linolenate
(18:3n3 or 6)
Arachidonic acid
arachidate
glycerol
1-linoleoylglycerol (18:2)
1-linolenoylglycerol (18:3)
2-linoleoylglycerol (18:2)
Drought effect
7D/7W (B73)
14D/14W (B73)
7D/7W (Lo964)
14D/14W (Lo964)
Up-abundance (p<0.05)
Up-abundance (0.05<p<0.10)
Down-abundance (p<0.05)
Down-abundance (0.05<p<0.10)
No Sig. Difference
Oleoyl-CoA
1-linoleoyl-GPC (18:2)
1-oleoyl-2-linoleoyl-glycerol (18:1/18:2)
1-linoleoyl-GPE (18:2)
1-oleoyl-3-linoleoyl-glycerol (18:1/18:2)
1-linolenoyl-GPC (18:3)
Unsaturated fatty acid Biosynthesis

Figure 5.7. Metabolite-metabolite network based on significant correlations. Metabolites were represented as nodes, different colors of nodes displayed metabolites in different pathways. Red: lipids and derivatives; blue: amino acids; yellow: nucleic acids; light blue: carbohydrates; light green: amino acid derivatives; purple: vitamin metabolism; and black: aminobenzoate metabolism. Node color, distribution, and connections show the interrelationship between the accumulation patterns and biochemical characteristics of the compounds.

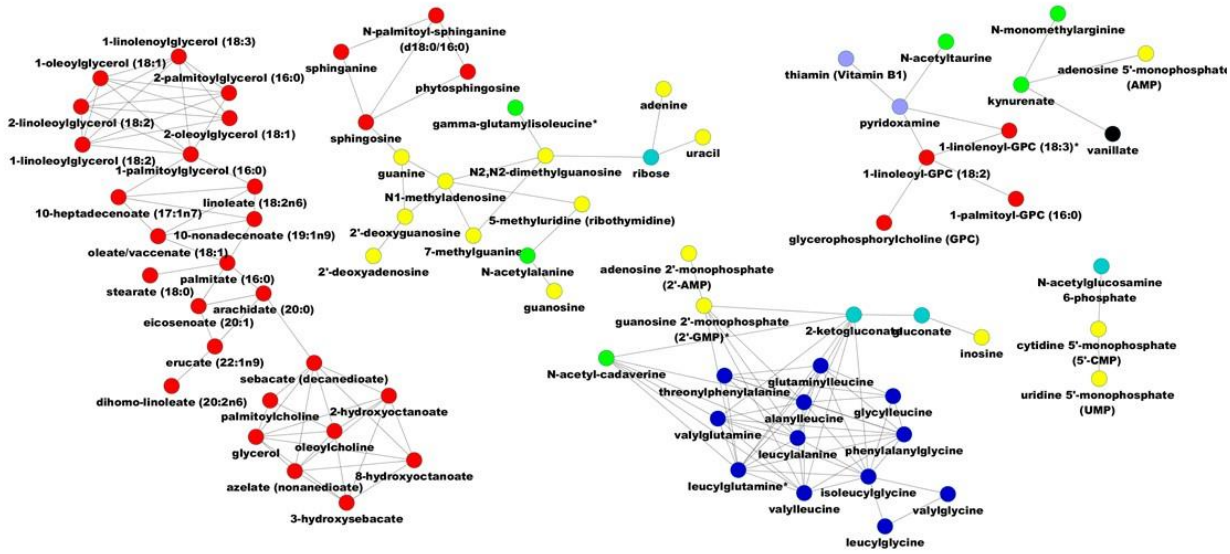
1-linolenoylglycerol (18:3)
1-oleoylglycerol (18:1)
2-palmitoylglycerol (16:0)
2-linoleoylglycerol (18:2)
2-oleoylglycerol (18:1)
1-linoleoylglycerol (18:2)
1-palmitoylglycerol (16:0)
linoleate (18:2n6)
10-heptadecenoate (17:1n7)
10-nonadecenoate (19:1n9)
oleate/vaccenate (18:1)
palmitate (16:0)
stearate (18:0)
arachidate (20:0)
eicosenoate (20:1)
erucate (22:1n9)
sebacate (decanedioate)
dihomo-linoleate (20:2n6)
palmitoylcholine
2-hydroxyoctanoate
glycerol
oleoylcholine
8-hydroxyoctanoate
azelate (nonanedioate)
3-hydroxysebacate
N-palmitoyl-sphinganine (d18:0/16:0)
sphinganine
phytosphingosine
sphingosine
gamma-glutamylisoleucine*
adenine
uracil
guanine
N2,N2-dimethylguanosine
ribose
N1-methyladenosine
5-methyluridine (ribothymidine)
2'-deoxyguanosine
7-methylguanine
2'-deoxyadenosine
N-acetylalanine
guanosine
N-monomethylarginine
N-acetyltaurine
thiamin (Vitamin B1)
adenosine 5'-monophosphate (AMP)
kynurenate
pyridoxamine
1-linolenoyl-GPC (18:3)*
vanillate
1-linoleoyl-GPC (18:2)
1-palmitoyl-GPC (16:0)
glycerophosphorylcholine (GPC)
adenosine 2'-monophosphate (2'-AMP)
guanosine 2'-monophosphate (2'-GMP)*
2-ketogluconate
gluconate
inosine
N-acetyl-cadaverine
glutaminylleucine
threonylphenylalanine
glycylleucine
alanylleucine
valylglutamine
leucylalanine
phenylalanylglycine
leucylglutamine*
isoleucylglycine
valylleucine
valylglycine
leucylglycine
N-acetylglucosamine 6-phosphate
cytidine 5'-monophosphate (5'-CMP)
uridine 5'-monophosphate (UMP)

CHAPTER 6

EFFECTS OF HYDROGEN PEROXIDE ON DIFFERENT TOXIGENIC AND ATOXIGENIC ISOLATES OF *ASPERGILLUS FLAVUS*

Fountain, J.C., Scully, B.T., Chen, Z., Gold, S.E., Glenn, A.E., Abbas, H.K., Lee, R.D., Kemerait, R.C., Guo, B. (2015). Effects of hydrogen peroxide on different toxigenic and atoxigenic isolates of *Aspergillus flavus*. *Toxins* 7:2985-2999. doi:10.3390/toxins7082985.

Abstract

Drought stress in the field has been shown to exacerbate aflatoxin contamination of maize and peanut. Drought and heat stress also produce reactive oxygen species (ROS) in plant tissues. Given the potential correlation between ROS and exacerbated aflatoxin production under drought and heat stress, the objectives of this study were to examine the effects of hydrogen peroxide (H_2O_2)-induced oxidative stress on the growth of different toxigenic (+) and atoxigenic (−) isolates of *Aspergillus flavus* and to test whether aflatoxin production affects the H_2O_2 concentrations that the isolates could survive. Ten isolates were tested: NRRL3357 (+), A9 (+), AF13 (+), Tox4 (+), A1 (−), K49 (−), K54A (−), AF36 (−), and Aflaguard (−); and one *A. parasiticus* isolate, NRRL2999 (+). These isolates were cultured under a H_2O_2 gradient ranging from 0 to 50 mM in two different media, aflatoxin-conducive yeast extract-sucrose (YES) and non-conducive yeast extract-peptone (YEP). Fungal growth was inhibited at a high H_2O_2 concentration, but specific isolates grew well at different H_2O_2 concentrations. Generally the toxigenic isolates tolerated higher concentrations than did atoxigenic isolates. Increasing H_2O_2 concentrations in the media resulted in elevated aflatoxin production in toxigenic isolates. In YEP media, the higher concentration of peptone (15%) partially inactivated the H_2O_2 in the media. In the 1% peptone media, YEP did not affect the H_2O_2 concentrations that the isolates could survive in comparison with YES media, without aflatoxin production. It is interesting to note that the commercial biocontrol isolates, AF36 (−), and Aflaguard (−), survived at higher levels of stress than other atoxigenic isolates, suggesting that this testing method could potentially be of use in the selection of biocontrol isolates. Further studies will be needed to investigate the mechanisms behind the variability among isolates with regard to their degree of oxidative stress tolerance and the role of aflatoxin production.

Introduction

The contamination of agricultural products with aflatoxins produced by *Aspergillus flavus* poses a serious threat to human health and food security, particularly in developing countries [1, 2]. Research into aflatoxin contamination prevention began in the 1960s following the outbreak of what was termed turkey X disease which resulted in the deaths of over 100,000 turkey poults due to aflatoxin contaminated feed [3]. These efforts were intensified in the area of pre-harvest host resistance following outbreaks in US maize in the 1970s, and their importance has been further underscored by the 2004 Kenya outbreak which resulted in 125 human deaths due to direct aflatoxicosis from consumption of contaminated maize [4, 5].

The contamination of oilseed crops, such as maize and peanut, with aflatoxin has been shown to be exacerbated by the presence of drought stress and related abiotic stresses [6, 7]. Host drought tolerance and reduced aflatoxin accumulation are also correlated [6, 7]. Given this observation, it is important to better understand the mechanisms at play in this relationship and how they may relate to both environmental stress tolerance and to the regulation of aflatoxin production in the pathogen.

Aflatoxin production in the *Aspergilli* is a complex process under a high degree of regulation through multiple mechanisms [8, 9]. Numerous studies have shown that aflatoxin production can be exacerbated by reactive oxygen species (ROS) and their reactive products including oxylipins [10, 11]. For example, Jayashree and Subramanyam [12] demonstrated that peroxidized lipids can stimulate the production of aflatoxin in *A. parasiticus* and accumulate to high levels during trophophase growth which coincides with aflatoxin production initiation in toxigenic isolates. Additional studies have also demonstrated that toxigenic isolates exhibit elevated oxygen consumption, greater mycelial ROS accumulation, and greater peroxisome

number than atoxigenic isolates, indicating a reasonable link between ROS and aflatoxin accumulation [12 – 16] . Recent molecular studies have also revealed that aflatoxin production is regulated by stress-related transcription factor pathways mediated by AtfB and AP-1, as well as the Velvet A (VeA) signaling pathway in response to *in vitro* applied ROS [14 – 16]. The growth and development of *A. flavus* is also regulated by ROS. For example, Grintzalis *et al.*, [17] demonstrated that ROS can regulate the production of aflatoxin and sclerotial differentiation in a concentration-dependent manner.

This proposed link between ROS and aflatoxin production has several implications with regard to the pathogen's biology and host defense against aflatoxin contamination. Given the correlation observed between elevated aflatoxin production and ROS accumulation, it has been proposed that aflatoxin production or associated mechanisms may provide some advantages in the drought and heat stress environments with high ROS to compete with other microorganisms [16, 18 – 20]. This opens the possibility that ROS may also function in the host-pathogen interaction between *Aspergillus* spp. and their host plants as a form of "cross-kingdom communication" [16, 19]. This seems plausible given the observed correlation between drought stress, which results in the accumulation of ROS in host plant tissues, and the exacerbation of aflatoxin contamination in oilseed crops such as maize and peanut [6, 7, 21, 22].

Given this correlation among drought and heat stresses, ROS and aflatoxin production, it is possible that the ability to produce aflatoxin may influence the growth of *Aspergillus* spp. isolates when exposed to drought stress-derived ROS such as hydrogen peroxide (H_2O_2) Therefore, the objectives of this study were twofold: to examine the effects of H_2O_2-induced oxidative stress on the growth of different isolates of toxigenic (+) and atoxigenic (−) isolates of *Aspergillus flavus*, and to test whether aflatoxin production affects the concentrations of H_2O_2 in

which the isolates could grow and survive. To test this, the differences in oxidative stress tolerance between toxigenic (+) and atoxigenic (−) isolates were examined using hydrogen peroxide (H_2O_2) as oxidative stress encountered during drought stress in both aflatoxin conducive and non-conducive media. Overall, for the isolates tested, toxigenic isolates generally tolerated higher levels of oxidative stress than did atoxigenic isolates. The reduction in aflatoxin production did not affect the survival levels of ROS induced by supplemental H_2O_2 in aflatoxin non-conducive 1% peptone YEP media. In addition, selected commercially available atoxigenic biological control isolates were able to tolerate greater levels of stress than non-selected isolates indicating the potential utility of this experimental method in screening local atoxigenic isolates for use as biological control agents in developing countries [23].

Materials and Methods

Isolate Collection

The isolates of *A. flavus* and *A. parasiticus* utilized in the study were collected from various sources as follows. The *A. flavus* isolate NRRL3357 and the *A. parasiticus* isolate NRRL2999 were obtained from the Northern Regional Research Center, USDA-ARS, Peoria, IL. The *A. flavus* isolates K49 and K54A were obtained from Dr. Hamed Abbas, USDA-ARS Biological Control of Pests Research Unit (Stoneville, MS, USA). The *A. flavus* isolates A1, A9, AF13, AF36, Aflaguard, and Tox4 were obtained from Dr. Kenneth Damann, Department of Plant Pathology and Crop Physiology, Louisiana State University (Baton Rouge, LA, USA). All isolates were shipped on potato dextrose agar (PDA) and were re-cultured on V8 agar (20% V8, 1% $CaCO_3$, 3% agar).

Culture Conditions and Biomass Measurement

The isolates were cultured on V8 agar plates at 32 °C from 5–7 days prior to use in the experiment. Conidia were then harvested from the plates in sterile water with 0.1% (*v*/*v*) Tween 20 and stored at 4 °C for further use. Four media were utilized in this study including: 1% YES (2% yeast extract, 1% sucrose), 15% YES (2% yeast extract, 15% sucrose), 1% YEP (2% yeast extract, 1% peptone), and 15% YEP (2% yeast extract, 15% peptone). The YES media is a toxin-conducive media and the YEP media is a toxin non-conducive media [36]. The concentrations of the media components were chosen based on optimized conditions determined by Davis *et al.*, [34].The media were supplemented with a gradient of hydrogen peroxide (H_2O_2; 3% stabilized solution) ranging from 0–50 mM. The media were then transferred to sterile 125 mL Erlenmeyer flasks with a total volume of 50 mL. The cultures were then inoculated with 100 μL of conidial suspension (~4.0×10^6 conidia/mL) from their respective isolates and plugged with a sterile cotton ball. The cultures were then incubated under stationary conditions at 32 °C in the dark for 7 days. Following incubation, the cultures were removed and the fungal mycelia were collected from each culture by filtration through non-sterilized Whatman no. 1 filter paper (GE Healthcare Life Sciences, Pittsburgh, PA, USA). The collected mycelia were then dried at 80 °C for 3–5 days and their dry biomass was recorded. In addition, a fraction of the culture filtrates were collected into amber glass vials and stored at 4 °C for use in aflatoxin measurement. Each assay was repeated at least three times.

Aflatoxin Measurement

The collected culture filtrates were then used to visualize the production of aflatoxin by the isolates in each medium and H_2O_2 combination using a modified thin layer chromatography

(TLC) method based on that employed by Guo *et al.*, [37]. Briefly, 500 μL of each culture filtrate was mixed with an equal volume of benzene in a 2 mL microfuge tube. The solution was then vortexed vigorously for 30 s. and then centrifuged at 10,000 × g at 25 °C for 2 min. The organic supernatant was then transferred to a 7 mL amber glass vial and was allowed to evaporate. The aflatoxin-containing residue was then dissolved in 100 μL methylene chloride and mixed by gentle inversion. For TLC analysis, 10 μL of each aflatoxin extract were spotted onto a silica-coated plate (10 × 20 cm; Z185329; Sigma Aldrich, St. Louis, MO, USA) along with an aflatoxin B_1 standard (A6636; Sigma Aldrich, St. Louis, MO, USA). The plates were then developed in diethyl ether: methanol: water (96:3:1) and allowed to dry under the fume hood. The presence or absence of aflatoxin was then confirmed by viewing the plates under UV light (365 nm). The plates were then photographed using a Nikon Coolpix L110 digital camera (Nikon, Tokyo, Japan).

Hydrogen Peroxide Degradation Assay

In order to evaluate the potential for the supplemented H_2O_2 to be inactivated by the culture media carbon sources, the concentration of H_2O_2 within non-inoculated culture media was monitored over time. Briefly, each medium (1% YES, 15% YES, 1% YEP, and 15% YEP) and a water control were supplemented with H_2O_2 to a concentration of 30 mM. The supplemented media were then placed at 32 °C in the dark, the same conditions employed in the culture experiment. The levels of H_2O_2 were then measured every 24 h for 72 h using an Amplex Red hydrogen peroxide/peroxidase kit (Life Technologies, Carlsbad, CA, USA) according to the manufacturer's instructions. A standard curve based on reaction H_2O_2 concentration was generated in order to calculate the H_2O_2 levels present in the culture media (Figure 6.2A).

Fluorescence measurements performed during the assay were done using a Biotek Synergy HT plate reader (Biotek, Winooski, VT, USA). The assay was repeated twice for each of three biological replicates.

Results and Discussion

Oxidative Stress Tolerance in Toxin-Conducive Media

In order to determine the effects of oxidative stress encountered during drought on toxigenic and atoxigenic isolates, we simulated this stress *in vitro* using H_2O_2 supplemented aflatoxin production conducive media. The applied concentrations of H_2O_2 were based on those utilized in previous studies [14] and based on the range of hydrogen peroxide levels previously observed to be cytotoxic to plant cells [24, 25].

In the aflatoxin production-conducive 15% sucrose YES media at the higher concentrations of supplemental H_2O_2, fungal growth was inhibited, but the different isolates grew well at different concentrations of H_2O_2. The toxigenic isolates including *A. flavus* Tox4, A9, AF13, and NRRL3357; and *A. parasiticus* NRRL2999 were able to grow well at levels of oxidative stress up to 40, 40, 35, 25, and 25 mM H_2O_2, respectively (Table 6.1). The atoxigenic isolates including *A. flavus* K49, AF36, Aflaguard, A1, and K54A, however, were only able to survive oxidative stress up to 30, 25, 25, 20, and 15 mM H_2O_2, respectively (Table 6.1). This indicates that there is a great deal of variability among the isolates with regard to their degree of oxidative stress tolerance with or without aflatoxin production in the natural environment.

However, the toxigenic isolate NRRL3357 survived only to 25 mM H_2O_2, a level comparable to most of the atoxigenic isolates examined in the study. Previous studies have shown that toxigenic isolates accumulate elevated levels of aflatoxin in response to increasing

oxidative stress *in vitro* [12, 13]. This was also observed here in the toxigenic isolates with increasing levels of H_2O_2-induced stress resulting in elevated levels of aflatoxin production in the toxigenic isolates grown in toxin-conducive 15% YES media (Figure 6.1A). These results are similar to those observed by Roze *et al.*, [26] where isolates produced greater levels of aflatoxin with increased levels of oxidative stress. Nonetheless, the production of aflatoxin as observed in NRRL3357 was lower in comparison to other examined isolates. Therefore, it is likely that aflatoxin production alone may not directly contribute to the stress tolerance in toxigenic isolates in general as observed here but other factors which are in need of further investigation.

Additional studies have also shown that toxigenic isolates exhibit enhanced antioxidant enzyme activities during the initiation of aflatoxin production, which may enhance the oxidative stress tolerance of the isolates [12, 13]. Narasaiah *et al.*, [20] suggested that the production of aflatoxin biosynthetic pathway intermediates may also function to remediate oxidative stress through the consumption and sequestration of ROS during their biosynthesis. However, the specific roles of these compounds in oxidative stress responses of *A. flavus* isolates have yet to be demonstrated. This apparent co-expression of antioxidant enzymes and aflatoxin production in response to H_2O_2-induced oxidative stress can have two possible interpretations: (1) aflatoxin production can function in further enhancing oxidative stress tolerance beyond that afforded by the antioxidant enzymes alone; or (2) aflatoxin and/or pathway intermediates may cause additional oxidative stress for as yet unknown reasons, and antioxidant enzymes are elevated in activity to counter this stress [18]. Continuing studies in the laboratory will examine the effects of these intermediate compounds and aflatoxin in enhancing or diminishing oxidative stress tolerance in *Aspergillus* spp.

Another trend was observed in the atoxigenic isolates. It was found that the atoxigenic isolates exhibiting the highest levels of oxidative stress tolerance were the K49, AF36, and Aflaguard biological control isolates (Table 6.1). These isolates have been selected due to their adaptation to local environments in the U.S., and their performance as effective biological controls for remediating aflatoxin contamination in maize and peanut [27 – 29].

Since environmental stress adaptation and competitive capabilities against toxigenic isolates likely are key indicators of biocontrol isolate performance, the selection of local adapted atoxigenic isolates for use as biological controls is preferred to introducing non-adapted isolates [23]. This concept has been demonstrated in sub-Saharan Africa with the selection of local adapted atoxigenic isolates for use as biological controls, and through the utilization of blends of isolates to enhance the diversity of the biological controls for broader efficacy in remediating aflatoxin contamination [23, 30, 31].

Given the need, therefore, to rapidly and efficiently screen atoxigenic isolates for utility as biological control agents, an effective, low cost, and technically simple method is needed. Several available screening methods are currently used based on competitive inhibition of aflatoxin production in which potential biological control isolates are co-inoculated with toxigenic isolates onto maize kernels [31], or into coconut liquid media [32]. These methods examine the effectiveness of potential biological control isolates in inhibiting aflatoxin production by toxigenic isolates, but do not evaluate their environmental stress tolerance, which is necessary if the isolate will be deployed in multiple, non-native environments. Since H_2O_2-induced oxidative stress occurs in organisms in response to abiotic stresses such as drought and heat [33], it is possible that the method used in this study could be utilized to screen potential biological control isolates for environmental stress tolerance *in vitro* prior to deployment in field

trials. This seems plausible given that atoxigenic isolates that have been selected for their performance as biological controls and permanence in the field (K49, AF36, and Aflaguard) possess elevated oxidative stress tolerance in comparison to non-selected atoxigenic isolates (A1 and K54A). Continuing studies in the laboratory will also examine the potential of this H_2O_2 gradient method in predicting atoxigenic isolate performance.

Effects of Carbon Source on Aflatoxin Production and Isolate Oxidative Stress Tolerance

In order to examine the role of aflatoxin production in oxidative stress responses, the isolates were cultured in a toxin non-conducive media, 15% peptone YEP, under the same conditions used previously with the toxin-conducive 15% sucrose YES media. If aflatoxin production functions at least in part in oxidative stress responses, it would be expected that the oxidative stress tolerance of the toxigenic isolates would be affected in non-conducive YEP media supplemented with H_2O_2 while the atoxigenic isolates would not be significantly affected. However, it was found that culturing the isolates in 15% peptone YEP media increased the levels of H_2O_2 that both the toxigenic and atoxigenic isolates could tolerate in comparison to their observed growth in 15% sucrose YES (Tables 6.1 and 6.2). Specifically, the toxigenic isolates Tox4, A9, AF13, NRRL3357, and NRRL2999 were able to survive up to 50, 50, 50, 40, and 30 mM H_2O_2, respectively, and the atoxigenic isolates Aflaguard, A1, K49, AF36, and K54A were able to survive up to 45, 40, 35, 35, and 30 mM H_2O_2, respectively (Table 6.2).

Unexpectedly, modifying the carbon source availability in the culture media enhanced the survival of toxigenic isolates of *Aspergillus* spp. However, the additional enhancement of the tolerance of the atoxigenic isolates to higher concentrations of H_2O_2 indicates that there is a medium-specific response that may be affecting the results. In addition, the survival of the

isolates at H_2O_2 concentrations potentially higher than 50 mM seems unlikely given the previously described oxidative stress tolerance of plant apoplasts with cell death occurring within 24 h in cultured *Arabidopsis thaliana* cells exposed to comparable levels of H_2O_2 [24]. Therefore, it is possible that peptone may act as an "inactivator or chelator" of H_2O_2 when utilized as a medium carbon source.

To determine whether or not changing the culture medium carbon source introduced artifacts into the system, we measured the concentration of H_2O_2 in non-inoculated culture media supplemented with 30 mM H_2O_2 over time with carbon source concentration of 15% and a minimum concentration of 1% under the same conditions used in the previous experiments and in earlier studies by Davis *et al.*, [34]. It was found that yeast extract media supplemented with sucrose (YES) at either 1% or 15% concentrations, or with peptone (YEP) at a concentration of 1% exhibited a slow rate of H_2O_2 degradation over time not significantly different from that observed in a water control supplemented with 30 mM H_2O_2 implying naturally expected H_2O_2 degradation in solution (Figure 6.2). However, when the yeast extract media was supplemented with peptone at a 15% concentration, the detected H_2O_2 levels in the media reduced rapidly to 52.3% and 17.2% of initial levels within 24 h and 72 h, respectively in the absence of *A. flavus* inoculum (Figure 6.2B).

These results indicate that elevated levels of peptone in yeast extract-based culture media can inhibit H_2O_2 from supplemented media thereby reducing the oxidative stress experienced by the fungi cultured in the media. This is especially true when peptone is present in higher numbers of molecules than H_2O_2 as seen in the present study (H_2O_2 to peptone peptide ratio of 2:5 in 15% YEP and 6:1 in 1% YEP assuming average peptide size of 2 kDa). This implies that the inactivating capabilities of peptone may be concentration dependent with higher levels of

peptone being able to sequester more H_2O_2 than lower levels of peptone. If this is the case, it would be expected that if isolates were cultured at higher peptone concentrations, they would experience less H_2O_2-derived oxidative stress over a shorter time period resulting in the appearance of enhanced stress tolerance. Given that this system serves as the basis of suppressing aflatoxin production in order to examine the effects of oxidative stress in some molecular studies [15], it is important to consider the potential of the peptide fragments found in peptone to react with H_2O_2 molecules to prevent experimental bias in future studies.

Isolate Responses in Reduced Carbon Source Media

In order to verify that the increase in isolate survival in 15% peptone YEP was due to the sequestration of H_2O_2 when peptone was present in excess, we cultured select isolates in yeast extract media supplemented with either sucrose or peptone at a minimum concentration of 1%. For the 1% sucrose YES media, the selected atoxigenic isolates, AF13, NRRL3357, Aflaguard, and K54A, were able to survive H_2O_2 concentrations up to 35, 20, 20, and 15 mM, respectively (Table 6.3), which were comparable to the results observed in the 15% sucrose YES media (Table 6.1). For the 1% peptone YEP media, the select isolates were able to survive H_2O_2 concentrations up to 30, 20, 20, and 15 mM, respectively (Table 6.4), which was drastically reduced in comparison to the results observed in 15% peptone YEP media (Table 6.2). This combined with the observed reduction in H_2O_2 concentration in non-inoculated 15% peptone YEP media confirms that peptone sequestration of H_2O_2 is the likely cause of the enhanced isolate survival observed in 15% peptone YEP.

Comparing the responses of the isolates in the minimum carbon source media, several observations can be made. First, the level of H_2O_2 -induced stress that the isolates are able to

tolerate is similar between the media. This is interesting given that aflatoxin production is stimulated in response to increasing oxidative stress in the toxigenic isolates in the 1% YES media as observed in the 15% YES media while no aflatoxin is produced by the isolates cultured in 1% YEP media (Figure 6.1B). Second, while the difference between the isolates' response in the 1% carbon media is not pronounced, there are some slight differences particularly in the AF13 and NRRL3357 isolates. In both the 15% and 1% YES media, AF13 was able to tolerate 35 mM H_2O_2, but, in the 1% YEP medium, the isolate is only able to tolerate 30 mM H_2O_2 (Tables 6.1, 6.3, and 6.4). In addition, the absence of observable aflatoxin production in the NRRL3357 isolate in 1% YES supplemented with 20 mM H_2O_2 (Figure 6.1B) coincides with a reduction in fungal biomass in comparison to the lower H_2O_2 concentrations (Tables 6.3 and 6.4). While the reduction in aflatoxin production in 1% YEP media may result in a slight reduction in oxidative stress tolerance in the isolates, further studies will be needed to validate and determine the precise role of aflatoxin production in such responses.

The culture media also had an effect on fungal isolate development. The select isolates cultured in 1% sucrose YES medium had greater levels of conidiation than those cultured in 1% peptone YEP medium. In addition, increasing H_2O_2 concentrations to 5–10 mM also resulted in elevated conidiation in both media with a more pronounced effect observed in the YEP medium (Figure 6.3). Higher concentrations (>15 mM), however, resulted in reduced conidiation and growth (Figure 6.3). These results are consistent with previous observations that elevated ROS accumulation in *A. flavus* results in enhanced conidiation [35]. Overall, less conidiation was observed in YEP cultured isolates possibly indicative of delayed development in comparison to YES cultured isolates. While this slower growth is likely due to reduced energy availability

resulting from the use of peptides rather than sucrose as a carbon source, further studies are needed to better understand the isolate specific responses present in either medium.

Summary and Future Directions

The different isolates responded to the H_2O_2 gradient differently in terms of biomass and survivability. The isolates survived different concentrations of H_2O_2-induced oxidative stress with toxigenic isolates generally tolerating higher levels of oxidative stress than atoxigenic isolates regardless of culture conditions. Aflatoxin production was also found to be enhanced by increasing H_2O_2 concentrations. Using peptone as the carbon source in the growth media may possibly act as an "inactivator or chelator" of H_2O_2. This simple assay may also be used as a screening assay for local native biocontrol isolates of atoxigenic *A. flavus.*

Given these findings, future studies examining the oxidative stress responses of *Aspergillus* spp. using this media system should take into account the potential experimental bias associated with using elevated carbon source concentrations. In addition, further studies are needed to better characterize the role of aflatoxin production in the elevated oxidative stress caused by drought and heat stress in the field, which may afford *Aspergillus* spp. an advantage in competition with other microorganisms. The initial ROS caused by drought stress in the field may further induce the production of aflatoxin by the fungus that might accelerate increases in ROS levels resulting in potential damage to the fungus itself [26]. Since it has been demonstrated that drought and related abiotic stresses result in the accumulation of ROS in the tissues of maize lines which are susceptible to aflatoxin contamination while resistant maize lines accumulate less ROS in their tissues, the role of ROS, specifically H_2O_2, should be investigated as potential signaling molecules in the maize-*A. flavus* interaction [18, 21, 22].

Conclusions

The contamination of agricultural crops with aflatoxins is a major concern for global food security, particularly in developing countries. Given that abiotic stresses such as drought stress have been shown to exacerbate the contamination of staple food crops such as maize, it is vital to understand the role of potentially causative chemical signals in this stress interaction. Since H_2O_2 is produced by plants in response to both pathogen infection and abiotic stress [33], a H_2O_2 gradient was used to simulate abiotic stress in toxigenic and atoxigenic isolates of *A. flavus* and *A. parasiticus* in order to examine the effects of hydrogen peroxide on fungal growth and aflatoxin production.

Toxigenic and atoxigenic isolates exhibited different levels of oxidative stress tolerance with toxigenic isolates generally surviving higher levels of oxidative stress than atoxigenic isolates. The production of aflatoxin in toxigenic isolates was also stimulated in response to increasing levels of oxidative stress. In addition, the elite atoxigenic biological control isolates of *A. flavus* were able to tolerate greater levels of H_2O_2-induced oxidative stress than other tested atoxigenic isolates. This indicates that this H_2O_2 gradient method may have utility in screening local atoxigenic isolates for use as biological control agents in developing countries due to the low cost and low degree of technical difficulty. We also found that peptone may react with H_2O_2 and reduce the effects of oxidative stress when used as a carbon source in culture media.

By better understanding the signals involved the responses of *A. flavus* and other *Aspergilli* to their environment; it may be possible to identify the key mechanisms involved in the host-pathogen interaction between *A. flavus* and staple food crops such as maize. This will allow for finding novel strategies for managing aflatoxin contamination, and for the

enhancement of host resistance to aflatoxin contamination and abiotic stress through conventional breeding and biotechnology applications.

Acknowledgments

We thank Billy Wilson and Dr. Liming Yang for technical support in the laboratory. This work is partially supported by the U.S. Department of Agriculture Agricultural Research Service (USDA-ARS), the Georgia Agricultural Commodity Commission for Corn, the Georgia Peanut Commission, the Peanut Foundation, and AMCOE (Aflatoxin Mitigation Center of Excellence, Chesterfield, MO, USA). Mention of trade names or commercial products in this publication is solely for the purpose of providing specific information and does not imply recommendation or endorsement by the USDA. The USDA is an equal opportunity provider and employer.

References

1. Williams, J.H.; Grubb, J.A.; Davis, J.W.; Wang, J.S.; Jolly, P.E.; Ankrah, N.A.; Ellis, W.O.; Afriyie-Gyawu, E.; Johnson, N.M.; Robinson, A.G.; *et al*. HHIV and hepatocellular and esophageal carcinomas related to consumption of mycotoxin-prone foods in sub-Saharan Africa. *Am. J. Clin. Nutr.* **2010**, *92*, 154–160.
2. Williams, J.H.; Phillips, T.D.; Jolly, P.E.; Stiles, J.K.; Jolly, C.M.; Aggarwal, D. Human aflatoxicosis in developing countries: A review of toxicology, exposure, potential health consequences, and interventions. *Am. J. Clin. Nutr.* **2004**, *80*, 1106–1122.
3. Wogan, G.N. Chemical nature and biological effects of the aflatoxins. *Bacteriol. Rev*. **1966**, *30*, 460.

4. Azziz-Baumgartner, E.; Lindblade, K.; Gieseker, K.; Rogers, H.S.; Kieszak, S.; Njapau, H.; Schleicher, R.; McCoy, L.F.; Misore, A.; DeCock, K.; *et al*. the Aflatoxin Investigative Group. Case-control study of an acute aflatoxicosis outbreak, Kenya, 2004. *Environ. Health Perspect.* **2005**, *113*, 1779–1783.
5. Diener, U.L.; Cole, R.J.; Sanders, T.H.; Payne, G.A.; Lee, L.S.; Klich, M.A. Epidemiology of aflatoxin formation by *Aspergillus flavus*. *Annu. Rev. Phytopathol*. **1987**, *25*, 249–270.
6. Guo, B.Z.; Chen, Z.Y.; Lee, R.D.; Scully, B.T. Drought stress and preharvest aflatoxin contamination in agricultural commodity: Genetics, genomics and proteomics. *J. Int. Plant Biol.* **2008**, *50*, 1281–1291.
7. Guo, B.Z.; Yu, J.; Ni, X.; Lee, R.D.; Kemerait, R.C.; Scully, B.T. Crop stress and aflatoxin contamination: Perspectives and prevention strategies. In *Crop Stress and its Management: Perspectives and Strategies*; Venkateswarlu, B., Shankerk, A.K., Shanker, C., Makeswari, M., Eds.; Springer: New York, NY, USA, 2012; pp. 399–427.
8. Amaike, S.; Keller, N.P. *Aspergillus flavus*. *Ann. Rev. Phytopathol*. **2011**, *4*, 695–717.
9. Yu, J.; Chang, P.K.; Ehrlich, K.C.; Cary, J.W.; Bhatnager, D.; Cleveland, T.E.; Payne, G.A.; Linz, J.E.; Woloshuk, C.P.; Bennett, J.W. Clustered pathway genes in aflatoxin biosynthesis.
Appl. Environ. Microbiol. **2004**, *70*, 1253–1262.
10. Fabbri, A.; Fanelli, C.; Panfili, G.; Passi, S.; Fasella, P. Lipoperoxidation and aflatoxin biosynthesis by *Aspergillus parasiticus* and *A. flavus*. *J. Gen. Microbiol*. **1983**, *129*, 3447–3452.
11. Gao, X.; Kolomiets, M.V. Host-derived lipids and oxylipins are crucial signals in modulating mycotoxin production by fungi. *Toxin Rev*. **2009**, *28*, 79–88.

12. Jayashree, T.; Subramanyam, C. Oxidative stress as a prerequisite for aflatoxin production by *Aspergillus parasiticus. Free Rad. Biol. Med*. **2000**, *29*, 981–985.

13. Reverberi, M.; Punelli, M.; Smith, C.A.; Zjalic, S.; Scarpari, M.; Scala, V.; Cardinali, G.; Aspite, N.; Pinzari, F.; Payne, G.A. How peroxisomes affect aflatoxin biosynthesis in *Aspergillus flavus.*

PLoS ONE **2012**, *7*, e48097.

14. Reverberi, M.; Zjalic, S.; Ricelli, A.; Punelli, F.; Camera, E.; Fabbri, C.; Picardo, M.; Fanelli, C.; Fabbri, A.A. Modulation of antioxidant defense in *Aspergillus parasiticus* is involved in aflatoxin biosynthesis: A role for the ApyapA gene. *Eukaryotic Cell* **2008**, *7*, 988–1000.

15. Roze, L.V.; Chanda, A.; Wee, J.; Awad, D.; Linz J.E. Stress-related transcription factor AtfB integrates secondary metabolism with oxidative stress response in Aspergilli. *J. Biol. Chem.* **2011**, *286, 35137–35148.*

16. Roze, L.V.; Hong, S.Y.; Linz, J.E. Aflatoxin biosynthesis: Current frontiers. *Annu. Rev. Food Sci. Tech.* **2013**, *4*, 293–311.

17. Grintzalis, K.; Vernardis, S.I.; Klapa, M.I.; Georgiou, C.D. Role of oxidative stress in sclerotial differentiation and aflatoxin B1 biosynthesis in *Aspergillus flavus*. *Appl. Environ. Microbiol*. **2014,** *80, 5561-5571*.

18. Fountain, J.C.; Khera, P.; Yang, L.; Nayak, S.N.; Scully, B.T.; Lee, R.D.; Chen, Z.Y.; Kemerait, R.C.; Varshney, R.K.; Guo, B.Z. Resistance to *Aspergillus flavus* in maize and peanut: Molecular biology, breeding, environmental stress, and future perspectives. *Crop J*. **2015**, *3*, 229–237.

19. Fountain, J.C.; Scully, B.T.; Ni, X.; Kemerait, R.C.; Lee, R.D.; Chen, Z.Y.; Guo, B.Z. Environmental influences on maize-*Aspergillus flavus* interactions and aflatoxin production. *Front. Microbiol*. **2014**, *5*, 1–7.
20. Narasaiah, K.V.; Sashidhar, R.B.; Subramanyam C. Biochemical analysis of oxidative stress in the production of aflatoxin and its precursor intermediates. *Mycopathologia* **2006**, *162*, 179–189.
21. Kebede, H.; Abbas, H.K.; Fisher, D.K.; Bellaloui, N. Relationship between aflatoxin contamination and physiological responses of corn plants under drought and heat stress. *Toxins* **2012**, *4*, 1385–1403.
22. Yang, L.; Fountain, J.C.; Ni, X.; Ji, P.; Lee, R.D.; Scully, B.T.; Kemerait, R.C.; Guo, B.Z. Maize sensitivity to drought stress is associated with differential responses to reactive oxygen species. *Phytopathology* **2015**, *105* (Suppl. S2), 13.
23. Probst, C.; Bandyopadhyay, R.; Price, L.E.; Cotty, P.J. Identification of atoxigenic *Aspergillus flavus* isolates to reduce aflatoxin contamination of maize in Kenya. *Plant Dis.* **2011**, *95*, 212–218.
24. Desikan, R.; Reynolds, A.; Hancock, J.T.; Neill, S.J. Harpin and hydrogen peroxide both initiate programmed cell death but have differential effects on defense gene expression in Arabidopsis suspension cultures. *Biochem. J.* **1998**, *330*, 115–120.
25. Neill, S.J.; Desikan, R.; Clarke, A.; Hurst, R.D.; Hancock, J.T. Hydrogen peroxide and nitric oxide as signaling molecules in plants. *J. Exp. Bot.* **2002**, *53*, 1237–1247.
26. Roze, L.V.; Laivenieks, M.; Hong, S.Y.; Wee, J.; Wong, S.S.; Vanos, B.; Awad, D.; Ehrlich, K.C.; Linz, J.E. Aflatoxin biosynthesis is a novel source of reactive oxygen species

– A potential redox signal to initiate resistance to oxidative stress? *Toxins*. **2015,** *7, 1411-1430*.

27. Chang, P.K.; Abbas, H.K.; Weaver, M.A.; Ehrlich, K.C.; Scharfenstein, L.L.; Cotty, P.J. Identification of genetic defects in the atoxigenic biocontrol strain *Aspergillus flavus* K49 reveals the presence of a competitive recombinant group in field populations. *Int. J. Food Microbiol*. **2012**, *154*, 192–196.
28. Dorner, J.W.; Lamb, M.C. Development and commercial use of afla-Guard®, an aflatoxin biocontrol agent. *Mycotoxin Res*. **2006**, *22*, 33–38.
29. Garber, R.K.; Cotty, P.J. Formation of sclerotia and aflatoxins in developing cotton bolls infected by the S strain of *Aspergillus flavus* and potential for biocontrol with an atoxigenic strain. *Phytopathology* **1997**, *87*, 940–945.
30. Atehnkeng, J.; Ojiambo, P.S.; Cotty, P.J.; Bandyopadhyay, R. Field efficacy of a mixture of atoxigenic *Aspergillus flavus* Link: Fr vegetative compatibility groups in preventing aflatoxin contamination in maize (*Zea mays* L.). *Biol. Control* **2014**, *72*, 62–70.
31. Atehnkeng, J.; Ojiambo, P.S.; Ikotun, T.; Sikorad, R.A.; Cotty, P.J.; Bandyopadhyay, R. Evaluation of atoxigenic isolates of *Aspergillus flavus* as potential biocontrol agents for aflatoxin in maize. *Food Addit. Contam*. **2008**, *25*, 1264–1271.
32. Degola, F.; Berni, E.; Restivo, F.M. Laboratory tests for assessing efficacy of atoxigenic *Aspergillus flavus* strains as biocontrol agents. *Int. J. Food Microbiol*. **2011**, *146*, 235–243.
33. Farooq, M.; Wahid, A.; Kobayashi, N.; Fujita, D.; Basra, S.M.A. Plant drought: Effects, mechanisms, and management. *Agron. Sustain. Dev*. **2009**, *29*, 185–212.
34. Davis, N.D.; Diener, U.L.; Eldridge, D.W. Production of aflatoxins B1 and G1 by *Aspergillus flavus* in a semisynthetic medium. *Appl. Microbiol*. **1966**, *14*, 378–380.

35. Chang, P.K.; Scharfenstein, L.L.; Luo, M.; Mahoney, N.; Molyneux, R.J.; Yu, J.; Brown, R.L.; Campbell, B.C. Loss of *msnA*, a putative stress regulatory gene, in *Aspergillus parasiticus* and *Aspergillus flavus* increased production of conidia, aflatoxins and kojic acid. *Toxins* **2010**, *3*, 82–104.
36. Abdollahi, A.; Buchanan, R.L. Regulation of aflatoxin biosynthesis: Induction of aflatoxin production by various carbohydrates. *J. Food Sci*. **1981**, *46*, 633–635.
37. Guo, B.Z.; Russin, J.S.; Brown, R.L.; Cleveland, T.E.; Widstrom, N.W. Resistance to aflatoxin contamination in corn as influenced by relative humidity and kernel germination. *J. Food Protect*. **1996**, *59*, 276–281.

Table 6.1. Average dry weights (g) of *A. flavus* mycelia in H_2O_2 amended yeast extract-sucrose (YES) (15% sucrose) media.

Isolate	Toxin	Hydrogen Peroxide Concentrations (mM)										
		0	**5**	**10**	**15**	**20**	**25**	**30**	**35**	**40**	**45**	**50**
Tox4	+	1.08	1.10	1.13	1.09	1.07	1.05	1.05	1.06	1.09	0	0
A9	+	1.14	1.12	1.12	1.10	1.14	1.15	0.80	0.99	0.49	0	0
AF13	+	1.15	1.13	1.12	1.14	1.08	1.09	1.11	1.19	0	nt	nt
NRRL3357	+	1.17	1.14	1.12	1.11	0.64	0.34	0	nt	nt	nt	nt
NRRL2999	+	1.12	1.11	1.21	1.06	1.03	1.19	0	nt	nt	nt	nt
K49	−	1.12	1.11	1.09	1.11	0.88	0.90	0.47	nt	nt	nt	nt
AF36	−	1.19	1.17	1.14	1.11	0.95	1.07	0	nt	nt	nt	nt
Aflaguard	−	1.16	1.12	1.15	1.19	0.79	0.38	0	nt	nt	nt	nt
A1	−	1.15	1.15	1.13	1.21	0.82	0	0	nt	nt	nt	nt
K54A	−	1.12	1.16	1.11	0.81	0	0	0	nt	nt	nt	nt

Note: nt: not tested; +: toxigenic; −: atoxigenic.

Table 6.2. Average dry weights (g) of *A. flavus* mycelia in H_2O_2 amended yeast extract-peptone YEP (15% peptone) media.

Isolate	Toxin	Hydrogen Peroxide Concentrations (mM)										
		0	**5**	**10**	**15**	**20**	**25**	**30**	**35**	**40**	**45**	**50**
Tox4	+	1.55	nt	nt	nt	1.18	1.21	1.18	1.03	1.50	1.28	1.04
A9	+	2.21	nt	nt	nt	1.18	1.19	1.09	1.14	1.42	1.31	1.33
AF13	+	1.38	1.35	1.38	1.4	1.37	1.41	1.32	1.29	1.24	1.39	1.28
NRRL3357	+	1.39	1.35	1.52	1.33	1.30	1.04	0.80	0.78	0.83	0	nt
NRRL2999	+	1.70	nt	nt	nt	1.15	0.98	0.71	0	0	0	nt
K49	−	1.09	1.06	1.09	1.08	1.16	0.74	0.65	0.73	0	0	nt
AF36	−	1.40	nt	nt	nt	1.34	1.02	0.80	0.62	0	0	nt
Aflaguard	−	1.65	nt	nt	nt	1.14	0.98	0.75	0.58	1.36	1.13	nt
A1	−	1.53	nt	nt	nt	1.01	0.93	0.77	0.30	0.76	0	nt
K54A	−	1.05	1.07	1.04	1.06	1.05	1.00	0.74	0	0	0	nt

Note: nt: not tested; +: toxigenic; −: atoxigenic.

Table 6.3. Average dry weights (g) of *A. flavus* mycelia in H_2O_2 amended YES (1% sucrose) medium.

Isolate	Toxin	Hydrogen Peroxide Concentrations (mM)												
		0	**5**	**10**	**15**	**20**	**25**	**30**	**35**	**40**	**45**	**50**	**55**	**60**
AF13	+	0.52	0.54	0.56	0.51	0.55	0.54	0.50	0.38	0	0	0	0	0
NRRL3357	+	0.45	0.47	0.53	0.46	0.12	0	0	0	0	0	0	0	0
Aflaguard	−	0.56	0.55	0.55	0.49	0.30	0	0	0	0	0	0	0	0
K54A	−	0.30	0.33	0.40	0.16	0	0	0	0	0	0	0	0	0

Note: +: toxigenic; −: atoxigenic.

Table 6.4. Average dry weights (g) of *A. flavus* mycelia in H_2O_2 amended YEP (1% peptone) medium.

Isolate	Toxin	Hydrogen Peroxide Concentrations (mM)												
		0	**5**	**10**	**15**	**20**	**25**	**30**	**35**	**40**	**45**	**50**	**55**	**60**
AF13	+	0.27	0.28	0.25	0.27	0.28	0.29	0.26	0	0	0	0	0	0
NRRL3357	+	0.24	0.25	0.33	0.28	0.08	0	0	0	0	0	0	0	0
Aflaguard	−	0.27	0.31	0.28	0.29	0.22	0	0	0	0	0	0	0	0
K54A	−	0.12	0.15	0.16	0.15	0	0	0	0	0	0	0	0	0

Note: +: toxigenic; −: atoxigenic.

Figure 6.1. Aflatoxin production of select *A. flavus* isolates under H_2O_2-induced oxidative stress in toxin-conducive yeast extract-sucrose (YES) and non-conducive yeast extract-peptone (YEP) media visualized using thin layer chromatography (TLC). (A) Isolate NRRL3357 was cultured in YES media containing 15% sucrose and supplemented with H_2O_2 ranging from 0 (control check) to 10 mM. Increasing visible fluorescence over the concentration gradient indicates elevated levels of aflatoxin B_{1+2}. (B) Isolates AF13 and NRRL3357 were cultured on YES and YEP media containing reduced carbon source concentrations (1%). Elevated aflatoxin production was observed in response to oxidative stress in 1% YES media (compared to "0" control) while no aflatoxin production was observed in 1% YEP medium. An aflatoxin B_1 standard was included as a reference.

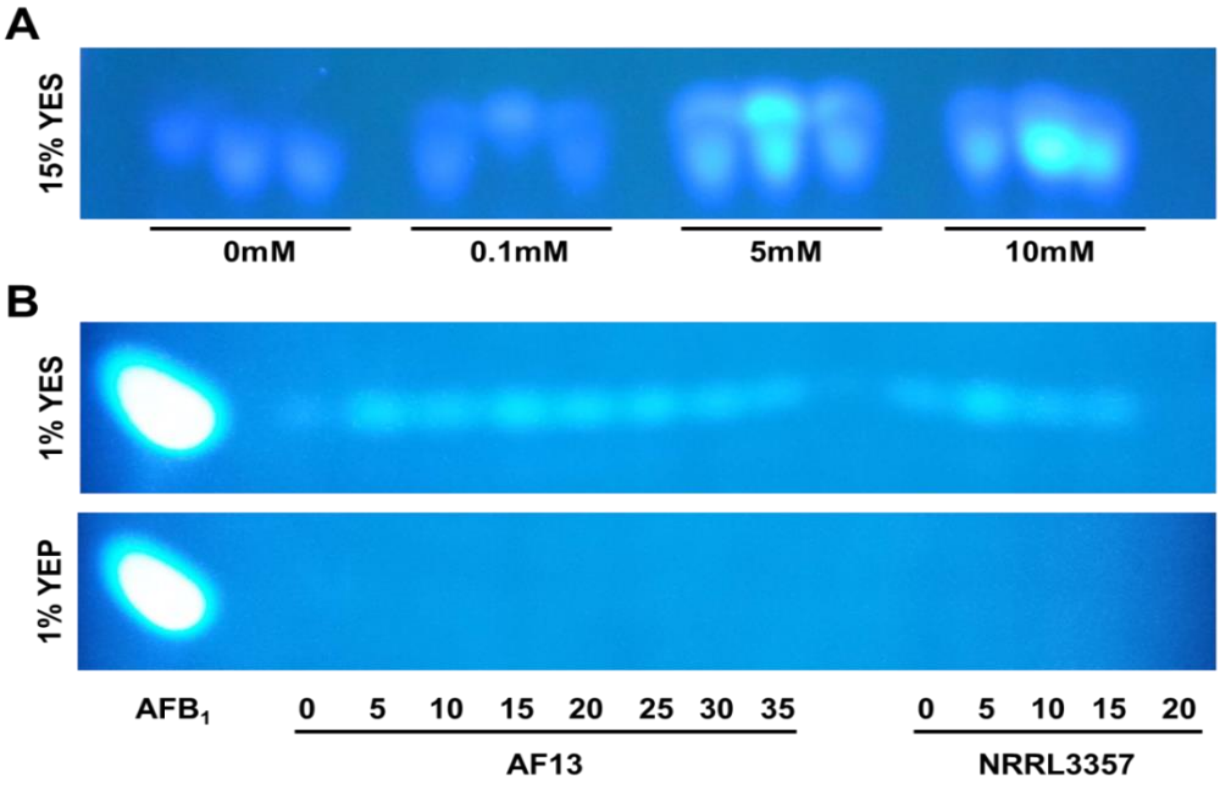
A
15% YES
0mM
0.1mM
5mM
10mM
B
1% YES
1% YEP
AFB1
0 5 10 15 20 25 30 35
AF13
0 5 10 15 20
NRRL3357

Figure 6.2. Quantification of H_2O_2 levels in non-inoculated culture media over time. (A) A standard curve was generated using stabilized H_2O_2 to quantify the H_2O_2 concentration in the media samples. (B) The concentration of H_2O_2 in non-inoculated YES and YEP culture media containing 15% or 1% carbon sources and initially supplemented to 30 mM H_2O_2 was monitored every 24 h for three days. The H_2O_2 concentration declined slowly over time in the YES media, the 1% peptone YEP media, and the water control, but plummeted sharply in YEP medium with 15% peptone (82.8% reduction in 72 h). This indicates that peptone molecules can potentially react with or inactivate H_2O_2.

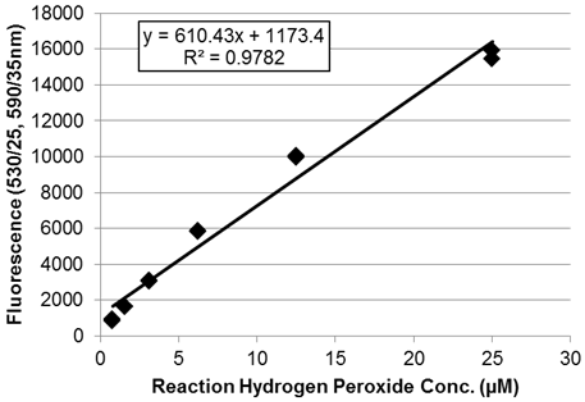
y = 610.43x + 1173.4
R² = 0.9782
Fluorescence (530/25, 590/35nm)
Reaction Hydrogen Peroxide Conc. (μM)
18000
16000
14000
12000
10000
8000
6000
4000
2000
0
0
5
10
15
20
25
30

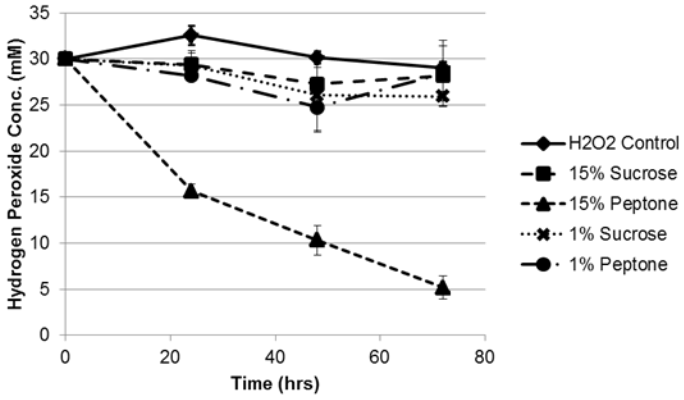
Hydrogen Peroxide Conc. (mM)
Time (hrs)
35
30
25
20
15
10
5
0
0
20
40
60
80
H2O2 Control
15% Sucrose
15% Peptone
1% Sucrose
1% Peptone

Figure 6.3. Growth behavior of selected *Aspergillus flavus* isolates under H_2O_2-induced oxidative stress in 1% carbon source yeast extract-sucrose (YES) and yeast extract-peptone (YEP) media. Isolates AF13, NRRL3357, Aflaguard, and K54A were cultured in 1% carbon source media and photographed for observation of their growth behavior in response to increasing H_2O_2 concentrations. Increased conidiation was observed from 5–15 mM with concentrations >15 mM resulting in reduced conidiation. Reduced growth and conidiation in YEP is likely due to reduced energy availability of carbohydrate.

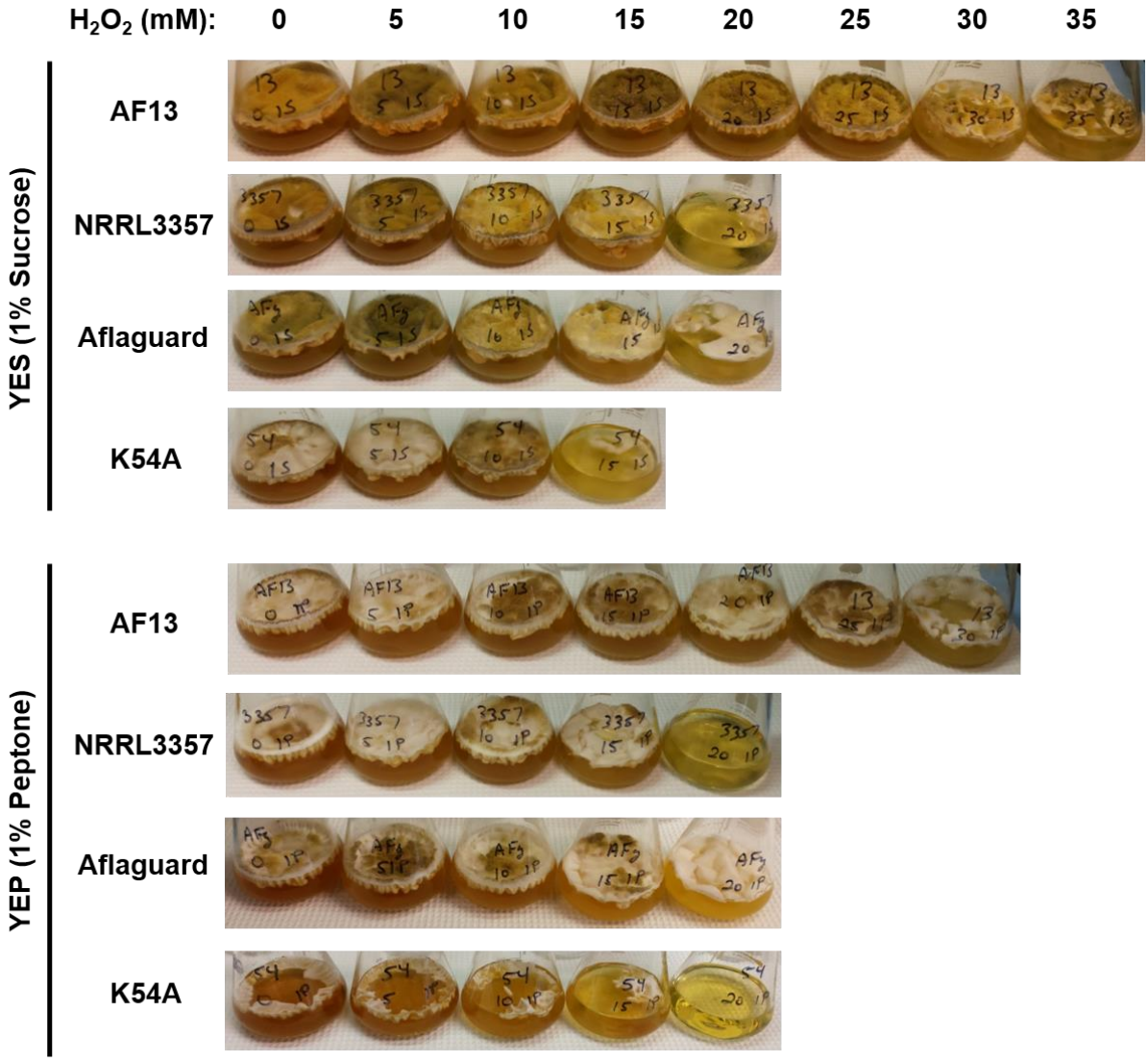
H_2O_2 (mM): 0 5 10 15 20 25 30 35
YES (1% Sucrose)
AF13
NRRL3357
Aflaguard
K54A
YEP (1% Peptone)
AF13
NRRL3357
Aflaguard
K54A

CHAPTER 7

OXIDATIVE STRESS AND CARBON METABOLISM INFLUENCE *ASPERGILLUS FLAVUS* TRANSCRIPTOME COMPOSITION AND SECONDARY METABOLITE PRODUCTION

Fountain, J.C., Bajaj, P., Pandey, M.K., Nayak, S.N., Yang, L., Kumar, V., Jayale, A.S., Chitikineni, A., Zhuang, W., Scully, B.T., Lee, R.D., Kemerait, R.C., Varshney, R.K., Guo, B. (2016). Oxidative stress and carbon metabolism influence *Aspergillus flavus* transcriptome composition and secondary metabolite production. *Nature Scientific Reports* 6:38747. doi:10.1038/srep38747. Reprinted here with permission of the publisher.

Abstract

Contamination of crops with aflatoxin is a serious global threat to food safety. Aflatoxin production by *Aspergillus flavus* is exacerbated by drought stress in the field and by oxidative stress *in vitro.* We examined transcriptomes of three toxigenic and three atoxigenic isolates of *A. flavus* in aflatoxin conducive and non-conducive media with varying levels of H_2O_2 to investigate the relationship of secondary metabolite production, carbon source, and oxidative stress. We found that toxigenic and atoxigenic isolates employ distinct mechanisms to remediate oxidative damage, and that carbon source affected the isolates' expression profiles. Iron metabolism, monooxygenases, and secondary metabolism appeared to participate in isolate oxidative responses. The results suggest that aflatoxin and aflatrem biosynthesis may remediate oxidative stress by consuming excess oxygen and that kojic acid production may limit iron-mediated, non-enzymatic generation of reactive oxygen species. Together, secondary metabolite production may enhance *A. flavus* stress tolerance, and may be reduced by enhancing host plant tissue antioxidant capacity through genetic improvement by breeding selection.

Introduction

Maize and peanut are staple food crops throughout the world with 1.02 billion and 45.65 million metric tons of production, respectively, in 2013[1]. These crops are particularly important in developing countries in Africa and Asia where aflatoxin contamination is most severe[2,3]. Contamination of maize and peanut with aflatoxins, the carcinogenic secondary metabolites of *Aspergillus flavus*, poses a global threat to food safety and security. Long term exposure to aflatoxin through contaminated foodstuffs has been associated with a myriad of hepatic diseases including cirrhosis, hepatitis, and hepatocellular carcinoma along with birth defects, immune deficiencies, and acute toxicity[4,5].

Given the importance of aflatoxin contamination remediation, extensive research has been performed since the 1970's to enhance host plant resistance[6-8]. However, a lack of diverse, resistant germplasm for aflatoxin contamination along with a high degree of environmental and genotype × environmental interaction influences on resistance has posed difficulties in breeding programs[9-11]. Environmental stresses including drought and heat stress can exacerbate aflatoxin contamination in maize and peanut[12,13]. This increase in aflatoxin contamination under drought stress in particular has motivated numerous research efforts endeavoring to address why *A. flavus* and other Aspergilli produce aflatoxin in stressed environments.

Over the last decade, several studies have elucidated the biosynthetic pathway for aflatoxin production and have begun to characterize upstream factors regulating its expression[14-16]. Aflatoxin biosynthesis is carried out by a 25 gene-cluster that is highly conserved among toxigenic isolates of *A. flavus*[16]. The production of aflatoxin has been shown to be regulated through several means, although the practical role of aflatoxin and various other secondary metabolites in *A. flavus* biology and/or its interactions with other organisms including plant host-

pathogen interactions is still not clear. Reactive oxygen species (ROS) and their reactive products including peroxidized lipids have been shown to induce and to be required for aflatoxin production[17]. Aflatoxin production has also been demonstrated to be under the regulation of oxidative stress-responsive signaling mediated by transcription factors such as AtfB, AP-1, and VeA[17-21]. Given that drought stress results in the accumulation of ROS and peroxidized lipids in host plant tissues, it is hypothesized that these compounds may exacerbate the production of aflatoxin during fungal colonization of stressed host tissues[22-25]. This correlation between ROS and aflatoxin production has also led to the hypothesis that aflatoxin production may function in the remediation of oxidative stress[8,17,21,26-28].

In addition to ROS, carbohydrate availability and metabolism have also been shown to influence aflatoxin production. Earlier studies by Davis and Diener[29] demonstrated the requirement of hexose sugars for the production of aflatoxins *in vitro* with compounds occurring later in carbohydrate metabolism (e.g. the tricarboxylic acid, TCA, cycle) being unable to support aflatoxin production. The close association of a simple sugar metabolic gene cluster with the aflatoxin biosynthetic gene cluster has also been demonstrated in *A. parasiticus*, though a similar association was not observed in all *Aspergillus spp.*[16,30]. In *A. flavus* isolates, supplementing culture media with alternative carbon sources such as peptone results in reduced or inhibited aflatoxin production[31,32]. The modulation of aflatoxin production through cultural methods including carbon source variation and ROS amendment has shown that isolates that produce aflatoxin tend to exhibit greater tolerance to oxidative stress, and that the reduction of aflatoxin production can adversely affect said tolerance[18,28].

In order to better understand the regulation of aflatoxin production in response to carbohydrate availability and oxidative stress, and to investigate the possible role of aflatoxin

production in stress responses, a global gene expression approach is needed. In this study, we examined the transcriptomes of toxigenic and atoxigenic isolates of *A. flavus* and their responses to increasing levels of oxidative stress and altered carbon source availability in culture medium. Understanding the molecular mechanisms linking stress responsive signaling and aflatoxin production pathways could provide insights into the practical role of aflatoxin production and considerations for enhancing host resistance for aflatoxin contamination.

Materials and Methods

Isolate collection

The *A. flavus* isolates used in the present study were collected from the following sources. The NRRL3357 isolate was obtained from the Northern Regional Research Center, USDA-ARS, Peoria, IL, USA. The AF13, AF36 (NRRL18543), Aflaguard (NRRL21882), and Tox4 isolates were obtained from Dr. Kenneth Damann, Department of Plant Pathology and Crop Physiology, Louisiana State University, Baton Rouge, LA, USA. The K54A isolate was obtained from the Biological Control of Pests Research Unit, USDA-ARS, Stoneville, MS, USA. NRRL3357, AF13, and Tox4 are aflatoxigenic. Aflaguard and AF36 are atoxigenic isolates which possess a complete aflatoxin biosynthetic pathway deletion and a point mutation in the polyketide synthase gene pksA, respectively[36]. The K54A isolate is atoxigenic isolate which has yet to be characterized. The collected isolates were received on potato dextrose agar (PDA) and upon receipt were maintained on V8 agar (20% V8, 1% $CaCO_3$, 3% agar).

Isolate culture conditions

Prior to the experiment, the isolates were grown on V8 agar at 32°C for 5 days. Fresh conidia were then harvested in 0.1% (v/v) Tween 20 buffer, and this conidial suspension (~4.0 x 10^6 conidia/mL) was immediately used for inoculation of liquid cultures. Two liquid media were used in the study, an aflatoxin production conducive yeast extract sucrose (YES; 2% yeast extract, 1% sucrose) medium and an aflatoxin production non-conducive yeast extract peptone (YEP; 2% yeast extract, 1% peptone) medium[31]. The concentrations of the media components were optimized based on the findings of Davis et al.[60] and our previous studies[32].

Prior to inoculation, the media were supplemented with different levels of hydrogen peroxide (H_2O_2, 3% stabilized solution) to induce moderate and more severe oxidative stress on the isolates. The concentrations were specific to the individual isolates and were based on our previous findings on the oxidative tolerance (growth inhibiting concentration of H_2O_2) of the isolates[32] as follows. NRRL3357 and Aflaguard were cultured in media supplemented with 0, 10, and 20 mM H_2O_2. AF13 and Tox4 were cultured in media supplemented with 0, 10, and 25 mM H_2O_2. AF36 and K54A cultured in media supplemented with 0 and 10 mM H_2O_2. For each culture, 50 mL of H_2O_2 supplemented medium was transferred to a sterile 125 mL Erlenmeyer flask, inoculated with 100 µL conidial suspension, and plugged with a sterile cotton ball. The isolates were then incubated in the dark at 32°C for 7 days under stationary conditions. This experiment was performed twice and considered as two biological replicates.

RNA extraction

Following incubation, mycelia were harvested from the flasks using a sterile spatula and immediately flash frozen in liquid nitrogen. The mycelia were then homogenized to a powder

using a chilled mortar and pestle and stored at -80°C until used in RNA extraction. Total RNA was then extracted using an RNeasy Plant Mini Kit with an on-column DNase digestion included during extraction according to the manufacturer's instructions (Qiagen, Hilden, Germany). The total RNA was quantified using a Nano-Drop ND1000 spectrophotometer (Thermo Scientific, Wilmington, DE, USA), and the quality of the RNA was determined by measuring the RNA integrity numbers (RINs) for each sample using an Agilent 2100 Bioanalyzer (Agilent, Santa Clara, CA, USA). Samples with RIN $\geq$ 5 were used for library preparation and RNA sequencing.

Library construction and Illumina sequencing

For library construction, 1µg of total RNA was used for each sample with biological replicates processed separately for later statistical comparison. Altogether, 32 libraries with 2 biological repeats (total of 64 libraries) were prepared for whole transcriptome sequencing using an Illumina TruSeq RNA Sequencing Kit according to the manufacturer's instructions (Illumina, San Diego, CA, USA). The prepared libraries were quantified using a Qubit 2.0 fluorometer (Thermo Scientific), and validated using an Agilent 2100 Bioanalyzer (Agilent). Cluster generation for these libraries was done using a cBot (Illumina), followed by 125bp paired-end sequencing using a HiSeq 2500 platform (Illumina).

Bioinformatic analysis

Raw sequencing reads obtained for each sample were checked for quality using FastQC v0.11.2 (http://www.bioinformatics.bbsrc.ac.uk/projects/fastqc). The data was then filtered for low quality reads (< Q20) and adapter sequences were removed using Trimmomatic v0.32[61]. The remaining reads were then checked for rRNA contamination by aligning the reads to the SILVA

database. Finally, using a Tuxedo protocol, the filtered, quality reads were aligned to the *A. flavus* NRRL3357 genome (GCF_000006275.2) using tophat2 v2.0.13 and bowtie2 v2.2.4[62,63]. The filtered reads were assembled by Cufflinks v2.2.1 using the RABT method to estimate their abundance[64,65]. The relative expression between isolate-treatment combinations was calculated in terms of Fragments Per Kilobase of exon per Million fragments mapped (FPKM) using the cuffdiff program. A gene was said to be significantly differentially expressed when $|\log_2(\text{fold change})| \geq 2$ with an adjusted p-value ≤ 0.05. The assembled transcripts were annotated against NCBI's non-redundant (nr) protein database using standalone blast-2.2.30+ followed by Gene Ontology (GO) and KEGG pathway analysis using Blast2GO.

Aflatoxin and kojic acid production assays

In order to validate the induction of kojic acid biosynthesis by increasing levels of H_2O_2, a modified method from Bentley[66] was utilized. Briefly, *A. flavus* isolates were cultured on potato dextrose agar (PDA), PDA amended with 1mM $FeCl_3$, and PDA amended with 1mM $FeCl_3$ along with 15mM H_2O_2. The presence of a bright orange coloration in the medium indicates the chelation of iron by kojic acid allowing for a qualitative comparison of kojic acid biosynthesis between the isolates.

The production of aflatoxin and kojic acid were also evaluated by thin layer chromatography according to methods used by Saruno et al.[67]. Briefly, liquid culture medium was collected while harvesting mycelia for RNA isolation, spotted onto a silica gel 20 thin layer chromatography (TLC) plate, and dried at room temperature. The plate was then developed in butanol-acetic acid-water (4:1:5) and dried with warm air. Aflatoxin and kojic acid present within the culture medium samples were then visualized by UV fluorescence with excitation

wavelengths of 365 and 254 nm, respectively, and photographed using a Nikon Coolpix L110 digital camera (Nikon, Tokyo, Japan).

Results

Transcriptome sequencing

To examine the transcriptomic responses of toxigenic and atoxigenic isolates of *A. flavus* to increasing levels of oxidative stress in aflatoxin production conducive and non-conducive media, we cultured three toxigenic (AF13, NRRL3357, and Tox4) and three atoxigenic (AF36, Aflaguard, and K54A) in either YES or YEP medium amended with different concentrations of H_2O_2 for RNA sequencing (Supplementary Table 7.1). In total, ~4.7 billion reads were generated from 64 libraries with an average of 73 million reads per library. Two of the 64 libraries sequenced contained low read counts and were excluded from the analysis. Following quality check, an average of 9 to 10% of the reads were removed, which were further filtered for rRNA contamination prior to mapping. Following quality filtration, 2.5 billion quality filtered reads with an average of 40.3 million reads per sample were obtained of which 92.27% were mapped to the *A. flavus* genome. The raw and processed RNA sequencing data can be accessed at http://ceg.icrisat.org/gt-bt/alfavus_1/home.asp.

Of the 13,487 genes present in the *A. flavus* NRRL3357 genome, the gene expression data analysis showed that a total of 11,144 genes (82.63% of the reference) were identified in the dataset (Supplementary Data 1). Of those detected, 9,158 genes (82.18 %) were found to possess an FPKM $\geq$ 2 in at least one isolate-treatment combination. Among these expressed genes, 319 genes (3.48 %) and 470 genes (5.13 %) were expressed uniquely in the toxigenic and atoxigenic isolates, respectively. Also, 529 genes (5.78 %) were expressed only in the conducive YES

medium while 460 genes (5.02 %) were expressed only in the non-conducive YEP medium (Figure 7.1, Supplementary Data 2). In total, 7,394 genes (80.74%) were expressed in both toxigenic and atoxigenic isolates when cultured in either medium (Figure 7.1, Supplementary Data 2).

Toxigenic isolate responses to oxidative stress are related to their ability to produce aflatoxin

On examining the level of oxidative tolerance of these isolates, our previous studies found that isolates with greater levels of aflatoxin production tend to tolerate greater levels of oxidative stress[32]. In order to examine the transcriptional responses of the toxigenic isolates to oxidative stress we identified the significantly differentially expressed genes in the isolates in YES medium in response to increasing levels of oxidative stress. Toxigenic isolates which produce greater levels of aflatoxin were found to exhibit fewer differentially expressed genes in response to stress than those which produced less aflatoxin (Table 7.1). For the transcripts observed to be differentially expressed in the toxigenic isolates, those involved in membrane transport, carbon metabolism, stress signaling, antioxidant mechanisms, and secondary metabolite production were enriched (Supplementary Data 3). Comparing high and moderate aflatoxin producing isolate GO enrichments also indicates that the high toxin producing isolates, Tox4 and AF13, exhibit similar responses at higher levels of stress as those employed by the moderate producing NRRL3357 isolate under less stress (Supplementary Data 3).

As expected, transcripts encoding components of the aflatoxin biosynthetic pathway were found to be up-regulated in response to increasing stress. These included *nor-1*, *verB*, *ver-1*, *omtA*, and *omtB* along with more cryptic members of the aflatoxin biosynthetic gene cluster

whose role(s) in aflatoxin production have yet to be identified including *aflS* and *aflV* (Figure 7.2A)[16]. In addition to these, transcripts encoding the production of additional secondary metabolites were differentially expressed in response to increasing stress. Transcripts encoding members of the isoprenoid biosynthetic pathway, which forms the basis for the production of the tremorogenic mycotoxin aflatrem[33], were also found to be up-regulated in the isolates in a similar manner observed for aflatoxin biosynthetic genes. The aflatrem biosynthetic components *atmB*, *atmC*, *atmD*, *atmG*, *atmM*, *atmP*, and *atmQ*[34] were expressed in all the toxigenic isolates in YES medium (Figure 7.2B). The *atmG* gene, encoding a putative geranylgeranyl pyrophosphate synthetase (GGPS), was consistently expressed in both the toxigenic and atoxigenic isolates regardless of H_2O_2 concentration or culture medium (Figure 7.2B). Also, a synaptic vesicle transporter SVOP transcript, which has been shown to be involved in kojic acid biosynthesis[35], was found to be upregulated in NRRL3357 at 10 mM H_2O_2 in YES while it was down-regulated in the more virulent Tox4 and AF13 isolates at 25 mM H_2O_2 (Figure 7.2C). Other kojic acid biosynthetic genes including *kojA*, *kojR*, and *kojT*[35] were stably expressed in all the toxigenic isolates regardless of treatment with H_2O_2 or culture medium (Figure 7.2C). Numerical FPKM data for that appearing in Figure 2 can be found in Supplementary Table 7.2.

Toxigenic and atoxigenic isolates exhibit similar yet distinct responses to oxidative stress

In comparison to the toxigenic isolates, the atoxigenic isolates exhibited distinct responses to oxidative stress, though there were some similarities. Among the atoxigenic isolates, those which are used as biological controls, Aflaguard and AF36, were previously found to tolerate higher levels of oxidative stress than non-adapted isolates including K54A[32]. In the present study, these biological control isolates exhibited fewer DEGs in comparison to K54A (Table 7.1). In addition,

the atoxigenic isolates, which generally tolerated lower levels of oxidative stress than the toxigenic isolates in the previous study[32], tended to exhibit greater numbers of significant DEGs than the toxigenic isolates, particularly at higher levels of stress (Table 7.1).

As in the toxigenic isolates, transcripts observed to be differentially expressed in the atoxigenic isolates included those involved in membrane transport, carbon metabolism, stress signaling, and antioxidant mechanisms (Supplementary Data 3). As expected, transcripts encoding components of the aflatoxin biosynthetic pathway were either not significantly regulated, or not expressed in the atoxigenic isolates (Figure 7.2A) depending on the mutation in the aflatoxin gene cluster present in each isolate[36,37]. Aflatrem biosynthetic genes were also found to be expressed in Aflaguard and AF36, but not in K54A while kojic acid biosynthesis genes were expressed in all of the atoxigenic isolates in YES medium (Figure 7.2).

Transcripts encoding chitin metabolic processes were down-regulated in response to increasing stress in the toxigenic isolates including those for chitinase and chitosanase (Supplementary Data 3). These same transcripts tended to be up-regulated in the atoxigenic isolates (Supplementary Data 3). Also, transcripts encoding antioxidant enzymes including thioredoxin peroxidase and thioredoxin reductase also tended to be upregulated in response to increasing stress in both the toxigenic and atoxigenic isolates (Supplementary Data 3). Cytochrome p450 monooxygenase genes, in addition to those expressed in the aflatoxin and aflatrem biosynthetic pathways, were also upregulated in both the toxigenic and atoxigenic isolates in response to increasing stress (Supplementary Data 3). Transcripts encoding products involved in aminobenzoate degradation were shown to be generally up-regulated in the toxigenic and atoxigenic isolates under increasing levels of stress (Supplementary Data 3). An exception to this was Tox4 which showed a significant down-regulation in an amidohydrolase family protein-

encoding transcript (AFLA_076800) (Supplementary Data 3). Also, transcripts encoding antibiosis and drug resistance proteins such as major facilitator superfamily (MFS) transporters and multidrug resistance proteins were up-regulated in the toxigenic isolates with increasing stress (Supplementary Data 3 and 4). In the atoxigenic isolates, transcripts encoding products capable of functioning in both antibiotic biosynthesis and additional pathways such as carbon metabolism and proteolysis were differentially expressed in response to increasing stress.

Medium carbon source affects secondary metabolite gene expression and production

Culturing the toxigenic and atoxigenic isolates in media with different carbon sources, sucrose or peptone, significantly altered the expression profiles of the isolates in response to increased levels of oxidative stress resulting in a clear segregation of expression patterns by carbon source (Figure 7.3; Supplementary Figure 7.1). As expected, culturing the toxigenic isolates in YEP medium resulted in low or no expression of several genes involved in aflatoxin and aflatrem biosynthesis (Figures 7.2 and 7.4). Exceptions to this included members of the sugar cluster (e.g. *aflYc* and *aflYd*) aflatoxin transporters (*aflT*), regulators of aflatoxin production (e.g. *aflR* and *VeA*), and the geranylgeranyl pyrophosphate synthetase gene (*atmG*) which functions upstream of aflatrem biosynthesis in the terpenoid biosynthetic pathway[16,34,38,39]. The expression of the kojic acid SVOP transporter was higher in YEP than in YES in both the toxigenic and atoxigenic isolates Aflaguard and AF36. The expression of this gene was higher in YES than YEP in K54A (Figure 7.2C). With this, the expression of metalloproteinases was down-regulated while siderophore biosynthesis genes were up-regulated in some isolates indicating possible iron deficiencies (Supplementary Data 4). The production of aflatoxin and kojic acid also corresponded to observed expression of their corresponding biosynthetic genes. Aflatoxin was

found to be produced by toxigenic isolates only in YES (Figure 7.5A) while kojic acid was produced in both YES and YEP (Figure 7.5B). Interestingly, kojic acid was produced at a higher level in YEP compared to YES (Figure 7.5B), and was found to be further stimulated by the addition of H_2O_2 in solid culture medium (Figure 7.5C).

Medium carbon source also affects antioxidant and energy metabolism responses

Culturing toxigenic and atoxigenic isolates in YES and YEP media resulted in the upregulation of transcripts encoding antioxidant enzymes including thioredoxin peroxidase, thioredoxin reductase, and components of glutathione metabolism (Supplementary Data 4). Cytochrome p450 monooxygenase genes were also upregulated in response to increasing stress in both the toxigenic and atoxigenic isolates in YEP. Transcripts encoding products involved in proteolysis and gluconeogenesis were also more prevalent with increasing stress in YEP. Chitin catabolic genes were also found to be up-regulated with increasing stress in YEP, particularly in isolates with less oxidative tolerance including NRRL3357, Aflaguard, AF36, and K54A (Supplementary Data 4). In addition, the upregulation of autophagy prevention genes such as *atg22* were observed in NRRL3357 in YEP medium (Supplementary Data 1 and 4)[40,41]. In addition, class 3 lipase expression was generally down-regulated in YEP in response to increasing stress, particularly at the highest examined concentrations of H_2O_2 relative to the control (Supplementary Data 4). A similar decrease was also observed in K54A in YES (Supplementary Data 3).

Expression of upstream regulators of oxidative stress responses and carbon utilization

In addition to annotated pathway components as previously described, we also examined the expression of several upstream regulators of secondary metabolite production and oxidative stress responses described in the literature. The expression of bZIP transcription factors such as *atf21* and *atfA*, which have been shown to regulate aflatoxin production in response to oxidative stress *in vitro* during earlier periods in fungal growth[20], were not significantly regulated in either YES or YEP media in the toxigenic isolates with increasing stress. They were, however, constitutively expressed at an elevated level in all isolates and treatments (Supplementary Data 5).

Several Cis_2His_2 (C_2H_2) transcription factors were also found to be expressed in the isolates with some previously uncharacterized members such as AFLA_078920 exhibiting higher expression in YES than YEP (Supplementary Data 5). Additional C_2H_2 transcription factors such as *creA* (AFLA_134680 and AFLA_134690) and *brlA* (AFLA_082850 and AFLA_082860) were also stably expressed during stress (Supplementary Data 5). In addition to these transcription factors, a mitogen activated protein kinase kinase kinase (MAPKKK), *bck1*, was found to be upregulated in response to increasing levels of oxidative stress (Supplementary Data 5). This MAPKK has been shown to function in coordination with Mkk2 and MpkA[42], both of which were stably expressed across all isolates and treatments in the study (Supplementary Data 5).

Discussion

Previously, we observed that the aflatoxin production capabilities of *A. flavus* isolates were correlated with the levels of H_2O_2 stress individual isolates could tolerate or survive[32]. Here, we

found a related trend with isolates with higher stress tolerance and aflatoxin production exhibiting fewer significant DEGs than atoxigenic, less tolerant isolates in both YES and YEP (Table 7.1). This may be due to the developmental stage of the tolerant isolates which after seven days in control cultures would exhibit stationary growth patterns[19]. The case for this is bolstered by the observation that other less tolerant isolates generally exhibited up-regulation in aminobenzoate degradation transcripts. These aminobenzoate compounds have been found to reduce both aflatoxin production and mycelial growth[43]. This may imply that more tolerant isolates may possess more rapid and intense responses to stress than the other isolates, and that the cause of this may be related to fungal development (Table 7.1). Isolate developmental stage may also explain the lack of significant differences in bZIP transcription factor expression observed in this study (Supplementary Data 5). Previously published experiments have mostly examined these genes' expression and function following approximately 72 hours of fungal growth[20].

In addition to developmental differences, the ability to produce secondary metabolites and antioxidant enzymes, to maintain cell wall integrity, to regulate primary metabolism to meet energetic requirements under stress, and to recycle damaged cellular components were all integral components of the responses of both the toxigenic and atoxigenic isolates (Figure 7.6). Cell wall integrity was maintained primarily through the down-regulation of chitinases and chitosanases, although these were found to be up-regulated in YEP under increasing stress indicating a possible reallocation of cellular resources to primary metabolism possibly due to carbon starvation[44-46]. This reallocation of resources may also be due to the limited availability of free glucose and carbon catabolite repression in response to upstream regulation by the C_2H_2 transcription factors creA and brlA (Supplementary Data 5) which have been shown to influence

the expression of extracellular chitinases in response to carbon starvation[40,47-51]. In addition, membrane integrity may also be of concern due to the observed regulation of lipase-encoding transcripts in YEP at higher levels of stress (Supplementary Data 4). Their product, a class 3 lipase, breaks down the ester linkages in membrane lipids[51]. A reduction in lipase activity may also reduce the formation of lipoperoxides through the reaction of free fatty acids with ROS[51].

The catabolism of amino acid components of peptone in the YEP medium would fuel the generation of TCA cycle intermediates such as succinate and fumarate with some being utilized to form acetyl-CoA, the major building block of polyketide and terpenoid mycotoxins such as aflatoxin and aflatrem[16,34]. Previous experiments have shown that aflatoxin production was limited or non-existent in YEP, and that supplementation of peptone medium with TCA intermediates would not restore aflatoxin production[52]. However, several monosaccharides such as glucose and fructose have been found to be conducive carbon sources for aflatoxin production[31]. This allows for the possibility that the lack of aflatoxin production observed in YEP (Figure 7.5A) may be due to limitations in acetyl or malonyl-CoA availably because of their being directed into primary energy production rather than mycotoxin biosynthesis. Further experimentation will be required to confirm this hypothesis.

In the conducive YES medium, aflatoxin production has been shown to be stimulated by increasing oxidative stress (Figure 7.5). Previous studies have also shown that oxidative stress also plays a role as it is required for the initiation of aflatoxin production in *A. flavus* and related species such as *A. parasiticus*[17]. Given the close association of increasing levels of ROS and antioxidant enzyme expression with aflatoxin production, several previous studies have proposed that the production of aflatoxin may function as a supplemental source of antioxidant protection for *A. flavus* and other Aspergilli against oxidative stress[21,27]. Increased oxygen consumption and

subsequent production of ROS during aflatoxin production in toxigenic isolates has also been demonstrated along with the localization of secondary ROS production to aflatoxisomes inside the fungal cells[26,28]. In a recent study, Roze et al.[28] found that this burst in ROS production likely from cytochrome p450 monooxygenase and oxidase activities in aflatoxin biosynthesis may contribute to enhancing oxidative tolerance in conidia. The prevalence of cytochrome p450 genes in both aflatoxin and aflatrem biosynthesis suggests that it is possible similar oxygen consumption and ROS production occurs in both systems (Figure 7.4)[34,53]. It is also possible that this secondary burst of ROS production may prime expression of antioxidant genes, and that these cytochrome p450 monooxygenase and oxidase enzymes may consume excess oxygen produced by detoxifying enzymes (e.g. CAT, SOD, thioredoxin, etc.) while breaking down ROS, fixing it into aflatoxin and aflatrem which are then secreted from the fungal cells. Therefore, aflatrem biosynthesis may function to enhance oxidative stress tolerance. Further study will be required to better understand the precise biochemical role of aflatoxin and aflatrem in the biology of *A. flavus* and its interactions with host organisms.

In addition to aflatoxin and aflatrem, kojic acid biosynthetic transcripts were also differentially expressed. Kojic acid has been previously described as an antioxidant and is thought to chelate free Fe cations to limit non-enzymatic ROS formation (e.g. Fenton reactions) or through direct reactions with ROS[54,55]. Excessive production of kojic acid may result in possible iron deficiencies which may be occurring here given the regulation of both the bck1/mkk2/mpkA signaling pathway and siderophore biosynthetic genes in the isolates (Supplementary Data 4 and 5)[42,56,57]. With the absence of aflatoxin production in atoxigenic isolates and in YEP, it is possible that kojic acid production may supplement the loss of aflatoxin production-derived stress tolerance. Also, the lack of aflatoxin production and aflatrem

biosynthesis gene expression, and the reduced levels of kojic acid produced in solid media assays (Figure 7.5C) may partially explain the reduced oxidative stress tolerance of the K54A isolate in comparison to the other examined isolates (Table 7.1).

Multidrug resistance genes and MFS transporters were also expressed both the toxigenic and atoxigenic isolates which function to enhance fungal tolerance to antibiotic compounds[38,58]. In the biological control isolates Aflaguard and AF36, several transcripts regulated in response to oxidative stress may function in antibiotic biosynthesis (Supplementary Data 3 and 4). Together, this indicates oxidative stress may stimulate mechanisms used by the isolates in competition with other organisms both in the host plant and in the soil, and highlights the possibility for the use of ROS in the study biological control competitiveness and drug discovery through the expression of cryptic pathways under oxidative stress[59].

The connection between oxidative stress and *A. flavus* secondary metabolite production also has implications for improving host plant resistance to aflatoxin contamination. Recent studies have shown that drought sensitive maize lines which have been previously demonstrated to be susceptible to aflatoxin contamination accumulate higher levels of ROS in their leaf and kernel tissues[24,25]. Given the previously mentioned correlation between drought stress and aflatoxin contamination[13], it is possible that these ROS or their reactive byproducts (e.g. H_2O_2 and peroxidized lipids) may function in signaling between *A. flavus* and susceptible plants resulting in exacerbated aflatoxin production during infection[8,21,22,24,25]. By enhancing the resistance of host tissues to oxidative damage through biomarker and drought tolerance selection in breeding programs, it may be possible to enhance plant resistance to pre-harvest aflatoxin contamination[18] and needs to be addressed further.

Conclusion

Transcriptomic analyses of toxigenic and atoxigenic isolates of *A. flavus* and their responses to H_2O_2-derived oxidative stress in aflatoxin conducive and non-conducive media revealed that aflatoxin and aflatrem biosynthetic gene expression coincides with the up-regulation of monooxygenase genes. This suggests that the fixation of excess oxygen into these mycotoxins prior to their secretion may provide a degree of oxidative tolerance in *A. flavus*. In addition, kojic acid production was also found to correlate with previously observed isolate tolerance to oxidative stress and may convey additional antioxidant protection in the absence of aflatoxin or aflatrem production by iron chelation. Toxigenic and atoxigenic isolates of *A. flavus* were found to employ similar mechanisms in oxidative stress responses with the exception of secondary metabolite production. Overall, the responses of the isolates focused on four major strategies in countering oxidative stress with individual variations that include cell wall maintenance and repair, enzymatic detoxification of ROS, enhancement and maintenance of primary metabolic needs, and secondary metabolite production. Together, these components work together as the basis of coordinated response to oxidative stress. This study also illustrated the potential roles of secondary metabolite production, including aflatoxin, aflatrem, and kojic acid, in antioxidant responses of *A. flavus*, and their connections to primary metabolism in oxidative stress responses.

Acknowledgements

We thank Billy Wilson, Hui Wang, Xiaohong Guo, and Xiangyun Ji for technical assistance in the laboratory. This work is partially supported by the U.S. Department of Agriculture Agricultural Research Service (USDA-ARS), the Georgia Agricultural Commodity Commission for Corn, the Georgia Peanut Commission, the Peanut Foundation, and AMCOE (Aflatoxin

Mitigation Center of Excellence. This work has been also undertaken as part of the CGIAR Research Program on Grain Legumes and the USAID University Linkages Program between USDA-ARS and ICRISAT. ICRISAT is a member of CGIAR Consortium. Mention of trade names or commercial products in this publication is solely for the purpose of providing specific information and does not imply recommendation or endorsement by the USDA.

Supplemental Information

Links to supplemental datasets, figures, and tables can be found in Appendix A. A manuscript describing a detailed analysis of toxigenic isolate transcriptional responses can be found in Appendix D.

References

1. FAOSTAT (2016) Available: http://faostat.fao.org/. Accessed on February 12, 2016.
2. Andrade, P. D. & Caldas, E. D. Aflatoxins in cereals: worldwide occurrence and dietary risk assessment. *World Mycotoxin J*. **8**, 415-431 (2015).
3. Torres, A. M., Barros, G. G., Palacios, S. A., Chulze, S. N. & Battilani, P. Review on pre-and post-harvest management of peanuts to minimize aflatoxin contamination. *Food Res. Int.* **62**, 11-19 (2014).
4. Kew, M. C. Aflatoxins as a cause of hepatocellular carcinoma. *J. Gastrointestin. Liver Dis.* **22**, 305-310 (2013).
5. Williams, J.H. *et al.* Human aflatoxicosis in developing countries: a review of toxicology, exposure, potential consequences, and interventions. *Am. J. Clin. Nutr*. 80, 1106-1122 (2004).

6. Diener, U. L., Asquith, R. L. & Dickens, J. W. Aflatoxin and *Aspergillus flavus* in corn. *So. Coop. Ser. Bull*. **279**, 112 (1983).
7. Diener, U. L. *et al*. Epidemiology of aflatoxin formation by *Aspergillus flavus*. *Ann. Rev. Phytopathol*. **25**, 249-270 (1987).
8. Fountain, J. C. *et al*. Environmental influences on maize-*Aspergillus flavus* interactions and aflatoxin production. *Front. Microbiol*. **5**, 40 (2014).
9. Guo, B., Chen, Z. Y., Lee, R. D. & Scully, B. T. Drought stress and preharvest aflatoxin contamination in agricultural commodity: genetics, genomics and proteomics. *J. Int. Plant Biol.* **50**, 1281-1291 (2008).
10. Pandey, M. K. *et al.* Advances in *Arachis* genomics for peanut improvement. *Biotech. Adv.* **30**, 639-651 (2012).
11. Williams, W. P. Breeding for resistance to aflatoxin accumulation in maize. *Mycotoxin Res.* **22**, 27-32 (2006).
12. Holbrook, C. C., Guo, B. Z., Wilson, D. M. & Timper, P. The US breeding program to develop peanut with drought tolerance and reduced aflatoxin contamination. *Peanut Sci.* **36**, 50-53 (2009).
13. Kebede, H., Abbas, H. K., Fisher, D. K. & Bellaloui, N. Relationship between aflatoxin contamination and physiological responses of corn plants under drought and heat stress. *Toxins*, **4**, 1385-1403 (2012).
14. Amaike, S. & Keller, N. P. *Aspergillus flavus*. *Ann. Rev. Phytopathol*. **49**, 107-133 (2011).
15. Guo, B.Z. *et al*. Crop stress and aflatoxin contamination: perspectives and prevention strategies. B. Venkateswarlu, A.K. Shankerk, C. Shanker, M. Makeswari (Eds.), Crop Stress and Its Management: Perspectives and Strategies, Springer, New York (2012), pp. 399–427.

16. Yu, J. *et al*. Clustered pathway genes in aflatoxin biosynthesis. *App. Environ. Microbiol.* **70**, 1253-1262 (2004).

17. Jayashree, T. & Subramanyam, C. Oxidative stress as a prerequisite for aflatoxin production by *Aspergillus parasiticus*. *Free Rad. Biol. Med.* **29**, 981–985 (2000).

18. Fountain, J. C. *et al.* Resistance to *Aspergillus flavus* in maize and peanut: Molecular biology, breeding, environmental stress, and future perspectives. *Crop J.* **3**, 229-237 (2015a).

19. Reverberi, M. *et al*. Modulation of antioxidant defense in *Aspergillus parasiticus* is involved in aflatoxin biosynthesis: a role for the ApyapA gene. *Eukaryot. Cell* **7**, 988–1000 (2008).

20. Roze, L. V., Chanda, A., Wee, J., Awad, D. & Linz, J. E. Stress-related transcription factor AtfB integrates secondary metabolism with oxidative stress response in aspergilli. *J. Biol. Chem.* **286**, 35137-35148 (2011).

21. Roze, L. V., Hong, S. Y. & Linz, J. E. Aflatoxin biosynthesis: current frontiers. *Annu. Rev. Food Sci. Tech.* **4**, 293–311 (2013).

22. Gao, X. *et al*. Inactivation of the lipoxygenase ZmLOX3 increases susceptibility of maize to *Aspergillus spp*. *Mol. Plant Mic. Interact*. **22**, 222-231 (2009).

23. Howe, G. A. & Schilmiller, A. L. Oxylipin metabolism in response to stress. *Curr. Op. Plant Biol.* **5**, 230-236 (2002).

24. Yang, L. *et al*. Differential accumulation of reactive oxygen and nitrogen species in maize lines with contrasting drought tolerance and aflatoxin resistance. *Phytopathology*, in press (2016).

25. Yang, L. *et al*. Stress sensitivity is associated with differential accumulation of reactive oxygen and nitrogen species in maize genotypes with contrasting levels of drought tolerance. *Int. J. Mol. Sci.* **16**, 24791-24819 (2015).

26. Narasaiah, K.V., Sashidhar, R.B. & Subramanyam, C. Biochemical analysis of oxidative stress in the production of aflatoxin and its precursor intermediates. *Mycopathologia* **162**, 179–189 (2006).

27. Reverberi, M., Ricelli, A., Zjalic, S., Fabbri, A. A. & Fanelli, C. Natural functions of mycotoxins and control of their biosynthesis in fungi. *App. Microbiol. Biotech.* **87**, 899–911 (2010).

28. Roze, L.V. *et al*. Aflatoxin biosynthesis is a novel source of reactive oxygen species – A potential redox signal to initiate resistance to oxidative stress? *Toxins* **7**, 1411–1430 (2015).

29. Davis, N. D. & Diener, U. L. Growth and aflatoxin production by *Aspergillus parasiticus* from various carbon sources. *App. Microbiol*. **16**, 158 (1968).

30. Yu, J., Chang, P. K., Bhatnagar, D. & Cleveland, T. E. Cloning of a sugar utilization gene cluster in *Aspergillus parasiticus*. *BBA Gene Struct. Exp*. **1493**, 211-214 (2000).

31. Abdollahi, A. & Buchanan, R. L. Regulation of aflatoxin biosynthesis: induction of aflatoxin production by various carbohydrates. *J. Food Sci.* **46**, 633-635 (1981).

32. Fountain, J. C. *et al.* Effects of hydrogen peroxide on different toxigenic and atoxigenic isolates of *Aspergillus flavus*. *Toxins* **7**, 2985-2999 (2015b).

33. Valdes, J. J., Cameron, J. E. & Cole, R. J. Aflatrem: a tremorgenic mycotoxin with acute neurotoxic effects. *Environ. Health Perspect*. **62**, 459 (1985).

34. Nicholson, M. J. *et al*. Identification of two aflatrem biosynthesis gene loci in *Aspergillus flavus* and metabolic engineering of *Penicillium paxilli* to elucidate their function. *Appl. Environ. Microbiol.* **75**, 7469-7481 (2009).

35. Terabayashi, Y. *et al*. Identification and characterization of genes responsible for biosynthesis of kojic acid, an industrially important compound from *Aspergillus oryzae*. *Fungal Genet. Biol*. **47**, 953-961 (2010).

36. Chang, P. K. *et al.* Identification of genetic defects in the atoxigenic biocontrol strain *Aspergillus flavus* K49 reveals the presence of a competitive recombinant group in field populations. *Int. J. Food Microbiol.* **154**, 192-196 (2012).

37. Chang, P. K., Horn, B. W. & Dorner, J. W. Sequence breakpoints in the aflatoxin biosynthesis gene cluster and flanking regions in nonaflatoxigenic *Aspergillus flavus* isolates. *Fungal Genet. Biol.* **42**, 914-923 (2005).

38. Chang, P. K., Yu, J. & Yu, J. H. aflT, a MFS transporter-encoding gene located in the aflatoxin gene cluster, does not have a significant role in aflatoxin secretion. *Fungal Genet. Biol.* **41**, 911-920 (2004).

39. Yu, J. H. & Keller, N. Regulation of secondary metabolism in filamentous fungi. *Annu. Rev. Phytopathol.* **43**, 437-458 (2005).

40. Yamazaki, H. *et al*. A chitinase gene, chiB, involved in the autolytic process of *Aspergillus nidulans*. *Curr. Genet*. **51**, 89-98 (2007).

41. Yang, Z., Huang, J., Geng, J., Nair, U. & Klionsky, D. J. Atg22 recycles amino acids to link the degradative and recycling functions of autophagy. *Mol. Biol. Cell* **17**, 5094-5104 (2006).

42. Jain, R. *et al*. The MAP kinase MpkA controls cell wall integrity, oxidative stress response, gliotoxin production and iron adaptation in *Aspergillus fumigatus*. *Mol. Microbiol*. **82**, 39-53 (2011).

43. Chipley, J. R. & Uraih, N. Inhibition of Aspergillus growth and aflatoxin release by derivatives of benzoic acid. *App. Environ. Microbiol*. **40**, 352-357 (1980).

44. Emri, T., Molnár, Z. & Pócsi, I. The appearances of autolytic and apoptotic markers are concomitant but differently regulated in carbon-starving *Aspergillus nidulans* cultures. *FEMS Microbiol. Letters* **251**, 297-303 (2005).

45. Nitsche, B. M., Jørgensen, T. R., Akeroyd, M., Meyer, V. & Ram, A. F. The carbon starvation response of *Aspergillus niger* during submerged cultivation: Insights from the transcriptome and secretome. *BMC Genomics* **13**, 1 (2012).

46. Emri, T., Molnár, Z., Szilágyi, M. & Pócsi, I. Regulation of autolysis in *Aspergillus nidulans*. *App. Biochem. Biotech.* **151**, 211-220 (2008).

47. Mogensen, J., Nielsen, H. B., Hofmann, G. & Nielsen, J. Transcription analysis using high-density micro-arrays of *Aspergillus nidulans* wild-type and creA mutant during growth on glucose or ethanol. *Fungal Genet. Biol*. **43**, 593-603 (2006).

48. Pócsi, I. *et al*. Asexual sporulation signalling regulates autolysis of *Aspergillus nidulans* via modulating the chitinase ChiB production. *J. App. Microbiol.* **107**, 514-523 (2009).

49. Roy, P., Lockington, R. A. & Kelly, J. M. CreA-mediated repression in *Aspergillus nidulans* does not require transcriptional auto-regulation, regulated intracellular localisation or degradation of CreA. *Fungal Genet. Biol.* **45**, 657-670 (2008).

50. Strauss, J. *et al*. The function of CreA, the carbon catabolite repressor of *Aspergillus nidulans*, is regulated at the transcriptional and post-transcriptional level. *Mol. Microbiol*. **32**, 169-178 (1999).

51. Bhattacharjee, S. Reactive oxygen species and oxidative burst: roles in stress, senescence and signal. *Curr. Sci. India*. **89**, 1113-1121 (2005).

52. Yan, S., Liang, Y., Zhang, J. & Liu, C. M. *Aspergillus flavus* grown in peptone as the carbon source exhibits spore density-and peptone concentration-dependent aflatoxin biosynthesis. *BMC Microbiol*. **12**, 106 (2012).

53. Duran, R. M., Cary, J. W. & Calvo, A. M. Production of cyclopiazonic acid, aflatrem, and aflatoxin by *Aspergillus flavus* is regulated by veA, a gene necessary for sclerotial formation. *App. Microbiol. Biotech.* **73**, 1158-1168 (2007).

54. Chang, P. K. *et al*. Loss of msnA, a putative stress regulatory gene, in *Aspergillus parasiticus* and *Aspergillus flavus* increased production of conidia, aflatoxins and kojic acid. *Toxins* **3**, 82-104 (2011).

55. Fenton, H. J. H. Oxidation of tartaric acid in presence of iron. *J. Chem. Soc. Trans*. **65**, 899-910 (1894).

56. Valiante, V., Heinekamp, T., Jain, R., Härtl, A. & Brakhage, A. A. The mitogen-activated protein kinase MpkA of *Aspergillus fumigatus* regulates cell wall signaling and oxidative stress response. *Fungal Genet. Biol.* **45**, 618-627 (2008).

57. Valiante, V., Jain, R., Heinekamp, T. & Brakhage, A. A. The MpkA MAP kinase module regulates cell wall integrity signaling and pyomelanin formation in *Aspergillus fumigatus*. *Fungal Genet. Biol.* **46**, 909-918 (2009).

58. Tobin, M. B., Peery, R. B. & Skatrud, P. L. Genes encoding multiple drug resistance-like proteins in *Aspergillus fumigatus* and *Aspergillus flavus*. *Gene* **200**, 11-23 (1997).

59. Brakhage, A. A. & Schroeckh, V. Fungal secondary metabolites–strategies to activate silent gene clusters. *Fungal Genet. Biol.* **48**, 15-22 (2011).

60. Davis, N. D., Diener, U. L. & Agnihotri, V. P. Production of aflatoxins B1 and G1 in chemically defined medium. *Mycopathol. Mycol. App*. **31**, 251-256 (1967).

61. Bolger, A., Lohse, M. & Usadel, B. Trimmomatic: a flexible trimmer for Illumina sequence data. *Bioinformatics*. **30**, 1-7 (2014).

62. Kim, D. *et al*. TopHat2: accurate alignment of transcriptomes in the presence of insertions, deletions and gene fusions. *Genome Biol*. **14**, R36 (2013).

63. Langmead, B., Trapnell, C., Pop, M. & Salzberg, S. Ultrafast and memory-efficient alignment of short DNA sequences to the human genome. *Genome Biol*. **10**, R25 (2009).

64. Roberts, A., Pimentel, H., Trapnell, C. & Pachter, L. Identification of novel transcripts in annotated genomes using RNA-Seq. *Bioinformatics*. **27**, 2325-2329 (2011).

65. Trapnell, C. *et al*. Differential analysis of gene regulation at transcript resolution with RNA-seq. *Nature Biotechnol*. **31**, 46-54 (2013).

66. Bentley, R. Preparation and analysis of kojic acid. *Methods in Enzymol.* **3**, 238-241 (1957).

67. Saruno, R., Kato, F. & Ikeno, T. Kojic acid, a tyrosinase inhibitor from *Aspergillus albus*. *Ag. Biol. Chem*. **43**, 1337-1338 (1979).

Table 7.1. Numbers of significantly differentially expressed genes (DEGs) in *Aspergillus flavus* isolates in YES (yeast extract sucrose) and YEP (yeast extract peptone) media in response to increasing oxidative stress.

Isolate	Toxin*	H_2O_2*	YES Medium			YEP Medium		
			0 v 10 mM	0 v 20/25 mM	10 v 20/25 mM	0 v 10 mM	0 v 20/25 mM	10 v 20/25 mM
Tox4	+++	40	4	29	57	19	78	44
AF13	+++	35	6	122	85	49	37	87
NRRL3357	+	20	53	117	112	27	446	738
Aflaguard	---	20	16	786	856	41	415	407
AF36	---	25	67			17		
K54A	-	15	142			224		

*Previously observed aflatoxin production and H_2O_2 tolerance in Fountain et al. (2015b). Toxin Production: '+++' High Aflatoxin Producer; '+' Moderate Aflatoxin Producer; '---' Atoxigenic Biological Control Isolate; '-' Atoxigenic Isolate.

Figure 7.1. Venn diagram of genes expressed in toxigenic and atoxigenic isolates in YES (yeast extract sucrose) and YEP (yeast extract peptone) media. Genes with FPKM ≥ 2 were considered to be expressed. Those genes expressed exclusively in YES (aflatoxin conducive) or YEP (aflatoxin non-conducive) medium in toxigenic (Tox4, AF13, and NRRL3357) and atoxigenic (Aflaguard, AF36, K54A) isolates were identified using Venny 2.1.0.

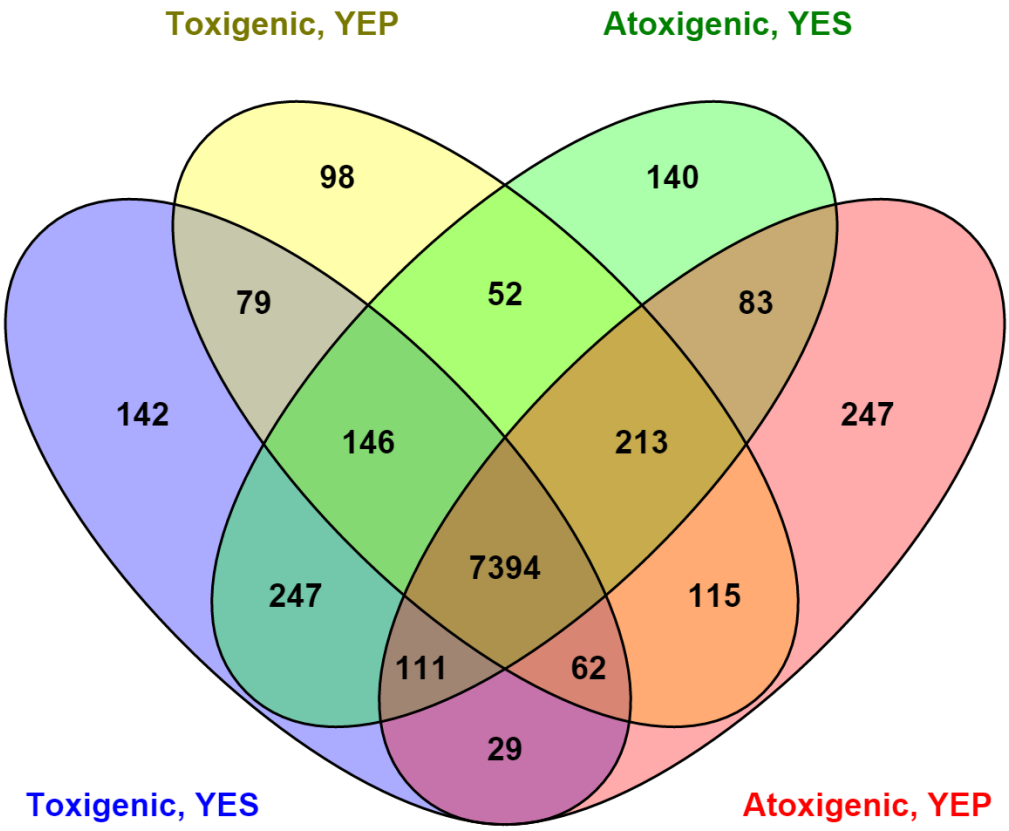
Toxigenic, YEP
Atoxigenic, YES
98
140
79
52
83
142
146
213
247
7394
247
115
111
62
29
Toxigenic, YES
Atoxigenic, YEP

Figure 7.2. Heatmap of secondary metabolite biosynthetic gene expression. Expression of genes involved in the biosynthesis of aflatoxin (A), aflatrem (B), and kojic acid (C) are plotted with colors corresponding to the FPKM's of the genes within each isolate and treatment combination. For each heatmap, individual keys are located at the base of each plot with FPKM values increasing from blue to red. Isolate and treatment labels at the top of the figure apply throughout.

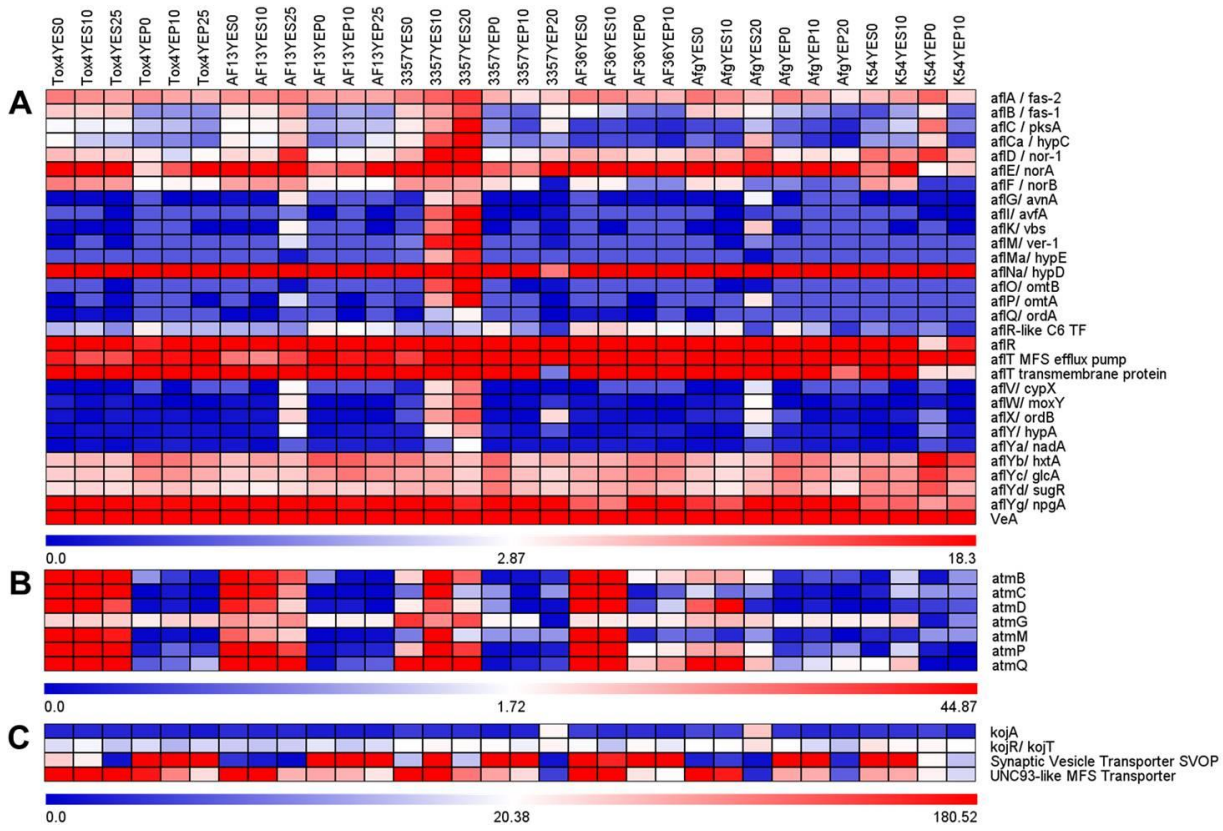
Tox4YES0
Tox4YES10
Tox4YES25
Tox4YEP0
Tox4YEP10
Tox4YEP25
AF13YES0
AF13YES10
AF13YES25
AF13YEP0
AF13YEP10
AF13YEP25
3357YES0
3357YES10
3357YES20
3357YEP0
3357YEP10
3357YEP20
AF36YES0
AF36YES10
AF36YEP0
AF36YEP10
AfgYES0
AfgYES10
AfgYES20
AfgYEP0
AfgYEP10
AfgYEP20
K54YES0
K54YES10
K54YEP0
K54YEP10
A
aflA / fas-2
aflB / fas-1
aflC / pksA
aflCa / hypC
aflD / nor-1
aflE/ norA
aflF / norB
aflG/ avnA
aflI/ avfA
aflK/ vbs
aflM/ ver-1
aflMa/ hypE
aflNa/ hypD
aflO/ omtB
aflP/ omtA
aflQ/ ordA
aflR-like C6 TF
aflR
aflT MFS efflux pump
aflT transmembrane protein
aflV/ cypX
aflW/ moxY
aflX/ ordB
aflY/ hypA
aflYa/ nadA
aflYb/ hxtA
aflYc/ glcA
aflYd/ sugR
aflYg/ npgA
VeA
0.0
2.87
18.3
B
atmB
atmC
atmD
atmG
atmM
atmP
atmQ
0.0
1.72
44.87
C
kojA
kojR/ kojT
Synaptic Vesicle Transporter SVOP
UNC93-like MFS Transporter
0.0
20.38
180.52

Figure 7.3. Principal component and multi-spatial analyses of *Aspergillus flavus* isolate expression profiles. Principle component (A) and multi-spatial (B) analyses of the expression profiles of the isolates in both YES (yeast extract sucrose) and YEP (yeast extract peptone) media with increasing levels of oxidative stress. The patterns present in the data indicate a clear segregation of the isolate profiles based mainly on culture medium carbon source.

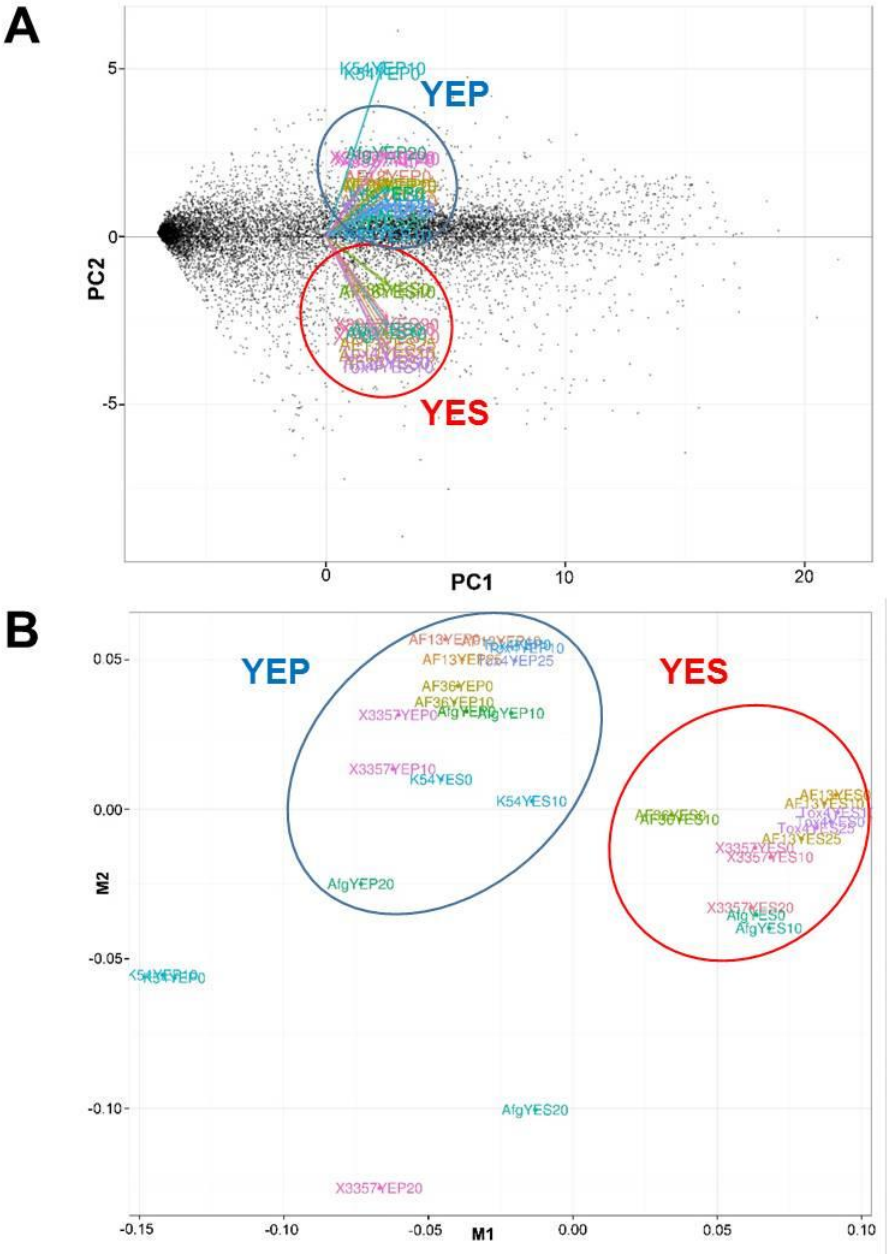
A
YEP
YES
PC1
PC2
B
YEP
YES
M1
M2

Figure 7.4. Differential expression of genes involved in glycolysis and secondary metabolite biosynthesis. The 6 x 3 tables beside the gene annotations indicate significant changes in gene expression between YES (yeast extract sucrose) and YEP (yeast extract peptone) media for each isolate when exposed to H_2O_2 (0, 10, and 20 or 25 mM). Green and red colors indicate significantly higher expression of the genes in YES and YEP, respectively. White color represents no significant difference between YES and YEP; and gray color represents comparisons not measured in the experiment. Red colored points in molecular models represent the occurrence of oxygen atoms. Red colored text for gene annotations represent cytochrome p450 monooxygenase-coding genes present in the aflatoxin and aflatrem biosynthetic pathways. Abbreviations: G6P, glucose-6-phosphate; F6P, fructose-6-phosphate; F1,6P, fructose-1,6-bisphosphate; Gly3P, glyceraldehyde-3-phosphate; Gly1,3PP, glyceraldehyde-1,3-bisphosphate; PEP, phosphoenolpyruvate.

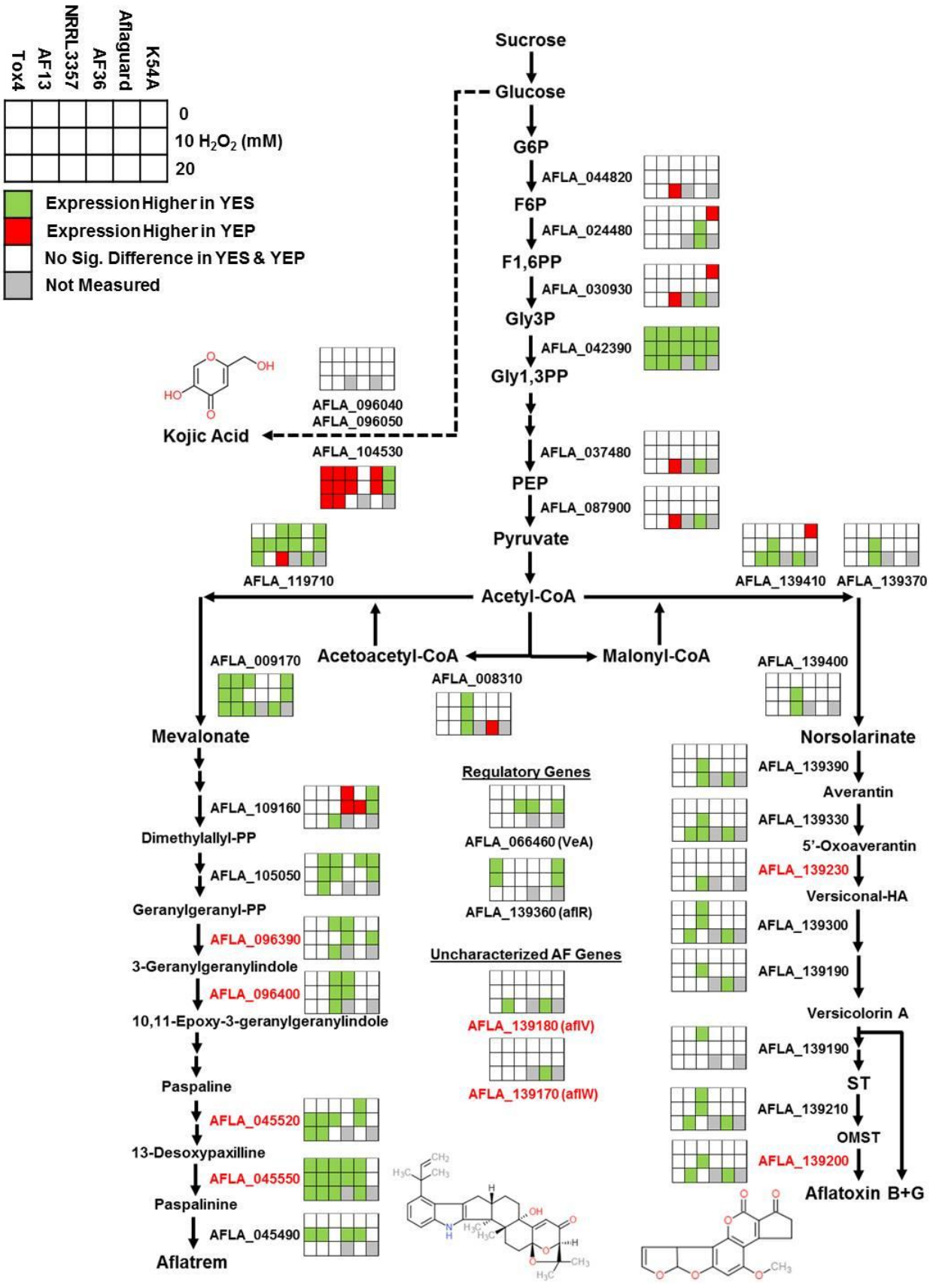
Tox4
AF13
NRRL3357
AF36
Aflaguard
K54A
0
10 H2O2 (mM)
20
Expression Higher in YES
Expression Higher in YEP
No Sig. Difference in YES & YEP
Not Measured
Sucrose
Glucose
G6P
AFLA_044820
F6P
AFLA_024480
F1,6PP
AFLA_030930
Gly3P
AFLA_042390
Gly1,3PP
AFLA_037480
PEP
AFLA_087900
Pyruvate
Acetyl-CoA
Acetoacetyl-CoA
Malonyl-CoA
AFLA_008310
AFLA_009170
Mevalonate
AFLA_109160
Dimethylallyl-PP
AFLA_105050
Geranylgeranyl-PP
AFLA_096390
3-Geranylgeranylindole
AFLA_096400
10,11-Epoxy-3-geranylgeranylindole
Paspaline
AFLA_045520
13-Desoxypaxilline
AFLA_045550
Paspalinine
AFLA_045490
Aflatrem
Kojic Acid
AFLA_096040
AFLA_096050
AFLA_104530
AFLA_119710
AFLA_139410
AFLA_139370
AFLA_139400
Norsolarinate
AFLA_139390
Averantin
AFLA_139330
5'-Oxoaverantin
AFLA_139230
Versiconal-HA
AFLA_139300
AFLA_139190
Versicolorin A
AFLA_139190
ST
AFLA_139210
OMST
AFLA_139200
Aflatoxin B+G
Regulatory Genes
AFLA_066460 (VeA)
AFLA_139360 (aflR)
Uncharacterized AF Genes
AFLA_139180 (aflV)
AFLA_139170 (aflW)

Figure 7.5. Aflatoxin and kojic acid production assays. Thin layer chromatography of liquid culture medium from the cultured isolates was performed for aflatoxin B1 (A) and kojic acid (B) with UV excitation at 365 and 254 nm, respectively. Aflatoxin was produced by the toxigenic isolates only in YES (yeast extract sucrose) while no aflatoxin production was observed for K54A in either medium. Kojic acid was shown to be produced by all isolates at a higher level in YEP (yeast extract peptone) than in YES (B), and seemed to be stimulated by the addition of H_2O_2 (C). In the solid medium assay based on Bentley[66] (C), the low production of kojic acid by K54A in the solid culture assay may be due to compositional differences in PDA and YES. Images are representative of three experimental replicates.

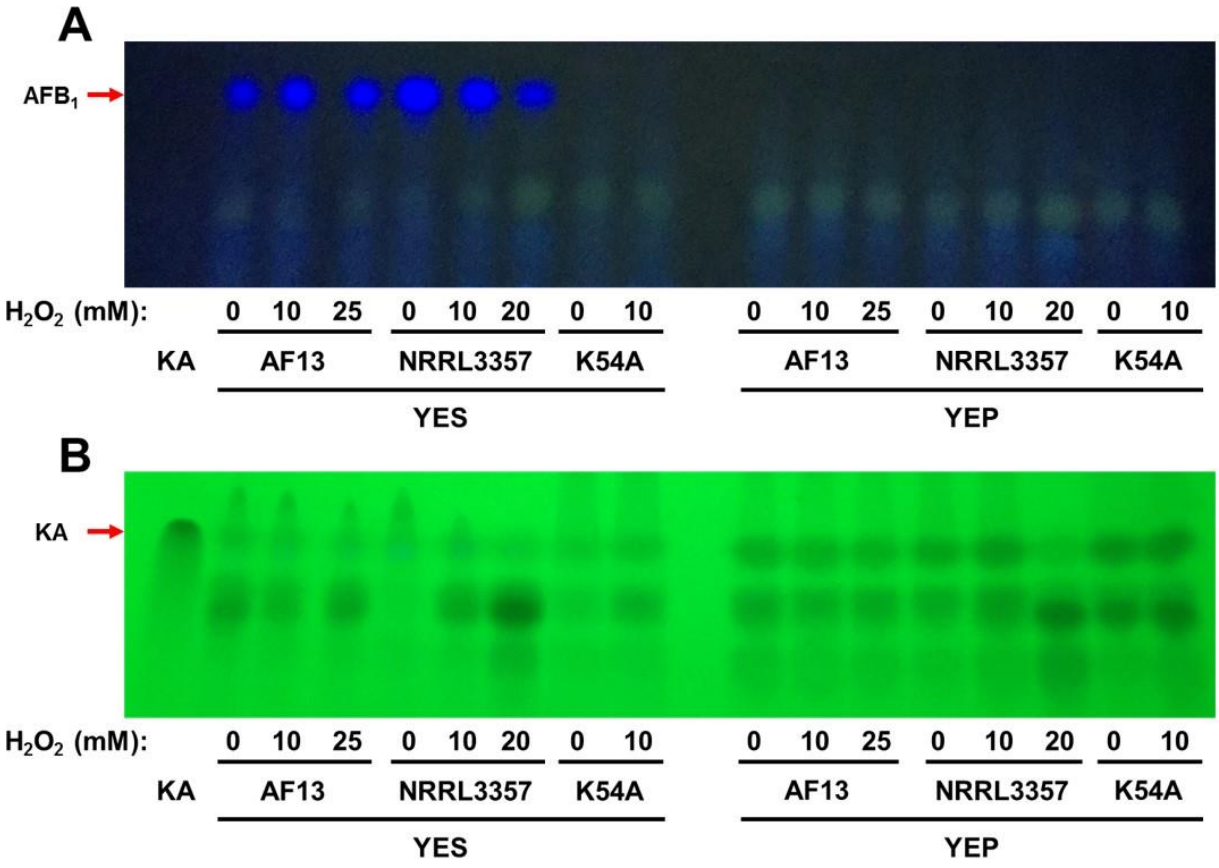
A
AFB1
H2O2 (mM): 0 10 25 0 10 20 0 10 0 10 25 0 10 20 0 10
KA AF13 NRRL3357 K54A AF13 NRRL3357 K54A
YES YEP
B
KA
H2O2 (mM): 0 10 25 0 10 20 0 10 0 10 25 0 10 20 0 10
KA AF13 NRRL3357 K54A AF13 NRRL3357 K54A
YES YEP

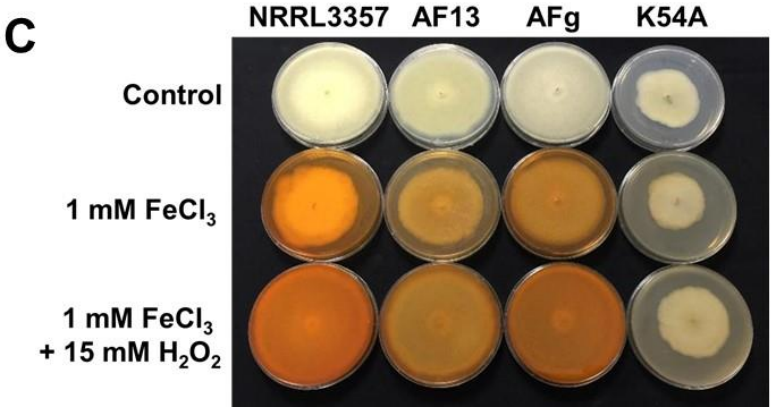
C
NRRL3357 AF13 AFg K54A
Control
1 mM FeCl3
1 mM FeCl3
+ 15 mM H2O2

Figure 7.6. Summary of the overall oxidative stress responses exhibited by *Aspergillus flavus* isolates. The isolates examined in this study exhibited four primary responses to imposed oxidative stress which were influenced by the provided culture medium carbon source (sucrose or peptone). These include: cell wall and cell membrane maintenance and repair through the regulation of chitinases and lipases along with associated signaling pathways; enzymatic detoxification of reactive oxygen species (ROS) through the thioredoxin and glutathione cycles along with enzymes such as catalase (CAT) and superoxide dismutase (SOD); enhancement and maintenance of primary metabolic needs in response to stress; and increased secondary metabolite production to either fix and secrete excess oxygen and ROS, or to limit their formation through co-factor binding or direct antioxidant activity.

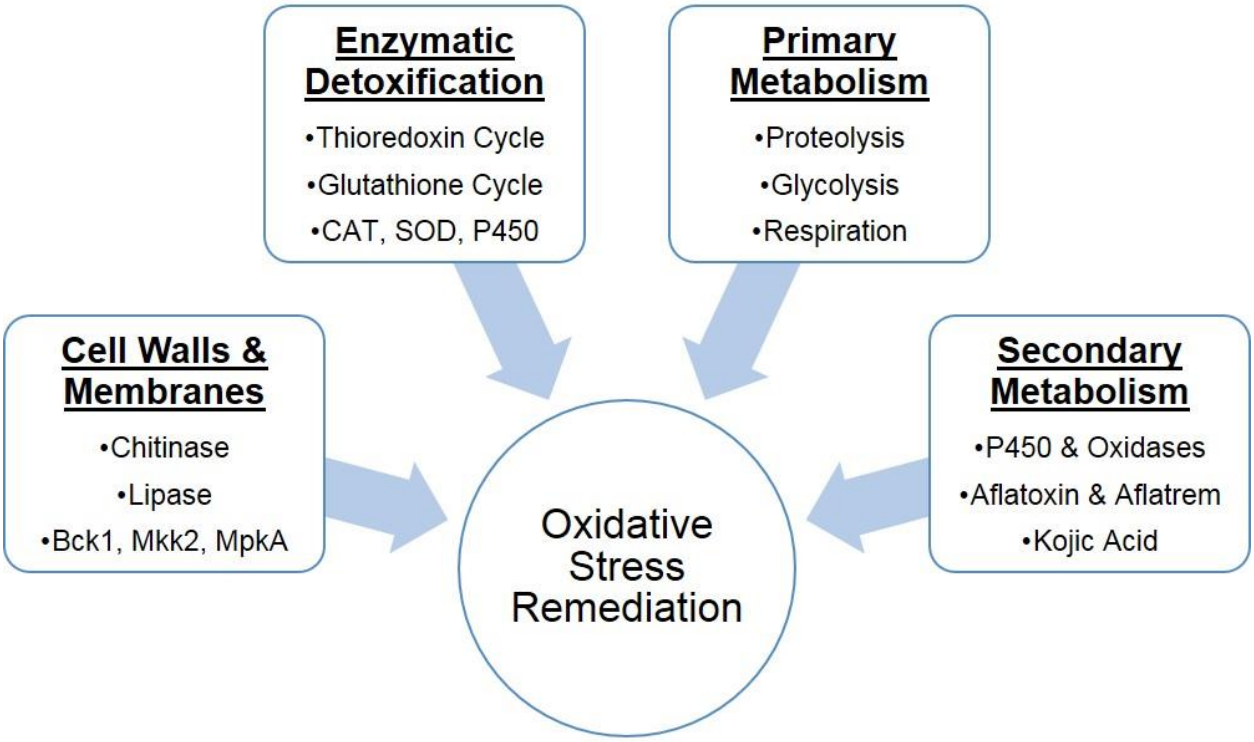
Enzymatic Detoxification
•Thioredoxin Cycle
•Glutathione Cycle
•CAT, SOD, P450
Primary Metabolism
•Proteolysis
•Glycolysis
•Respiration
Cell Walls & Membranes
•Chitinase
•Lipase
•Bck1, Mkk2, MpkA
Secondary Metabolism
•P450 & Oxidases
•Aflatoxin & Aflatrem
•Kojic Acid
Oxidative Stress Remediation

CHAPTER 8

ISOLATE-SPECIFIC OXIDATIVE STRESS RESPONSES AT THE PROTEIN LEVEL IN *ASPERGILLUS FLAVUS* ARE CORRELATED WITH AFLATOXIN PRODUCTION CAPABILITY

Fountain, J.C., Koh, J., Yang, L., Bajaj, P., Pandey, M.K., Nayak, S.N., Chen, W., Zhuang, W., Lee, R.D., Kemerait, R.C., Varshney, R.K., Chen, S., Guo, B. (2017). Isolate-specific oxidative stress responses at the protein level in *Aspergillus flavus* are correlated with aflatoxin production capability. Prepared for submission to *Proteomics*.

Abstract

Aspergillus flavus is a facultative pathogen of crops such as maize and peanut. It produces carcinogenic aflatoxins during infection, particularly in drought stressed host plants. Reactive oxygen species (ROS) have been shown to accumulate in host plant tissues during drought and to stimulate the production of aflatoxin by *A. flavus in vitro* and *in vivo*. Previous transcriptome studies of field isolates of *A. flavus* showed that oxidative stress may also regulate isolate development, carbohydrate metabolism, and the production of additional secondary metabolites. To examine these responses at the protein level, here we performed iTRAQ (Isobaric Tags for Relative and Absolute Quantification) proteomics for three isolates with varying levels of aflatoxin production: AF13 (+++), NRRL3357 (+), and K54A (-) in aflatoxin conducive medium amended with varying levels of H_2O_2. Proteomic analysis identified 1,173 proteins in at least two replicates with higher number of differentially expressed proteins in isolates with less oxidative stress tolerance. Weak correlation (r = 0.1114) was observed between the proteomic and the previously obtained transcriptomic data indicating the potential role of post-transcriptional regulation. The most common differentially expressed biochemical pathways included carbon metabolism, glutathione metabolism, oxidative stress regulation, and secondary metabolite biosynthesis. Highly toxigenic isolate exhibited greater expression of lytic enzymes and sclerotial developmental proteins, while less toxigenic isolate mainly displayed regulation of antioxidant and primary metabolic pathways. The environmental stress tolerance mechanisms employed by these isolates provide a direction for the enhancement of host resistance through the manipulation of host antioxidant capacity and lytic enzyme inhibition activity using biomarker selection in breeding programs and through novel approaches such as genome editing in crops.

Introduction

Aspergillus flavus (Link ex Fr, Teleomorph: *Petromyces flavus*) is a facultative plant pathogen, which is capable of infecting host plants, primarily maize and peanut. The infection of these crops by *A. flavus* poses a serious threat to human and animal health due to its production of carcinogenic mycotoxins, termed as aflatoxins (Amaike and Keller, 2011). Chronic exposure to aflatoxin can lead to increased likelihood of developing hepatocellular carcinoma and hepatitis with exposure to high levels resulting in acute aflatoxicosis and death (Williams et al. 2004, 2010). Outbreaks of aflatoxin contamination typically occur in regions prone to drought and can result in loss of life. For example, the 2004 Kenyan outbreak resulted in 317 cases of acute aflatoxicosis and 125 deaths (Azziz-Baumgartner et al. 2005). Aflatoxin contamination of crops such as maize, peanut, and others also leads to significant economic losses in the US, approaching $500 million per year with greater losses reported globally due to lost crop value and regulatory restrictions on import and export of contaminated foods (Wu, 2015).

Research efforts have been focused on prevention of both pre-and post-harvest aflatoxin contamination, of which post-harvest storage is the single most effective measure currently available for the reduction of aflatoxin contamination (Magan and Aldred, 2007; Torres et al. 2014). The post-harvest management can become more effective if resistance to pre-harvest colonization and aflatoxin production is employed to minimize the inoculum for post-harvest contamination. Pre-harvest aflatoxin contamination is managed mainly through the application of atoxigenic biological control isolates of *A. flavus*, such as Aflaguard (NRRL21882) and AF36 (NRRL18543) which compete with toxigenic isolates for available niches in the environment, and through host resistance (Abbas et al. 2011; Cotty and Bayman, 1993; Chen et al. 2016; Dorner and Lamb, 2006; Kelly et al. 2012). Host resistance to *A. flavus* colonization and

aflatoxin contamination is highly quantitative and is primarily a product of innate host immunity to pathogen infection rather than specific gene-for-gene resistance (Fountain et al. 2014, 2015a). This resistance is also highly influenced by abiotic stresses such as drought and heat stress (Guo et al. 2008).

Drought stress has been shown to stimulate the production of reactive oxygen species (ROS) in plant tissues which function in stress responsive signaling, but can also have deleterious effects on hosts if they accumulate in excessive concentrations (Baxter et al. 2014; de Carvalho, 2008). Recent studies have suggested that these ROS and their reactive byproducts such as oxylipins may influence the production of aflatoxin by *A. flavus* during colonization (Gao et al. 2009). Previous reports have shown that oxidative stress can stimulate the production of aflatoxin by *A. flavus* with medium amendment with oxylipins, ROS, or ROS production inducers resulting in greater aflatoxin production (Fabbri et al. 1983; Fountain et al. 2015b, Jayashree and Subramanyam, 2000; Narasaiah et al. 2006). Conversely, supplementation of medium with ROS scavengers and antioxidant compounds have been shown to reduce or inhibit aflatoxin production (Grintzalis et al. 2014). These results suggest that oxidative stress may indeed be a pre-requisite for aflatoxin production (Jayashree and Subramanyam, 2000).

Aflatoxin production is encoded by a highly conserved cluster of 25 genes housed within 70kb in the *A. flavus* genome (Yu et al. 2004). Although the biochemical processes involved in the biosynthesis of aflatoxin carried out by these encoded components have been well characterized (Payne and Brown, 1998; Roze et al. 2013), there is limited understanding on the regulating mechanisms wherein several transcription factors have been found to be involved in this regulatory process. For example, AflR is a key regulatory transcription factor for aflatoxin production whose silencing impedes aflatoxin production (McDonald et al. 2005). Other

transcription factors such as the bZIP transcription factors AtfA and AtfB also bind to aflatoxin gene promoters and regulate oxidative stress responses (Hong et al. 2013).

In addition to this, post-transcriptional modifications and interactions have been shown to be heavily involved in the regulation of secondary metabolite production and development in *Aspergillus spp*. For example, G-protein and protein kinase A (PkaA) signaling pathways are used to phosphorylate AflR to regulate aflatoxin production along with conidia and sclerotia development (Amare and Keller, 2014; Shimizu et al. 2003). AflR can also be regulated in a phosphorylation and PkaA-independent manner by RasA, a member of the small GTP-binding protein family, potentially through direct interaction (Shimizu et al. 2003). Post-transcriptional modifications have also been suggested based on the low correlation between their RNA sequencing gene expression levels and observed fold-changes in proteins, such as in the case of *A. flavus* responses to temperature stress (Bai et al. 2015).

Given the evident relationship between oxidative stress and aflatoxin production, and its implication for understanding the biological role of aflatoxin production in *A. flavus* both in the field and during host colonization, we previously examined the transcriptomes of several field isolates of *A. flavus* to oxidative stress when utilizing aflatoxin conducive or non-conducive substrates (Fountain et al. 2016a, 2016b). We observed that isolates producing higher levels of aflatoxin and possessing greater tolerance to oxidative stress exhibited less differential gene expression compared to less tolerant, atoxigenic isolates. Additional secondary metabolite genes including aflatrem and kojic acid genes were found to be up-regulated by oxidative stress suggesting a coordinated secondary metabolite role in oxidative stress responses. However, given that few genes were differentially expressed in the highly tolerant isolates, it is possible that post-transcriptional and protein level regulation plays a more definitive role in oxidative

stress tolerance. To examine the oxidative stress responses of *A. flavus* at the protein/enzymatic level, we examined the proteomic responses of select field isolates of *A. flavus* to oxidative stress in aflatoxin production conductive medium using isobaric tags for relative and absolute quantitation (iTRAQ) proteomics. Correlative analyses between these proteomic data and previously obtained transcriptomic data were also performed to examine for possible post-transcriptional regulation of responses. The selected isolates exhibited distinct responses to oxidative stress which provide insights into potential targets for enhancing host resistance and biological control performance.

Materials and Methods

Isolate collection

The AF13 isolate used in this study was obtained from Dr. Kenneth Damann, Department of Plant Pathology and Crop Physiology, Louisiana State University, Baton Rouge, LA. The NRRL3357 isolate was obtained from the USDA National culture repository, Peoria, IL. The K54A isolate was obtained from Dr. Hamed Abbas, USDA-ARS, Mycotoxin Res Unit, Stoneville, MS. All isolates were received on potato dextrose agar (PDA) and were sub-cultured on V8 agar (20% V8 juice, 1% $CaCO_3$, 2% agar) prior to use.

Isolate culture conditions

Conidia of each isolate were harvested from V8 agar plates five days after inoculation using sterile 0.1% Tween 20 solution. The isolates were then cultured in 125mL Erlenmeyer flasks containing 50mL yeast extract-sucrose (YES; 2% yeast extract, 1% sucrose) medium inoculated with 100µL conidia suspension (~$4.0x10^6$ conidia/mL). For oxidative stress treatments, the YES

medium was amended with H_2O_2 (3% stabilized solution) at concentrations as previously determined based on individual isolates' oxidative stress tolerance (Fountain et al. 2015b) with AF13 cultures amended with 0, 10, and 25mM H_2O_2; NRRL3357 with 0, 10, and 20mM H_2O_2; and K54A with 0 and 10mM H_2O_2. The isolates were then stationary cultured at 30°C for 7 days in the dark. Three biological replicate cultures were performed for each isolate and treatment combination. Following culturing, mycelia was recovered and stored at -80°C for protein isolation.

Protein isolation and quantitation

Proteins were isolated using a modified phenol/methanolic ammonium acetate method based on Zhuang et al. (2016) and Hurkman and Tanaka (1986). Briefly, the obtained mycelia tissue was ground to a fine powder using a mortar and pestle cooled in liquid nitrogen. The powdered tissue (200mg) was then incubated in extraction media (0.1M Tris-HCL pH 8.8, 10mM EDTA, 1.2% β-mercaptoethanol (*v*/*v*), 0.9 M Sucrose) for 20 min on ice with occasional vortexing. Tris-buffered phenol (pH 8.8) was then added and the samples incubated in ice for a further 10 min. Following centrifugation at 5,000 x g at 4°C for 20 min, proteins in the phenol phase were then precipitated in a separate tube in five volumes of cold 0.1M ammonium acetate in 100% methanol. The precipitated proteins were then pelleted by centrifugation at 5,000 x g at 4°C for 20 min and washed twice in both 0.1M ammonium acetate and then in cold 80% acetone. The pellet was then dissolved in 2D buffer (8M Urea, 4% CHAPS (*w*/*v*), 40mM Tris-base, 2M Thiourea) immediately prior to quantitation using an EZQ Protein Quantitation Kit (Invitrogen, Carlsbad, CA, USA) according to the manufacturer's instructions. One-dimensional polyacrylamide gel electrophoresis was then performed to validate protein quality (Figure S8.1).

Protein digestion and iTRAQ labeling

Following quantitation, for each sample 100µg of protein was dissolved in the dissolution buffer containing denaturant found in the iTRAQ Reagents – 8-plex kit (AB Sciex Inc., Foster City, CA, USA) then reduced, alkylated, digested with trypsin, and labeled according to the manufacturer's instructions. For the AF13 isolate, the 0, 10, and 25mM H_2O_2 treated samples were labeled with iTRAQ tags 113, 114, and 115, respectively. For the NRRL3357 isolate, the 0, 10, and 20mM H_2O_2 treated samples were labeled with tags 116, 117, and 118, respectively. Finally, for the K54A isolate, the 0 and 10mM H_2O_2 treated samples were labeled with tags 119 and 121, respectively. Each of the three biological replicates were processed separately with the same labeling strategy. Following labeling, each biological replicate of samples were mixed and aliquoted into four technical replicates.

Strong cation exchange fractionation, reverse phase nanoflow HPLC, and tandem mass spectrometry

Peptide fractionation, HPLC, and mass spectrometry were performed as described in our previous study (Yang et al. 2014). Briefly, each peptide mixture was lyophilized and dissolved in Solvent A (25% acetonitrile (*v*/*v*), 10 mM ammonium formate, pH 2.8) followed by fractionation on a Agilent HPLC System 1260 (Agilent Technologies, Santa Clara, CA, USA) with a polysulfoethyl column (2.1mm x 100mm, 5µL, 300Å; PolyLC, Columbia, MD, USA). Elution was performed with a flow rate of 200µL/min with a linear gradient of 0 – 20% Solvent B (25% acetonitrile, 0.5M ammonium formate, pH 6.8) over 50 min. Ramping up was then performed with 100% Solvent B for 5 min. Absorbance at 280nm was monitored, and a total of 10 fractions were collected. The collected fractions were then resuspended in LC solvent A (0.1% formic acid

in 3% acetonitrile) and used for analysis on a hybrid quadrupole Orbitrap (Q Exactive Plus) MS system (Thermo Fisher, Bremen, Germany) coupled with an Easy-nLC 1000 system (Thermo Fisher). Mass analysis was performed in positive ion mode with high collision dissociation energy. The scan range was 400–2,000 m/z with full MS resolution of 70,000 and 200–2,000 m/z with MS2 resolution of 17,500. The first mass was fixed at 115 m/z, and 445.12003 m/z (polysiloxane ion mass) was used for real-time mass calibration. Mass spectral data obtained in this study have been deposited in the ProteomeXchange (Vizcaino et al. 2014).

Peptide identification, relative quantification, and bioinformatics analysis.

Peptide sequences were identified based on the obtained MS/MS data using the ProteinPilot (v4.5) software (Applied Biosystems) against specified non-redundant databases (combined Uniprot, http://www.uniprot.org/uniprot/?query=aspergillus+flavus&sort=score; NCBI, https://www.ncbi.nlm.nih.gov/gquery/?term=aspergillus+flavus). Data normalization was performed using default settings along with differential expression and p-value estimation using ProteinPilot. Identified proteins were considered to be differentially expressed if it exhibited a fold change ≥ 1.2 or ≤ 0.8 with a p-value ≤ 0.05 in at least one isolate, and was detected in at least two experimental replications.

Functional classification and subcellular localization of the detected and differentially expressed proteins was performed using the Gene Ontology (GO) enrichment tool in FungiDB (Stajich et al. 2012). Functional and localization term consolidation was then performed using REVIGO (Supek et al. 2011). Visualization of GO biological process terms for each isolate was performed based on REVIGO outputs using R-studio and R (v3.3.0). Venn diagrams of differentially expressed proteins were created using Venny (v2.1). Heatmaps of expression

patterns, hierarchical clustering analysis, and principal components analysis (PCA) were performed using the Multi-experiment Viewer (MeV; v4.9.0) (Howe et al. 2010). Biological pathway enrichment analysis was performed using the metabolic pathway analysis tool in FungiDB using the Kyoto Encyclopedia of Genes and Genomes (KEGG) (Kanehisa and Goto, 2000). Finally, predicted protein-protein interactions were examined using STRING (v10.0) (Szklarczyk et al. 2015).

Results

Proteome profiling of *A. flavus* isolate responses to oxidative stress

In order to examine the differences in the responses of highly toxigenic, moderately toxigenic, and atoxigenic isolates of *A. flavus* to oxidative stress as encountered in the field during drought stress and the colonization of stressed host plant tissues, a comparative proteomic analysis was performed on select isolates following treatment with various levels of H_2O_2. We used an iTRAQ proteomics approach to identify differential proteins in response to stress. This study was performed with three biological replicates, each as an independent iTRAQ set (Figure 8.1A). Approximately 360,000 MS/MS spectra were generated for each biological replicate. Following filtration using a global false discovery rate (FDR) of 1%, 280,365 MS spectra were obtained (Table S8.1). For each replicate an average of 18,364 distinct peptides were identified using the ProteinPilot software coupled with both the NCBI and Uniprot databases, resulted in the identification of an average of 1,900 proteins in each replicate at a 1% global FDR. Of these 1,900 proteins, 799 (42.05%) were expressed in all three biological replicates and 1,173 (61.74%) were present in at least two biological replicates. These 1,173 proteins were then further examined in subsequent analyses.

Gene ontology (GO) enrichment analyses were then performed to provide an overview of cell components and pathways examined by the experiment. Examination of subcellular localization enrichment for the detected proteins showed that cytosolic, ribosomal, and organelle-associated proteins were enriched (Figure 8.1B). Biological functional annotation of the detected proteins was also consistent with the localization analysis with primary metabolism, protein metabolism, redox homeostasis, and asexual reproductive process being among the most enriched stress-related GO terms observed (Figure 8.1C).

Differential expression analysis of the detected proteins

Following protein identification and annotation, differential expression analysis was performed to examine the responses of each isolate to increasing levels of oxidative stress. Proteins were considered to be differentially expressed if they exhibited a fold change ≥ 1.2 or ≤ 0.8 with a *p*-value ≤ 0.05 (Figure 8.2A). The AF13 isolate, which was previously found to tolerate higher levels of oxidative stress and produce high levels of aflatoxin (Fountain et al. 2015b), exhibited 46 and 17 differentially expressed proteins (DEPs) under 10mM and 25mM H_2O_2 treatments, respectively, compared to 0mM H_2O_2 control (Table 8.1). The NRRL3357 isolate, which tolerates moderate levels of oxidative stress and produces moderately high levels of aflatoxin (Fountain et al. 2015b), exhibited 29 and 220 DEPs under the 10mM and 20mM H_2O_2 treatments, respectively (Table 8.1). Lastly, the K54A isolate, which previously tolerated the least amount of oxidative stress of isolates surveyed and is atoxigenic (Fountain et al. 2015b), exhibited 23 DEPs comparing between the control and the 10mM H_2O_2 treatment (Table 8.1). A list of the DEPs found within each isolate and treatment can be found in Table S8.2.

Comparison of the DEPs across isolates showed that the three isolates examined in this study exhibit highly distinct responses to oxidative stress with few commonly regulated DEPs being detected between them (Figure 8.2B). These distinctive responses can also be seen in the principal components analysis (PCA; Figure 8.2C), which showed clear differences in the overall expression profiles for the isolates in all treatments. Of the isolates, the NRRL3357 and K54A isolates exhibited more closely related responses to stress with numerically more commonly regulated proteins and closer relationships indicated in the PCA (Figure 8.2B and 8.2C). These distinct responses can also be observed in the hierarchical clustering analysis of protein expression between isolates (Figure 8.3). Here, a clear segregation of expression patterns can be observed, such as when comparing the responses of AF13 and NRRL3357. For example, NRRL3357 exhibited greater levels of variation in protein expression comparing the control and 20mM H_2O_2 treatment while having more commonality with K54A in the 10mM H_2O_2 treatment.

Functional classification of the differentially expressed proteins

The DEPs identified in response to increasing oxidative stress in each isolate were used for functional enrichment analyses based on biological process GO. The functional classification of the DEPs was done using FungiDB, a data repository for sequence and protein information for numerous plant and animal pathogenic fungi and fungal-like organisms (Stajich et al. 2012), and redundant GO terms were removed using REVIGO (Supek et al. 2011). The detected functional annotations for each isolate were consistent with oxidative stress responses.

AF13 showed enrichment for terms including carbohydrate and tricarboxylic acid cycle components, responses to oxidative stress, protein folding and metabolism, ATP biosynthesis,

and nitric oxide (NO) biosynthesis with increasing levels of H_2O_2 stress (Figure 8.4). NRRL3357 showed a greater variety of enriched terms than observed AF13. This isolate's terms included those found in AF13 and others such as co-enzyme metabolism, NADPH metabolism, and pyrimidine metabolism under increasing levels of stress (Figure 8.4). The DEPs observed in K54A in response to stress included several proteins lacking functional annotations and were, therefore, lacking in GO enrichment compared to the other isolates. The terms found in K54A included those involved in responses to oxidative stress, ATP biosynthesis, and NO biosynthesis (Figure 8.4). A complete list of the enriched GO terms for biological processes found in the isolates can be found in Table S8.3.

Sub-cellular localization of the differentially expressed proteins

In addition to biological processes, the cellular localization GO terms for the detected DEPS in each isolate were examined for enrichment in response to stress. Consistent with the protein extraction methodology and the localization analysis described for all 1,173 proteins, the DEPs tended to localize to the cytoplasm and membranes including the plasma membrane and organelle membranes. A complete list of the enriched GO terms for cellular localization found in the isolates can be found in Table S8.4.

For AF13, DEPs under moderate stress tended to localize in the cytoplasm, cell wall, cellular and mating projections, proteasome complexes, and telomeres. Conversely, under higher levels of stress, AF13 DEPs localized more to cytoplasmic and mitochondrial components, particularly to cytochrome complexes and electron transport complexes involved in ATP biosynthesis. For NRRL3357, DEPs under moderate stress localized to the cytoplasm and to membrane-associated components including vesicular transport components, the endoplasmic

reticulum, and the Golgi apparatus. Under higher levels of stress, other additional enriched locations including mitochondrial ATP synthase complexes and TCA cycle components, and ribosomes were also detected for the DEPs. For K54A, similar to NRRL3357, DEPs detected under stress tended to localize the cytoplasm, vesicular transport components, ribosomes, the Golgi apparatus, and the mitochondria. Overall for all isolates examined, it is clear that cytoplasm, mitochondria, and vesicle localized responses comprise the bulk of the responses of these isolates to H_2O_2.

KEGG pathway analysis of the differentially expressed proteins.

In addition to GO annotation, FungiDB was used to examine the pathway annotations for each DEP based on the Kyoto Encyclopedia of Genes and Genomes (KEGG) database (Kanehisa and Goto, 2000) followed by enrichment analysis. For AF13, under moderate levels of stress, several carbohydrate metabolism-related pathways were identified including starch and sucrose metabolism, glycolysis, and pyruvate metabolism (Figure 8.5). In addition, carbon fixation and N-glycan biosynthesis pathways were found to be represented by the DEPs. Under high stress, AF13 DEPs were enriched for pathways including glycolysis, amino and nucleotide sugar metabolism, and oxidative phosphorylation. For NRRL3357 under moderate stress, enriched pathways included carbohydrate metabolism components such as glycolysis, pyruvate metabolism and the TCA cycle (Figure 8.5). Amino acid metabolism, benzoate degradation, and fatty acid degradation pathways were also enriched. Under high stress, in addition to those observed under moderate stress, pathways such as the pentose phosphate pathway, N-glycan biosynthesis, and glutathione metabolism were enriched. One component of the aflatoxin biosynthetic pathway, versicolorin A dehydrogenase/ketoreductase (ver-1) was increased (Table

S8.2). While other aflatoxin biosynthesis proteins including polyketide synthase A (pksA), versicolorin B synthase (vbs), and dimethylsterigmatosystin 6-O-methyltransferase (omtB) were detected in the analysis, only ver-1 was found to be differentially expressed in NRRL3357 under high stress conditions. Conversely, one cyclopiazonic acid (CPA) biosynthetic component, a dimethylallyl tryptophan synthase (dmaT; AFLA_139480) was decreased in NRRL3357 but increased in AF13 (Table S8.2). For K54A, under stress the pathways enriched included arginine and proline metabolism, limonene and pinene degradation, glycolysis (Figure 8.5), and oxidative phosphorylation. Overall, for all of the isolates respiration-related pathways such as glycolysis, the TCA cycle, and oxidative phosphorylation along with amino acid and complex macromolecular catabolism comprise a bulk of the pathways differentially regulated in the isolates treated with H_2O_2 (Table 8.2). A complete list of the enriched KEGG biological pathways found in the isolates can be found in Table S8.5.

Correlation analysis between the transcriptome and proteome data

Previously, we examined the transcriptional responses of six field isolates of *A. flavus* ranging from highly toxigenic to atoxigenic commercial biological control isolates to increasing levels of oxidative stress in both aflatoxin production conducive and non-conducive media (Fountain et al. 2016a, 2016b). Three of these isolates were used in the present study to examine their protein-level responses to oxidative stress under the same experimental conditions. Using the available transcriptome data, a correlation analysis was performed between expression levels observed in both studies to examine for possible post-transcriptional regulation of oxidative stress responses.

When comparing expression levels between the experiments, it became clear that genes exhibiting higher overall levels of expression in each isolate were more likely to be detected in

the proteomics analysis (Figure 8.6A-C). Pearson correlation between significantly differentially expressed genes (DEGs) and their corresponding proteins were found to be low (r = 0.3075) (Figure 8.6D). Similarly, correlating the expression observed for significant DEPs to their corresponding transcript expression in the previous transcriptome study resulted in a lower correlation (r = 0.1114) (Figure 8.6E). Despite a low degree of correlation between the expression levels in the two experiments, the two datasets did show consistency in terms of the trend of changes, with only 24.9% of transcripts showing opposite patterns compared to the DEPs (Figure 8.6F).

Examining the level of correlation between the two experiments at the pathway level found that the degree of correlation varied by pathway and isolate. Some pathways when examining proteins in all isolates and treatments found higher degrees of correlation between the RNA and protein level expression patterns. For example, glutathione metabolism and the pentose phosphate pathway exhibited higher levels of correlation than that observed for the entire dataset (Figure 8.6E, Table 8.2). Conversely, for pathways such as purine metabolism and alanine, aspartate, and glutamate metabolism, negative correlations between the datasets was observed (Table 8.2). However, examining each pathway correlation by isolate did reveal some variation in the correlation observed. The isolates which expressed greater numbers of DEPs, NRRL3357 and K54A, tended to exhibit higher correlations for each pathway compared to AF13. For example, the glutathione metabolism pathway components in AF13 exhibited a correlation of r = 0.0823 while NRRL3357 and K54A exhibited a correlation of r = 0.7172 and r = 0.4914, respectively (Figure S8.2). Overall, the higher levels of correlation observed in these pathways may be indicative of their ongoing active expression and importance in oxidative stress responses.

Protein-protein interaction analysis

Given that proteins function through interacting with other proteins and molecules, understanding the potential interactions occurring between DEPs is an important aspect to consider. To examine the interactions between DEPs detected in response to oxidative stress in the examined isolates, these proteins were searched for potential physical, co-expression, and co-occurrence types of interactions in the STRING database (Szklarczyk et al. 2015). For AF13, branches of the interaction network were defined by pathway and molecular function including carbohydrate metabolism and antioxidant enzymes (Figure S8.3A). For NRRL3357, a more extensive interaction network was obtained than in the other isolates with k-means clustering analysis dividing the network into several key interacting pathway components including antioxidant enzymes, carbohydrate metabolism enzymes, pentose phosphate pathway, oxidative phosphorylation, and translation regulation (Figure 8.7 and S8.3B). For K54A, a number of smaller interaction groups were identified and consisted of protein folding, translation, vesicle trafficking, and carbohydrate metabolism pathway components (Figure S8.3C). Overall, several hub proteins exhibiting physical and co-expression interactions with multiple proteins in diverse pathways were identified in all three isolates. These included protein folding and degradation enzymes such as heat shock proteins (e.g. hsp70 and hsp90), alcohol dehydrogenase (adh1), malate dehydrogenase, G-protein complex proteins (e.g. cpcB), and ATP synthase (α subunit). Additional DEPs not exhibiting interactions with other proteins found in this analysis also likely play indirect roles in oxidative stress responses in isolates of *A. flavus*. A list of all abbreviations and protein names along with the specific node interactions can be found in Table S8.6.

Discussion

The production of aflatoxin by *A. flavus* and related species of fungi is regulated in concert with other secondary metabolites, developmental processes, and stress-responsive enzymes in response to environmental stress (Brakhage, 2013; Roze et al. 2013). Specifically, oxidative stress has been shown to be a pre-requisite and stimulator of aflatoxin production (Jayashree and Subramanyam, 2000; Narasaiah et al. 2006). This is of particular interest given the observation that drought stress results in compromised host resistance to aflatoxin contamination, and that drought stress results in the accumulation of ROS in host plant tissues (Guo et al. 2008; Yang et al. 2015, 2016). Previously, we have explored differences in oxidative stress responses between field isolates of *A. flavus* with varying degrees of aflatoxin production ranging from highly toxigenic isolates to atoxigenic commercial biological controls in culture and at the transcriptome levels (Fountain et al. 2015b, 2016a, 2016b). These studies suggested that aflatoxin production along with additional secondary metabolites such as aflatrem and kojic acid, antioxidant enzyme expression, and carbohydrate metabolism may play significant roles in *A. flavus* oxidative stress responses. In order to further explore these responses at the protein and enzymatic level, and to examine for the possibility of post-transcriptional regulation of oxidative stress responses, we examined the proteomes of select isolates of *A. flavus* to increasing levels of H_2O_2-derived oxidative stress in an aflatoxin production-conducive medium.

Previously, it was found that isolates which produce higher levels of aflatoxin tended to exhibit fewer significant DEGs in response to increasing levels of oxidative stress compared to less toxigenic or atoxigenic isolates (Fountain et al. 2016a, 2016b). At the protein level, the three isolates examined showed similar numbers of DEPs when comparing the control and 10mM H_2O_2 moderate stress treatment (Table 8.1). However, when comparing the numbers of DEPs at

the higher level of stress, 20 or 25mM H_2O_2, the moderately high aflatoxin producing isolate, NRRL3357, exhibited a much greater number of DEPs compares to the high aflatoxin producing isolate, AF13 (Table 8.1). This suggests that the ability to produce higher levels of aflatoxin tends to correlate with greater levels of stress tolerance resulting in less vigorous overall responses to oxidative stress. However, the lack of correlation under moderate stress may also be indicative of responses which occur at time points not examined in this study.

The lack of a similar trend of increasing numbers of DEPs under moderate stress with decreasing stress tolerance as seen for DEGs previously (Fountain et al. 2016a) may also be indicative of both experimental variation and in possible post-transcriptional regulation of responses to stress. Post-transcriptional modifications and signaling play a significant role in the regulation of secondary metabolite production and reproductive development in *Aspergillus spp.* and other fungi. For example, phospho-relay signaling networks including MAP kinase components such as AnFus3, AnSte7, Anste11, and AnSte50 in *A. nidulans* have been shown to regulate both conidiation and sterigmatocystin production (Bayram et al. 2012). Other kinase signaling components such as G-protein-mediated regulation of aflR through G-protein/cAMP/protein kinase A (pkaA) have also been shown to regulate development and mycotoxin production in *Aspergillus spp*. including *A. nidulans* and *A. parasiticus* (Roze et al. 2004; Shimizu et al. 2001, 2003). Similar cAMP protein kinase regulators were also found to be differentially expressed here in NRRL3357 under higher levels of oxidative stress (Table S8.2). Another indication of possible post-transcriptional regulation of protein expression is the low degree of correlation between the transcriptome and proteome data observed here (Figure 8.6). Bai et al. (2015) observed a similar low degree of correlation ($r = 0.14$) between transcript and protein expression when examining heat stress responses in *A. flavus* which was interpreted as

being due to post-transcriptional regulation. While these low degrees of correlation may indeed be due to post-transcription modification and regulation of translation, it is also likely that inherent experimental error due to differences in RNA and protein turnover and biological variation between experimental replicates contribute to such weak correlations (Vogel and Marcotte, 2012). Therefore, additional studies will be required to explore the role of post-transcriptional regulation in *A. flavus* oxidative stress responses.

Comparison of the detected DEPs for each isolate under increasing levels of oxidative stress revealed distinctive, isolate-specific responses with few commonly regulated proteins detected between isolates (Figure 8.2B). However, NRRL3357 and K54A did exhibit more commonality than either isolate showed with AF13, suggesting a correlation of stress responses with overall oxidative stress tolerance and aflatoxin production capability. The particular DEPs exhibited by the isolates also points to distinct overall strategies with implications for host resistance and interactions with other soilborne microbes. For example, AF13 tended to exhibit increased expression of lytic enzymes such as α-amylase, chitinase, β-glucosidase, glucanase, and α-mannosidase, while NRRL3357 showed decreased expression of the same enzymes (Table S8.2). These enzymes have been shown to be involved in the colonization of host plant tissues with their inhibitors, such as the α-amylase-inhibiting 14-kDa trypsin inhibitor, being found to accumulate in resistant maize kernel tissues (Brown et al. 2001; Chen et al. 1999, 2015; Mellon et al. 2007). Increased lytic enzyme expression suggests that AF13 may more readily colonize host tissues with higher ROS content, particularly under drought stress (Yang et al. 2015, 2016). Increased hydrolytic enzyme expression has also been found to provide benefits for fungi in competition with other microbes in soil and plant environments, such as in the case of *Tricoderma spp*. biological controls (Benitez et al. 2004). Therefore, increased isolate potency in

terms of competitive and host colonizing capability through enhanced lytic enzyme expression may be correlated with overall oxidative stress tolerance and warrants further investigation.

Differences in the overall strategies employed by the examined isolates could also be seen with regard to primary metabolism. The moderately toxigenic and atoxigenic isolates tended to show greater degrees of regulation in carbohydrate metabolism and mitochondrial oxidative phosphorylation (Figure 8.4 and 8.5, Table S8.2). Inhibition of oxidative phosphorylation by the application of exogenous compounds such as resveratrol has been shown to compromise fungal oxidative stress tolerance by altering mitochondrial respiration (Madrigal-Perez and Ramos-Gomez, 2016). For carbohydrate metabolism, the active production of glycolysis and TCA cycle intermediates provide the basic components for the biosynthesis of macromolecules, which could be useful in the repair of cellular components with oxidative damage. In addition to glycolysis and the TCA cycle, the pentose phosphate pathway was also stimulated in response to stress in both toxigenic isolates (Figure 8.5). This pathway has been shown to be a source of reduced co-factors such as NADPH, which are utilized in the glutathione pathway for non-specific antioxidant activity (Mittler, 2002; Stincone et al. 2015). Interestingly, the moderately toxigenic isolate showed decreased NADPH-generating enzymes in the pentose phosphate pathway which may contribute to reduced stress tolerance compared to the highly toxigenic isolate. Alternatively, this may relate to a reduction in demand for reduced coenzymes due to stress alleviation already provided by the glutathione pathway or other mechanisms at the timepoint examined in the study.

The differential expression of antioxidant enzyme systems in response to increasing stress may also provide insight into the specific ROS detrimental to these fungi, and to which they are responding. While relatively stable, H_2O_2 is also a weaker ROS resulting in a lesser

degree of oxidative stress compared to other species such as superoxide ($O_2^{\cdot -}$), hydroperoxyl (HO_2.), and hydroxyl ($OH^{\cdot -}$) radicals, which while possessing significantly shorter half-lives can result in significantly greater damage to cellular components (Das and Roychoudhury, 2014; Heller and Tudzynski, 2011). Previous studies have explored the effects of specific ROS on aflatoxin production and isolate development in *A. flavus*. For example, Grintzalis et al. (2014) treated *A. flavus* with numerous broad and specific ROS and antioxidant enzyme inhibitors to identify which ROS would stimulate aflatoxin and/or sclerotial development. They found that H_2O_2 specifically regulates sclerotia development, and that peroxidized lipids, superoxide, hydroxyl, and thiol radicals tended to have a greater role in aflatoxin production regulation.

Here, we observed that non-specific antioxidant mechanisms such as glutathione metabolism and heat shock proteins tended to be the main ROS scavenging systems increased in response to increasing stress (Table S8.2, Figure 8.7), while catalase was found to be decreased in NRRL3357 under increasing stress (Figure 8.7). This suggests that other ROS such as the hydroxyl radical are more likely to be the source of continuing stress the isolates are responding to. These toxic ROS can be generated non-enzymatically through iron cation-mediated interconversions such as the Fenton reactions (Fenton, 1894). This coupled with the observations that biosynthetic mechanisms for iron chelating compounds such as kojic acid (Fountain et al. 2016a, 2016b; Terabayashi et al. 2010) and CPA (Chang et al. 2009; Yu et al. 2011) were regulated in this system (Table S8.2, Fountain et al. 2016a, 2016b) suggests that ROS such as $OH^{\cdot -}$ may be one of the main causes of oxidative damage in this experiment.

These ROS can also interact with other compounds to form other damaging radicals including reactive nitrogen species (RNS) such as nitric oxide (NO). These compounds have been found to influence isolate development through RNS bursts. Specifically, NO bursts have

been found to be involved in the initiation of both conidiation and sclerotia formation in *Aspergillus spp*. and other fungi (Arasimowicz-Jelonek and Floryszak-Wieczorek, 2016). This burst of NO is countered by increase in detoxifying enzyme expression, specifically a series of flavohemoproteins, to prevent excess nitrosative stress (Baidya et al. 2011). Here, AF13 showed increases in nitric oxide synthase (NOS) and the sclerotia component protein sspA (Li and Rollins, 2009) accompanied by a decrease in flavohemoprotein expression while NRRL3357 showed the opposite pattern of expression (Table S8.2). This suggests, as was previously hypothesized (Fountain et al. 2016b), that isolate development rates may be influenced by oxidative stress. This may also contribute to the different responses observed between the highly and moderately toxigenic isolates at the time point examined in this study. However, such differences in growth rates may also be reflective of different growth patterns observed for these isolates. In addition, the patterns of NOS and flavohemoprotein expression may be a function of mycotoxin production regulation in this system, and for developmental regulation (Baidya et al. 2011). Further studies into developmental effects on oxidative stress responses may provide further insights into the dynamics of this response and potential impacts on interactions with other organisms.

Isolate secondary metabolism components were also found to be differentially expressed in response to increasing stress. However, very few such proteins were detected in this experiment likely due to either limitations of the protein isolation or iTRAQ protocols employed (Wu et al. 2006), or due to time dependent regulation of expression given that the majority of aflatoxin production occurs 2 – 6 days in stationary culture (Davis et al. 1966). Previously, we observed that the moderately toxigenic isolate, NRRL3357 showed significant increases in aflatoxin gene expression under high levels of oxidative stress (Fountain et al. 2016a, 2016b).

This corresponds to the observed increase in ver-1 protein expression observed here in NRRL3357 (Table S8.1). It has been proposed that the production of secondary metabolites such as aflatoxin may provide supplemental antioxidant protection to *A. flavus* and other Aspergilli either through the fixation of ROS into toxin molecules, or through the stimulation of antioxidant enzyme expression through localized ROS bursts (Fountain et al. 2016a; Narasaiah et al. 2006; Roze et al 2015). The continued expression of ver-1 in NRRL3357 may, therefore, be indicative of ongoing aflatoxin production which may provide some antioxidant benefits.

The regulation of aflatoxin biosynthetic components has serious implications for host resistance. Under drought stress, it has been shown that drought sensitive, aflatoxin contamination susceptible varieties of maize accumulate higher levels of ROS and RNS under drought compared to drought tolerant, aflatoxin resistant varieties (Yang et al. 2015, 2016). Given this correlation, the observed stimulation of aflatoxin production by ROS (Fountain et al. 2015b; Jayashree and Subramanyam, 2000; Narasaiah et al. 2006), the role of RNS in fungal development and mycotoxin production regulation (Arasimowicz-Jelonek and Floryszak-Wieczorek, 2016; Baidya et al. 2011; Marcos et al. 2016), and the regulation of aflatoxin production by nitrogen availability through transcription factors such as AreA (Chang et al. 2000; Tudzynski, 2014), the responses of *A. flavus* to host-derived stress may provide insights into mechanisms to enhance host resistance. Current molecular breeding practices have been successful in developing both maize and peanut lines with degrees of aflatoxin resistance and drought tolerance (Fountain et al. 2015a). While progress has been made, additional measures will be necessary to further enhance available resistance to aflatoxin contamination. The isolate responses observed here show the importance of the ability of the fungus to colonize host tissues, acquire nutrition, and prevent and remediate oxidative damage for environmental stress

tolerance. Utilizing novel advances in biotechnology such as transgenic and genome editing approaches, these components may be targeted by enhancing host expression of lytic enzyme inhibiters and antioxidant enzymes, or through the use of novel RNA interference approaches such as host-induced gene silencing (HIGS) of aflatoxin biosynthetic genes (Thakare et al. 2017). These approaches provide a future direction for enhancing both drought tolerance and aflatoxin contamination resistance in both maize and peanut. In addition, these same fungal pathways also provide biomarkers for the selection of novel atoxigenic biological control isolates among native populations of *A. flavus* or *A. parasiticus* for use in aflatoxin remediation.

Acknowledgements

We thank Ning Zhu, Billy Wilson, and Hui Wang for technical assistance in the laboratory. This work is partially supported by the U.S. Department of Agriculture Agricultural Research Service (USDA-ARS), the Georgia Agricultural Commodity Commission for Corn, the Georgia Peanut Commission, the Peanut Foundation, and AMCOE (Aflatoxin Mitigation Center of Excellence, Chesterfield, MO, USA). This work has also been undertaken as part of the CGIAR Research Program on Grain Legumes and the USAID University Linkages Program between USDA-ARS and ICRISAT. ICRISAT is a member of CGIAR Consortium. Mention of trade names or commercial products in this publication is solely for the purpose of providing specific information and does not imply recommendation or endorsement by the USDA. The USDA is an equal opportunity provider and employer.

Supplemental Information

Supplemental datasets, figures, and tables can be found in Appendix C.

References

1. Abbas, H. K., Weaver, M. A., Horn, B. W., Carbone, I., Monacell, J. T., & Shier, W. T. (2011). Selection of *Aspergillus flavus* isolates for biological control of aflatoxins in corn. Toxin Rev. 30(2-3), 59-70.
2. Amaike, S. & Keller, N. P. *Aspergillus flavus*. *Ann. Rev. Phytopathol*. 49, 107-133 (2011).
3. Amare, M. G., & Keller, N. P. (2014). Molecular mechanisms of *Aspergillus flavus* secondary metabolism and development. *Fungal Genetics and Biology*, *66*, 11-18.
4. Arasimowicz-Jelonek, M., & Floryszak-Wieczorek, J. (2016). Nitric Oxide in the Offensive Strategy of Fungal and Oomycete Plant Pathogens. *Frontiers in plant science*, *7*.
5. Azziz-Baumgartner, E., Lindblade, K., Gieseker, K., Rogers, H. S., Kieszak, S., Njapau, H., ... & Rubin, C. (2005). Case-control study of an acute aflatoxicosis outbreak, Kenya, 2004. Environ. Health Perspect. 113, 1779-1783.
6. Bai, Y., Wang, S., Zhong, H., Yang, Q., Zhang, F., Zhuang, Z., ... & Wang, S. (2015). Integrative analyses reveal transcriptome-proteome correlation in biological pathways and secondary metabolism clusters in *A. flavus* in response to temperature. *Scientific reports*, *5*, 14582.
7. Baidya, S., Cary, J. W., Grayburn, W. S., & Calvo, A. M. (2011). Role of nitric oxide and flavohemoglobin homolog genes in *Aspergillus nidulans* sexual development and mycotoxin production. *Applied and environmental microbiology*, *77*(15), 5524-5528.
8. Baxter, A., Mittler, R., & Suzuki, N. (2014). ROS as key players in plant stress signalling. J. Exp. Bot. 65(5), 1229-1240.

9. Bayram, Ö., Bayram, Ö. S., Ahmed, Y. L., Maruyama, J. I., Valerius, O., Rizzoli, S. O., ... & Braus, G. H. (2012). The *Aspergillus nidulans* MAPK module AnSte11-Ste50-Ste7-Fus3 controls development and secondary metabolism. *PLoS Genet*, *8*(7), e1002816.
10. Benítez, T., Rincón, A. M., Limón, M. C., & Codón, A. C. (2004). Biocontrol mechanisms of Trichoderma strains. *International microbiology*, *7*(4), 249-260.
11. Brakhage, A. A. (2013). Regulation of fungal secondary metabolism. *Nature Reviews Microbiology*, *11*(1), 21-32.
12. Brown, R. L., Chen, Z. Y., Cleveland, T. E., Cotty, P. J., & Cary, J. W. (2001). Variation in in vitro α-amylase and protease activity is related to the virulence of *Aspergillus flavus* isolates. *Journal of food protection*, *64*(3), 401-404.
13. Chang, P. K., Ehrlich, K. C., & Fujii, I. (2009). Cyclopiazonic acid biosynthesis of *Aspergillus flavus* and *Aspergillus oryzae*. *Toxins*, *1*(2), 74-99.
14. Chang, P. K., Yu, J., Bhatnagar, D., & Cleveland, T. E. (2000). Characterization of the *Aspergillus parasiticus* major nitrogen regulatory gene, areA. *Biochimica et Biophysica Acta (BBA)-Gene Structure and Expression*, *1491*(1), 263-266.
15. Chen, Z. Y., Brown, R. L., Russin, J. S., Lax, A. R., & Cleveland, T. E. (1999). A corn trypsin inhibitor with antifungal activity inhibits *Aspergillus flavus* α-amylase. *Phytopathology*, *89*(10), 902-907.
16. Chen, Z. Y., Rajasekaran, K., Brown, R. L., Sayler, R. J., & Bhatnagar, D. (2015). Discovery and confirmation of genes/proteins associated with maize aflatoxin resistance. *World Mycotoxin Journal*, *8*(2), 211-224.
17. Chen, Z. Y., Warburton, M. L., Hawkins, L., Wei, Q., Raruang, Y., Brown, R. L., ... & Bhatnagar, D. (2016). Production of the 14 kDa trypsin inhibitor protein is important for

maize resistance against *Aspergillus flavus* infection/aflatoxin accumulation. World Mycotoxin J. 9(2), 215-228.

18. Cotty, P. J., & Bayman, P. (1993). Competitive exclusion of a toxigenic strain of *Aspergillus flavus* by an atoxigenic strain. Phytopathol. 83(12), 1283-1287.
19. Cruz de Carvalho, M. H. (2008). Drought stress and reactive oxygen species: production, scavenging and signaling. Plant signaling & behavior, 3(3), 156-165.
20. Das, K., & Roychoudhury, A. (2014). Reactive oxygen species (ROS) and response of antioxidants as ROS-scavengers during environmental stress in plants. *Frontiers in Environmental Science*, *2*, 53.
21. Davis, N. D., Diener, U. L., & Eldridge, D. W. (1966). Production of aflatoxins B1 and G1 by *Aspergillus flavus* in a semisynthetic medium. *Applied microbiology*, *14*(3), 378-380.
22. Dorner, J. W., & Lamb, M. C. (2006). Development and commercial use of afla-guard, an aflatoxin biocontrol agent. Mycotoxin Res. 22(1), 33-38.
23. Fabbri, A. A., Fanelli, C., Panfili, G., Passi, S., & Fasella, P. (1983). Lipoperoxidation and aflatoxin biosynthesis by *Aspergillus parasiticus* and *A. flavus*. Microbiology, 129(11), 3447-3452.
24. Fenton, H. J. H. (1894). LXXIII.—Oxidation of tartaric acid in presence of iron. *Journal of the Chemical Society, Transactions*, *65*, 899-910.
25. Fountain, J. C., Bajaj, P., Nayak, S. N., Yang, L., Pandey, M. K., Kumar, V., ... & Varshney, R. K. (2016b). Responses of *Aspergillus flavus* to Oxidative Stress Are Related to Fungal Development Regulator, Antioxidant Enzyme, and Secondary Metabolite Biosynthetic Gene Expression. *Frontiers in Microbiology*, *7*.

26. Fountain, J. C., Bajaj, P., Pandey, M., Nayak, S. N., Yang, L., Kumar, V., ... & Lee, R. D. (2016a). Oxidative stress and carbon metabolism influence *Aspergillus flavus* transcriptome composition and secondary metabolite production. *Scientific Reports*, *6*.

27. Fountain, J. C., Khera, P., Yang, L., Nayak, S. N., Scully, B. T., Lee, R. D., ... & Guo, B. (2015a). Resistance to *Aspergillus flavus* in maize and peanut: Molecular biology, breeding, environmental stress, and future perspectives. The Crop Journal, 3(3), 229-237.

28. Fountain, J. C., Scully, B. T., Chen, Z. Y., Gold, S. E., Glenn, A. E., Abbas, H. K., ... & Guo, B. (2015b). Effects of hydrogen peroxide on different toxigenic and atoxigenic isolates of *Aspergillus flavus*. *Toxins*, *7*(8), 2985-2999.

29. Fountain, J. C., Scully, B. T., Ni, X., Kemerait, R. C., Lee, R. D., Chen, Z. Y., & Guo, B. (2014). Environmental influences on maize-*Aspergillus flavus* interactions and aflatoxin production. Front. Microbiol. 5.

30. Gao, X., Brodhagen, M., Isakeit, T., Brown, S. H., Göbel, C., Betran, J., ... & Kolomiets, M. V. (2009). Inactivation of the lipoxygenase ZmLOX3 increases susceptibility of maize to *Aspergillus spp*. Molecular plant-microbe interactions, 22(2), 222-231.

31. Grintzalis, K., Vernardis, S. I., Klapa, M. I., & Georgiou, C. D. (2014). Role of oxidative stress in sclerotial differentiation and aflatoxin B1 biosynthesis in *Aspergillus flavus*. *Applied and environmental microbiology*, *80*(18), 5561-5571.

32. Guo, B., Chen, Z. Y., Lee, R. D., & Scully, B. T. (2008). Drought stress and preharvest aflatoxin contamination in agricultural commodity: genetics, genomics and proteomics. J. Int. Plant Biol. 50(10), 1281-1291.

33. Heller, J., & Tudzynski, P. (2011). Reactive oxygen species in phytopathogenic fungi: signaling, development, and disease. *Annual review of phytopathology*, *49*, 369-390.

34. Hong, S. Y., Roze, L. V., & Linz, J. E. (2013). Oxidative stress-related transcription factors in the regulation of secondary metabolism. *Toxins*, *5*(4), 683-702.

35. Howe, E., Holton, K., Nair, S., Schlauch, D., Sinha, R., & Quackenbush, J. (2010). Mev: multiexperiment viewer. In *Biomedical informatics for cancer research* (pp. 267-277). Springer US.

36. Hurkman, W. J., & Tanaka, C. K. (1986). Solubilization of plant membrane proteins for analysis by two-dimensional gel electrophoresis. *Plant physiology*, *81*(3), 802-806.

37. Jayashree, T., & Subramanyam, C. (2000). Oxidative stress as a prerequisite for aflatoxin production by *Aspergillus parasiticus*. *Free Radical Biology and Medicine*, *29*(10), 981-985.

38. Kanehisa, M., & Goto, S. (2000). KEGG: kyoto encyclopedia of genes and genomes. *Nucleic acids research*, *28*(1), 27-30.

39. Kelley, R. Y., Williams, W. P., Mylroie, J. E., Boykin, D. L., Harper, J. W., Windham, G. L., ... & Shan, X. (2012). Identification of maize genes associated with host plant resistance or susceptibility to *Aspergillus flavus* infection and aflatoxin accumulation. PLoS One, 7(5), e36892.

40. Li, M., & Rollins, J. A. (2009). The development-specific protein (Ssp1) from Sclerotinia sclerotiorum is encoded by a novel gene expressed exclusively in sclerotium tissues. *Mycologia*, *101*(1), 34-43.

41. Madrigal-Perez, L. A., & Ramos-Gomez, M. (2016). Resveratrol Inhibition of Cellular Respiration: New Paradigm for an Old Mechanism. *International journal of molecular sciences*, *17*(3), 368.

42. Magan, N., & Aldred, D. (2007). Post-harvest control strategies: minimizing mycotoxins in the food chain. Int. J. Food Microbiol. 119(1), 131-139.

43. Marcos, A. T., Ramos, M. S., Marcos, J. F., Carmona, L., Strauss, J., & Cánovas, D. (2016). Nitric oxide synthesis by nitrate reductase is regulated during development in Aspergillus. *Molecular microbiology*, *99*(1), 15-33.

44. McDonald, T., Brown, D., Keller, N. P., & Hammond, T. M. (2005). RNA silencing of mycotoxin production in Aspergillus and Fusarium species. *Molecular plant-microbe interactions*, *18*(6), 539-545.

45. Mellon, J. E., Cotty, P. J., & Dowd, M. K. (2007). *Aspergillus flavus* hydrolases: their roles in pathogenesis and substrate utilization. *Applied microbiology and biotechnology*, *77*(3), 497-504.

46. Mittler, R. (2002). Oxidative stress, antioxidants and stress tolerance. *Trends in plant science*, *7*(9), 405-410.

47. Narasaiah, K. V., Sashidhar, R. B., & Subramanyam, C. (2006). Biochemical analysis of oxidative stress in the production of aflatoxin and its precursor intermediates. Mycopathologia, 162(3), 179-189.

48. Payne, G. A., & Brown, M. P. (1998). Genetics and physiology of aflatoxin biosynthesis. *Annual review of phytopathology*, *36*(1), 329-362.

49. Roze, L. V., Beaudry, R. M., Keller, N. P., & Linz, J. E. (2004). Regulation of aflatoxin synthesis by FadA/cAMP/protein kinase A signaling in *Aspergillus parasiticus*. *Mycopathologia*, *158*(2), 219-232.

50. Roze, L. V., Hong, S. Y., & Linz, J. E. (2013). Aflatoxin biosynthesis: current frontiers. *Annual review of food science and technology*, *4*, 293-311.

51. Roze, L. V., Laivenieks, M., Hong, S. Y., Wee, J., Wong, S. S., Vanos, B., ... & Linz, J. E. (2015). Aflatoxin biosynthesis is a novel source of reactive oxygen species—a potential redox signal to initiate resistance to oxidative stress?. *Toxins*, *7*(5), 1411-1430.

52. Shimizu, K., & Keller, N. P. (2001). Genetic involvement of a cAMP-dependent protein kinase in a G protein signaling pathway regulating morphological and chemical transitions in *Aspergillus nidulan*s. *Genetics*, *157*(2), 591-600.

53. Shimizu, K., Hicks, J. K., Huang, T. P., & Keller, N. P. (2003). Pka, Ras and RGS protein interactions regulate activity of AflR, a Zn (II) 2Cys6 transcription factor in *Aspergillus nidulans*. *Genetics*, *165*(3), 1095-1104.

54. Stajich, J. E., Harris, T., Brunk, B. P., Brestelli, J., Fischer, S., Harb, O. S., ... & Stoeckert, C. J. (2012). FungiDB: an integrated functional genomics database for fungi. *Nucleic acids research*, *40*(D1), D675-D681.

55. Stincone, A., Prigione, A., Cramer, T., Wamelink, M., Campbell, K., Cheung, E., ... & Keller, M. A. (2015). The return of metabolism: biochemistry and physiology of the pentose phosphate pathway. *Biological Reviews*, *90*(3), 927-963.

56. Supek, F., Bošnjak, M., Škunca, N., & Šmuc, T. (2011). REVIGO summarizes and visualizes long lists of gene ontology terms. *PloS one*, *6*(7), e21800.

57. Szklarczyk, D., Franceschini, A., Wyder, S., Forslund, K., Heller, D., Huerta-Cepas, J., ... & Kuhn, M. (2015). STRING v10: protein–protein interaction networks, integrated over the tree of life. *Nucleic acids research*, 43 D447-D452 gku1003.

58. Terabayashi, Y., Sano, M., Yamane, N., Marui, J., Tamano, K., Sagara, J., ... & Higa, Y. (2010). Identification and characterization of genes responsible for biosynthesis of kojic acid,

an industrially important compound from *Aspergillus oryzae*. *Fungal Genetics and Biology*, *47*(12), 953-961.

59. Thakare, D., Zhang, J., Wing, R. A., Cotty, P. J., & Schmidt, M. A. (2017). Aflatoxin-free transgenic maize using host-induced gene silencing. *Science Advances*, *3*(3), e1602382.
60. Torres, A. M., Barros, G. G., Palacios, S. A., Chulze, S. N., & Battilani, P. (2014). Review on pre-and post-harvest management of peanuts to minimize aflatoxin contamination. Food Res. Int. 62, 11-19.
61. Tudzynski, B. (2014). Nitrogen regulation of fungal secondary metabolism in fungi. *Frontiers in microbiology*, *5*, 656.
62. Vizcaíno, J. A., Deutsch, E. W., Wang, R., Csordas, A., Reisinger, F., Rios, D., ... & Binz, P. A. (2014). ProteomeXchange provides globally coordinated proteomics data submission and dissemination. *Nature biotechnology*, *32*(3), 223-226.
63. Vogel, C., & Marcotte, E. M. (2012). Insights into the regulation of protein abundance from proteomic and transcriptomic analyses. *Nature Reviews Genetics*, *13*(4), 227-232.
64. Williams J.H., Grubb J.A., Davis J.W., Wang J.S., Jolly P.E., Ankrah, N.A., et al. HIV and hepatocellular and esophageal carcinomas related to consumption of mycotoxin-prone foods in sub-Saharan Africa. *Am. J. Clin. Nutr.* 92, 154–160 (2010).
65. Williams, J.H., Phillips, T.D., Jolly, P.E., Stiles, J.K., Jolly, C.M., Aggarwal, D. Human aflatoxicosis in developing countries: a review of toxicology, exposure, potential consequences, and interventions. *Am. J. Clin. Nutr. 80*, 1106-1122 (2004).
66. Wu, F. (2015). Global impacts of aflatoxin in maize: trade and human health. World Mycotoxin J., 8(2), 137-142.

67. Wu, W. W., Wang, G., Baek, S. J., & Shen, R. F. (2006). Comparative study of three proteomic quantitative methods, DIGE, cICAT, and iTRAQ, using 2D gel-or LC− MALDI TOF/TOF. *Journal of proteome research*, *5*(3), 651-658.

68. Yang, L., Fountain, J.C., Chu, Y., Ni, X., Lee, R.D., Kemerait, R.C., et al. (2016). Differential accumulation of reactive oxygen and nitrogen species in maize lines with contrasting drought tolerance and aflatoxin resistance. Phytopathology 106,S2.16.

69. Yang, L., Fountain, J.C., Wang, H., Ni, X., Ji, P., Lee, R.D., et al. (2015). Stress sensitivity is associated with differential accumulation of reactive oxygen and nitrogen species in maize genotypes with contrasting levels of drought tolerance. Int. J. Mol. Sci. 16, 24791–24819.

70. Yang, L., Jiang, T., Fountain, J. C., Scully, B. T., Lee, R. D., Kemerait, R. C., ... & Guo, B. (2014). Protein profiles reveal diverse responsive signaling pathways in kernels of two maize inbred lines with contrasting drought sensitivity. *International journal of molecular sciences*, *15*(10), 18892-18918.

71. Yu, J., Chang, P. K., Ehrlich, K. C., Cary, J. W., Bhatnagar, D., Cleveland, T. E., ... & Bennett, J. W. (2004). Clustered pathway genes in aflatoxin biosynthesis. *Applied and environmental microbiology*, *70*(3), 1253-1262.

72. Yu, J., Fedorova, N. D., Montalbano, B. G., Bhatnagar, D., Cleveland, T. E., Bennett, J. W., & Nierman, W. C. (2011). Tight control of mycotoxin biosynthesis gene expression in *Aspergillus flavus* by temperature as revealed by RNA-Seq. *FEMS microbiology letters*, *322*(2), 145-149.

73. Zhang, M., Koh, J., Liu, L., Shao, Z., Liu, H., Hu, S., ... & Wang, Q. (2016). Critical Role of COI1-Dependent Jasmonate Pathway in AAL toxin induced PCD in Tomato Revealed by Comparative Proteomics. *Scientific reports*, *6*.

Table 8.1. Numbers of significantly, differentially expressed proteins.

Isolate	Toxin[a]	H_2O_2 (mM)[a]	0 v 10 mM	0 v 20/25 mM
AF13	+++	35	46	17
NRRL3357	+	20	29	220
K54A	-	15	23	

[a]Aflatoxin production capability (+++, high; +, moderately high; -, atoxigenic) and maximum [H_2O_2] tolerance observed in Fountain et al. 2015.

Table 8.2. Significantly enriched KEGG pathways in all isolates and treatments, and their correlation with transcriptome data.

ID	Annotation	Results	P-value	Benjamini	Bonferroni	r[1]
ec00480	Glutathione metabolism	20	5.72E-05	0.0002	0.0014	0.6866
ec00030	Pentose phosphate pathway	13	0.0004	0.0008	0.0098	0.3760
ec00062	Fatty acid elongation	6	0.0490	0.0490	1.0000	0.1453
ec00620	Pyruvate metabolism	34	3.70E-14	8.88E-13	8.88E-13	0.1085
ec00281	Geraniol degradation	10	0.0069	0.0098	0.1668	0.0958
ec00020	Citrate cycle (TCA cycle)	23	2.89E-11	1.73E-10	6.93E-10	0.0673
ec00640	Propanoate metabolism	31	0.0371	0.0405	0.8904	0.0467
ec00410	beta-Alanine metabolism	12	0.0003	0.0007	0.0081	0.0051
ec00290	Valine, leucine and isoleucine biosynthesis	10	0.0007	0.0013	0.0170	0.0019
ec00010	Glycolysis / Gluconeogenesis	34	2.65E-13	3.18E-12	6.37E-12	-0.0109
ec00280	Valine, leucine and isoleucine degradation	29	1.86E-11	1.48E-10	4.45E-10	-0.0196
ec00720	Carbon fixation pathways in prokaryotes	26	0.0009	0.0015	0.0216	-0.0369
ec00500	Starch and sucrose metabolism	18	0.0215	0.0257	0.5149	-0.0433
ec00710	Carbon fixation in photosynthetic organisms	15	2.40E-06	1.15E-05	5.77E-05	-0.0465
ec00630	Glyoxylate and dicarboxylate metabolism	18	5.49E-06	2.20E-05	0.0001	-0.0666
ec00260	Glycine, serine and threonine metabolism	30	0.0269	0.0307	0.6456	-0.0707
ec00040	Pentose and glucuronate interconversions	24	0.0160	0.0214	0.3845	-0.0830
ec00071	Fatty acid degradation	22	0.0001	0.0003	0.0026	-0.0975
ec00970	Aminoacyl-tRNA biosynthesis	11	0.0022	0.0035	0.0519	-0.1023
ec00072	Synthesis and degradation of ketone bodies	4	0.0208	0.0257	0.4996	-0.1410
ec00983	Drug metabolism - other enzymes	13	0.0425	0.0443	1.0000	-0.1561
ec00230	Purine metabolism	28	0.0002	0.0006	0.0053	-0.1591
ec00250	Alanine, aspartate and glutamate metabolism	16	0.0003	0.0007	0.0080	-0.3449

[1]Pearson correlation of protein and RNA fold changes. Transcriptome data obtained from Fountain et al. 2016.

Figure 8.1. Comparative iTRAQ proteomics analysis. A. Design of the iTRAQ proteomics analysis. Column headings describe the isobaric tag molecular weights utilized for each sample. The rows represent the independent replicated runs of the experiment which are considered as three biological replicates. B. Subcellular localization enrichment for the 1,173 proteins detected in at least two biological replicates. C. Select functional enrichment analysis for gene ontology (GO) biological functions related to oxidative stress responses.

A

iTRAQ Tag / iTRAQ Set	113	114	115	116	117	118	119	121
1	0mM H_2O_2 AF13	10mM H_2O_2 AF13	25mM H_2O_2 AF13	0mM H_2O_2 NRRL3357	10mM H_2O_2 NRRL3357	20mM H_2O_2 NRRL3357	0mM H_2O_2 K54A	10mM H_2O_2 K54A
2	0mM H_2O_2 AF13	10mM H_2O_2 AF13	25mM H_2O_2 AF13	0mM H_2O_2 NRRL3357	10mM H_2O_2 NRRL3357	20mM H_2O_2 NRRL3357	0mM H_2O_2 K54A	10mM H_2O_2 K54A
3	0mM H_2O_2 AF13	10mM H_2O_2 AF13	25mM H_2O_2 AF13	0mM H_2O_2 NRRL3357	10mM H_2O_2 NRRL3357	20mM H_2O_2 NRRL3357	0mM H_2O_2 K54A	10mM H_2O_2 K54A

B

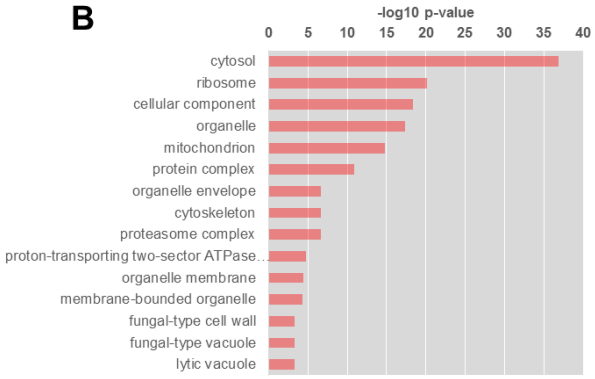

C

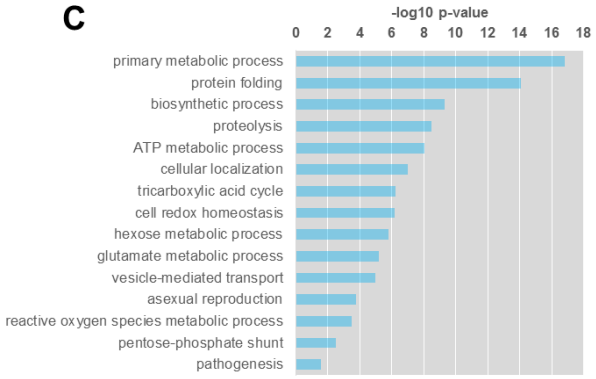

Figure 8.2. Differential expression analysis. A. Volcano plot of detected proteins indicating significantly (red) and non-significantly (blue) differentially expressed proteins. B. Venn diagrams of proteins increased or decreased in expression in response to increasing stress levels in AF13 (blue), NRRL3357 (yellow), and K54A (green). C. Principal components analysis of the protein expression profiles detected for each isolate. Isolate groups are delineated with the colored circles.

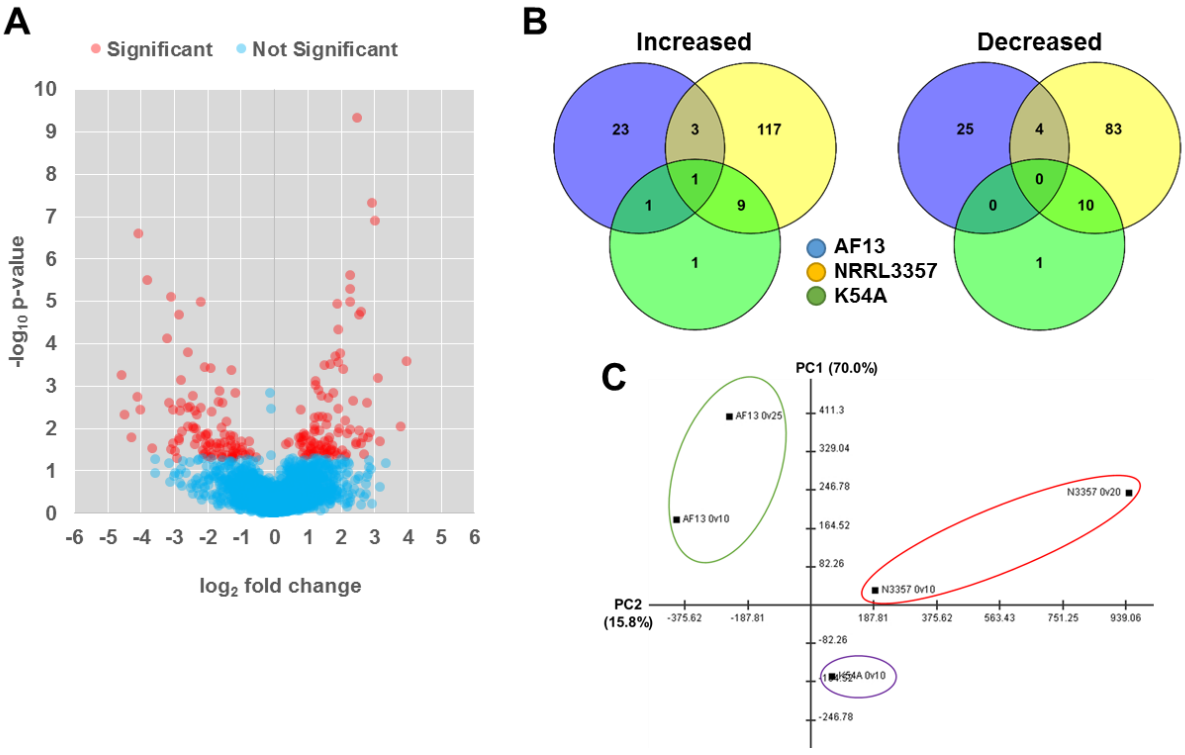
A
Significant
Not Significant
-log10 p-value
log2 fold change
B
Increased
Decreased
23
3
117
1
1
9
1
25
4
83
0
0
10
1
AF13
NRRL3357
K54A
C
PC1 (70.0%)
PC2 (15.8%)
AF13 0v25
AF13 0v10
N3357 0v20
N3357 0v10
K54A 0v10

Figure 8.3. Heatmap and hierarchical clustering analyses of protein relative expression patterns. The heatmap represents the observed fold changes in expression for the 799 proteins found to be expressed in all three biological replicates of the experiment. Blue color represents decreased patterns. Red color represents increased patterns. Hierarchical clustering analysis of the proteins shows several distinct clades with unique expression patterns showing isolate-specific responses to stress. Overall differences in isolate expression can also be visualized in the sample-level tree.

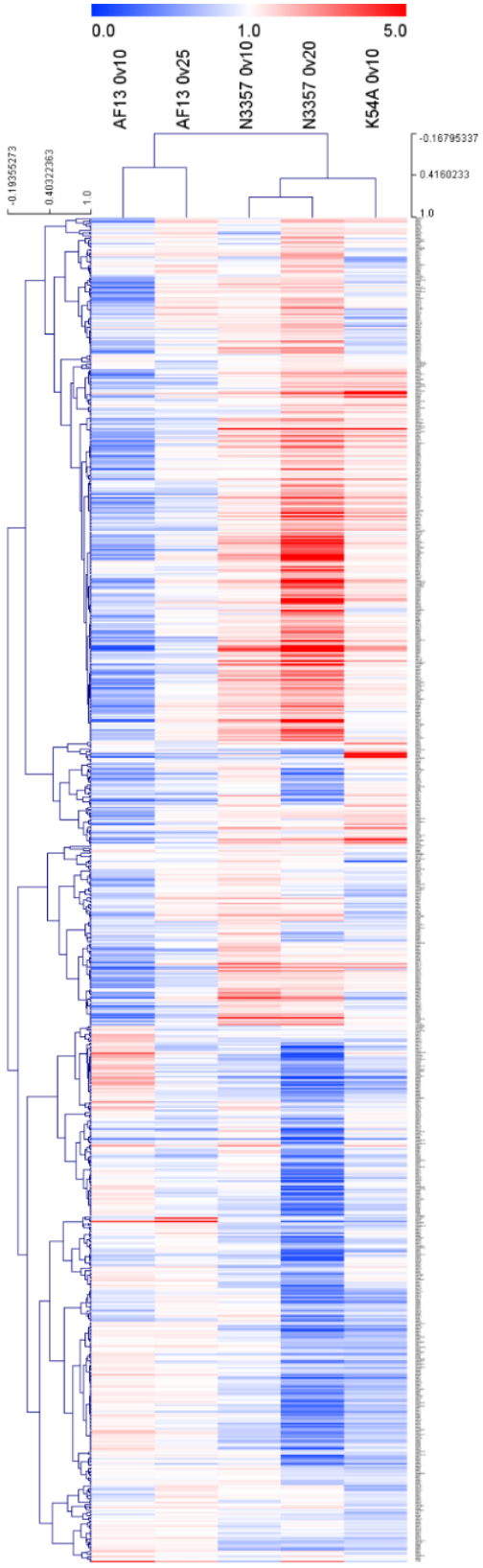
0.0
1.0
5.0
AF13 0v10
AF13 0v25
N3357 0v10
N3357 0v20
K54A 0v10
-0.19355273
0.40322363
1.0
-0.16795337
0.4160233
1.0

Figure 8.4. Gene ontology (GO) enrichment for protein biological functions under increasing levels of oxidative stress. Biological function GO term enrichment analysis was performed for DEPs obtained from each isolate and treatment. The size and shade are indicative of the p-values for each GO term enrichment with increasing size and opacity corresponding to increased significance.

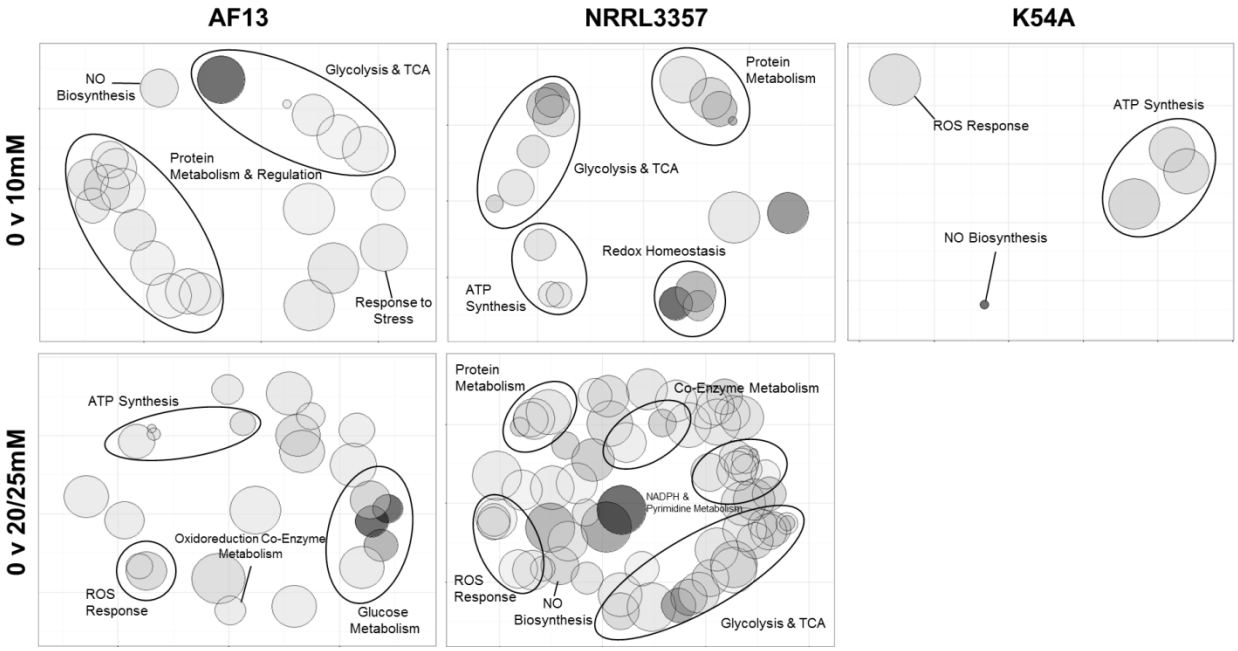
AF13
NRRL3357
K54A
0 v 10mM
0 v 20/25mM
NO Biosynthesis
Glycolysis & TCA
Protein Metabolism & Regulation
Response to Stress
Protein Metabolism
Glycolysis & TCA
Redox Homeostasis
ATP Synthesis
ROS Response
ATP Synthesis
NO Biosynthesis
ATP Synthesis
Oxidoreduction Co-Enzyme Metabolism
ROS Response
Glucose Metabolism
Protein Metabolism
Co-Enzyme Metabolism
NADPH & Pyrimidine Metabolism
ROS Response
NO Biosynthesis
Glycolysis & TCA

Figure 8.5. Carbohydrate metabolic pathway components differentially expressed in response to increasing oxidative stress. Enzymes found to be differentially expressed in the glycolysis/gluconeogenesis (blue), pentose phosphate (red), fermentation (yellow), and tricarboxylic acid (TCA) cycle (green) pathways are plotted based on their associations found in the KEGG database. Larger fonts correspond to compounds in the pathways while smaller, italicized fonts represent enzymes. The 2 x 3 heatmaps represent each isolate and fold change in expression observed relative to the control for each H_2O_2 treatment. Red and blue colors represent significantly higher and lower expression, respectively; white color represents no significant change in expression; and gray color represents treatments not measured in this experiment. Abbreviations: G6P, glucose-6-phosphate; F6P, fructose-6-phosphate; F1,6 P, fructose-1,6-bisphosphate; Gly3P, glyceraldehyde-3-phosphate; Gly1,3PP, glyceraldehyde-1,3-bisphosphate; PEP, phosphoenolpyruvate; 6PGLac, 6-phosphogluconolactone; 6PGlu, 6-phosphogluconate; Ribu5P, ribulose-5-phosphate; Rib5P, ribose-5-phosphate.

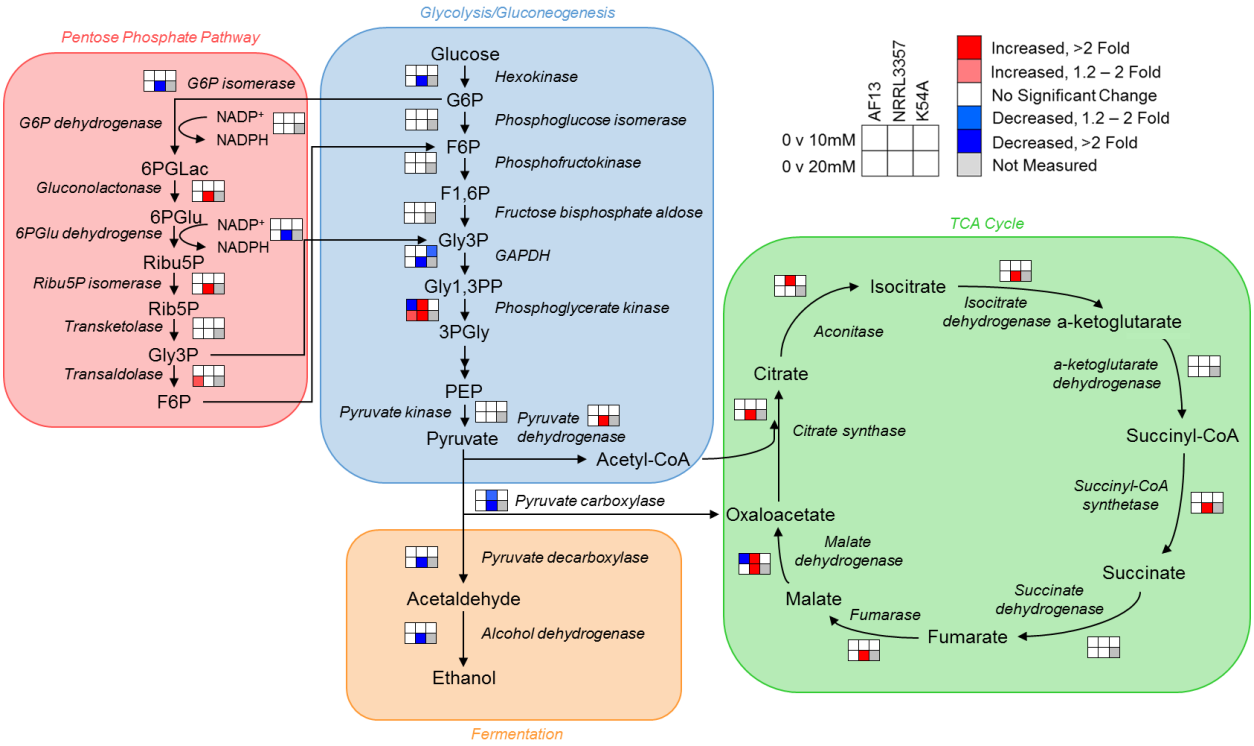
Glycolysis/Gluconeogenesis
Pentose Phosphate Pathway
TCA Cycle
Fermentation
Glucose
Hexokinase
G6P
Phosphoglucose isomerase
F6P
Phosphofructokinase
F1,6P
Fructose bisphosphate aldose
Gly3P
GAPDH
Gly1,3PP
Phosphoglycerate kinase
3PGly
PEP
Pyruvate kinase
Pyruvate
Pyruvate dehydrogenase
Acetyl-CoA
Pyruvate carboxylase
Pyruvate decarboxylase
Acetaldehyde
Alcohol dehydrogenase
Ethanol
G6P isomerase
G6P dehydrogenase
NADP+
NADPH
6PGLac
Gluconolactonase
6PGlu
6PGlu dehydrogense
Ribu5P
Ribu5P isomerase
Rib5P
Transketolase
Gly3P
Transaldolase
F6P
Citrate
Aconitase
Isocitrate
Isocitrate dehydrogenase
a-ketoglutarate
a-ketoglutarate dehydrogenase
Succinyl-CoA
Citrate synthase
Succinyl-CoA synthetase
Succinate
Oxaloacetate
Malate dehydrogenase
Malate
Succinate dehydrogenase
Fumarase
Fumarate
AF13
NRRL3357
K54A
0 v 10mM
0 v 20mM
Increased, >2 Fold
Increased, 1.2 – 2 Fold
No Significant Change
Decreased, 1.2 – 2 Fold
Decreased, >2 Fold
Not Measured

Figure 8.6. Correlative comparison of iTRAQ proteomics and previously obtained transcriptome data. The expression of transcripts detected (red) and undetected (blue) in the iTRAQ proteomics data were compared between the control and 10mM H_2O_2 treatment for AF13 (A), NRRL3357 (B), and K54A (C) with transcripts exhibiting higher levels of expression being more likely to be detected in the proteomics analysis. Pearson correlations of significantly differentially expressed transcripts with their corresponding proteins (D) or significant DEPs with their corresponding transcripts (E) showed a low degree of correlation between the datasets. A majority of protein and transcript fold changes showed either agreement or were not changed with regard to up or down regulation and fold regulation with 24.6% showing opposite responses between the datasets (F).

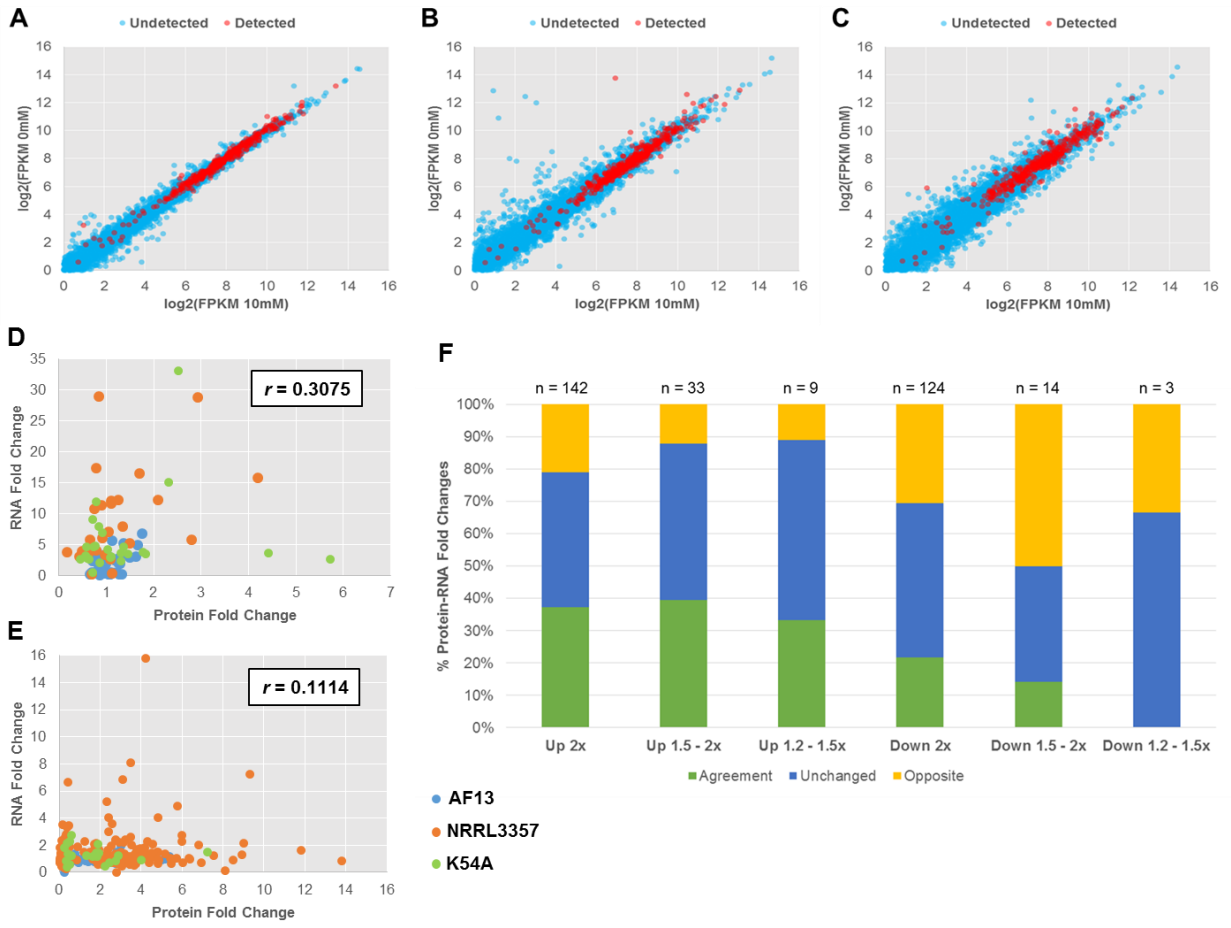
A
Undetected
Detected
log2(FPKM 0mM)
log2(FPKM 10mM)
B
Undetected
Detected
log2(FPKM 0mM)
log2(FPKM 10mM)
C
Undetected
Detected
log2(FPKM 0mM)
log2(FPKM 10mM)
D
r = 0.3075
RNA Fold Change
Protein Fold Change
E
r = 0.1114
RNA Fold Change
Protein Fold Change
F
n = 142
n = 33
n = 9
n = 124
n = 14
n = 3
% Protein-RNA Fold Changes
Up 2x
Up 1.5 - 2x
Up 1.2 - 1.5x
Down 2x
Down 1.5 - 2x
Down 1.2 - 1.5x
Agreement
Unchanged
Opposite
AF13
NRRL3357
K54A

Figure 8.7. Protein-protein interactions predicted for DEPs found in NRRL3357 in response to increasing oxidative stress. The STRING database was used to examine up- (A) and down- (B) regulated proteins in NRRL3357 detected in both H_2O_2 treatments. Each node in the network represents a DEP. Interactions are shown by the blue lines connecting each node with the weight of each line representing the confidence of the interaction based on available evidence in the database. Clusters of interest are indicated by the colored labels.

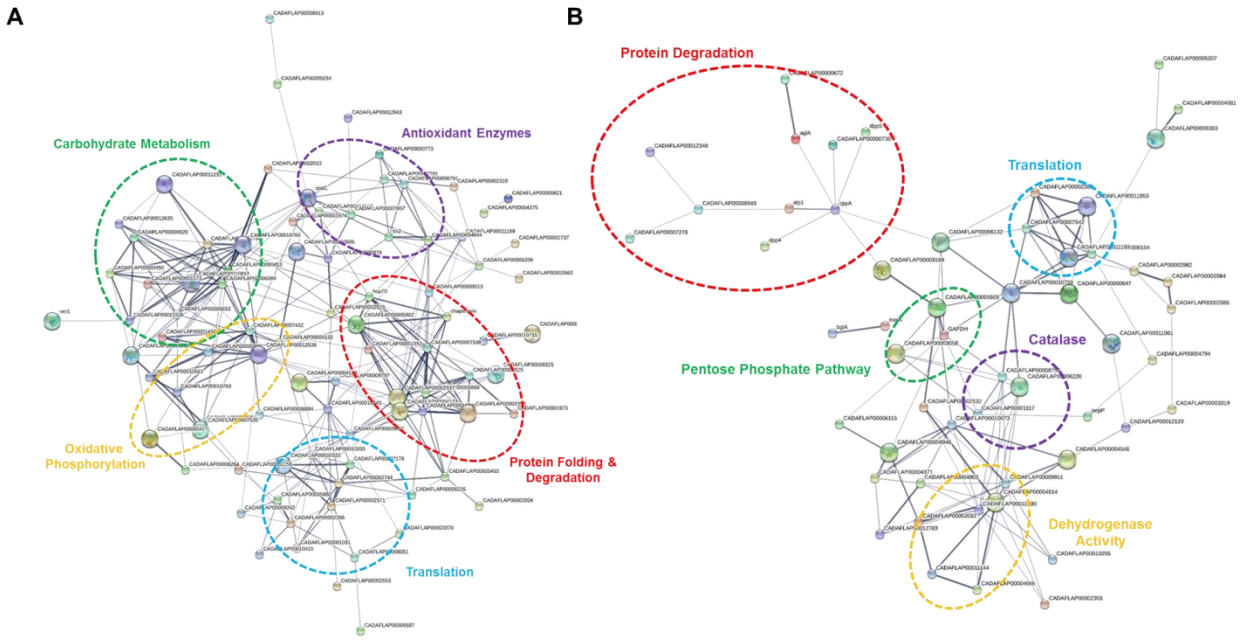
A
Carbohydrate Metabolism
Antioxidant Enzymes
Oxidative Phosphorylation
Protein Folding & Degradation
Translation
B
Protein Degradation
Translation
Catalase
Pentose Phosphate Pathway
Dehydrogenase Activity

CHAPTER 9

SUMMARY AND FUTURE DIRECTIONS

Summary and Conclusions

This dissertation, which has combined both field and laboratory approaches to study drought stress and associated oxidative stress related to aflatoxin production, provides a basis for developing novel strategies and practical solutions to mitigate the aflatoxin issue. The identified pathways and mechanisms described here serve as potential targets suitable for manipulation using biotechnology to enhance host plant resistance. Therefore, in this summary chapter there are two objectives: first, to bridge the review articles found in Chapters 1 & 2 of this dissertation and current literature published in the last four years relevant to this research; and second, to outline possible and proposed methods of testing the hypotheses originating here to improve host resistance and to mitigate the aflatoxin safety issue.

In addition to the threat posed by aflatoxin to human and animal health which have been long established (Kew, 2013; Williams et al. 2004), recent estimates of the economic losses in terms of food crop value and yield are in excess of $500 million annually in the US alone (Wu, 2015). These impacts serve as the impetuses for developing strategies to mitigate aflatoxin contamination. Historically, these strategies have focused on post-harvest storage conditions and plant breeding for pre-harvest host resistance (Amaike and Keller, 2011). Host plant resistance to aflatoxin contamination has been a major focus of plant breeding and pathology research since the mid 1970's (Diener et al. 1983, 1987; Fountain et al. 2014). These efforts have identified potential sources of genetic resistance to aflatoxin contamination in both maize and peanut primarily through screening of germplasm for stable resistance across multiple environments or growing seasons, or through the development of genetic mapping populations and germplasm collections for association studies (Fountain et al. 2015a; Guo et al. 2017; Wahl et al. 2016). These identified sources of genetic resistance are highly influenced by the environment with

significant genotype x environmental interactions hampering the identification of stable quantitative trait loci (QTL) and the development of molecular markers for enhancing resistance in breeding programs (Dhakal et al. 2016; Farfan et al. 2015; Fountain et al. 2015a; Warburton and Williams, 2014; Zhuang et al. 2016). Understanding the roles of this environmental stress and its influence on this plant-pathogen interaction is critical to developing lines with stable, deployable resistance. Of the identified environmental stresses capable of affecting aflatoxin resistance, drought stress is of particular concern, and has been shown to result in significant increases in aflatoxin contamination in both maize and peanut (Guo et al. 2008a, 2008b; Pitt et al. 2013). Therefore, understanding the effects of drought stress on both the host and pathogen to provide novel methods of enhancing host resistance to aflatoxin contamination represents the long term goal of our current research to mitigate this problem.

Drought stress has been shown to result in oxidative stress in plant tissues. This oxidative stress results from the disruption of redox homeostasis and the generation of reactive oxygen species (ROS) (de Carvalho et al. 2008; Das and Roychoudhury, 2014). These ROS naturally function in both biotic and abiotic stress-responsive signaling pathways under normal circumstances, however can cause oxidative damage to cellular components when accumulating in excess (Baxter et al. 2014). These ROS can also react with and induce the formation of reactive nitrogen species (RNS) which also function in cellular signaling processes and can cause cellular damage when over accumulating and the initiation of apoptosis during pathogen defense responses (Lehmann et al. 2015; Wang et al. 2013). In this dissertation research, it was found that drought sensitive, aflatoxin contamination susceptible maize lines accumulate higher levels of ROS in their kernel tissues under drought stress along with higher levels of simple sugars and peroxidized lipids (Yang et al. 2015, 2016a, 2016b).

These compounds have also been shown to be involved in the regulation of aflatoxin production in several species of *Aspergillus* fungi. Since 2000 with the first publication by Jayashree and Subramanyam (2000), it has been repeatedly observed that ROS and associated oxidative stress provided by oxidized or peroxidized compounds such as oxylipins stimulate the production of aflatoxin, and regulate the development of conidia and sclerotia (Amare and Keller, 2014; Grintzalis et al. 2014; Reverberi et al. 2012). The integration of stress responsive signaling pathways and mycotoxin production regulation has also been a focus of several studies which have shown a link between aflatoxin production regulation and oxidative stress mitigation responses (Roze et al. 2011, 2013). Studies such as that published by Roze et al. (2015) also suggest that aflatoxin biosynthesis may be a source of partial oxidative stress alleviation with isolates possessing non-functional aflatoxin biosynthesis genes exhibiting significantly reduced conidial survival under oxidative stress. In this dissertation, transcriptomic and proteomic studies of *A. flavus* isolate responses to oxidative stress have also shown that the expression of genes involved in aflatoxin biosynthesis was enhanced by oxidative stress, and that fungal developmental rates and pathogenicity may also be affected (Fountain et al. 2016a, 2016b, 2017). These same studies have also suggested a coordinated role of secondary metabolite production in oxidative stress alleviation in *A. flavus* (Fountain et al. 2016a, 2016b, 2017).

Together, these observations of ROS and metabolite accumulation in plants under drought stress and their role in aflatoxin production regulation suggests that ROS may function in crosstalk between host plants and *A. flavus* during infection resulting in exacerbated aflatoxin contamination under drought. Proteomic examination of maize rachis and kernel tissues have also shown that antioxidant enzymes such as catalase and superoxide dismutase accumulate in drought tolerant, aflatoxin resistant maize lines in response to either drought stress or *A. flavus*

infection (Pechanova et al. 2011, 2015; Yang et al. 2014). Given these observations and those described in this dissertation, increases in host tissue antioxidant capacity may provide benefits to both drought tolerance and to aflatoxin contamination resistance.

Future Directions

Transgenic and Genome Editing Approaches

The global data obtained in this dissertation research provide insights for potential novel avenues for the enhancement of aflatoxin contamination resistance in host plants using genetic engineering (e.g. genome editing and genetic transformation) to manipulating the levels of stress-responsive compounds independently or in tandem to reduce the production of aflatoxin in grain hosts. While several pathways were found to correlate with drought sensitivity in maize, the complexity of their biosynthesis or their essential nature may preclude their use in mutation studies employing genome editing approaches. Therefore, compounds and pathways whose manipulation will avoid potential lethal or interfering effects including antioxidant enzymes, starch and carbohydrate biosynthetic regulators, and lipoxygenases whose products or targets (ROS, sugars, and oxylipins) were common to both the host and pathogen responses under drought/oxidative stress were considered.

By manipulating antioxidant gene expression to enhance antioxidant capacity, lipoxygenase expression to regulate lipid signaling pathways, and starch biosynthetic mechanisms to reduce seed simple sugar content, improved host aflatoxin resistance and drought tolerance may be possible. In addition, by better understanding the responses of field isolates to oxidative stress and how this correlated with observed pathogenicity, biological controls may be better selected for field applications from among native isolates, or the capabilities of existing

formulated isolate may be enhanced to improve their efficacy. Together, these approaches will provide a novel avenue to search for and produce practical solutions to this aflatoxin safety issue.

The application of biotechnologies, specifically traditional genetic transformation using *Agrobacterium tumefaciens* or biolistics, and clustered regularly interspaced short palindromic repeats (CRISPR)/Cas9 genome editing, allow for the possibility of enhancing host resistance rapidly through the targeted manipulation of traits identified in previous studies. Given the observed correlation between host oxidative stress under drought stress and exacerbated aflatoxin contamination, a promising future direction, as an example as described below, will be to test whether the enhancement or reduction of host antioxidant capacity through the manipulation of antioxidant gene expression using these technologies may improve host resistance.

Under this proposed project, the objective would be to test the hypothesis that antioxidant capacity and ROS content in maize and peanut kernel/seed tissues are related to aflatoxin contamination resistance using genetic engineering technologies including transgenic and genome editing. This may be addressed through two approaches: first positively by the overexpression of antioxidant enzymes in these crops to reduce ROS content and enhance resistance, and secondly in a negative approach through the knock-down of expression through mutagenesis of antioxidant mechanisms to repress resistance. The first approach, the enhancement of host resistance to aflatoxin contamination under drought stress using genetic engineering, will focus on increasing the expression of the antioxidant enzyme catalase in both maize and peanut. Additional genes such as ascorbate peroxidase and superoxide dismutase may also be explored. This will be accomplished through the introduction of an overexpression cassette consisting of a selectable marker, a seed-specific constitutive promoter, a complete

coding sequence of the respective plant catalase, and a transcriptional terminator. Seed specific promoters such as gamma-zein in maize (Thakare et al. 2017) are useful for this application since aflatoxin contamination is a problem primarily in seed tissues, and in order to avoid gene silencing by the host due to excessive over-expression which may occur when utilizing non-specific constitutive promoters (Schubert et al. 2004; Weinhold et al. 2013). The transformation cassettes would be delivered into maize and peanut using *Agrobacterium tumefaciens*-mediated transformation or through the use of biolistics. Successful transformants will be identified through the culture of transformed callus tissues on herbicide-selective medium, and transplanted in the greenhouse to produce T_0 plants and T_1 seeds.

The second approach will focus on the mutation and functional disruption of antioxidant enzyme-encoding genes using CRISPR/Cas9 genome editing. This technology employs the Cas9 nuclease to introduce point mutations in DNA which are homologous to a single guide RNA (sgRNA). While in bacteria this mechanism is hypothesized to function in bacteriophage resistance, it has since been found that synthetic sgRNAs can be used to introduce point mutations into select target DNA sequences in other organisms including plants (Song et al. 2016). It has also been found that multiple sgRNAs homologous to different DNA sequences can be introduced simultaneously to mutate multiple genes, and that this system can be used to introduce foreign DNA into plant genomes through homology directed repair (Shi et al. 2017). In this experiment, a sgRNA construct would be assembled with homologous sequences to 2 – 3 selected antioxidant genes and introduced into maize callus tissues using biolistics. The diploid nature of the maize genome and the relative ease of transformation will allow for an attempt to simultaneously mutate multiple genes. However, for peanut, only one antioxidant gene mutatuion using CRISPR/Cas9 would initially be attempted. This is due to the allotetraploid

nature of the peanut genome, and the associated difficulty in obtaining simultaneous mutagenesis for all four functional alleles of the selected genes to produce the desired phenotypes. Also, the gold particles used in biolistics may be coated with Cas9 protein generated using overexpression in *Escherichia coli*. This will avoid potential pitfalls associated with Cas9 over-expression in the host such as off-target mutation and the need for Cas9 codon optimization in maize or peanut to improve translation (Song et al. 2016). The sgRNA constructs could then be introduced as described in maize and in peanut.

Following transformation using either approach, generated T_0 plants would be self-pollinated to generate T_1 seeds in both maize and peanut. The transformants would then be evaluated to confirm the proper insertion or deletion of target DNA. For the overexpression mutants in both maize and peanut, validation of functional insertion of the construct would be done using PCR to amplify each component of the construct followed by Sanger sequencing. Lines containing all components would be used for RNA isolation and quantitative RT-PCR (qPCR) to examine for gene expression relative to untransformed controls. Temporal patterns of overexpression in seeds/kernels may be examined using qPCR at regular intervals to examine for possible growth-stage specificity in expression. Tissue-specific overexpression of the selected genes will also be validated using qPCR by examining various tissues including whole seeds/kernels, endosperm, cotyledons, embryos, leaves, stems, roots, silk, and pods at the determined time of optimum expression from the time course experiment. For CRISPR/Cas9 mutagenized plants, the genomic DNA sequence of each of the selected antioxidant enzyme-encoding genes will be sequenced using Sanger sequencing to confirm Cas9 induced mutations and their positions within the genes. Putative functional changes in protein structure due to the induced mutations will also be determined by *in silico* analyses.

To examine for differences in aflatoxin contamination, T_1 seeds would be used for a kernel screening assay (KSA; Brown et al. 1995). Briefly, seeds/kernels will be surface sterilized and inoculated with a conidia suspension of *A. flavus* and placed in a moisture chamber at 30°C for one week. At the conclusion, infection severity, conidiation, and aflatoxin content will be measured and comparisons drawn between transformed and non-transformed seeds. It is expected that catalase overexpressing seeds will accumulate less aflatoxin than their controls while the opposite is expected for the CRISPR/Cas9 mutagenized seeds. While this method is quick and technically simple, it does not routinely agree with results obtained from *in vivo* inoculation.

In order to test the hypothesis with regard to drought stress *in vivo,* these transformed lines (T_2 plants) would cultivated in the greenhouse or in microplots with controllable irrigation, and inoculated with *A. flavus* with and without drought stress as follows. For maize, drought stress will be introduced at 14 days after pollination with simultaneous inoculation of ears with *A. flavus* inoculum using a side needle injection method (Guo et al. 2017; Windham et al. 2003). Non-inoculated and irrigated controls along with an inoculation only treatment and a needle wounding control will also be performed. Kernels will be collected at 7 and 14 days after inoculation, and at maturity. In peanut, the same treatment design will be used with *A. flavus* inoculum grown on cracked wheat will be introduced into the soil at flowering. Drought stress will be introduced at 100 days after planting and maintained until maturity (140 days after planting) as described by Clevenger et al. (2016). Seeds from each treatment will be collected and used for analysis.

To examine changes in antioxidant enzyme activity in the generated mutants, crude protein extractions would be performed from seed/kernel tissues at selected time points as

described by Yang et al. (2015). These extracts will be used to determine catalase, superoxide dismutase, and ascorbate peroxidase activity levels using spectrophotometric methods (Venisse et al. 2001; Yang et al. 2015) to confirm increases or decreases in overall activity based following transformation. The content of H_2O_2 and superoxide in the seeds/kernels at these time points will also be determined using spectrophotometric methods (Yang et al. 2015). For both KSA and *in vivo* samples, aflatoxin present in these tissues will be extracted using methanol and quantified using spectrophotometric methods (Fountain et al. 2016a; Guo et al. 2017; Lee et al. 2004; Yang et al. 2017).

It is expected that overexpression mutants will exhibit higher levels of antioxidant enzyme activity and lower levels of ROS accumulation during drought treatment and *A. flavus* inoculation. This should result in reduced aflatoxin contamination compared to the untransformed lines under the same conditions. Conversely, in the CRISPR/Cas9 mutated lines, reductions in antioxidant enzyme activity and increases in H_2O_2 and superoxide content are expected with associated increases in aflatoxin contamination. While these methods will not be able to examine the co-localization of the ROS and fungal infection and aflatoxin production, these experiments will provide evidence as to whether host tissue ROS content is correlated with aflatoxin resistance, and that using these techniques to enhance antioxidant capacity is a valid approach to enhance resistance.

Investigating the Relationship between ROS and Secondary Metabolite Production

While the development of novel techniques of enhancing host resistance is the primary objective, additional hypotheses were also generated related to fungal biology during the course of this dissertation research which warrant further investigation. Two examples of this are that

aflatoxin production provides a form of oxidative stress alleviation to *A. flavus* (Fountain et al. 2015b), and that other secondary metabolites such as kojic acid may supplement these beneficial effects in the absence of aflatoxin production (Fountain et al. 2016a). These hypotheses can be tested through a combination of mutagenesis and medium supplementation assays described as follows.

The concept of aflatoxin production providing oxidative stress alleviation to the fungus has been previously proposed in the literature with the observation of a positive correlation between aflatoxin production and the accumulation of ROS and their reactive byproducts in fungal tissues (Jayashree and Subramanyam, 2000; Narasaiah et al. 2006; Roze et al. 2013). More recently, Roze et al. (2015) showed that deletion of aflatoxin biosynthetic genes resulted in reduced conidial oxidative stress tolerance expressed as reduced conidial germination rates under high levels of oxidative stress provided by H_2O_2. It was hypothesized in this work that the biosynthetic process of producing aflatoxin, not the compound itself, was the source of the antioxidant benefit with the cause likely being secondary ROS bursts stimulating the production of higher levels of antioxidant enzymes in fungal tissues, particularly the next generation of conidia.

To test this, aflatoxin could be supplemented into culture medium while culturing either atoxigenic field isolates of *A. flavus*, or with isolates possessing point mutations or deletions in their aflatoxin biosynthetic pathways with and without the addition of increasing concentrations of H_2O_2 or other oxidative stress-causing agent. If aflatoxin has a direct benefit, increased levels of fungal growth would be expected under higher levels of stress. However, this approach may not produce a detectable response. *Aspergillus flavus* compartmentalizes the final phases of aflatoxin production to specialized vesicles for exocytosis and not to the cytoplasm (Chanda et

al. 2009), and accumulates relatively low levels of aflatoxin in mycelia tissues while the surrounding medium may contain high concentrations of aflatoxin (Hesseltine et al. 1966). Together, this implies a unidirectional active transport of aflatoxin out of the fungal tissues possibly limiting the efficacy of aflatoxin supplementation on oxidative stress responses, and pointing more toward individual biosynthetic processes rather than aflatoxin itself as being the source of the potential antioxidant benefits.

An alternative approach could be to supplement intermediates from the biosynthetic pathway occurring at points concurrent or beyond those inhibited in mutant isolates either in the form of pure compounds or culture filtrates/mycelial extracts from isolates which produce necessary compound (e.g. supplementing averantin to a Δ*pksA* or Δ*nor-1* isolate). This in combination with growing selected isolates across a gradient of increasing concentrations of H_2O_2 could be done for multiple mutant isolates possessing different aflatoxin biosynthetic gene deletions to identify which steps in aflatoxin production provide the observed antioxidant benefits. This would be shown by reduced fungal growth or conidial germination under high levels of oxidative stress in a particular mutant compared to the wild type isolate which would be recovered by supplementation with the missing intermediate(s). In addition, histochemical staining methods similar to those previously employed (Yang et al. 2015) can be used to quantify ROS accumulation in fungal tissues as a measure of oxidative stress tolerance and alleviation.

The second hypothesis regarding kojic acid was based on the observations that kojic acid accumulates at higher concentrations in medium not conducive for aflatoxin production (Fountain et al. 2016a), significant reductions in fungal growth were not observed when culturing the isolates in this non-conducive medium (YEP; Fountain et al. 2015b), and that kojic acid is an iron-chelating antioxidant compound (Terabayashi et al. 2010). It is hypothesized that

the lack of significant reductions in fungal growth in the aflatoxin non-conducive medium were due to these increases in kojic acid, which may interfere with observing the full effects of the loss of aflatoxin production on oxidative stress tolerance. To counter this interference and test the hypothesis, two methods could be performed. First, double and single mutants of a kojic acid biosynthetic gene (e.g. Δ*kojA*) and an aflatoxin gene (e.g. Δ*pksA*) can be cultured across an increasing gradient of H_2O_2 in an aflatoxin conducive medium and compared for growth and ROS accumulation in their tissues. If significant reductions in oxidative stress tolerance are observed in the double mutant, supplementation of aflatoxin biosynthetic intermediates can be performed as previously described to look for possible recovery effects. Reduction in growth in the single kojic acid gene mutant would also confirm the role of kojic acid in oxidative stress tolerance. Second, iron cations can be introduced by adding $FeCl_3$ into the culture medium to chelate produced kojic acid and prevent it from functioning in antioxidant reactions allowing for observation of the effects of the loss of aflatoxin on oxidative stress tolerance. A related test could also be performed using $FeCl_2$ instead of $FeCl_3$. Iron (II) is the initial reactant in Fenton reactions in which remove an electron from Fe^{2+} is removed by H_2O_2 resulting in Fe^{3+} and $OH^{\cdot -}$, a more toxic ROS (Fenton, 1894). This could be combined with the supplementation of $OH^{\cdot -}$ specific antioxidant compounds such as dimethylsulfoxide (DMSO) to test whether $OH^{\cdot -}$ is one of the primary ROS responsible for exacerbated aflatoxin production.

These approaches, if successful, will improve our understanding of the role of ROS in this host plant-pathogen interaction and fungal biology related to aflatoxin production, provide for the development of bio-markers for selection of drought tolerant germplasm in breeding programs, and provide a novel method for mitigating pre-harvest aflatoxin contamination in maize and peanut under drought stress to compliment current efforts to enhance resistance

through traditional breeding. This will also represent the first utilization of CRISPR/Cas9 genome editing in the investigation of aflatoxin resistance in maize and peanut. It will also be suitable for funding under federal grants including the USDA-NIFA Agricultural and Food Research Initiative (AFRI), and by local and national stakeholder groups such as the National Corn Grower's Association, the Georgia Corn Commission, the Peanut Foundation, the National Peanut Board, and the Georgia Peanut Commission.

References

1. Amaike, S., & Keller, N. P. (2011). *Aspergillus flavus*. *Annual review of phytopathology*, *49*, 107-133.
2. Amare, M. G., & Keller, N. P. (2014). Molecular mechanisms of *Aspergillus flavus* secondary metabolism and development. *Fungal Genetics and Biology*, *66*, 11-18.
3. Atehnkeng, J., Donner, M., Ojiambo, P. S., Ikotun, B., Augusto, J., Cotty, P. J., & Bandyopadhyay, R. (2016). Environmental distribution and genetic diversity of vegetative compatibility groups determine biocontrol strategies to mitigate aflatoxin contamination of maize by *Aspergillus flavus*. *Microbial biotechnology*, *9*(1), 75-88.
4. Baxter, A., Mittler, R., & Suzuki, N. (2014). ROS as key players in plant stress signaling. *J. Exp. Bot. 65*(5), 1229-1240.
5. Brown, R. L., Cleveland, T. E., Payne, G. A., Woloshuk, C. P., Campbell, K. W., & White, D. G. (1995). Determination of resistance to aflatoxin production in maize kernels and detection of fungal colonization using an *Aspergillus flavus* transformant expressing *Escherichia coli* β-glucuronidase. *Phytopathology*, *85*(9), 983-989.

6. Chanda, A., Roze, L. V., Kang, S., Artymovich, K. A., Hicks, G. R., Raikhel, N. V., ... & Linz, J. E. (2009). A key role for vesicles in fungal secondary metabolism. *Proceedings of the National Academy of Sciences*, 106(46), 19533-19538.
7. Clevenger, J., Marasigan, K., Liakos, V., Sobolev, V., Vellidis, G., Holbrook, C., & Ozias-Akins, P. (2016). RNA sequencing of contaminated seeds reveals the state of the seed permissive for pre-harvest aflatoxin contamination and points to a potential susceptibility factor. *Toxins*, *8*(11), 317.
8. Cruz de Carvalho, M. H. (2008). Drought stress and reactive oxygen species: production, scavenging and signaling. *Plant Signaling & Behavior*, *3*(3), 156-165.
9. Das, K., & Roychoudhury, A. (2014). Reactive oxygen species (ROS) and response of antioxidants as ROS-scavengers during environmental stress in plants. *Frontiers in Environmental Science*, *2*, 53.
10. Dhakal, R., Windham, G. L., Williams, W. P., & Subudhi, P. K. (2016). Quantitative trait loci (QTL) for reducing aflatoxin accumulation in corn. *Molecular Breeding*, *36*(12), 164.
11. Diener, U. L., Asquith, R. L., and Dickens, J. W. (1983). Aflatoxin and *Aspergillus flavus* in corn. *So. Coop. Ser. Bull. 279*, 112 pp.
12. Diener, U. L., Cole, R. J., Sanders, T. H., Payne, G. A., Lee, L. S., & Klich, M. A. (1987). Epidemiology of aflatoxin formation by *Aspergillus flavus*. *Annual Review of Phytopathology*, *25*(1), 249-270.
13. Farfan, I. D. B., Gerald, N., Murray, S. C., Isakeit, T., Huang, P. C., Warburton, M., ... & Kolomiets, M. (2015). Genome wide association study for drought, aflatoxin resistance, and important agronomic traits of maize hybrids in the sub-tropics. *PloS one*, *10*(2), e0117737.

14. Fenton, H.J.H. (1894). Oxidation of tartaric acid in presence of iron. *J. Chem. Soc. Trans.* 65, 899-910.

15. Fountain, J. C., Bajaj, P., Pandey, M., Nayak, S. N., Yang, L., Kumar, V., ... & Lee, R. D. (2016a). Oxidative stress and carbon metabolism influence *Aspergillus flavus* transcriptome composition and secondary metabolite production. *Scientific Reports*, *6*.

16. Fountain, J. C., Bajaj, P., Nayak, S. N., Yang, L., Pandey, M. K., Kumar, V., ... Varshney, R. K. , & Guo, B. (2016b). Responses of *Aspergillus flavus* to Oxidative Stress Are Related to Fungal Development Regulator, Antioxidant Enzyme, and Secondary Metabolite Biosynthetic Gene Expression. *Frontiers in Microbiology*, *7*.

17. Fountain, J. C., Bajaj, P., Yang, L., Pandey, M. K., Nayak, S. N., Koh, J., Kumar, V., Jayale, A.S., Chitikineni, A., Lee, R.D., Kemerait, R.C., Chen, S., Varshney, R. K., Guo, B. (2017). Integrated Transcriptome and Proteome Analyses Reveal a Close Association between Secondary Metabolite Production Capabilities and Aspergillus flavus Isolate Oxidative Stress Tolerance. *Proceedings of the Plant and Animal Genome Conference,* January 14-18, San Diego, CA.

18. Fountain, J. C., Khera, P., Yang, L., Nayak, S. N., Scully, B. T., Lee, R. D., ... & Guo, B. (2015a). Resistance to *Aspergillus flavus* in maize and peanut: Molecular biology, breeding, environmental stress, and future perspectives. *The Crop Journal*, *3*(3), 229-237.

19. Fountain, J. C., Scully, B. T., Chen, Z. Y., Gold, S. E., Glenn, A. E., Abbas, H. K., ... & Guo, B. (2015b). Effects of hydrogen peroxide on different toxigenic and atoxigenic isolates of *Aspergillus flavus*. *Toxins*, *7*(8), 2985-2999.

20. Fountain, J., Scully, B., Ni, X., Kemerait, R., Lee, D., Chen, Z. Y., & Guo, B. (2014). Environmental influences on maize-*Aspergillus flavus* interactions and aflatoxin production. *Frontiers in Microbiology*, 5, 40.
21. Grintzalis, K.; Vernardis, S.I.; Klapa, M.I.; Georgiou, C.D. (2014). Role of oxidative stress in sclerotial differentiation and aflatoxin B1 biosynthesis in *Aspergillus flavus*. *Appl. Environ. Microbiol. 80, 5561-5571*.
22. Guo, B., Chen, Z. Y., Lee, R. D., & Scully, B. T. (2008). Drought stress and preharvest aflatoxin contamination in agricultural commodity: genetics, genomics and proteomics. *Journal of Integrative Plant Biology*, *50*(10), 1281-1291.
23. Guo, B., Ji, X., Ni, X., Fountain, J. C., Li, H., Abbas, H. K., ... & Scully, B. T. (2017). Evaluation of maize inbred lines for resistance to pre-harvest aflatoxin and fumonisin contamination in the field. *The Crop Journal, in press*.
24. Guo, B., Yu, J., Holbrook, C. C., Cleveland, T. E., Nierman, W. C., & Scully, B. T. (2009). Strategies in prevention of preharvest aflatoxin contamination in peanuts: aflatoxin biosynthesis, genetics and genomics. *Peanut Science*, *36*(1), 11-20.
25. Hesseltine, C. W., Shotwell, O. L., Ellis, J. J., & Stubblefield, R. D. (1966). Aflatoxin formation by *Aspergillus flavus. Bacteriological reviews*, 30(4), 795.
26. Holbrook, C. C., Guo, B. Z., Wilson, D. M., & Timper, P. (2009). The US breeding program to develop peanut with drought tolerance and reduced aflatoxin contamination. *Peanut Science*, *36*(1), 50-53.
27. Jayashree, T., & Subramanyam, C. (2000). Oxidative stress as a prerequisite for aflatoxin production by *Aspergillus parasiticus*. *Free Radical Biology and Medicine*, *29*(10), 981-985.

28. Kew, M. C. Aflatoxins as a cause of hepatocellular carcinoma. *J. Gastrointestin. Liver Dis.* 22, 305-310 (2013).

29. Lee, N. A., Wang, S., Allan, R. D., & Kennedy, I. R. (2004). A rapid aflatoxin B1 ELISA: development and validation with reduced matrix effects for peanuts, corn, pistachio, and soybeans. *Journal of agricultural and food chemistry*, *52*(10), 2746-2755.

30. Lehmann, S., Serrano, M., L'Haridon, F., Tjamos, S. E., & Metraux, J. P. (2015). Reactive oxygen species and plant resistance to fungal pathogens. *Phytochemistry*, *112*, 54-62.

31. Narasaiah, K. V., Sashidhar, R. B., & Subramanyam, C. (2006). Biochemical analysis of oxidative stress in the production of aflatoxin and its precursor intermediates. *Mycopathologia*, 162(3), 179-189.

32. Reverberi, M., Punelli, M., Smith, C. A., Zjalic, S., Scarpari, M., Scala, V., ... & Fabbri, A. A. (2012). How peroxisomes affect aflatoxin biosynthesis in *Aspergillus flavus*. *PLoS One*, *7*(10), e48097.

33. Roze, L. V., Chanda, A., Wee, J., Awad, D., & Linz, J. E. (2011). Stress-related transcription factor AtfB integrates secondary metabolism with oxidative stress response in aspergilli. *Journal of Biological Chemistry*, *286*(40), 35137-35148.

34. Roze, L. V., Hong, S. Y., & Linz, J. E. (2013). Aflatoxin biosynthesis: current frontiers. *Annual review of food science and technology*, *4*, 293-311.

35. Roze, L. V., Laivenieks, M., Hong, S. Y., Wee, J., Wong, S. S., Vanos, B., ... & Linz, J. E. (2015). Aflatoxin biosynthesis is a novel source of reactive oxygen species—a potential redox signal to initiate resistance to oxidative stress?. *Toxins*, *7*(5), 1411-1430.

36. Schubert, D., Lechtenberg, B., Forsbach, A., Gils, M., Bahadur, S., & Schmidt, R. (2004). Silencing in Arabidopsis T-DNA transformants: the predominant role of a gene-specific RNA sensing mechanism versus position effects. *The Plant Cell*, *16*(10), 2561-2572.

37. Shi, J., Gao, H., Wang, H., Lafitte, H. R., Archibald, R. L., Yang, M., ... & Habben, J. E. (2017). ARGOS8 variants generated by CRISPR-Cas9 improve maize grain yield under field drought stress conditions. *Plant biotechnology journal*, *15*(2), 207-216.

38. Song, G., Jia, M., Chen, K., Kong, X., Khattak, B., Xie, C., ... & Mao, L. (2016). CRISPR/Cas9: a powerful tool for crop genome editing. *The Crop Journal*, *4*(2), 75-82.

39. Terabayashi, Y., Sano, M., Yamane, N., Marui, J., Tamano, K., Sagara, J., ... & Higa, Y. (2010). Identification and characterization of genes responsible for biosynthesis of kojic acid, an industrially important compound from *Aspergillus oryzae*. *Fungal Genetics and Biology*, *47*(12), 953-961.

40. Thakare, D., Zhang, J., Wing, R. A., Cotty, P. J., & Schmidt, M. A. (2017). Aflatoxin-free transgenic maize using host-induced gene silencing. *Science Advances*, *3*(3), e1602382.

41. Venisse, J. S., Gullner, G., & Brisset, M. N. (2001). Evidence for the involvement of an oxidative stress in the initiation of infection of pear by *Erwinia amylovora*. *Plant Physiology*, *125*(4), 2164-2172.

42. Wahl, N., Murray, S. C., Isakeit, T., Krakowsky, M., Windham, G. L., Williams, W. P., ... & Scully, B. (2016). Identification of Resistance to Aflatoxin Accumulation and Yield Potential in Maize Hybrids in the Southeast Regional Aflatoxin Trials (SERAT). *Crop Science*, 57(1), 202-215.

43. Wang, Y., Loake, G. J., & Chu, C. (2013). Cross-talk of nitric oxide and reactive oxygen species in plant programed cell death. *Frontiers in Plant Science*, *4*, 314.

44. Warburton, M. L., & Williams, W. P. (2014). Aflatoxin resistance in maize: what have we learned lately?. *Advances in Botany*, *2014*.

45. Weinhold, A., Kallenbach, M., & Baldwin, I. T. (2013). Progressive 35S promoter methylation increases rapidly during vegetative development in transgenic *Nicotiana attenuata* plants. *BMC plant biology*, *13*(1), 99.

46. Williams, J.H., Phillips, T.D., Jolly, P.E., Stiles, J.K., Jolly, C.M. & Aggarwal, D. Human aflatoxicosis in developing countries: a review of toxicology, exposure, potential consequences, and interventions. *Am. J. Clin. Nutr*. 80, 1106-1122 (2004).

47. Windham, G. L., Williams, W. P., Buckley, P. M., & Abbas, H. K. (2003). Inoculation techniques used to quantify aflatoxin resistance in corn. *Journal of Toxicology: Toxin Reviews*, *22*(2-3), 313-325.

48. Wu, F. (2015). Global impacts of aflatoxin in maize: trade and human health. *World Mycotoxin J.*, *8*(2), 137-142.

49. Yang, L., Fountain, J.C., Chu, Y., Ni, X., Lee, R.D., Kemerait, R.C., et al. (2016a). Differential accumulation of reactive oxygen and nitrogen species in maize lines with contrasting drought tolerance and aflatoxin resistance. *Phytopathology 106*, S2.16.

50. Yang, L., Fountain, J.C., Ni, X., Lee, R.D., Chen, S., Scully, B.T., Kemerait, R.C., Guo, B. (2016b). Differential metabolome analysis of field-grown maize kernels in response to drought stress. *Phytopathology 106*, S4.160.

51. Yang, L., Fountain, J.C., Wang, H., Ni, X., Ji, P., Lee, R.D., et al. (2015). Stress sensitivity is associated with differential accumulation of reactive oxygen and nitrogen species in maize genotypes with contrasting levels of drought tolerance. *Int. J. Mol. Sci. 16*, 24791–24819.

52. Zhang, Y., Cui, M., Zhang, J., Zhang, L., Li, C., Kan, X., ... & Yin, Z. (2016). Confirmation and fine mapping of a major QTL for aflatoxin resistance in maize using a combination of linkage and association mapping. *Toxins*, *8*(9), 258.

APPENDIX A

SUPPLEMENTARY INFORMATION FOR PUBLISHED CHAPTERS

Supplemental datasets, figures, and tables for the following previously published chapters can be found online at the following websites.

Chapter 4: Yang and Fountain et al. (2015). *Int. J. Mol. Sci.* 16:24791-24819. doi:10.3390/ijms161024791. http://www.mdpi.com/1422-0067/16/10/24791

Chapter 7: Fountain et al. (2016). *Sci. Rep.* 6:38747. doi:10.1038/srep38747. https://www.nature.com/articles/srep38747

Appendix D: Fountain et al. (2016). *Front. Microbiol.* 7:2048. doi:10.3389/fmicb.2016.02048. http://journal.frontiersin.org/article/10.3389/fmicb.2016.02048/full

APPENDIX B

SUPPLEMENTARY INFORMATION FOR CHAPTER 5

Note: Supplemental tables/datafiles will be available online upon publication.

Figure S5.1. Effect of drought treatment on plant phenotype of selected maize lines. Representative images of six selected maize lines collected at well-watered and drought treated conditions.

Irrigation						
Drought treatment (7 day)						
Irrigation						
Drought treatment (14 day)						
	B73	Lo1016	A638	Lo964	Va35	Grace E-5

Figure S5.2. Hierarchical cluster analysis of differential abundance in all tested samples.

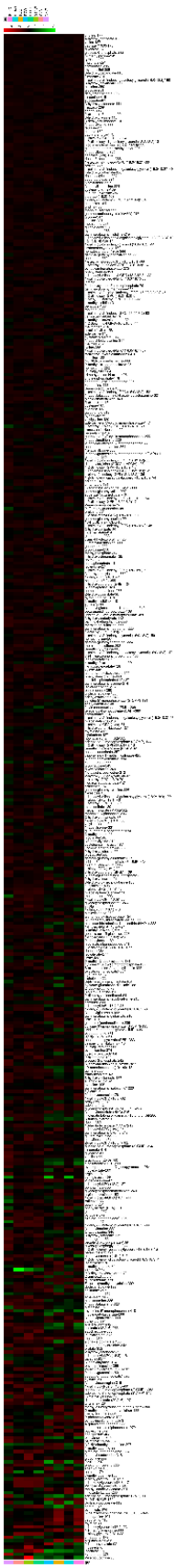

Figure S5.3. Venn diagram showing the overlap of differentially expressed metabolites in maize kernles at different developing stage (A) and different genotypes. S7D, S14D, S7W and S14W refers to the metabolites from B73 with and without drought treatments for 7 and 14 DAI; R7D, R14D, R7W and R14W refers to the metabolites from Lo964 with and without drought treatments for 7 and 14 DAI.

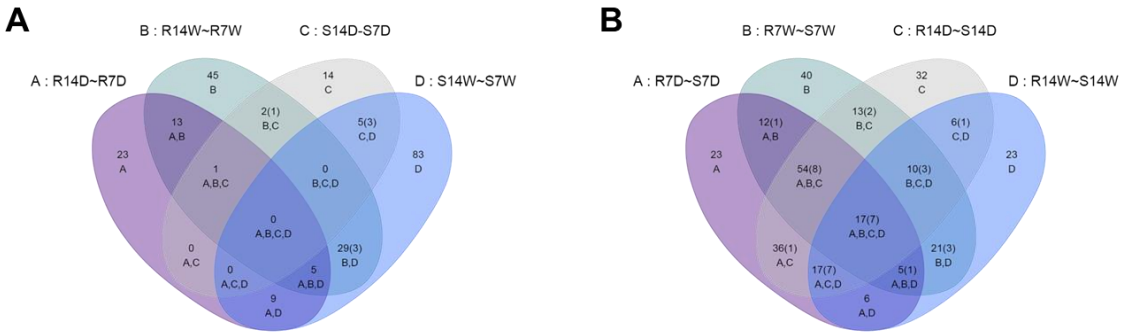
A
B : R14W~R7W
C : S14D-S7D
A : R14D~R7D
D : S14W~S7W
45
B
14
C
13
A,B
2(1)
B,C
5(3)
C,D
23
A
1
A,B,C
0
B,C,D
83
D
0
A,B,C,D
0
A,C
29(3)
B,D
0
A,C,D
5
A,B,D
9
A,D
B
B : R7W~S7W
C : R14D~S14D
A : R7D~S7D
D : R14W~S14W
40
B
32
C
12(1)
A,B
13(2)
B,C
6(1)
C,D
23
A
54(8)
A,B,C
10(3)
B,C,D
23
D
17(7)
A,B,C,D
36(1)
A,C
21(3)
B,D
17(7)
A,C,D
5(1)
A,B,D
6
A,D

Figure S5.4. Correlation analysis between metabolite and metabolite in maize kernels. X- and Y-axes were categorized into different metabolites, grouped by pathway.

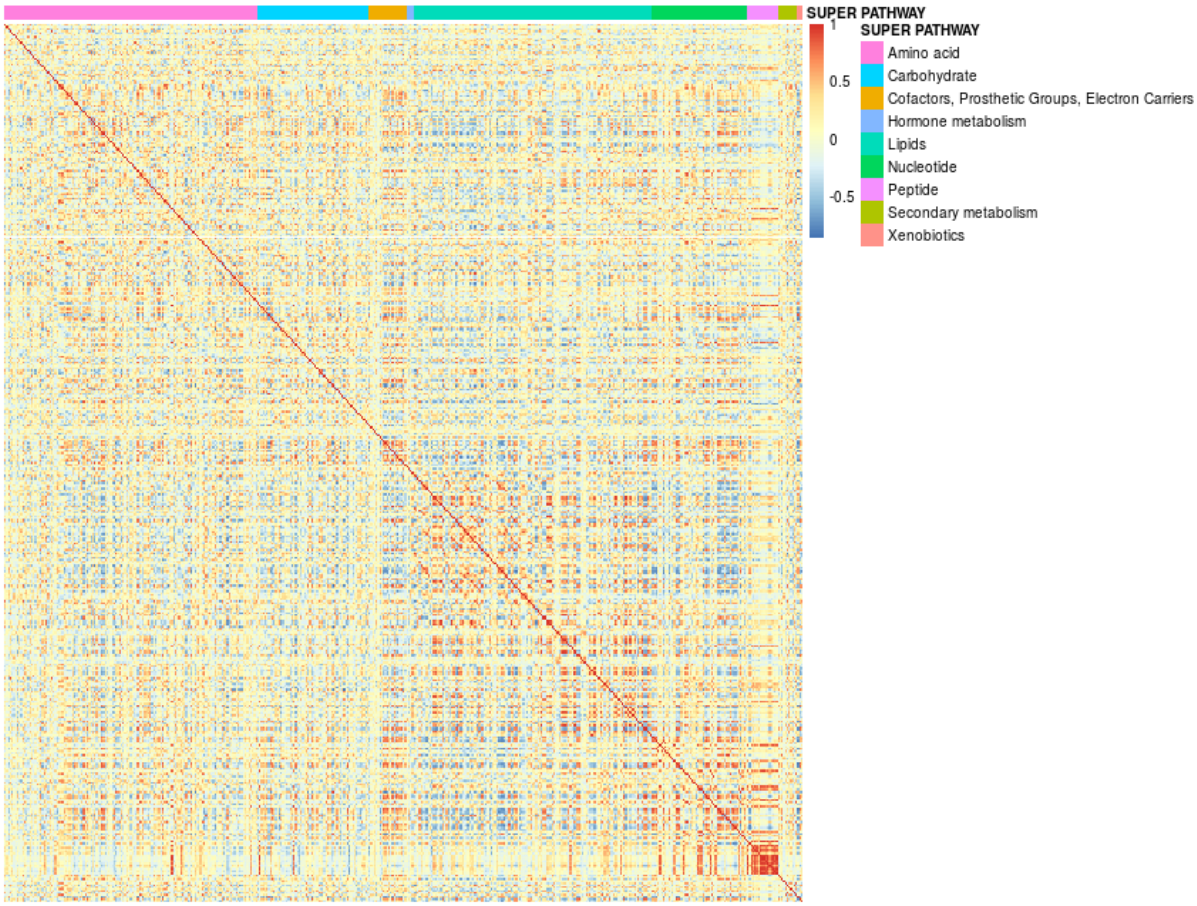
SUPER PATHWAY
SUPER PATHWAY
Amino acid
Carbohydrate
Cofactors, Prosthetic Groups, Electron Carriers
Hormone metabolism
Lipids
Nucleotide
Peptide
Secondary metabolism
Xenobiotics
1
0.5
0
-0.5

Figure S5.5. Metabolic networks constructed by the differentially accumulated metabolites in maize developing kernels in response to drought stress. (A) and (B) refer to the metabolic networks in B73 at 7 and 14 DAI; (C) and (D) refer to the metabolic networks in Lo964 at 7 and 14 DAI.

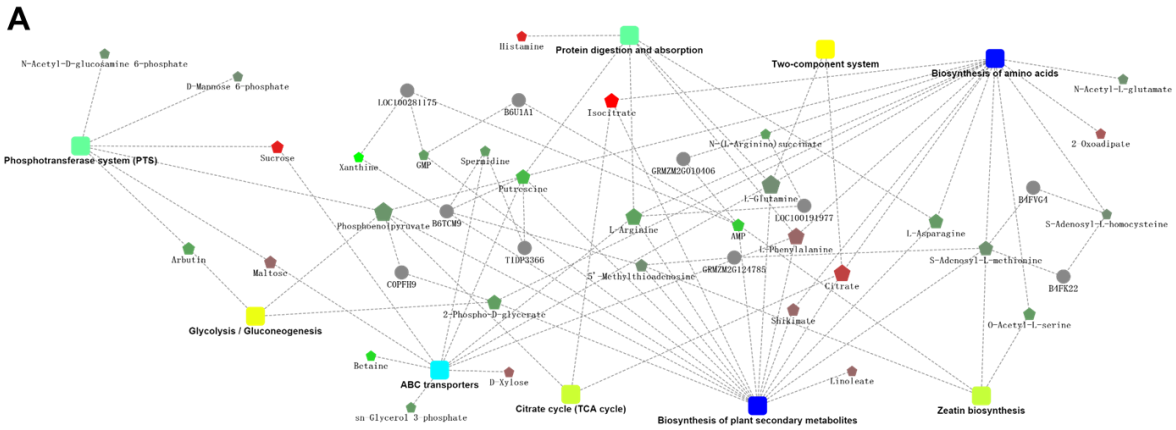
A
Histamine
Protein digestion and absorption
Two-component system
Biosynthesis of amino acids
N-Acetyl-D-glucosamine 6-phosphate
D-Mannose 6-phosphate
N-Acetyl-L-glutamate
LOC100281175
B6U1A1
Isocitrate
2 Oxoadipate
Phosphotransferase system (PTS)
Sucrose
N-(L-Arginino)succinate
Xanthine
GMP
Spermidine
GRMZM2G010406
Putrescine
L-Glutamine
B4FVG4
Phosphoenolpyruvate
B6TCM9
LOC100191977
S-Adenosyl-L-homocysteine
L-Arginine
AMP
L-Asparagine
Arbutin
T1DP3366
L-Phenylalanine
S-Adenosyl-L-methionine
Maltose
S-Methylthioadenosine
GRMZM2G124785
Citrate
COPFH9
B4FK22
2-Phospho-D-glycerate
Shikimate
Glycolysis / Gluconeogenesis
O-Acetyl-L-serine
Betaine
ABC transporters
D-Xylose
Linoleate
Citrate cycle (TCA cycle)
Biosynthesis of plant secondary metabolites
Zeatin biosynthesis
sn-Glycerol 3-phosphate
B
Pyrimidine metabolism
B4FSZ8
Methylmalonate
3-Aminoisobutyric acid
Thymidine
dCMP
Lysine biosynthesis
Q8RUR9
GMP
Biosynthesis of amino acids
N6-(L-1,3-Dicarboxypropyl)-L-lysine
beta-Alanine
LOC100280755
1D-myo-Inositol 3-phosphate
Lysine degradation
L-2-Aminoadipate
B6SMK8
Protein digestion and absorption
Sedoheptulose 7-phosphate
Carbon fixation in photosynthetic organisms
L-Tryptophan
LOC100282482
L-Aspartate
LOC100273302
D-Xylose
Hypotaurine
Taurine
Orthophosphate
Taurine and hypotaurine metabolism
ABC transporters
Glycerol

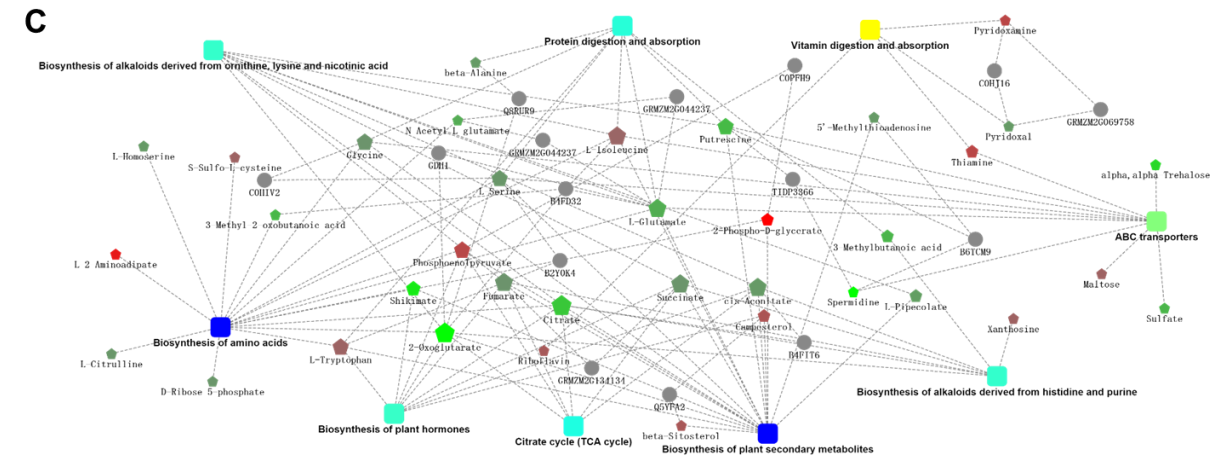
C
Biosynthesis of alkaloids derived from ornithine, lysine and nicotinic acid
Protein digestion and absorption
Vitamin digestion and absorption
ABC transporters
Biosynthesis of amino acids
Biosynthesis of plant hormones
Citrate cycle (TCA cycle)
Biosynthesis of plant secondary metabolites
Biosynthesis of alkaloids derived from histidine and purine
beta-Alanine
N-Acetyl-L-glutamate
Glycine
L-Homoserine
S-Sulfo-L-cysteine
3-Methyl-2-oxobutanoic acid
L-2-Aminoadipate
L-Citrulline
D-Ribose-5-phosphate
L-Tryptophan
Shikimate
Phosphoenolpyruvate
2-Oxoglutarate
Fumarate
Citrate
Riboflavin
Succinate
cis-Aconitate
Campesterol
beta-Sitosterol
L-Isoleucine
L-Serine
L-Glutamate
Putrescine
2-Phospho-D-glycerate
3-Methylbutanoic acid
Spermidine
L-Pipecolate
Xanthosine
Sulfate
Maltose
alpha,alpha-Trehalose
Thiamine
Pyridoxal
Pyridoxamine
5'-Methylthioadenosine
GRMZM2G044237
GRMZM2G069758
Q8RUR9
B4FD32
B2Y0K4
B4FIT6
GRMZM2G134134
Q5YFA2
COPFH9
COHJ16
COHIV2
GDH1
TIDP3366
B6TCM9
B6U1A1
D
Purine metabolism
Zeatin biosynthesis
ABC transporters
antothenate and CoA biosynthesis
Betaine
Guanosine
Deoxyadenosine
Spermidine
Inosine
B4FH67
TIDP3366
GRMZM2G037379
B6TCM9
LOC100285737
D-Ribose
Thiamine
Q5YFA2
Sulfate
Deoxyguanosine
Putrescine
beta-Sitosterol
Nicotinate
NRH2
B6SWM0
B6TYF3
L-Ornithine
Citrate
Campesterol
COPFH9
Allantoate
L-Isoleucine
O-Acetyl-L-serine
C4J0R4
AMP
5'-Methylthioadenosine
LOC100281175
LKRSDH
gpm602a
L-Asparagine
NIT2
L-Tryptophan
B6TPU3
Guanine
L-2-Aminoadipate
PhosphoenolPyruvate
Pyruvate
L-Cysteine
L-Aspartate
beta-Alanine
2-Phospho-D-glycerate
2,3-Dihydroxy-3-methylbutanoate
sn-Glycerol-3-phosphate
Uracil
GRMZM2G044237
alpha-Isopropylmalate
3-Methyl-2-oxobutanoic acid
B4FD32
Q8RUR9
L-Citrulline
N6-(L-1,3-Dicarboxypropyl)-L-lysine
2-Oxoglutarate
Shikimate
L-Glutamate
LOC100273676
S-Adenosyl-L-methionine
imc2319
GDH1
LKRSDH
GRMZM2G124785
Biosynthesis of amino acids
Biosynthesis of plant hormones
Biosynthesis of plant secondary metabolites
Citrate cycle (TCA cycle)

Figure S5.6. Statistical comparison design. Statistical comparisons between samples from each lines, indicated by arrows, were conducted between 7 and 14 DAI within each lines, 7 and 14-day well-watering within each lines, drought treatment and well-watered conditions within each lines, and drought treatment or well-watered conditions between two lines.

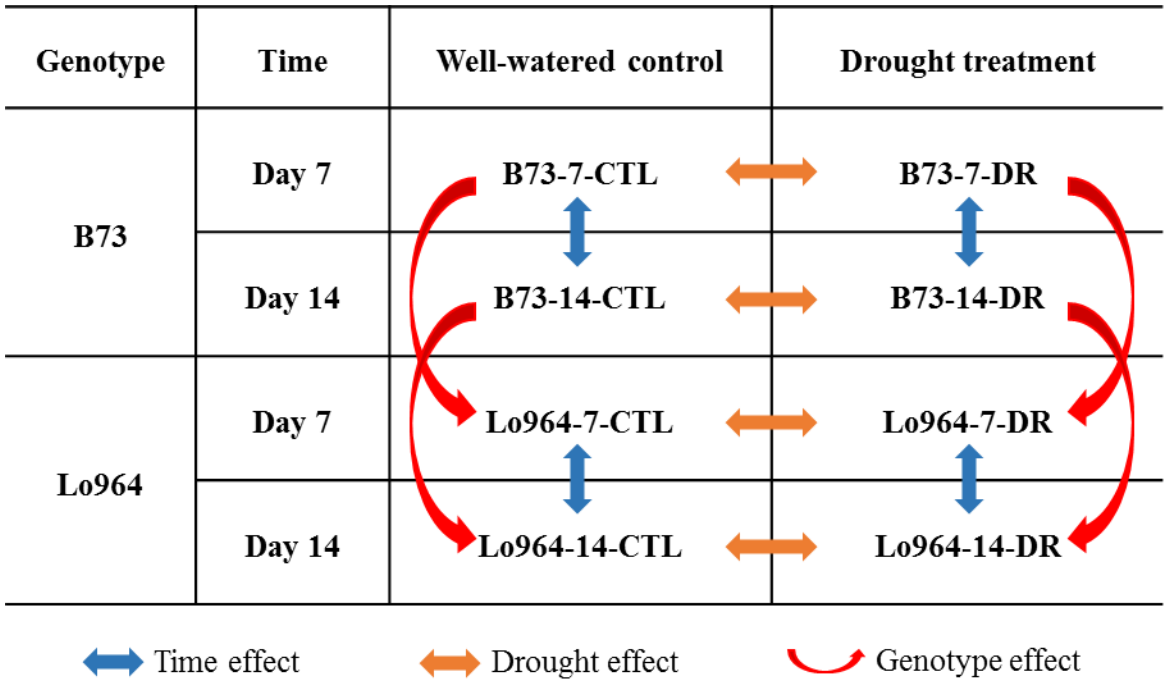
Genotype
Time
Well-watered control
Drought treatment
B73
Day 7
B73-7-CTL
B73-7-DR
Day 14
B73-14-CTL
B73-14-DR
Lo964
Day 7
Lo964-7-CTL
Lo964-7-DR
Day 14
Lo964-14-CTL
Lo964-14-DR
Time effect
Drought effect
Genotype effect

APPENDIX C

SUPPLEMENTARY INFORMATION FOR CHAPTER 8

Figure S8.1. One-dimensional polyacrylamide gel electrophoresis (1D-PAGE). An aliquot of the isolated proteins used for iTRAQ proteomics was used for 1D-PAGE to check the quality and quantity of the samples used. The lanes are as labeled with the first lane containing a protein size ladder ranging from 10 – 260kDa. No protein degradation or inconsistency in detected intensity was detected between the samples prior to iTRAQ analysis.

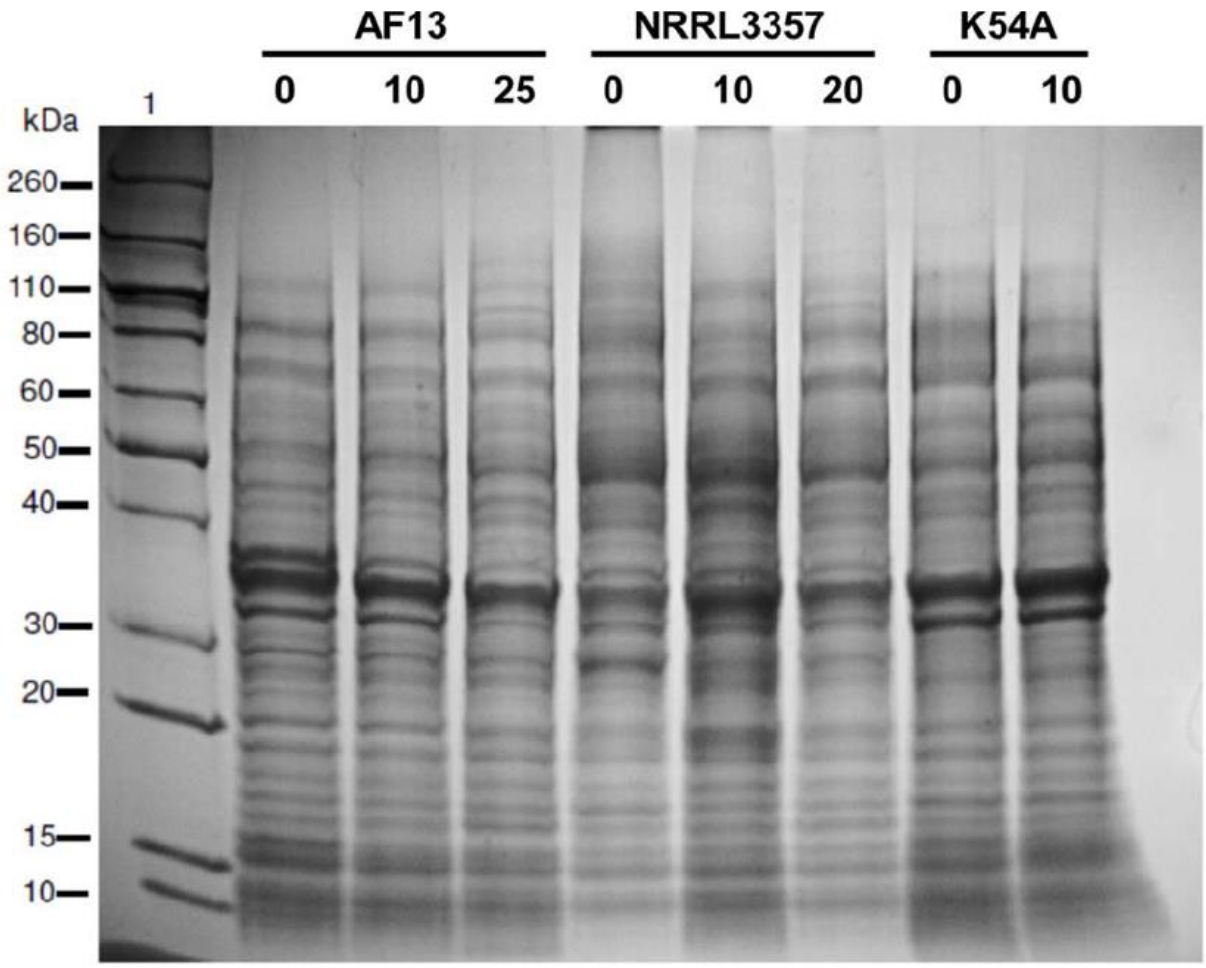
AF13
NRRL3357
K54A
0
10
25
0
10
20
0
10
kDa
1
260
160
110
80
60
50
40
30
20
15
10

Figure S8.2. Pearson correlations of proteome and transcriptome data for select metabolic pathways. Pearson correlations of detected protein expression with corresponding transcripts when comparing the control and 10mM H_2O_2 treatments were performed for proteins involved in glutathione metabolism, the pentose phosphate pathway, and aminobenzoate degradation for all isolates (overall plots) and for each individual isolate. Greater degrees of correlation could be observed within each pathway both overall and within each isolate than observed for all proteins and transcripts. Isolate-to isolate variation in correlation was also observed within each pathway likely corresponding to the degree of differential expression observed for the proteins and transcripts in each pathway.

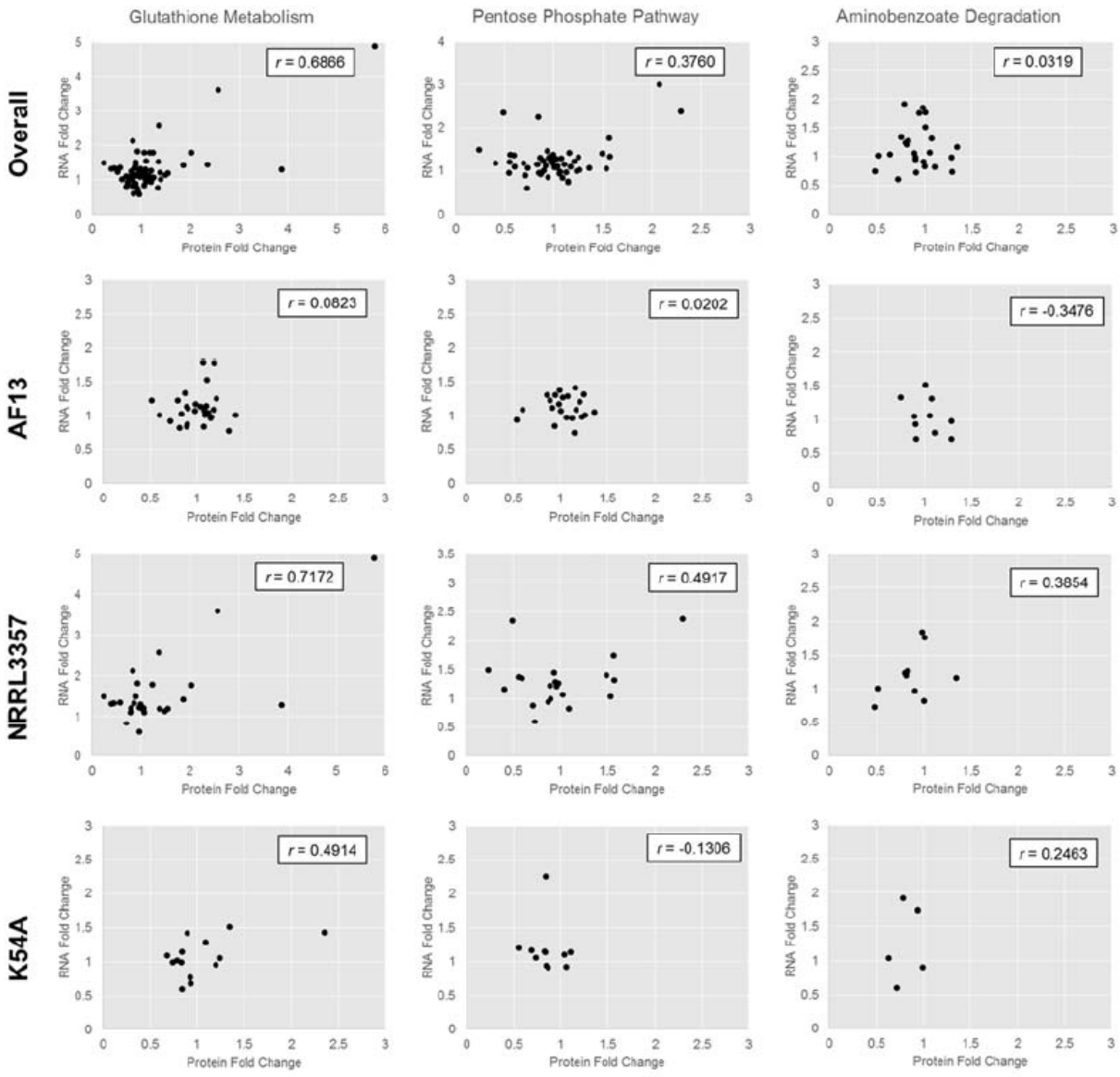
Glutathione Metabolism
Pentose Phosphate Pathway
Aminobenzoate Degradation
Overall
AF13
NRRL3357
K54A
r = 0.6866
r = 0.3760
r = 0.0319
r = 0.0823
r = 0.0202
r = -0.3476
r = 0.7172
r = 0.4917
r = 0.3854
r = 0.4914
r = -0.1306
r = 0.2463
RNA Fold Change
Protein Fold Change

Figure S8.3. STRING interaction networks for differentially expressed proteins observed in each isolate in response to increasing levels of oxidative stress. STRING interaction plots for AF13 (A), NRRL3357 (B), and K54A (C) were performed. Nodes are colored based on software default parameters. Distance between nodes and their position relative to each other indicate their relatedness in terms of biological function, protein-protein interaction, and co-expression. Lines connecting nodes represent different forms of evidence for a relationship between the proteins connected by the nodes. Of note are the following colored lines representing available evidence of interactions: light blue: known interactions from curated databases; pink: experimentally determined interactions; dark blue: gene co-occurance; yellow: textmining; and black: co-expression.

A

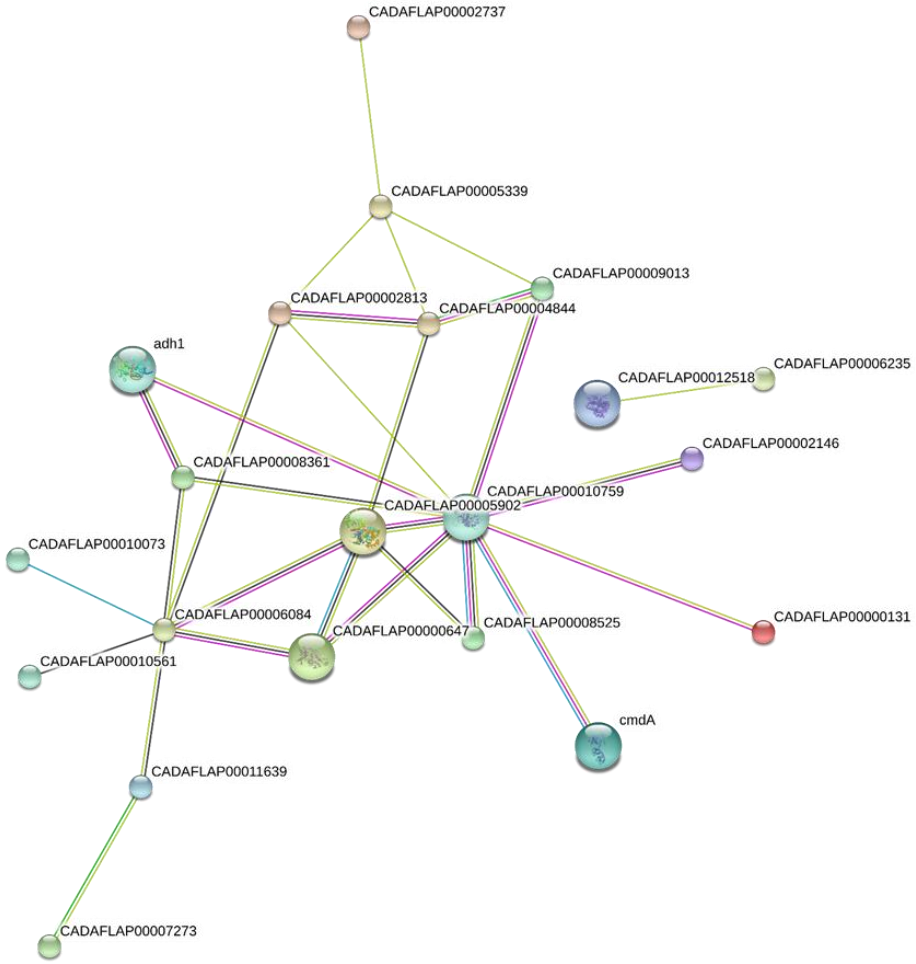
CADAFLAP00002737
CADAFLAP00005339
CADAFLAP00009013
CADAFLAP00002813
CADAFLAP00004844
adh1
CADAFLAP00012518
CADAFLAP00006235
CADAFLAP00002146
CADAFLAP00008361
CADAFLAP00010759
CADAFLAP00005902
CADAFLAP00010073
CADAFLAP00006084
CADAFLAP00000647
CADAFLAP00008525
CADAFLAP00000131
CADAFLAP00010561
cmdA
CADAFLAP00011639
CADAFLAP00007273

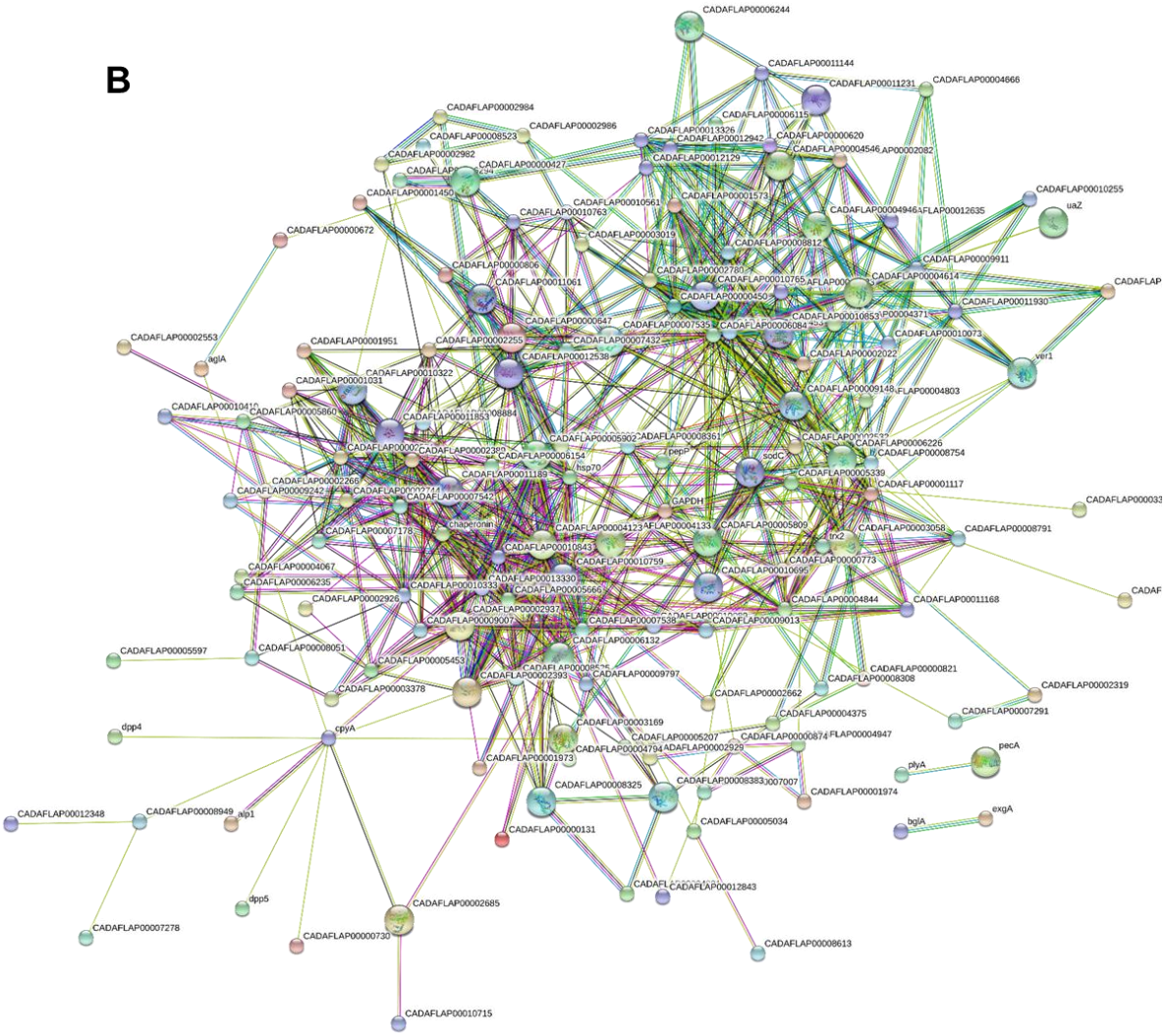
B
CADAFLAP00006244
CADAFLAP00011144
CADAFLAP00011231
CADAFLAP00004666
CADAFLAP00002984
CADAFLAP00002986
CADAFLAP00008523
CADAFLAP00006115
CADAFLAP00012942
CADAFLAP00000620
CADAFLAP00002982
CADAFLAP00004546
CADAFLAP00012129
CADAFLAP00000427
CADAFLAP00001450
CADAFLAP00001573
CADAFLAP00010255
CADAFLAP00010561
CADAFLAP00010763
CADAFLAP00004946
CADAFLAP00012635
uaZ
CADAFLAP00000672
CADAFLAP00003019
CADAFLAP00008812
CADAFLAP00000911
CADAFLAP00000806
CADAFLAP00011061
CADAFLAP00004614
CADAFLAP00000450
CADAFLAP00011930
CADAFLAP00002553
CADAFLAP00001951
CADAFLAP00002255
CADAFLAP00007432
CADAFLAP00010973
aglA
CADAFLAP00012538
CADAFLAP00002022
ver1
CADAFLAP00010322
CADAFLAP00001031
CADAFLAP00009148
CADAFLAP00004803
CADAFLAP00005860
CADAFLAP00008361
CADAFLAP00006226
CADAFLAP00002266
CADAFLAP00011189
CADAFLAP00005339
CADAFLAP00001117
CADAFLAP00009242
CADAFLAP00007542
GAPDH
CADAFLAP00007178
CADAFLAP00004123
CADAFLAP00005809
CADAFLAP00003058
CADAFLAP00008791
CADAFLAP00010843
trx2
CADAFLAP00004067
CADAFLAP00010759
CADAFLAP00000773
CADAFLAP00006235
CADAFLAP00013330
CADAFLAP00010333
CADAFLAP00005666
CADAFLAP00002926
CADAFLAP00004844
CADAFLAP00011168
CADAFLAP00009007
CADAFLAP00007538
CADAFLAP00009013
CADAFLAP00006132
CADAFLAP00005597
CADAFLAP00008051
CADAFLAP00005453
CADAFLAP00000821
CADAFLAP00002393
CADAFLAP00009797
CADAFLAP00008308
CADAFLAP00003378
CADAFLAP00002662
CADAFLAP00002319
CADAFLAP00004375
CADAFLAP00007291
dpp4
cpyA
CADAFLAP00003169
CADAFLAP00005207
CADAFLAP00000874
CADAFLAP00004947
CADAFLAP00004794
CADAFLAP00002929
pecA
CADAFLAP00001973
plyA
CADAFLAP00008325
CADAFLAP00008383
CADAFLAP00007007
CADAFLAP00001974
CADAFLAP00012348
CADAFLAP00008949
alp1
exgA
bglA
CADAFLAP00000131
CADAFLAP00005034
CADAFLAP00012843
dpp5
CADAFLAP00002685
CADAFLAP00007278
CADAFLAP00000738
CADAFLAP00008613
CADAFLAP00010715

C

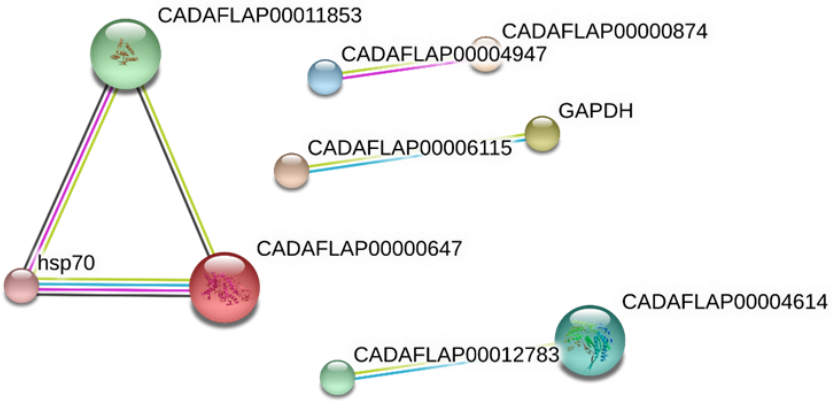
CADAFLAP00011853
CADAFLAP00000874
CADAFLAP00004947
GAPDH
CADAFLAP00006115
hsp70
CADAFLAP00000647
CADAFLAP00004614
CADAFLAP00012783

Table S8.1. Summary of generated iTRAQ proteomics data

Data	*FDR Type*	FDR	Rep 1	Rep 2	Rep 3	Average
Proteins	Global	1%	2,147	1,907	1,646	1,900
Distinct Peptides	Global	1%	19,936	17,479	17,677	18,364
Spectra	Global	1%	67,246	66,352	74,767	69,455

Table S8.2. Differentially expressed proteins in A. flavus isolates in response to oxidative stress.

Gene ID	Uniprot ID	Annotation	Fold Change	p-value
		AF13 0 v 10mM		
AFLA_095660	B8NKY3	Immunoglobulin G-binding protein H, putative	5.1563	0.0068
AFLA_021870	A0A0D9MMH9	Glucanase	4.9830	0.0015
AFLA_033400	A0A0D9N9J1	alpha-1,2-Mannosidase	3.0115	0.0295
AFLA_026140	B8N0S9	Alpha-amylase	2.9625	0.0081
AFLA_045980	A0A0D9N070	Prolyl oligopeptidase family protein	2.3179	0.0008
AFLA_097750	C5H8J2	SspA	1.8977	0.0320
AFLA_027070	B8N394	Acetyl-coenzyme A synthetase	1.8851	0.0122
AFLA_057770	B8NE46	Probable pectate lyase A	1.8573	0.0174
AFLA_006960	B8NQL4	Molecular chaperone and allergen Mod-E/Hsp90/Hsp1	1.8458	0.0132
AFLA_125270	A0A0D9MSQ9	Uncharacterized protein	1.8241	0.0272
AFLA_130150	A0A0D9NA25	Uncharacterized protein	1.8014	0.0104
AFLA_078900	B8MXV3	Beta-hexosaminidase	1.7422	0.0205
AFLA_102010	B8NU30	Class V chitinase, putative	1.7272	0.0056
AFLA_124500	B8NML4	Nitric oxide synthase, putative	1.6632	0.0162
AFLA_051140	A0A0D9MWN4	Beta-glucosidase	1.4575	0.0509
AFLA_076170	B8MX30	Uncharacterized protein	1.2767	0.0001
AFLA_139480	C9K205	Dimethylallyl tryptophan synthase	1.1705	0.0399
AFLA_076180	B8MX31	Uncharacterized protein	1.0849	0.0034
AFLA_029850	B8N1C0	Cysteine-rich secreted protein	0.9040	0.0016
AFLA_040120	B8NAG7	Flavohemoprotein	0.7818	0.0239
AFLA_071010	B8NK52	Heat shock protein (Sti1), putative	0.5110	0.0150
AFLA_034380	B8N244	Catalase, putative	0.4921	0.0033
AFLA_099650	B8NTN4	Woronin body major protein, putative	0.4431	0.0015
AFLA_063320	B8NFJ8	Uncharacterized protein	0.4424	0.0248
AFLA_122720	A0A0D9MR79	Variant SH3 domain protein	0.4400	0.0254
AFLA_022480	B8N5C0	26S proteasome regulatory particle subunit Rpn8, putative	0.3797	0.0087
AFLA_026020	Q52QR9	Calmodulin A	0.3513	0.0289
AFLA_027710	B8N0Z6	Peptidyl-prolyl cis-trans isomerase	0.3390	0.0466
AFLA_056260	B8ND65	Nascent polypeptide-associated complex (NAC) subunit, putative	0.3336	0.0411
AFLA_133940	B8NFW5	Uncharacterized protein	0.2663	0.0236
AFLA_045750	B8NBK0	Antigenic mitochondrial protein HSP60, putative	0.2607	0.0198
AFLA_054750	B8ND04	Malate dehydrogenase, NAD-dependent	0.2599	0.0205
AFLA_093280	B8NKS4	Disulfide isomerase (TigA), putative	0.2564	0.0202
AFLA_060110	B8NEA2	Uncharacterized protein	0.2151	0.0155
AFLA_050270	B8NSS6	Conserved lysine-rich protein, putative	0.1869	0.0097
AFLA_070490	B8NK00	Uncharacterized protein	0.1845	0.0203
AFLA_031780	B8N3U4	Telomere and ribosome associated protein Stm1, putative	0.1715	0.0031
AFLA_088570	B8MWG7	Uncharacterized protein	0.1676	0.0068
AFLA_117640	B8NVS7	CipC-like antibiotic stress responsive protein	0.1645	0.0091
AFLA_042700	A0A0D9MTF9	RNA recognition motif	0.1563	0.0232
AFLA_007700	B8NXF1	Uncharacterized protein	0.1456	0.0117
AFLA_069370	B8NIQ9	Phosphoglycerate kinase	0.1434	0.0025

Table S8.2. Cont.

Gene ID	Uniprot ID	Annotation	Fold Change	p-value
AFLA_073480	B8MW01	Tropomyosin, putative	0.1337	0.0088
AFLA_033620	B8N439	RNA binding protein, putative	0.1317	0.0441
AFLA_052860	B8NS55	Chaperone/heat shock protein Hsp12, putative	0.1170	0.0306
AFLA_028800	B8N3H7	Eukaryotic translation initiation factor 5A	0.0783	0.0284
		AF13 0 v 25mM		
AFLA_095660	B8NKY3	Immunoglobulin G-binding protein H, putative	15.5847	0.0003
AFLA_048690	A0A0D9N9P4	Alcohol dehydrogenase GroES-like domain protein	5.3708	0.0373
AFLA_004950	B8NQA4	Cytochrome c oxidase subunit Va, putative	2.7840	0.0240
AFLA_121090	B8NWS2	Uncharacterized protein	2.7659	0.0288
AFLA_078650	B8MXS8	ATP synthase subunit alpha	1.9208	0.0177
AFLA_069370	B8NIQ9	Phosphoglycerate kinase	1.7182	0.0340
AFLA_099010	B8NUD9	Transaldolase	1.7166	0.0157
AFLA_006960	B8NQL4	Molecular chaperone and allergen Mod-E/Hsp90/Hsp1	1.5606	0.0136
AFLA_119460	A0A0D9MQY3	NAD dependent epimerasedehydratase family protein	1.4746	0.0404
AFLA_111100	B8N9G4	Mitochondrial peroxiredoxin Prx1, putative	1.4179	0.0330
AFLA_039410	B8NCN4	Cell wall serine-threonine-rich galactomannoprotein Mp1	1.3686	0.0534
AFLA_071350	B8NJ18	UDP-N-acetylglucosamine pyrophosphorylase	1.3415	0.0281
AFLA_029850	B8N1C0	Cysteine-rich secreted protein	0.9290	0.0033
AFLA_076170	B8MX30	Uncharacterized protein	0.9241	0.0412
AFLA_034380	B8N244	Catalase, putative	0.5908	0.0395
AFLA_007700	B8NXF1	Uncharacterized protein	0.5875	0.0197
AFLA_060110	B8NEA2	Uncharacterized protein	0.4245	0.0155
		NRRL3357 0 v 10mM		
AFLA_007700	B8NXF1	Uncharacterized protein	4.8380	0.0000
AFLA_112130	A0A0D9MS17	Hydrophobic surface binding protein A	4.5253	0.0071
AFLA_054750	B8ND04	Malate dehydrogenase, NAD-dependent	4.3005	0.0449
AFLA_050270	B8NSS6	Conserved lysine-rich protein, putative	3.4445	0.0424
AFLA_069370	B8NIQ9	Phosphoglycerate kinase	3.2011	0.0188
AFLA_097190	B8NU47	Uncharacterized protein	3.1380	0.0470
AFLA_012200	B8NYQ1	Hsp70 chaperone (HscA), putative	2.9971	0.0033
AFLA_130310	B8NPF9	Protein disulfide-isomerase	2.9678	0.0056
AFLA_045750	B8NBK0	Antigenic mitochondrial protein HSP60, putative	2.8139	0.0003
AFLA_044620	B8NB87	Mitochondrial Hsp70 chaperone (Ssc70), putative	2.4698	0.0034
AFLA_040120	B8NAG7	Flavohemoprotein	2.3532	0.0135
AFLA_034050	B8N211	Aconitate hydratase, mitochondrial	2.2716	0.0086
AFLA_022380	B8N5B0	Molecular chaperone Hsp70	2.2652	0.0358
AFLA_028910	B8N3I8	Polyadenylate-binding protein	2.2287	0.0506
AFLA_033100	B8N3Y7	Phosphatidylinositol transporter, putative	2.2080	0.0045
AFLA_035620	B8N4E9	Hsp70 chaperone BiP/Kar2, putative	2.1612	0.0308
AFLA_093280	B8NKS4	Disulfide isomerase (TigA), putative	2.1103	0.0263
AFLA_119660	B8NWC9	ATP synthase subunit beta	2.0259	0.0443
AFLA_038700	A0A0D9NC88	Peptide hydrolase	1.7118	0.0036
AFLA_008310	A0A0D9MUN9	Thiolase N-terminal domain protein	1.6783	0.0239
AFLA_122720	A0A0D9MR79	Variant SH3 domain protein	1.6142	0.0112
AFLA_095660	B8NKY3	Immunoglobulin G-binding protein H, putative	1.5212	0.0031

Table S8.2. Cont.

Gene ID	Uniprot ID	Annotation	Fold Change	p-value
AFLA_027810	A0A0D9MQC0	Subtilase family protein	1.2614	0.0237
AFLA_023500	A0A0D9N0I0	Ser-Thr-rich glycosyl-phosphatidyl-inositol-anchored membrane	1.2208	0.0149
AFLA_136640	B8NGN7	Translation elongation factor EF-2 subunit, putative	0.8556	0.0337
AFLA_108790	B8N8T4	Aldehyde dehydrogenase AldA, putative	0.6861	0.0480
AFLA_112120	B8N9R6	Pyruvate carboxylase	0.6007	0.0325
AFLA_110600	B8N9B4	Aminopeptidase	0.5475	0.0417
AFLA_045980	A0A0D9N070	Prolyl oligopeptidase family protein	0.4090	0.0004
		NRRL3357 0 v 20mM		
AFLA_105920	P41749	Endopolygalacturonase A	13.8028	0.0089
AFLA_028800	B8N3H7	Eukaryotic translation initiation factor 5A	11.8265	0.0015
AFLA_019230	B8N6F9	Mismatched base pair and cruciform DNA recognition protein, put	9.3129	0.0061
AFLA_112130	A0A0D9MS17	Hydrophobic surface binding protein A	8.9999	0.0197
AFLA_057240	A0A0D9MQY5	RNA recognition motif	8.9178	0.0215
AFLA_089380	A0A0D9MZ41	Endo-chitosanase	8.5050	0.0006
AFLA_045750	B8NBK0	Antigenic mitochondrial protein HSP60, putative	8.0881	0.0000
AFLA_069370	B8NIQ9	Phosphoglycerate kinase	7.5484	0.0000
AFLA_093220	B8NKR8	Ran-specific GTPase-activating protein 1, putative	6.9233	0.0159
AFLA_136570	B8NGN0	Cytochrome c	6.8061	0.0024
AFLA_043730	B8NAZ8	Nuclear protein export protein Yrb2, putative	6.3921	0.0411
AFLA_048510	B8NSI8	UV excision repair protein (RadW), putative	6.3291	0.0164
AFLA_025760	B8N351	50S ribosomal protein L12	6.0343	0.0300
AFLA_066270	B8NID1	RNA-binding La domain protein	5.9871	0.0220
AFLA_031780	B8N3U4	Telomere and ribosome associated protein Stm1, putative	5.9799	0.0000
AFLA_091060	B8NLH9	Allergen Asp F3	5.7723	0.0109
AFLA_003440	B8NQW0	Translation initiation factor 4B	5.7504	0.0000
AFLA_044620	B8NB87	Mitochondrial Hsp70 chaperone (Ssc70), putative	5.5549	0.0000
AFLA_082510	B8MYW2	TCTP family protein	5.5169	0.0099
AFLA_030860	A0A0D9MYG7	Uncharacterized protein	5.4935	0.0231
AFLA_106310	B8N837	Chaperonin, putative	5.4231	0.0216
AFLA_091990	B8NKN3	Peptidyl-prolyl cis-trans isomerase	5.1617	0.0022
AFLA_006520	A0A0D9N6X4	Scd6-like Sm domain protein	4.8678	0.0386
AFLA_076710	A0A0D9N180	Malate dehydrogenase	4.8412	0.0000
AFLA_028910	B8N3I8	Polyadenylate-binding protein	4.8204	0.0000
AFLA_033100	B8N3Y7	Phosphatidylinositol transporter, putative	4.8118	0.0000
AFLA_126870	B8NMS4	Uncharacterized protein	4.7704	0.0102
AFLA_004950	B8NQA4	Cytochrome c oxidase subunit Va, putative	4.6372	0.0002
AFLA_132540	B8NH30	Thioredoxin	4.5661	0.0130
AFLA_099000	Q8NK14	Cu,Zn-superoxide dismutase (Fragment)	4.5307	0.0172
AFLA_089270	A0A0D9N5A3	Basic region leucine zipper	4.3982	0.0394
AFLA_057670	B8NE36	Neutral protease 2	4.3020	0.0121
AFLA_091270	B8NKG1	Fumarate hydratase, putative	4.3014	0.0066
AFLA_093660	B8NKW2	Solid-state culture expressed protein (Aos23), putative	4.2034	0.0004
AFLA_117850	B8NW38	RPEL repeat protein	4.1850	0.0230
AFLA_002560	B8NPV3	60S ribosomal protein L37a	4.0878	0.0301
AFLA_112910	B8N9Z5	Uncharacterized protein	4.0491	0.0319

Table S8.2. Cont.

Gene ID	Uniprot ID	Annotation	Fold Change	p-value
AFLA_133920	B8NFW3	Acyl CoA binding protein family	3.9799	0.0516
AFLA_111100	B8N9G4	Mitochondrial peroxiredoxin Prx1, putative	3.8786	0.0002
AFLA_135540	B8NHE9	ATP synthase oligomycin sensitivity conferral protein, putative	3.8065	0.0100
AFLA_094630	B8NM07	Triosephosphate isomerase	3.7901	0.0003
AFLA_022470	B8N5B9	Adenylate kinase	3.7778	0.0034
AFLA_043390	B8NAW4	Hsp70 chaperone (BiP), putative	3.7297	0.0126
AFLA_012200	B8NYQ1	Hsp70 chaperone (HscA), putative	3.7234	0.0000
AFLA_136600	B8NGN3	GrpE protein homolog	3.6832	0.0271
AFLA_006300	B8NQF0	Nucleoside diphosphate kinase	3.6605	0.0380
AFLA_035620	B8N4E9	Hsp70 chaperone BiP/Kar2, putative	3.6524	0.0000
AFLA_132990	B8NH75	Ribosomal protein L34 protein, putative	3.6256	0.0412
AFLA_008910	B8NXS1	Uncharacterized protein	3.5379	0.0346
AFLA_035510	A0A0D9N8A2	KH domain protein	3.5028	0.0002
AFLA_056260	B8ND65	Nascent polypeptide-associated complex (NAC) subunit, putative	3.4917	0.0148
AFLA_032890	B8N1Y5	Uncharacterized protein	3.4883	0.0017
AFLA_023500	A0A0D9N0I0	Ser-Thr-rich glycosyl-phosphatidyl-inositol-anchored membrane fa	3.4875	0.0123
AFLA_073480	B8MW01	Tropomyosin, putative	3.4259	0.0334
AFLA_071010	B8NK52	Heat shock protein (Sti1), putative	3.3882	0.0014
AFLA_029390	B8N174	HMG box protein, putative	3.3548	0.0253
AFLA_037490	B8N2H4	Eukaryotic translation initiation factor 3 subunit J	3.2690	0.0305
AFLA_022380	B8N5B0	Molecular chaperone Hsp70	3.2121	0.0003
AFLA_033690	B8N446	60S ribosomal protein L31e	3.2025	0.0269
AFLA_054750	B8ND04	Malate dehydrogenase, NAD-dependent	3.2016	0.0319
AFLA_036640	B8N4G1	PH domain protein	3.1291	0.0160
AFLA_033620	B8N439	RNA binding protein, putative	3.0908	0.0150
AFLA_021820	B8N7G0	Nuclear movement protein NudC	3.0902	0.0191
AFLA_069010	B8NJU1	S-adenosylmethionine synthase	3.0484	0.0003
AFLA_007700	B8NXF1	Uncharacterized protein	3.0378	0.0019
AFLA_025990	B8N0R4	Clathrin light chain	3.0098	0.0381
AFLA_113000	B8NA04	Integral ER membrane protein Scs2, putative	3.0067	0.0126
AFLA_087950	B8MWA5	Isocitrate dehydrogenase LysB	2.9508	0.0520
AFLA_135200	B8NHB5	Uncharacterized protein	2.9388	0.0184
AFLA_067940	B8NIK7	Uncharacterized protein	2.9382	0.0282
AFLA_139300	Q5VD95	Ver-1	2.9378	0.0401
AFLA_080240	B8MY87	ATP synthase delta chain, mitochondrial, putative	2.9047	0.0421
AFLA_076450	B8MX58	Electron transfer flavoprotein alpha subunit, putative	2.8451	0.0379
AFLA_041260	B8NCF1	Ribosome associated DnaJ chaperone Zuotin, putative	2.8222	0.0195
AFLA_080390	B8MYA2	6-phosphogluconolactonase, putative	2.7764	0.0180
AFLA_051770	B8NSY4	Thioredoxin reductase	2.7696	0.0015
AFLA_004090	B8NR25	Uncharacterized protein	2.7423	0.0351
AFLA_086710	B8N031	Inorganic diphosphatase, putative	2.7256	0.0052
AFLA_093280	B8NKS4	Disulfide isomerase (TigA), putative	2.6680	0.0021
AFLA_002670	B8NPW4	Curved DNA-binding protein (42 kDa protein)	2.6656	0.0017
AFLA_031960	B8N3W2	40S ribosomal protein S7e	2.5888	0.0248
AFLA_079910	B8MY54	Glutathione peroxidase	2.5725	0.0549

Table S8.2. Cont.

Gene ID	Uniprot ID	Annotation	Fold Change	p-value
AFLA_022270	B8N599	Uncharacterized protein	2.5672	0.0031
AFLA_012160	B8NYP6	Acetyl-CoA acetyltransferase, putative	2.5492	0.0307
AFLA_078380	B8MXQ1	Acetyl-coA hydrolase Ach1, putative	2.5228	0.0111
AFLA_128280	B8NP45	M protein repeat protein	2.4778	0.0012
AFLA_056850	B8NDC4	Electron transfer flavoprotein, beta subunit, putative	2.4733	0.0053
AFLA_122720	A0A0D9MR79	Variant SH3 domain protein	2.4677	0.0250
AFLA_030180	B8N1F3	Protein mitochondrial targeting protein (Mas1), putative	2.4320	0.0511
AFLA_076680	B8MX81	Acetyltransferase component of pyruvate dehydrogenase complex	2.4213	0.0434
AFLA_106390	B8N845	Ribose 5-phosphate isomerase A	2.4122	0.0304
AFLA_068840	B8NJS4	Aminomethyltransferase	2.3874	0.0336
AFLA_014930	B8N6I0	Cofactor for methionyl-and glutamyl-tRNA synthetase, putative	2.3539	0.0009
AFLA_091030	B8NLH6	Uncharacterized protein	2.3419	0.0526
AFLA_034050	B8N211	Aconitate hydratase, mitochondrial	2.3298	0.0041
AFLA_060260	B8NEB7	Heat shock protein Hsp30/Hsp42, putative	2.3249	0.0031
AFLA_061880	B8NEJ0	Pyridoxine biosynthesis protein	2.3126	0.0104
AFLA_007020	B8NRD5	Citrate synthase	2.3122	0.0102
AFLA_120630	B8NWM6	Glyoxylate/hydroxypyruvate reductase, putative	2.3036	0.0220
N/A	A0A0D9MZ11	ATP synthase D chain mitochondrial ATP5H	2.2920	0.0113
AFLA_119660	B8NWC9	ATP synthase subunit beta	2.2785	0.0053
AFLA_080930	B8MYF5	EF hand domain protein	2.1823	0.0089
AFLA_131280	B8NFM7	Actin cortical patch assembly protein Pan1, putative	2.1482	0.0197
AFLA_099650	B8NTN4	Woronin body major protein, putative	2.1429	0.0005
AFLA_075060	B8MWP8	Transformer-SR ribonucleoprotein, putative	2.1380	0.0396
AFLA_048610	B8NSJ8	Succinyl-CoA synthetase alpha subunit, putative	2.0954	0.0184
AFLA_052400	B8NS09	Isocitrate lyase	2.0952	0.0292
AFLA_026470	B8N0W2	Aspartate aminotransferase	2.0949	0.0349
AFLA_046470	A0A0D9MT15	Peptidylprolyl isomerase	2.0230	0.0450
AFLA_095570	B8NMC5	RNA annealing protein Yra1, putative	2.0178	0.0405
AFLA_007000	B8NQL8	Ubiquinol-cytochrome C reductase complex core protein 2, putativ	2.0151	0.0226
AFLA_040120	B8NAG7	Flavohemoprotein	1.9342	0.0426
AFLA_134120	B8NG73	Orotate phosphoribosyltransferase	1.9075	0.0450
AFLA_025980	B8N0R3	Hsp90 co-chaperone Cdc37	1.8733	0.0462
AFLA_022480	B8N5C0	26S proteasome regulatory particle subunit Rpn8, putative	1.8507	0.0266
AFLA_029440	B8N179	NADH-cytochrome b5 reductase	1.8281	0.0087
AFLA_134340	B8NG94	BAR domain protein	1.8252	0.0151
AFLA_032870	B8N1Y3	cAMP-dependent protein kinase regulatory subunit	1.8226	0.0302
AFLA_127390	B8NNC8	Proteasome regulatory particle subunit Rpt5, putative	1.8044	0.0184
AFLA_042700	A0A0D9MTF9	RNA recognition motif	1.8035	0.0372
AFLA_035540	B8N4E1	Signal transducing adapter molecule, putative	1.7254	0.0302
AFLA_045330	B8NBF8	Eukaryotic translation initiation factor subunit eIF-4F, putative	1.6279	0.0247
AFLA_088570	B8MWG7	Uncharacterized protein	1.4967	0.0412
AFLA_029850	B8N1C0	Cysteine-rich secreted protein	0.9015	0.0015
AFLA_106350	B8N841	ATP citrate lyase subunit (Acl), putatibe	0.5678	0.0525
AFLA_070990	B8NK50	UTP-glucose-1-phosphate uridylyltransferase Ugp1, putative	0.5061	0.0318
AFLA_044820	B8NBA7	Glucose-6-phosphate isomerase	0.4950	0.0215

Table S8.2. Cont.

Gene ID	Uniprot ID	Annotation	Fold Change	p-value
AFLA_056170	B8NDX6	Catalase	0.4613	0.0410
AFLA_133990	B8NFX0	Secretory pathway gdp dissociation inhibitor	0.4509	0.0293
AFLA_036110	B8N2C6	4-hydroxyphenylpyruvate dioxygenase	0.4451	0.0142
AFLA_092640	B8NLP8	Alkaline phosphatase	0.4391	0.0296
AFLA_078650	B8MXS8	ATP synthase subunit alpha	0.4391	0.0390
AFLA_020380	B8N500	Stomatin family protein	0.4267	0.0482
AFLA_069590	B8NIT1	Adenosylhomocysteinase	0.4243	0.0335
AFLA_051530	B8NSW0	Methylmalonate-semialdehyde dehydrogenase, putative	0.4211	0.0485
AFLA_126670	B8NMQ4	Uncharacterized protein	0.4207	0.0408
AFLA_109320	B8N8Y6	3-hydroxyisobutyrate dehydrogenase	0.4204	0.0261
AFLA_079480	B8MY11	Oligopeptidase family protein	0.4130	0.0435
AFLA_050690	B8NRS8	Mitochondrial ADP,ATP carrier protein (Ant), putative	0.4082	0.0248
AFLA_031570	B8N3S3	Pyruvate decarboxylase PdcA, putative	0.4008	0.0192
AFLA_083370	B8MZ48	Glutathione oxidoreductase Glr1, putative	0.3978	0.0145
AFLA_038790	B8NCH3	Adenosine deaminase family protein	0.3923	0.0157
AFLA_122180	B8NX31	Uncharacterized protein	0.3909	0.0301
AFLA_044090	B8NB34	Uricase	0.3831	0.0295
AFLA_001890	A0A0D9MRR2	GMC oxidoreductase	0.3791	0.0232
AFLA_028260	B8N151	Probable glucan 1,3-beta-glucosidase A	0.3789	0.0276
AFLA_060110	B8NEA2	Uncharacterized protein	0.3676	0.0432
AFLA_097750	C5H8J2	SspA	0.3621	0.0263
AFLA_027070	B8N394	Acetyl-coenzyme A synthetase	0.3552	0.0135
AFLA_057770	B8NE46	Probable pectate lyase A	0.3498	0.0206
AFLA_117760	B8NVT9	Phytase, putative	0.3470	0.0041
AFLA_110260	B8N980	Flavin-binding monooxygenase-like protein	0.3425	0.0090
AFLA_034870	A0A0D9N8E0	Taurine catabolism dioxygenase TauD TfdA family protein	0.3376	0.0025
AFLA_110600	B8N9B4	Aminopeptidase	0.3318	0.0094
AFLA_078900	B8MXV3	Beta-hexosaminidase	0.3236	0.0220
AFLA_017100	A0A0D9MRY2	Beta-galactosidase	0.3185	0.0013
AFLA_046730	B8NBU8	Uncharacterized protein	0.3156	0.0296
AFLA_099220	B8NUG0	Uncharacterized protein	0.3150	0.0387
AFLA_125270	A0A0D9MSQ9	Uncharacterized protein	0.3106	0.0023
AFLA_077860	B8MXJ9	Uncharacterized protein	0.3018	0.0145
AFLA_031760	B8N3U2	Glutaminase, putative	0.3012	0.0217
AFLA_039410	B8NCN4	Cell wall serine-threonine-rich galactomannoprotein Mp1	0.3002	0.0269
AFLA_036090	B8N2C4	Homogentisate 1,2-dioxygenase (HmgA), putative	0.2844	0.0425
AFLA_128530	B8NP70	Delta-1-pyrroline-5-carboxylate dehydrogenase PrnC	0.2811	0.0143
AFLA_124380	A0A0D9N439	Ricin-type beta-trefoil lectin domain-like protein	0.2726	0.0121
AFLA_074520	B8MWJ5	Probable alpha-galactosidase A	0.2726	0.0514
AFLA_110690	B8N9C3	Cytochrome c peroxidase Ccp1, putative	0.2689	0.0372
AFLA_124500	B8NML4	Nitric oxide synthase, putative	0.2678	0.0039
AFLA_036440	B8N2F9	Alanine aminotransferase, putative	0.2636	0.0476
AFLA_056350	B8ND74	2-methylcitrate dehydratase, putative	0.2536	0.0410
AFLA_036070	B8N2C2	Maleylacetoacetate isomerase MaiA	0.2498	0.0455
AFLA_008990	A0A0D9MP25	Carboxypeptidase	0.2484	0.0258

Table S8.2. Cont.

Gene ID	Uniprot ID	Annotation	Fold Change	p-value
AFLA_103940	B8NV99	Glutamate carboxypeptidase, putative	0.2475	0.0129
AFLA_122110	A0A0D9N4R3	Peroxidase	0.2412	0.0376
AFLA_042090	B8NCX4	Fasciclin domain family protein	0.2401	0.0140
AFLA_036840	B8N4I0	6-phosphogluconate dehydrogenase, decarboxylating	0.2376	0.0230
AFLA_047350	B8NC10	Probable Xaa-Pro aminopeptidase pepP	0.2373	0.0144
AFLA_112470	B8N9V1	Cobalamin-independent methionine synthase MetH/D	0.2364	0.0003
AFLA_112120	B8N9R6	Pyruvate carboxylase	0.2363	0.0028
AFLA_051980	B8NT05	G-protein complex beta subunit CpcB	0.2274	0.0394
AFLA_038700	A0A0D9NC88	Peptide hydrolase	0.2230	0.0316
AFLA_133150	B8NH91	Catechol dioxygenase, putative	0.2226	0.0510
AFLA_086900	B8N050	Alpha-mannosidase	0.2199	0.0135
AFLA_090690	B8NLE2	Mycelial catalase Cat1	0.2178	0.0000
AFLA_130150	A0A0D9NA25	Uncharacterized protein	0.2168	0.0031
AFLA_086800	B8N040	Epoxide hydrolase, putative	0.2052	0.0519
AFLA_139480	C9K205	Dimethylallyl tryptophan synthase	0.1989	0.0046
AFLA_055060	B8ND35	NAD-dependent formate dehydrogenase AciA/Fdh	0.1975	0.0167
AFLA_030140	B8N1E9	60S acidic ribosomal protein P0	0.1961	0.0098
AFLA_055230	B8ND52	Actin Act1	0.1924	0.0237
AFLA_037960	B8N2M1	Glucosamine-fructose-6-phosphate aminotransferase	0.1894	0.0038
AFLA_014520	B8N5V9	Multicopper oxidase, putative	0.1838	0.0017
AFLA_038530	B8NC58	Extracellular metalloproteinase mep	0.1832	0.0087
AFLA_029310	B8N3M8	Alcohol dehydrogenase, zinc-containing, putative	0.1766	0.0044
AFLA_101930	B8NU22	Succinate-semialdehyde dehydrogenase, putative	0.1668	0.0002
AFLA_102010	B8NU30	Class V chitinase, putative	0.1642	0.0032
AFLA_055450	B8NDQ4	Translation elongation factor eEF-1 subunit gamma, putative	0.1419	0.0007
AFLA_025100	B8N2Y6	Glyceraldehyde-3-phosphate dehydrogenase	0.1397	0.0037
AFLA_110160	B8N970	Probable dipeptidyl peptidase 4	0.1381	0.0171
AFLA_076180	B8MX31	Uncharacterized protein	0.1368	0.0193
AFLA_136640	B8NGN7	Translation elongation factor EF-2 subunit, putative	0.1365	0.0000
AFLA_002090	B8NQR5	Extracellular serine carboxypeptidase, putative	0.1354	0.0175
AFLA_026140	B8N0S9	Alpha-amylase	0.1321	0.0498
AFLA_101230	B8NTV2	Glutaminase GtaA	0.1257	0.0350
AFLA_021870	A0A0D9MMH9	Glucanase	0.1221	0.0219
AFLA_108100	B8N8L6	Argininosuccinate synthase	0.1211	0.0036
AFLA_108790	B8N8T4	Aldehyde dehydrogenase AldA, putative	0.1165	0.0000
AFLA_025510	B8N327	GPI anchored protein, putative	0.1109	0.0024
AFLA_033400	A0A0D9N9J1	alpha-1,2-Mannosidase	0.1093	0.0269
AFLA_006960	B8NQL4	Molecular chaperone and allergen Mod-E/Hsp90/Hsp1	0.1079	0.0001
AFLA_101160	B8NUR3	40S ribosomal protein S9	0.0965	0.0062
AFLA_027810	A0A0D9MQC0	Subtilase family protein	0.0836	0.0530
AFLA_051140	A0A0D9MWN4	Beta-glucosidase	0.0706	0.0000
AFLA_139470	B8NI10	Beta-cyclopiazonate dehydrogenase	0.0613	0.0035
AFLA_045980	A0A0D9N070	Prolyl oligopeptidase family protein	0.0585	0.0000
AFLA_076170	B8MX30	Uncharacterized protein	0.0576	0.0018
AFLA_070490	B8NK00	Uncharacterized protein	0.0511	0.0157

Table S8.2. Cont.

Gene ID	Uniprot ID	Annotation	Fold Change	p-value
AFLA_108410	B8N8P6	Dipeptidase	0.0441	0.0046
AFLA_119040	B8NVX6	Muramidase, putative	0.0429	0.0117
AFLA_034640	B8N270	Peptide hydrolase	0.0418	0.0005
		K54A 0 v 10mM		
AFLA_112130	A0A0D9MS17	Hydrophobic surface binding protein A	7.2344	0.0120
AFLA_030880	B8N1M3	Uncharacterized protein	4.0270	0.0296
AFLA_003440	B8NQW0	Translation initiation factor 4B	2.8918	0.0309
AFLA_007700	B8NXF1	Uncharacterized protein	2.7634	0.0329
AFLA_031780	B8N3U4	Telomere and ribosome associated protein Stm1, putative	2.4727	0.0096
AFLA_133920	B8NFW3	Acyl CoA binding protein family	2.2300	0.0386
AFLA_039410	B8NCN4	Cell wall serine-threonine-rich galactomannoprotein Mp1	1.9187	0.0022
AFLA_097190	B8NU47	Uncharacterized protein	1.9056	0.0146
AFLA_057240	A0A0D9MQY5	RNA recognition motif	1.8539	0.0230
AFLA_004950	B8NQA4	Cytochrome c oxidase subunit Va, putative	1.8204	0.0089
AFLA_080930	B8MYF5	EF hand domain protein	1.6398	0.0377
AFLA_044620	B8NB87	Mitochondrial Hsp70 chaperone (Ssc70), putative	1.3370	0.0207
AFLA_071350	B8NJ18	UDP-N-acetylglucosamine pyrophosphorylase	0.6057	0.0357
AFLA_124500	B8NML4	Nitric oxide synthase, putative	0.5997	0.0544
AFLA_078650	B8MXS8	ATP synthase subunit alpha	0.5153	0.0207
AFLA_025100	B8N2Y6	Glyceraldehyde-3-phosphate dehydrogenase	0.5114	0.0269
AFLA_042090	B8NCX4	Fasciclin domain family protein	0.5080	0.0384
AFLA_122110	A0A0D9N4R3	Peroxidase	0.5028	0.0205
AFLA_101160	B8NUR3	40S ribosomal protein S9	0.4074	0.0278
AFLA_055060	B8ND35	NAD-dependent formate dehydrogenase AciA/Fdh	0.4053	0.0488
AFLA_108410	B8N8P6	Dipeptidase	0.3654	0.0067
AFLA_108790	B8N8T4	Aldehyde dehydrogenase AldA, putative	0.3300	0.0468
AFLA_045980	A0A0D9N070	Prolyl oligopeptidase family protein	0.2662	0.0004

Table S8.3. Biological function GO terms enriched among DEPs in A. flavus isolates in response to oxidative stress.

GO Term	Name	Result Count	p-value
	AF13 0 v 10mM		
GO:0005975	carbohydrate metabolic process	8	0.0001
GO:0006457	protein folding	3	0.0010
GO:0071704	organic substance metabolic process	16	0.0077
GO:0006809	nitric oxide biosynthetic process	1	0.0084
GO:0046209	nitric oxide metabolic process	1	0.0084
GO:0042026	protein refolding	1	0.0084
GO:0044238	primary metabolic process	15	0.0101
GO:0051130	positive regulation of cellular component organization	1	0.0126
GO:0032270	positive regulation of cellular protein metabolic process	1	0.0126
GO:0043243	positive regulation of protein complex disassembly	1	0.0126
GO:0051247	positive regulation of protein metabolic process	1	0.0126
GO:0045727	positive regulation of translation	1	0.0126
GO:0045901	positive regulation of translational elongation	1	0.0126
GO:0045905	positive regulation of translational termination	1	0.0126
GO:0043244	regulation of protein complex disassembly	1	0.0126
GO:0006449	regulation of translational termination	1	0.0126
GO:0006452	translational frameshifting	1	0.0126
GO:0006950	response to stress	3	0.0130
GO:0046516	hypusine metabolic process	1	0.0167
GO:0008612	peptidyl-lysine modification to hypusine	1	0.0167
GO:0006108	malate metabolic process	1	0.0209
GO:0018205	peptidyl-lysine modification	1	0.0209
GO:0016052	carbohydrate catabolic process	2	0.0222
GO:0006448	regulation of translational elongation	1	0.0250
GO:0010608	posttranscriptional regulation of gene expression	1	0.0291
GO:0006417	regulation of translation	1	0.0291
GO:0008152	metabolic process	21	0.0296
GO:0009891	positive regulation of biosynthetic process	1	0.0332
GO:0031328	positive regulation of cellular biosynthetic process	1	0.0332
GO:0010557	positive regulation of macromolecule biosynthetic process	1	0.0332
GO:0010604	positive regulation of macromolecule metabolic process	1	0.0332
GO:0009820	alkaloid metabolic process	1	0.0373
GO:0051128	regulation of cellular component organization	1	0.0373
GO:0006096	glycolysis	1	0.0414
GO:0048518	positive regulation of biological process	1	0.0414
GO:0031325	positive regulation of cellular metabolic process	1	0.0414
GO:0048522	positive regulation of cellular process	1	0.0414
GO:0009893	positive regulation of metabolic process	1	0.0414
GO:0006414	translational elongation	1	0.0414
	AF13 0 v 25mM		
GO:0006007	glucose catabolic process	2	0.0006
GO:0019320	hexose catabolic process	2	0.0006
GO:0046365	monosaccharide catabolic process	2	0.0006

Table S8.3. Cont.

GO Term	Name	Result Count	p-value
GO:0044724	single-organism carbohydrate catabolic process	2	0.0009
GO:0006006	glucose metabolic process	2	0.0009
GO:0019318	hexose metabolic process	2	0.0014
GO:0005996	monosaccharide metabolic process	2	0.0020
GO:0016052	carbohydrate catabolic process	2	0.0025
GO:0044723	single-organism carbohydrate metabolic process	2	0.0079
GO:0006950	response to stress	2	0.0111
GO:0009117	nucleotide metabolic process	2	0.0118
GO:0008152	metabolic process	9	0.0132
GO:0006753	nucleoside phosphate metabolic process	2	0.0134
GO:0006096	glycolysis	1	0.0140
GO:0015986	ATP synthesis coupled proton transport	1	0.0154
GO:0015985	energy coupled proton transport, down electrochemical gradient	1	0.0154
GO:0006740	NADPH regeneration	1	0.0209
GO:0006098	pentose-phosphate shunt	1	0.0209
GO:0006739	NADP metabolic process	1	0.0209
GO:0055086	nucleobase-containing small molecule metabolic process	2	0.0214
GO:0015991	ATP hydrolysis coupled proton transport	1	0.0223
GO:0006979	response to oxidative stress	1	0.0223
GO:0015988	energy coupled proton transmembrane transport	1	0.0223
GO:0019362	pyridine nucleotide metabolic process	1	0.0292
GO:0046496	nicotinamide nucleotide metabolic process	1	0.0292
GO:0019637	organophosphate metabolic process	2	0.0303
GO:0072524	pyridine-containing compound metabolic process	1	0.0306
GO:0006754	ATP biosynthetic process	1	0.0333
GO:0009206	purine ribonucleoside triphosphate biosynthetic process	1	0.0347
GO:0009142	nucleoside triphosphate biosynthetic process	1	0.0347
GO:0009201	ribonucleoside triphosphate biosynthetic process	1	0.0347
GO:0009145	purine nucleoside triphosphate biosynthetic process	1	0.0347
GO:1901575	organic substance catabolic process	2	0.0356
GO:0015992	proton transport	1	0.0360
GO:0006818	hydrogen transport	1	0.0360
GO:0046034	ATP metabolic process	1	0.0360
GO:0050896	response to stimulus	2	0.0393
GO:0006733	oxidoreduction coenzyme metabolic process	1	0.0401
GO:0006091	generation of precursor metabolites and energy	1	0.0401
GO:0042451	purine nucleoside biosynthetic process	1	0.0415
GO:0046129	purine ribonucleoside biosynthetic process	1	0.0415
GO:0055114	oxidation-reduction process	4	0.0426
GO:0009056	catabolic process	2	0.0438
GO:0044710	single-organism metabolic process	5	0.0460
GO:0009163	nucleoside biosynthetic process	1	0.0469
GO:0042455	ribonucleoside biosynthetic process	1	0.0469
GO:1901659	glycosyl compound biosynthetic process	1	0.0469
GO:0009152	purine ribonucleotide biosynthetic process	1	0.0482

Table S8.3. Cont.

GO Term	Name	Result Count	p-value
	NRRL3357 0 v 10mM		
GO:0045454	cell redox homeostasis	2	0.0024
GO:0019725	cellular homeostasis	2	0.0026
GO:0006091	generation of precursor metabolites and energy	2	0.0034
GO:0042592	homeostatic process	2	0.0034
GO:0006006	glucose metabolic process	2	0.0039
GO:0042026	protein refolding	1	0.0059
GO:0019318	hexose metabolic process	2	0.0061
GO:0065008	regulation of biological quality	2	0.0067
GO:0006457	protein folding	2	0.0079
GO:0043086	negative regulation of catalytic activity	1	0.0088
GO:0044092	negative regulation of molecular function	1	0.0088
GO:0005996	monosaccharide metabolic process	2	0.0090
GO:0006094	gluconeogenesis	1	0.0118
GO:0019319	hexose biosynthetic process	1	0.0147
GO:0006108	malate metabolic process	1	0.0147
GO:0046364	monosaccharide biosynthetic process	1	0.0147
GO:0006508	proteolysis	3	0.0165
GO:0006096	glycolysis	1	0.0291
GO:0015986	ATP synthesis coupled proton transport	1	0.0320
GO:0015985	energy coupled proton transport, down electrochemical gradient	1	0.0320
GO:0044723	single-organism carbohydrate metabolic process	2	0.0333
GO:0009060	aerobic respiration	1	0.0377
GO:0006099	tricarboxylic acid cycle	1	0.0377
GO:0019538	protein metabolic process	5	0.0381
GO:0043648	dicarboxylic acid metabolic process	1	0.0406
GO:0015991	ATP hydrolysis coupled proton transport	1	0.0462
GO:0045333	cellular respiration	1	0.0462
GO:0015988	energy coupled proton transmembrane transport	1	0.0462
GO:0044238	primary metabolic process	10	0.0482
	NRRL3357 0 v 20mM		
GO:0071704	organic substance metabolic process	82	<0.0001
GO:0019318	hexose metabolic process	9	<0.0001
GO:0008152	metabolic process	115	<0.0001
GO:0006006	glucose metabolic process	8	<0.0001
GO:0044281	small molecule metabolic process	31	<0.0001
GO:0044238	primary metabolic process	75	<0.0001
GO:0005996	monosaccharide metabolic process	9	<0.0001
GO:0006979	response to oxidative stress	6	<0.0001
GO:0005975	carbohydrate metabolic process	23	<0.0001
GO:0019320	hexose catabolic process	6	<0.0001
GO:0046365	monosaccharide catabolic process	6	<0.0001
GO:0006007	glucose catabolic process	6	<0.0001
GO:0016052	carbohydrate catabolic process	8	0.0001
GO:0006753	nucleoside phosphate metabolic process	12	0.0001

Table S8.3. Cont.

GO Term	Name	Result Count	p-value
GO:0046129	purine ribonucleoside biosynthetic process	6	0.0001
GO:0042451	purine nucleoside biosynthetic process	6	0.0001
GO:0044723	single-organism carbohydrate metabolic process	10	0.0001
GO:0006457	protein folding	7	0.0001
GO:0044724	single-organism carbohydrate catabolic process	6	0.0001
GO:0009117	nucleotide metabolic process	11	0.0002
GO:0055086	nucleobase-containing small molecule metabolic process	13	0.0002
GO:0015985	energy coupled proton transport, down electrochemical gradient	4	0.0002
GO:0015986	ATP synthesis coupled proton transport	4	0.0002
GO:0042455	ribonucleoside biosynthetic process	6	0.0002
GO:1901659	glycosyl compound biosynthetic process	6	0.0002
GO:0009163	nucleoside biosynthetic process	6	0.0002
GO:0019538	protein metabolic process	30	0.0003
GO:1901564	organonitrogen compound metabolic process	23	0.0003
GO:0009206	purine ribonucleoside triphosphate biosynthetic process	5	0.0004
GO:0009201	ribonucleoside triphosphate biosynthetic process	5	0.0004
GO:0009145	purine nucleoside triphosphate biosynthetic process	5	0.0004
GO:0009142	nucleoside triphosphate biosynthetic process	5	0.0004
GO:0044710	single-organism metabolic process	55	0.0005
GO:0006508	proteolysis	13	0.0005
GO:0019752	carboxylic acid metabolic process	17	0.0005
GO:0043436	oxoacid metabolic process	17	0.0006
GO:0006082	organic acid metabolic process	17	0.0006
GO:0006739	NADP metabolic process	4	0.0006
GO:0006098	pentose-phosphate shunt	4	0.0006
GO:0006740	NADPH regeneration	4	0.0006
GO:0072522	purine-containing compound biosynthetic process	6	0.0006
GO:1901575	organic substance catabolic process	14	0.0007
GO:0009056	catabolic process	15	0.0007
GO:1901293	nucleoside phosphate biosynthetic process	7	0.0007
GO:0044237	cellular metabolic process	59	0.0007
GO:0019637	organophosphate metabolic process	13	0.0009
GO:0006732	coenzyme metabolic process	7	0.0016
GO:0009152	purine ribonucleotide biosynthetic process	5	0.0018
GO:0019362	pyridine nucleotide metabolic process	4	0.0019
GO:0046496	nicotinamide nucleotide metabolic process	4	0.0019
GO:0009165	nucleotide biosynthetic process	6	0.0019
GO:0006414	translational elongation	3	0.0022
GO:0046390	ribose phosphate biosynthetic process	5	0.0022
GO:0009260	ribonucleotide biosynthetic process	5	0.0022
GO:0072524	pyridine-containing compound metabolic process	4	0.0022
GO:0006164	purine nucleotide biosynthetic process	5	0.0025
GO:0006754	ATP biosynthetic process	4	0.0030
GO:0045454	cell redox homeostasis	4	0.0030
GO:0090407	organophosphate biosynthetic process	8	0.0031

Table S8.3. Cont.

GO Term	Name	Result Count	p-value
GO:0019725	cellular homeostasis	4	0.0034
GO:0006818	hydrogen transport	4	0.0039
GO:0015992	proton transport	4	0.0039
GO:0046034	ATP metabolic process	4	0.0039
GO:0051186	cofactor metabolic process	7	0.0042
GO:0006094	gluconeogenesis	2	0.0049
GO:0043648	dicarboxylic acid metabolic process	3	0.0052
GO:0006091	generation of precursor metabolites and energy	4	0.0056
GO:0006733	oxidoreduction coenzyme metabolic process	4	0.0056
GO:0042592	homeostatic process	4	0.0056
GO:0055114	oxidation-reduction process	36	0.0062
GO:0006950	response to stress	8	0.0068
GO:0006108	malate metabolic process	2	0.0073
GO:0019319	hexose biosynthetic process	2	0.0073
GO:0046939	nucleotide phosphorylation	2	0.0073
GO:0046364	monosaccharide biosynthetic process	2	0.0073
GO:0042278	purine nucleoside metabolic process	6	0.0084
GO:0046128	purine ribonucleoside metabolic process	6	0.0084
GO:1901566	organonitrogen compound biosynthetic process	11	0.0091
GO:0006520	cellular amino acid metabolic process	11	0.0100
GO:0009119	ribonucleoside metabolic process	6	0.0113
GO:0015672	monovalent inorganic cation transport	4	0.0125
GO:0016051	carbohydrate biosynthetic process	3	0.0146
GO:1901137	carbohydrate derivative biosynthetic process	6	0.0155
GO:0009116	nucleoside metabolic process	7	0.0156
GO:1901657	glycosyl compound metabolic process	7	0.0156
GO:0009144	purine nucleoside triphosphate metabolic process	5	0.0158
GO:0009199	ribonucleoside triphosphate metabolic process	5	0.0158
GO:0009205	purine ribonucleoside triphosphate metabolic process	5	0.0158
GO:0072593	reactive oxygen species metabolic process	2	0.0167
GO:0006801	superoxide metabolic process	2	0.0167
GO:0006221	pyrimidine nucleotide biosynthetic process	2	0.0167
GO:0009141	nucleoside triphosphate metabolic process	5	0.0167
GO:0065008	regulation of biological quality	4	0.0173
GO:0072521	purine-containing compound metabolic process	6	0.0180
GO:0006220	pyrimidine nucleotide metabolic process	2	0.0205
GO:0006412	translation	9	0.0234
GO:0006096	glycolysis	2	0.0247
GO:0006793	phosphorus metabolic process	15	0.0263
GO:0009072	aromatic amino acid family metabolic process	3	0.0326
GO:0016054	organic acid catabolic process	3	0.0353
GO:0046395	carboxylic acid catabolic process	3	0.0353
GO:1901605	alpha-amino acid metabolic process	6	0.0361
GO:0009060	aerobic respiration	2	0.0391
GO:0072528	pyrimidine-containing compound biosynthetic process	2	0.0391

Table S8.3. Cont.

GO Term	Name	Result Count	p-value
GO:0006099	tricarboxylic acid cycle	2	0.0391
GO:0009150	purine ribonucleotide metabolic process	5	0.0401
GO:0006790	sulfur compound metabolic process	3	0.0413
GO:0006575	cellular modified amino acid metabolic process	3	0.0413
GO:0009259	ribonucleotide metabolic process	5	0.0438
GO:0019693	ribose phosphate metabolic process	5	0.0438
GO:0006228	UTP biosynthetic process	1	0.0450
GO:0006730	one-carbon metabolic process	1	0.0450
GO:0006183	GTP biosynthetic process	1	0.0450
GO:0000303	response to superoxide	1	0.0450
GO:0006637	acyl-CoA metabolic process	1	0.0450
GO:1901701	cellular response to oxygen-containing compound	1	0.0450
GO:0042823	pyridoxal phosphate biosynthetic process	1	0.0450
GO:0034599	cellular response to oxidative stress	1	0.0450
GO:0070887	cellular response to chemical stimulus	1	0.0450
GO:0035383	thioester metabolic process	1	0.0450
GO:0019430	removal of superoxide radicals	1	0.0450
GO:0006084	acetyl-CoA metabolic process	1	0.0450
GO:0046036	CTP metabolic process	1	0.0450
GO:0042026	protein refolding	1	0.0450
GO:0006165	nucleoside diphosphate phosphorylation	1	0.0450
GO:0046209	nitric oxide metabolic process	1	0.0450
GO:0010035	response to inorganic substance	1	0.0450
GO:0009208	pyrimidine ribonucleoside triphosphate metabolic process	1	0.0450
GO:0034614	cellular response to reactive oxygen species	1	0.0450
GO:0042822	pyridoxal phosphate metabolic process	1	0.0450
GO:0006241	CTP biosynthetic process	1	0.0450
GO:0006106	fumarate metabolic process	1	0.0450
GO:1901700	response to oxygen-containing compound	1	0.0450
GO:0009148	pyrimidine nucleoside triphosphate biosynthetic process	1	0.0450
GO:0009209	pyrimidine ribonucleoside triphosphate biosynthetic process	1	0.0450
GO:0006090	pyruvate metabolic process	1	0.0450
GO:0006809	nitric oxide biosynthetic process	1	0.0450
GO:0009052	pentose-phosphate shunt, non-oxidative branch	1	0.0450
GO:0046051	UTP metabolic process	1	0.0450
GO:0000302	response to reactive oxygen species	1	0.0450
GO:0071451	cellular response to superoxide	1	0.0450
GO:0006163	purine nucleotide metabolic process	5	0.0476
GO:0006796	phosphate-containing compound metabolic process	14	0.0492
	K54A 0 v 10mM		
GO:0006809	nitric oxide biosynthetic process	1	0.0048
GO:0046209	nitric oxide metabolic process	1	0.0048
GO:0015986	ATP synthesis coupled proton transport	1	0.0260
GO:0015985	energy coupled proton transport, down electrochemical gradient	1	0.0260
GO:0015991	ATP hydrolysis coupled proton transport	1	0.0376

Table S8.3. Cont.

GO Term	Name	Result Count	p-value
GO:0015988	energy coupled proton transmembrane transport	1	0.0376
GO:0006979	response to oxidative stress	1	0.0376

Table S8.4. Cell localization GO terms enriched among DEPs in A. flavus isolates in response to oxidative stress.

GO Term	Name	Result Count	p-value
	AF13 0 v 10mM		
GO:0000782	telomere cap complex	1	0.0113
GO:0005854	nascent polypeptide-associated complex	1	0.0113
GO:0005823	central plaque of spindle pole body	1	0.0113
GO:0000783	nuclear telomere cap complex	1	0.0113
GO:0005737	cytoplasm	14	0.0152
GO:0009277	fungal-type cell wall	2	0.0187
GO:0000131	incipient cellular bud site	1	0.0187
GO:0005618	cell wall	2	0.0233
GO:0030312	external encapsulating structure	2	0.0284
GO:0008541	proteasome regulatory particle, lid subcomplex	1	0.0298
GO:0005788	endoplasmic reticulum lumen	1	0.0298
GO:0000784	nuclear chromosome, telomeric region	1	0.0335
GO:0000781	chromosome, telomeric region	1	0.0335
GO:0044450	microtubule organizing center part	1	0.0371
GO:0005934	cellular bud tip	1	0.0371
GO:0005937	mating projection	1	0.0480
GO:0042995	cell projection	1	0.0480
	AF13 0 v 25mM		
GO:0005737	cytoplasm	8	0.0005
GO:0098800	inner mitochondrial membrane protein complex	2	0.0010
GO:0044455	mitochondrial membrane part	2	0.0012
GO:0005739	mitochondrion	4	0.0014
GO:0098798	mitochondrial protein complex	2	0.0017
GO:0044429	mitochondrial part	3	0.0028
GO:0005754	mitochondrial proton-transporting ATP synthase, catalytic core	1	0.0037
GO:0045267	proton-transporting ATP synthase, catalytic core	1	0.0037
GO:0005743	mitochondrial inner membrane	2	0.0066
GO:0019866	organelle inner membrane	2	0.0071
GO:0045277	respiratory chain complex IV	1	0.0073
GO:0045261	proton-transporting ATP synthase complex, catalytic core F(1)	1	0.0073
GO:0005751	mitochondrial respiratory chain complex IV	1	0.0073
GO:0000275	mitochondrial proton-transporting ATP synthase complex, catalytic core	1	0.0073
GO:0031966	mitochondrial membrane	2	0.0096
GO:0098796	membrane protein complex	2	0.0113
GO:0044444	cytoplasmic part	5	0.0135
GO:0005753	mitochondrial proton-transporting ATP synthase complex	1	0.0145
GO:0005740	mitochondrial envelope	2	0.0154
GO:0070069	cytochrome complex	1	0.0158
GO:0033178	proton-transporting two-sector ATPase complex, catalytic domain	1	0.0170
GO:0045259	proton-transporting ATP synthase complex	1	0.0170
GO:0044424	intracellular part	8	0.0175
GO:0005746	mitochondrial respiratory chain	1	0.0194
GO:0098803	respiratory chain complex	1	0.0206

Table S8.4. Cont.

GO Term	Name	Result Count	p-value
GO:0070469	respiratory chain	1	0.0206
GO:0005622	intracellular	8	0.0215
GO:0031967	organelle envelope	2	0.0259
GO:0031975	envelope	2	0.0273
GO:0005625	obsolete soluble fraction	1	0.0348
GO:0016469	proton-transporting two-sector ATPase complex	1	0.0372
GO:0044464	cell part	8	0.0391
GO:0005623	cell	8	0.0397
	NRRL3357 0 v 10mM		
GO:0012510	trans-Golgi network transport vesicle membrane	1	0.0088
GO:0030130	clathrin coat of trans-Golgi network vesicle	1	0.0088
GO:0030125	clathrin vesicle coat	1	0.0088
GO:0030665	clathrin-coated vesicle membrane	1	0.0088
GO:0005905	coated pit	1	0.0088
GO:0030136	clathrin-coated vesicle	1	0.0088
GO:0030132	clathrin coat of coated pit	1	0.0088
GO:0030140	trans-Golgi network transport vesicle	1	0.0088
GO:0005783	endoplasmic reticulum	2	0.0090
GO:0044459	plasma membrane part	1	0.0147
GO:0030133	transport vesicle	1	0.0176
GO:0030660	Golgi-associated vesicle membrane	1	0.0176
GO:0045261	proton-transporting ATP synthase complex, catalytic core F(1)	1	0.0176
GO:0030658	transport vesicle membrane	1	0.0176
GO:0005798	Golgi-associated vesicle	1	0.0205
GO:0005886	plasma membrane	1	0.0205
GO:0044433	cytoplasmic vesicle part	1	0.0263
GO:0012506	vesicle membrane	1	0.0263
GO:0030135	coated vesicle	1	0.0263
GO:0030662	coated vesicle membrane	1	0.0263
GO:0030120	vesicle coat	1	0.0263
GO:0030659	cytoplasmic vesicle membrane	1	0.0263
GO:0045259	proton-transporting ATP synthase complex	1	0.0291
GO:0030118	clathrin coat	1	0.0291
GO:0031982	vesicle	1	0.0320
GO:0031988	membrane-bounded vesicle	1	0.0320
GO:0000139	Golgi membrane	1	0.0320
GO:0031410	cytoplasmic vesicle	1	0.0320
GO:0016023	cytoplasmic membrane-bounded vesicle	1	0.0320
GO:0005737	cytoplasm	4	0.0332
GO:0033178	proton-transporting two-sector ATPase complex, catalytic domain	1	0.0349
GO:0044431	Golgi apparatus part	1	0.0434
GO:0005794	Golgi apparatus	1	0.0462
	NRRL3357 0 v 20mM		
GO:0005737	cytoplasm	26	<0.0001
GO:0045261	proton-transporting ATP synthase complex, catalytic core F(1)	3	0.0006

Table S8.4. Cont.

GO Term	Name	Result Count	p-value
GO:0044444	cytoplasmic part	16	0.0012
GO:0045259	proton-transporting ATP synthase complex	3	0.0022
GO:0030125	clathrin vesicle coat	2	0.0030
GO:0030130	clathrin coat of trans-Golgi network vesicle	2	0.0030
GO:0030140	trans-Golgi network transport vesicle	2	0.0030
GO:0005905	coated pit	2	0.0030
GO:0030665	clathrin-coated vesicle membrane	2	0.0030
GO:0030136	clathrin-coated vesicle	2	0.0030
GO:0012510	trans-Golgi network transport vesicle membrane	2	0.0030
GO:0030132	clathrin coat of coated pit	2	0.0030
GO:0033178	proton-transporting two-sector ATPase complex, catalytic domain	3	0.0035
GO:0032991	macromolecular complex	16	0.0057
GO:0044459	plasma membrane part	2	0.0073
GO:0030658	transport vesicle membrane	2	0.0100
GO:0030660	Golgi-associated vesicle membrane	2	0.0100
GO:0030133	transport vesicle	2	0.0100
GO:0005886	plasma membrane	2	0.0131
GO:0005798	Golgi-associated vesicle	2	0.0131
GO:0005840	ribosome	7	0.0149
GO:0016469	proton-transporting two-sector ATPase complex	3	0.0204
GO:0030120	vesicle coat	2	0.0205
GO:0044433	cytoplasmic vesicle part	2	0.0205
GO:0030659	cytoplasmic vesicle membrane	2	0.0205
GO:0030135	coated vesicle	2	0.0205
GO:0012506	vesicle membrane	2	0.0205
GO:0030662	coated vesicle membrane	2	0.0205
GO:0030118	clathrin coat	2	0.0247
GO:0031410	cytoplasmic vesicle	2	0.0292
GO:0031988	membrane-bounded vesicle	2	0.0292
GO:0031982	vesicle	2	0.0292
GO:0016023	cytoplasmic membrane-bounded vesicle	2	0.0292
GO:0000139	Golgi membrane	2	0.0292
GO:0030529	ribonucleoprotein complex	7	0.0305
GO:0005853	eukaryotic translation elongation factor 1 complex	1	0.0450
GO:0045239	tricarboxylic acid cycle enzyme complex	1	0.0450
GO:0045254	pyruvate dehydrogenase complex	1	0.0450
GO:0005952	cAMP-dependent protein kinase complex	1	0.0450
GO:0043234	protein complex	9	0.0484
	K54A 0 v 10mM		
GO:0012510	trans-Golgi network transport vesicle membrane	1	0.0072
GO:0030130	clathrin coat of trans-Golgi network vesicle	1	0.0072
GO:0030125	clathrin vesicle coat	1	0.0072
GO:0030665	clathrin-coated vesicle membrane	1	0.0072
GO:0005905	coated pit	1	0.0072
GO:0030140	trans-Golgi network transport vesicle	1	0.0072

Table S8.4. Cont.

GO Term	Name	Result Count	p-value
GO:0030136	clathrin-coated vesicle	1	0.0072
GO:0030132	clathrin coat of coated pit	1	0.0072
GO:0044459	plasma membrane part	1	0.0119
GO:0044446	intracellular organelle part	3	0.0137
GO:0044422	organelle part	3	0.0137
GO:0045261	proton-transporting ATP synthase complex, catalytic core F(1)	1	0.0143
GO:0030658	transport vesicle membrane	1	0.0143
GO:0030133	transport vesicle	1	0.0143
GO:0030660	Golgi-associated vesicle membrane	1	0.0143
GO:0031090	organelle membrane	2	0.0152
GO:0005798	Golgi-associated vesicle	1	0.0166
GO:0005886	plasma membrane	1	0.0166
GO:0030135	coated vesicle	1	0.0213
GO:0030659	cytoplasmic vesicle membrane	1	0.0213
GO:0012506	vesicle membrane	1	0.0213
GO:0030120	vesicle coat	1	0.0213
GO:0030662	coated vesicle membrane	1	0.0213
GO:0044433	cytoplasmic vesicle part	1	0.0213
GO:0045259	proton-transporting ATP synthase complex	1	0.0237
GO:0030118	clathrin coat	1	0.0237
GO:0000139	Golgi membrane	1	0.0260
GO:0031982	vesicle	1	0.0260
GO:0031410	cytoplasmic vesicle	1	0.0260
GO:0016023	cytoplasmic membrane-bounded vesicle	1	0.0260
GO:0031988	membrane-bounded vesicle	1	0.0260
GO:0015935	small ribosomal subunit	1	0.0283
GO:0033178	proton-transporting two-sector ATPase complex, catalytic domain	1	0.0283
GO:0044444	cytoplasmic part	3	0.0288
GO:0005743	mitochondrial inner membrane	1	0.0330
GO:0044431	Golgi apparatus part	1	0.0353
GO:0019866	organelle inner membrane	1	0.0353
GO:0005794	Golgi apparatus	1	0.0376
GO:0032991	macromolecular complex	3	0.0435
GO:0044391	ribosomal subunit	1	0.0491

Table S8.5. KEGG pathway terms enriched among DEPs in *A. flavus* isolates in response to oxidative stress.

Pathway ID	Name	Result Count	p-value
	AF13 0 v 10mM		
ec00513	Various types of N-glycan biosynthesis	2	0.0008
ec00710	Carbon fixation in photosynthetic organisms	2	0.0045
ec00680	Methane metabolism	2	0.0056
ec00720	Carbon fixation pathways in prokaryotes	2	0.0064
ec00500	Starch and sucrose metabolism	3	0.0087
ec00620	Pyruvate metabolism	2	0.0165
ec00630	Glyoxylate and dicarboxylate metabolism	2	0.0185
ec00965	Betalain biosynthesis	1	0.0365
ec00010	Glycolysis / Gluconeogenesis	2	0.0367
ec00603	Glycosphingolipid biosynthesis - globo series	1	0.0405
	AF13 0 v 25mM		
ec00190	Oxidative phosphorylation	2	0.0163
ec00010	Glycolysis / Gluconeogenesis	2	0.0181
ec00520	Amino sugar and nucleotide sugar metabolism	2	0.0260
	NRRL3357 0 v 10mM		
ec00720	Carbon fixation pathways in prokaryotes	4	<0.0001
ec00620	Pyruvate metabolism	4	<0.0001
ec00020	Citrate cycle (TCA cycle)	3	0.0001
ec00630	Glyoxylate and dicarboxylate metabolism	3	0.0002
ec00710	Carbon fixation in photosynthetic organisms	2	0.0012
ec00640	Propanoate metabolism	2	0.0020
ec00310	Lysine degradation	2	0.0053
ec00280	Valine, leucine and isoleucine degradation	2	0.0057
ec00071	Fatty acid degradation	2	0.0064
ec00380	Tryptophan metabolism	2	0.0095
ec00010	Glycolysis / Gluconeogenesis	2	0.0109
ec00903	Limonene and pinene degradation	1	0.0264
ec00362	Benzoate degradation	1	0.0329
ec00072	Synthesis and degradation of ketone bodies	1	0.0329
	NRRL3357 0 v 20mM		
ec00720	Carbon fixation pathways in prokaryotes	9	<0.0001
ec00020	Citrate cycle (TCA cycle)	10	<0.0001
ec00710	Carbon fixation in photosynthetic organisms	8	<0.0001
ec00630	Glyoxylate and dicarboxylate metabolism	10	<0.0001
ec00620	Pyruvate metabolism	9	<0.0001
ec00010	Glycolysis / Gluconeogenesis	9	0.0002
ec00640	Propanoate metabolism	6	0.0002
ec00680	Methane metabolism	5	0.0009
ec00250	Alanine, aspartate and glutamate metabolism	6	0.0019
ec00190	Oxidative phosphorylation	7	0.0026
ec00270	Cysteine and methionine metabolism	6	0.0027
ec00195	Photosynthesis	4	0.0048
ec00450	Selenocompound metabolism	3	0.0056

Table S8.5. Cont.

Pathway ID	Name	Result Count	p-value
ec00350	Tyrosine metabolism	6	0.0071
ec00480	Glutathione metabolism	5	0.0115
ec00030	Pentose phosphate pathway	4	0.0118
ec00500	Starch and sucrose metabolism	7	0.0212
ec00603	Glycosphingolipid biosynthesis - globo series	2	0.0296
ec00513	Various types of N-glycan biosynthesis	2	0.0296
ec00520	Amino sugar and nucleotide sugar metabolism	6	0.0308
ec00330	Arginine and proline metabolism	6	0.0308
ec00040	Pentose and glucuronate interconversions	4	0.0428
	K54A 0 v 10mM		
ec00190	Oxidative phosphorylation	2	0.0098
ec00010	Glycolysis / Gluconeogenesis	2	0.0109
ec00330	Arginine and proline metabolism	2	0.0158
ec00903	Limonene and pinene degradation	1	0.0264

Table S8.6. Annotations of specific proteins in the protein-protein interaction analysis for NRRL3357.

ID	STRING ID	Annotation
AFLA_073480	CADAFLAP00000131	Tropomyosin, putative
AFLA_074520	aglA	Alpha-galactosidase, putative
AFLA_075060	CADAFLAP00000288	Transformer-SR ribonucleoprotein, putative
AFLA_076170	CADAFLAP00000399	Putative uncharacterized protein
AFLA_076180	CADAFLAP00000400	Putative uncharacterized protein
AFLA_076450	CADAFLAP00000427	Electron transfer flavoprotein alpha subunit, putative
AFLA_076680	CADAFLAP00000450	Pyruvate dehydrogenase complex, dihydrolipoamide acetyltransferase
AFLA_076710	CADAFLAP00000453	Malate dehydrogenase, NAD-dependent
AFLA_077860	CADAFLAP00000568	Putative uncharacterized protein
AFLA_078380	CADAFLAP00000620	Acetyl-coA hydrolase Ach1, putative
AFLA_078650	CADAFLAP00000647	ATP synthase subunit alpha
AFLA_078900	CADAFLAP00000672	Beta-N-acetylhexosaminidase NagA, putative
AFLA_079480	CADAFLAP00000730	Oligopeptidase family protein
AFLA_079910	CADAFLAP00000773	Glutathione peroxidase
AFLA_080240	CADAFLAP00000806	ATP synthase delta chain, mitochondrial, putative
AFLA_080390	CADAFLAP00000821	6-phosphogluconolactonase, putative
AFLA_080930	CADAFLAP00000874	EF hand domain protein
AFLA_082510	CADAFLAP00001031	TCTP family protein
AFLA_083370	CADAFLAP00001117	Glutathione oxidoreductase Glr1, putative
AFLA_086710	CADAFLAP00001450	Inorganic diphosphatase, putative
AFLA_086800	CADAFLAP00001459	Epoxide hydrolase, putative
AFLA_086900	CADAFLAP00001469	Alpha-mannosidase
AFLA_087950	CADAFLAP00001573	Isocitrate dehydrogenase LysB
AFLA_088570	CADAFLAP00001635	Putative uncharacterized protein
AFLA_023500	CADAFLAP00001726	Extracellular conserved serine-rich protein
AFLA_025100	GAPDH	Glyceraldehyde 3-phosphate dehydrogenase (EC 1.2.1.12)
AFLA_025510	CADAFLAP00001927	GPI anchored protein, putative
AFLA_025760	CADAFLAP00001951	50S ribosomal protein L12
AFLA_025980	CADAFLAP00001973	Hsp90 co-chaperone Cdc37
AFLA_025990	CADAFLAP00001974	Clathrin light chain
AFLA_026140	taa	Alpha-amylase, putative
AFLA_026470	CADAFLAP00002022	Aspartate aminotransferase (EC 2.6.1.1)
AFLA_027070	CADAFLAP00002082	Acetyl-coenzyme A synthetase FacA
AFLA_027810	alp1	Alkaline protease
AFLA_028260	exgA	Exo-beta-1,3-glucanase (Exg1), putative
AFLA_028800	CADAFLAP00002255	Eukaryotic translation initiation factor eIF-5A
AFLA_028910	CADAFLAP00002266	Polyadenylate-binding protein
AFLA_029310	CADAFLAP00002306	Alcohol dehydrogenase, zinc-containing, putative
AFLA_029390	CADAFLAP00002314	HMG box protein, putative
AFLA_029440	CADAFLAP00002319	NADH-cytochrome b5 reductase, putative
AFLA_029850	CADAFLAP00002360	Cysteine-rich secreted protein
AFLA_030140	CADAFLAP00002389	60S ribosomal protein P0
AFLA_030180	CADAFLAP00002393	Protein mitochondrial targeting protein (Mas1), putative
AFLA_030860	CADAFLAP00002461	RNAPII degradation factor Def1, putative

Table S8.6. Cont.

ID	STRING ID	Annotation
AFLA_031570	CADAFLAP00002532	Pyruvate decarboxylase PdcA, putative
AFLA_031760	CADAFLAP00002551	Glutaminase, putative
AFLA_031780	CADAFLAP00002553	Telomere and ribosome associated protein Stm1, putative
AFLA_031960	CADAFLAP00002571	40S ribosomal protein S7e
AFLA_032870	CADAFLAP00002662	cAMP-dependent protein kinase regulatory subunit PkaR
AFLA_032890	CADAFLAP00002664	Putative uncharacterized protein
AFLA_033100	CADAFLAP00002685	Phosphatidylinositol transporter, putative
AFLA_033400	mns1B	Mannosidase MsdS
AFLA_033620	CADAFLAP00002737	RNA binding protein, putative
AFLA_033690	CADAFLAP00002744	60S ribosomal protein L31e
AFLA_034050	CADAFLAP00002780	Mitochondrial aconitate hydratase, putative
AFLA_034640	CADAFLAP00002839	Aminopeptidase Y, putative
AFLA_034870	CADAFLAP00002862	Putative uncharacterized protein
AFLA_035510	CADAFLAP00002926	RNA binding effector protein Scp160, putative
AFLA_035540	CADAFLAP00002929	Signal transducing adapter molecule, putative
AFLA_035620	CADAFLAP00002937	Hsp70 chaperone BiP/Kar2, putative
AFLA_036070	CADAFLAP00002982	Maleylacetoacetate isomerase MaiA
AFLA_036090	CADAFLAP00002984	Homogentisate 1,2-dioxygenase (HmgA), putative
AFLA_036110	CADAFLAP00002986	4-hydroxyphenylpyruvate dioxygenase, putative
AFLA_036440	CADAFLAP00003019	Alanine aminotransferase, putative
AFLA_036640	CADAFLAP00003039	PH domain protein
AFLA_036840	CADAFLAP00003058	6-phosphogluconate dehydrogenase, decarboxylating (EC 1.1.1.44)
AFLA_037490	HCR1	Eukaryotic translation initiation factor 3 subunit EifCj, putative
AFLA_037960	CADAFLAP00003169	Glucosamine-fructose-6-phosphate aminotransferase
AFLA_014520	CADAFLAP00003337	Multicopper oxidase, putative
AFLA_014930	CADAFLAP00003378	Cofactor for methionyl-and glutamyl-tRNA synthetase, putative
AFLA_017100	lacA	Beta-galactosidase (EC 3.2.1.23)
AFLA_019230	CADAFLAP00003808	Mismatched base pair and cruciform DNA recognition protein, putative
AFLA_020380	CADAFLAP00003923	Stomatin family protein
AFLA_021820	CADAFLAP00004067	Nuclear movement protein NudC
AFLA_021870	cbhA	Cellobiohydrolase celD
AFLA_022270	CADAFLAP00004112	Putative uncharacterized protein
AFLA_022380	CADAFLAP00004123	Molecular chaperone Hsp70
AFLA_022470	CADAFLAP00004132	Adenylate kinase, putative
AFLA_022480	CADAFLAP00004133	26S proteasome regulatory particle subunit Rpn8, putative
AFLA_105920	pecA	Polygalacturonase A Precursor (EC 3.2.1.15)(Pectinase)(PGL)(P2C)
AFLA_106310	chaperonin	Chaperonin, putative
AFLA_106350	CADAFLAP00004371	ATP citrate lyase subunit (Acl), putatibe
AFLA_106390	CADAFLAP00004375	Ribose 5-phosphate isomerase A
AFLA_108100	CADAFLAP00004546	Argininosuccinate synthase (EC 6.3.4.5)
AFLA_108410	CADAFLAP00004576	Dipeptidase, putative
AFLA_108790	CADAFLAP00004614	Aldehyde dehydrogenase AldA, putative
AFLA_109320	CADAFLAP00004666	3-hydroxyisobutyrate dehydrogenase
AFLA_110160	dpp4	Extracellular dipeptidyl-peptidase Dpp4
AFLA_110260	CADAFLAP00004760	Flavin-binding monooxygenase-like protein

Table S8.6. Cont.

ID	STRING ID	Annotation
AFLA_110600	CADAFLAP00004794	Aminopeptidase
AFLA_110690	CADAFLAP00004803	Cytochrome c peroxidase Ccp1, putative
AFLA_111100	CADAFLAP00004844	Mitochondrial peroxiredoxin Prx1, putative
AFLA_112120	CADAFLAP00004946	Pyruvate carboxylase, putative
AFLA_112130	CADAFLAP00004947	Clathrin heavy chain
AFLA_112470	CADAFLAP00004981	Cobalamin-independent methionine synthase MetH/D
AFLA_112910	CADAFLAP00005025	Putative uncharacterized protein
AFLA_113000	CADAFLAP00005034	Integral ER membrane protein Scs2, putative
AFLA_038530	CADAFLAP00005181	Elastinolytic metalloproteinase Mep
AFLA_038700	CADAFLAP00005198	Putative uncharacterized protein
AFLA_038790	CADAFLAP00005207	Adenosine deaminase family protein
AFLA_039410	CADAFLAP00005268	Antigenic cell wall protein MP1
AFLA_040120	CADAFLAP00005339	Flavohemoprotein
AFLA_041260	CADAFLAP00005453	Ribosome associated DnaJ chaperone Zuotin, putative
AFLA_042090	CADAFLAP00005536	Fasciclin domain family protein
AFLA_042700	CADAFLAP00005597	Pre-mRNA splicing factor (Prp24), putative
AFLA_043390	CADAFLAP00005666	Hsp70 chaperone (BiP), putative
AFLA_043730	CADAFLAP00005700	Nuclear protein export protein Yrb2, putative
AFLA_044090	uaZ	Uricase (EC 1.7.3.3)(Urate oxidase)
AFLA_044620	hsp70	Mitochondrial Hsp70 chaperone (Ssc70), putative
AFLA_044820	CADAFLAP00005809	Glucose-6-phosphate isomerase (EC 5.3.1.9)
AFLA_045330	CADAFLAP00005860	Eukaryotic translation initiation factor subunit eIF-4F, putative
AFLA_045750	CADAFLAP00005902	Antigenic mitochondrial protein HSP60, putative
AFLA_045980	dpp5	Secreted dipeptidyl peptidase DppV
AFLA_046470	CADAFLAP00005974	Putative uncharacterized protein
AFLA_046730	CADAFLAP00006000	Putative uncharacterized protein
AFLA_047350	pepP	Prolidase pepP, putative
AFLA_054750	CADAFLAP00006084	Malate dehydrogenase, NAD-dependent
AFLA_055060	CADAFLAP00006115	NAD-dependent formate dehydrogenase AciA/Fdh
AFLA_055230	CADAFLAP00006132	Actin Act1
AFLA_055450	CADAFLAP00006154	Translation elongation factor eEF-1 subunit gamma, putative
AFLA_056170	CADAFLAP00006226	Catalase (EC 1.11.1.6)
AFLA_056260	CADAFLAP00006235	Nascent polypeptide-associated complex (NAC) subunit, putative
AFLA_056350	CADAFLAP00006244	2-methylcitrate dehydratase, putative
AFLA_056850	CADAFLAP00006294	Electron transfer flavoprotein, beta subunit, putative
AFLA_057240	CADAFLAP00006333	RNP domain protein
AFLA_057670	CADAFLAP00006376	Neutral protease 2, putative
AFLA_057770	plyA	Pectate lyase A
AFLA_060110	CADAFLAP00006620	Putative uncharacterized protein
AFLA_060260	CADAFLAP00006635	Heat shock protein Hsp30/Hsp42, putative
AFLA_061880	CADAFLAP00006797	Pyridoxine biosynthesis protein
AFLA_131280	CADAFLAP00007007	Actin cortical patch assembly protein Pan1, putative
AFLA_132540	trx2	Thioredoxin TrxA
AFLA_132990	CADAFLAP00007178	Ribosomal protein L34 protein, putative
AFLA_133150	CADAFLAP00007194	Catechol dioxygenase, putative

Table S8.6. Cont.

ID	STRING ID	Annotation
AFLA_133920	CADAFLAP00007271	Acyl CoA binding protein family
AFLA_133990	CADAFLAP00007278	Secretory pathway gdp dissociation inhibitor
AFLA_134120	CADAFLAP00007291	Orotate phosphoribosyltransferase
AFLA_134340	CADAFLAP00007312	BAR domain protein
AFLA_135200	CADAFLAP00007398	Putative uncharacterized protein
AFLA_135540	CADAFLAP00007432	ATP synthase
AFLA_136570	CADAFLAP00007535	Cytochrome c
AFLA_136600	CADAFLAP00007538	GrpE protein homolog
AFLA_136640	CADAFLAP00007542	Translation elongation factor EF-2 subunit, putative
AFLA_139300	ver1	Ver-1
AFLA_139470	cpaC	FAD dependent oxidoreductase, putative
AFLA_139480	cpaB	Dimethylallyl tryptophan synthase, putative
AFLA_066270	CADAFLAP00008051	RNA-binding La domain protein
AFLA_067940	CADAFLAP00008218	Putative uncharacterized protein
AFLA_068840	CADAFLAP00008308	Glycine cleavage system T protein
AFLA_069010	CADAFLAP00008325	S-adenosylmethionine synthetase (EC 2.5.1.6)
AFLA_069370	CADAFLAP00008361	Phosphoglycerate kinase (EC 2.7.2.3)
AFLA_069590	CADAFLAP00008383	Adenosylhomocysteinase (EC 3.3.1.1)
AFLA_070490	CADAFLAP00008473	Putative uncharacterized protein
AFLA_070990	CADAFLAP00008523	UTP-glucose-1-phosphate uridylyltransferase Ugp1, putative
AFLA_071010	CADAFLAP00008525	Heat shock protein (Sti1), putative
AFLA_089270	CADAFLAP00008613	BZIP transcription factor HacA
AFLA_089380	CADAFLAP00008624	Extracellular chitosanase CsnC, putative
AFLA_090690	CADAFLAP00008754	Mycelial catalase Cat1
AFLA_091030	CADAFLAP00008788	Putative uncharacterized protein
AFLA_091060	CADAFLAP00008791	Allergen Asp F3
AFLA_091270	CADAFLAP00008812	Fumarate hydratase, putative
AFLA_091990	CADAFLAP00008884	Peptidyl-prolyl cis-trans isomerase (EC 5.2.1.8)
AFLA_092640	CADAFLAP00008949	Alkaline phosphatase (EC 3.1.3.1)
AFLA_093220	CADAFLAP00009007	Ran-specific GTPase-activating protein 1, putative
AFLA_093280	CADAFLAP00009013	Disulfide isomerase (TigA), putative
AFLA_093660	CADAFLAP00009051	Solid-state culture expressed protein (Aos23), putative
AFLA_094630	CADAFLAP00009148	Triosephosphate isomerase (EC 5.3.1.1)
AFLA_095570	CADAFLAP00009242	RNA annealing protein Yra1, putative
AFLA_095660	CADAFLAP00009251	Immunoglobulin G-binding protein H, putative
AFLA_124380	CADAFLAP00009496	Putative uncharacterized protein
AFLA_124500	CADAFLAP00009508	Nitric oxide synthase, putative
AFLA_125270	CADAFLAP00009585	Tyrosinase
AFLA_126670	CADAFLAP00009725	Putative uncharacterized protein
AFLA_126870	CADAFLAP00009745	Putative uncharacterized protein
AFLA_127390	CADAFLAP00009797	Proteasome regulatory particle subunit Rpt5, putative
AFLA_128280	CADAFLAP00009886	M protein repeat protein
AFLA_128530	CADAFLAP00009911	Delta-1-pyrroline-5-carboxylate dehydrogenase PrnC
AFLA_130150	CADAFLAP00010073	NAD+ dependent glutamate dehydrogenase, putative
AFLA_130310	CADAFLAP00010089	Protein disulfide isomerase Pdi1, putative

Table S8.6. Cont.

ID	STRING ID	Annotation
AFLA_001890	CADAFLAP00010255	Cellobiose dehydrogenase
AFLA_002090	CADAFLAP00010275	Extracellular serine carboxypeptidase, putative
AFLA_002560	CADAFLAP00010322	60S ribosomal protein L37a
AFLA_002670	CADAFLAP00010333	Curved DNA-binding protein (42 kDa protein)
AFLA_003440	CADAFLAP00010410	Translation initiation factor 4B
AFLA_004090	CADAFLAP00010475	Putative uncharacterized protein
AFLA_004950	CADAFLAP00010561	Cytochrome c oxidase subunit Va, putative
AFLA_006300	CADAFLAP00010695	Nucleoside diphosphate kinase (EC 2.7.4.6)
AFLA_006520	CADAFLAP00010715	CRAL/TRIO domain protein
AFLA_006960	CADAFLAP00010759	Molecular chaperone and allergen Mod-E/Hsp90/Hsp1
AFLA_007000	CADAFLAP00010763	Ubiquinol-cytochrome C reductase complex core protein 2, putative
AFLA_007020	CADAFLAP00010765	Citrate synthase
AFLA_048510	CADAFLAP00010843	UV excision repair protein (RadW), putative
AFLA_048610	CADAFLAP00010853	Succinyl-CoA synthetase alpha subunit, putative
AFLA_050270	CADAFLAP00011019	Conserved lysine-rich protein, putative
AFLA_050690	CADAFLAP00011061	Mitochondrial ADP,ATP carrier protein (Ant), putative
AFLA_051140	bglA	Beta-glucosidase, putative
AFLA_051530	CADAFLAP00011144	Methylmalonate-semialdehyde dehydrogenase, putative
AFLA_051770	CADAFLAP00011168	Thioredoxin reductase (EC 1.8.1.9)
AFLA_051980	CADAFLAP00011189	G-protein complex beta subunit CpcB
AFLA_052400	CADAFLAP00011231	Isocitrate lyase AcuD
AFLA_097190	CADAFLAP00011457	Putative uncharacterized protein
AFLA_097750	sspA	Putative uncharacterized protein
AFLA_099000	sodC	Superoxide dismutase [Cu-Zn] (EC 1.15.1.1)
AFLA_099220	CADAFLAP00011660	Putative uncharacterized protein
AFLA_099650	CADAFLAP00011702	Woronin body major protein, putative
AFLA_101160	CADAFLAP00011853	40S ribosomal protein S9
AFLA_101230	CADAFLAP00011860	Glutaminase GtaA
AFLA_101930	CADAFLAP00011930	Succinate-semialdehyde dehydrogenase, putative
AFLA_102010	CADAFLAP00011938	Class V chitinase, putative
AFLA_103940	CADAFLAP00012129	Glutamate carboxypeptidase, putative
AFLA_117760	CADAFLAP00012348	Phytase, putative
AFLA_117850	CADAFLAP00012357	RPEL repeat protein
AFLA_119040	CADAFLAP00012476	Muramidase, putative
AFLA_119660	CADAFLAP00012538	ATP synthase subunit beta (EC 3.6.3.14)
AFLA_120630	CADAFLAP00012635	Glyoxylate/hydroxypyruvate reductase, putative
AFLA_122110	CADAFLAP00012783	Bifunctional catalase-peroxidase Cat2
AFLA_122180	CADAFLAP00012790	Putative uncharacterized protein
AFLA_122720	CADAFLAP00012843	Actin binding protein, putative
AFLA_007700	CADAFLAP00012881	Putative uncharacterized protein
AFLA_008310	CADAFLAP00012942	Acetyl-CoA-acetyltransferase, putative
AFLA_008910	CADAFLAP00013001	Putative uncharacterized protein
AFLA_008990	cpyA	Carboxypeptidase CpyA/Prc1, putative
AFLA_012160	CADAFLAP00013326	Acetyl-CoA acetyltransferase, putative
AFLA_012200	CADAFLAP00013330	Hsp70 chaperone (HscA), putative

APPENDIX D

RESPONSES OF *ASPERGILLUS FLAVUS* TO OXIDATIVE STRESS ARE RELATED TO FUNGAL DEVELOPMENT REGULATOR, ANTIOXIDANT ENZYME, AND SECONDARY METABOLITE BIOSYNTHETIC GENE EXPRESSION

Fountain, J.C., Bajaj, P., Nayak, S.N., Yang, L., Pandey, M.K., Kumar, V., Jayale, A.S., Chitikineni, A., Lee, R.D., Kemerait, R.C., Varshney, R.K., Guo, B. (2016). Responses of *Aspergillus flavus* to oxidative stress are related to fungal development regulator, antioxidant enzyme, and secondary metabolite biosynthetic gene expression. *Frontiers in Microbiology* 7:2048. doi:10.3389/fmicb.2016.02048. Reprinted here with permission of the publisher.

Abstract

The infection of maize and peanut with *Aspergillus flavus* and subsequent contamination with aflatoxin pose a threat to global food safety and human health, and is exacerbated by drought stress. Drought stress-responding compounds such as reactive oxygen species (ROS) are associated with fungal stress responsive signaling and secondary metabolite production, and can stimulate the production of aflatoxin by *A. flavus in vitro*. These secondary metabolites have been shown to possess diverse functions in soil-borne fungi including antibiosis, competitive inhibition of other microbes, and abiotic stress alleviation. Previously, we observed that isolates of *A. flavus* showed differences in oxidative stress tolerance which correlated with their aflatoxin production capabilities. In order to better understand these isolate-specific oxidative stress responses, we examined the transcriptional responses of field isolates of *A. flavus* with varying levels of aflatoxin production (NRRL3357, AF13, and Tox4) to H_2O_2-induced oxidative stress using an RNA sequencing approach. These isolates were cultured in an aflatoxin-production conducive medium amended with various levels of H_2O_2. Whole transcriptomes were sequenced using an Illumina HiSeq platform with an average of 40.43 million filtered paired-end reads generated for each sample. The obtained transcriptomes were then used for differential expression, gene ontology, pathway, and co-expression analyses. Isolates which produced higher levels of aflatoxin tended to exhibit fewer differentially expressed genes than isolates with lower levels of production. Genes found to be differentially expressed in response to increasing oxidative stress included antioxidant enzymes, primary metabolism components, antibiosis-related genes, and secondary metabolite biosynthetic components specifically for aflatoxin, aflatrem, and kojic acid. The expression of fungal development-related genes including aminobenzoate degradation genes and conidiation regulators were found to be regulated in

response to increasing stress. Aflatoxin biosynthetic genes and antioxidant enzyme genes were also found to be co-expressed and highly correlated with fungal biomass under stress. This suggests that these secondary metabolites may be produced as part of coordinated oxidative stress responses in *A. flavus* along with antioxidant enzyme gene expression and developmental regulation.

Introduction

The contamination of crops with aflatoxin, a carcinogenic secondary metabolite of the facultative plant parasite *Aspergillus flavus* (Guo et al., 1996), is a threat to human health, global food safety and security (Williams et al., 2010; Guo et al., 2012; Andrade and Caldas, 2015). Aflatoxin contamination of staple and dietary supplemental crops such as maize and peanut result in both losses in crop value in international trade due to restrictions on aflatoxin content (Matumba et al. 2015; Wu, 2015), and negative impacts in human and animal health (Williams et al. 2004, 2010; Kew, 2013). These concerns are the impetus for investigations into the biology of this organism and its interactions with host plants related to aflatoxin contamination (Amaike and Keller, 2011; Diener et al. 1983, 1987; Guo et al., 2012; Fountain et al., 2014).

The aflatoxin biosynthetic pathway has been well characterized in *A. flavus* and in other aflatoxigenic species of *Aspergillus* such as *A. parasiticus*, and sterigmatocystin producing species such as *A. nidulans* (Amaike and Keller, 2011). Aflatoxin biosynthesis is encoded by a cluster of 25 genes which has been highly conserved among *Aspergillus spp*. and has been well characterized (Yu et al. 2004). While the biosynthetic mechanisms involved in aflatoxin production have been well characterized, little is known regarding the biological role of aflatoxin in *A. flavus* or other *Aspergillus spp.* Secondary metabolites produced by soil-dwelling fungi

exhibit various biological activities including fungivory resistance, stress tolerance, and quorum sensing (Reverberi et al. 2008, 2010; Roze et al. 2013).

Recent studies have shown that reactive oxygen species (ROS) and their reactive products such as peroxidized lipids (oxylipins) are required for the production of aflatoxin and can stimulate aflatoxin production if applied *in vitro* (Jayashree and Subramanyam, 2001). Induction of oxylipin and ROS accumulation in *A. flavus* mycelia through peroxisome proliferation has also been linked with increased aflatoxin production and antioxidant enzyme activity (Reverberi et al. 2012). Similarly, several studies have also been performed examining the effects of antioxidants on the growth and aflatoxin production of Aspergilli. For example, phenolic compounds such as caffeic acid tannic acid derived from tree nuts have been shown to inhibit aflatoxin production in *A. flavus* (Mahoney et al. 2010). Other synthetic phenolic compounds such as butylated hydroxyanisole (BHA) and propyl paraben (PP) have also been found to have a similar effect as a function of medium pH and water activity (Nesci et al. 2003; Passone et al. 2005). Treatment with BHA as also been shown to inhibit sclerotial differentiation in *A. flavus*. Oxidative stress responsive signaling mechanisms have been found to be involved in the regulation of aflatoxin production such as the stress responsive transcription factors AtfB, AP-1, and VeA (Baidya et al. 2014; Hong et al. 2013; Reverberi et al. 2008; Roze et al. 2011, 2013; Sakamoto et al. 2008). Also, VeA along with VelB and LaeA form the Velvet protein complex to regulate both secondary metabolite production and reproductive development in *A. flavus* and other *Aspergillus spp.* (Park et al. 2012). The consumption and/or generation of ROS have also been found to co-localize to vesicles known as aflatoxisomes where the final phases of aflatoxin production are carried out (Chanda et al. 2009, 2010; Roze et al. 2015).

Because of the close association of ROS and aflatoxin production, it has been hypothesized that aflatoxin production may serve as a component of oxidative stress alleviation mechanisms employed by *Aspergillus spp*. in addition to antioxidant enzymes, altered carbon metabolism, and the production of other secondary metabolites (Fountain et al. 2014, 2016; Narasaiah et al. 2006; Roze et al. 2013). The tolerance of *A. flavus* and *A. parasiticus* isolates to oxidative stress has been shown to be correlated with their levels of aflatoxin production. For example, Roze et al. (2015) showed that conidia of isolates with higher levels of aflatoxin production also exhibited greater viability when cultured in ROS-amended medium.

This correlation between ROS and aflatoxin production has also lead to the hypothesis that host plant-derived ROS and oxylipins may function in the host-parasite interaction between *A. flavus* or other Aspergilli and their host plants. Host plant resistance to aflatoxin contamination have been identified, and this resistance has been found to be heavily influenced by environmental stresses, particularly drought stress (Diener et al. 1983, 1987; Fountain et al. 2014; Guo et al. 2008; Holbrook et al. 2009; Jiang et al. 2012; Kebede et al. 2012; Pandey et al. 2012; Williams, 2006). Interestingly, these aforementioned ROS and oxylipins have also been shown to accumulate in the tissues of host plants during drought stress, and their levels have been correlated with aflatoxin contamination resistance (Gao et al. 2009; Yang et al. 2015, 2016). Host plant tissue antioxidant enzyme activity and capacity has also been found to be correlated with reduced *A. flavus* growth and aflatoxin production in model species such as buckwheat (Chitarrini et al. 2014).

In our previous studies, isolates of *A. flavus* were found to exhibit different degrees of oxidative stress tolerance which appeared to correlate with their aflatoxin production capability suggesting that aflatoxin production may contribute to stress tolerance (Fountain et al. 2015).

However, the observed stress tolerance of the toxigenic isolates cultured in aflatoxin non-conducive medium was reduced yet comparable indicating that factors in addition to aflatoxin production also contributed to the observed differences. In order to better understand the differences in isolate-specific responses to oxidative stress, and to further explore the potential role of aflatoxin production in stress alleviation in *A. flavus*, we examined the global transcriptional responses of several isolates of *A. flavus* to increasing oxidative stress, which has been summarized in an overview-type publication (Fountain et al. 2016). Here, we present a detailed analysis of changes in the transcriptomes of different toxigenic *A. flavus* isolates with distinguished aflatoxin production capabilities to increasing oxidative stress in an aflatoxin conducive culture medium. By examining the oxidative stress responses of *A. flavus*, the biological role of aflatoxin production in stress responses and in competition with other soil-dwelling organisms may be better understood.

Materials and Methods

The methodologies presented here are adapted from Fountain et al. (2016) and describe the data generation and analysis procedures for the toxigenic isolates examined in this study.

Isolate Culture Conditions

The *A. flavus* toxigenic isolates utilized in this study were obtained as previously described (Fountain et al. 2015). The isolates AF13, NRRL3357, and Tox4 were initially cultured on V8 agar (20% V8, 1% $CaCO_3$, 3% agar) at 32°C for 5 days. Conidia were collected from the cultures by washing the plates with sterile 0.1% (v/v) Tween 20. This conidial suspension (~4.0 x 10^6 conidia/mL) was used to inoculate liquid cultures of yeast extract sucrose (YES; 2% yeast

extract, 1% sucrose) medium containing various concentrations of hydrogen peroxide (H_2O_2, 3% stabilized solution). For AF13 and Tox4, the YES medium was supplemented with 0, 10, and 25 mM H_2O_2 representing a control, moderately high, and high levels of stress, respectively. For NRRL3357, the YES medium was supplemented with 0, 10, and 20 mM H_2O_2 due to the lower concentration of H_2O_2 the isolate could tolerate (Fountain et al. 2015). The experiment was performed in 125 mL Erlenmeyer flasks containing 50 mL H_2O_2 amended YES medium and 100 µL conidial suspension plugged with a sterile cotton ball. The cultures were incubated at 32°C for 7 days in the dark with two biological replicates for each isolate/treatment combination. Mycelia were then harvested from each culture, immediately frozen in liquid nitrogen, and stored at -80°C.

RNA Isolation

The harvested mycelia were homogenized in a chilled mortar and pestle to a fine powder, and then used for total RNA isolation. Total RNA was isolates using an RNeasy Plant Mini Kit with DNase digestion according to the manufacturer's instructions (Qiagen, Hilden, Germany). The isolated RNA was then quantified using a Nano-Drop ND1000 spectrophotometer (Thermo Scientific, Wilmington, DE, USA) and the RNA integrity numbers (RINs) for each sample were validated using an Agilent 2100 Bioanalyzer (Agilent, Santa Clara, CA, USA). Samples with an RIN $\geq$ 5 were used for RNA sequencing.

Library Construction and Illumina Sequencing

The cDNA libraries for each sample and biological replicate were generated from 1µg of total RNA. A total of 18 libraries were generated for the toxigenic *A. flavus* isolate samples and used

for transcriptome sequencing using an Illumina TruSeq RNA Sequencing Kit according to the manufacturer's instructions (Illumina, San Diego, CA, USA). Following quantitation using a Qubit 2.0 fluorometer (Thermo Scientific), and validation using an Agilent 2100 Bioanalyzer (Agilent), the libraries were used for cluster generation using a cBot (Illumina), and paired-end sequencing using a HiSeq 2500 platform according to the manufacturer's instructions (Illumina).

Bioinformatics Analysis

Initial quality checks on raw sequencing reads were performed using FastQC v0.11.2 with low quality reads being removed using Trimmomatic v0.32, along with rRNA contamination following alignment with the SILVA database. The remaining, high quality reads were used for differential expression analysis using the tuxedo protocol. Briefly, alignment of filtered reads to the *A. flavus* NRRL3357 reference genome (GCF_000006275.2) was done using tophat2 v2.0.13 and bowtie2 v2.2.4. Cufflinks v2.2.1 and cuffdiff were used to assemble the transcripts and determine transcript abundance in terms of Fragments Per Kilobase of exon per Million fragments mapped (FPKM). A gene was considered significantly differentially expressed when $|\log_2(\text{fold change})| \geq 2$ with an adjusted p-value ≤ 0.05. Tophat2 alignments were used to perform RABT (reference annotation based transcript) assembly for both genes and isoforms. The assemblies were then compared and merged using cuffmerge and used for analysis.

The assembled transcripts were annotated using a standalone blast 2.2.30+ and analyzed through Blast2GO and KEGG for gene ontology (GO) and pathway analysis, respectively. Heatmaps of select secondary metabolites biosynthesis genes and principal components analysis (PCA) of the gene expression profiles of the isolates was performed with multiple experiment viewer (MeV) v4.9.0. For promoter analysis of select genes, upstream gene sequences containing

conserved transcription factor binding domains were obtained using FungiDB (http://fungidb.org/) followed by sequence analysis using MEME 4.11.2 (Bailey et al. 2009; Stajich et al. 2012). Co-expression analysis was performed using the weighted correlation network analysis (WGCNA) package in R v3.3.0 (Langfelder and Horvath, 2008)

Quantitative RT-PCR Validation

In order to validate the RNA sequencing results, we selected several genes for expression analysis on a subset of samples using quantitative RT-PCR (qPCR). Using total RNA remaining following library construction, we synthesized cDNA using a Taqman reverse transcriptase kit (Thermo-Fisher) according to the manufacturer's instructions. Reverse transcription was carried out using a PTC-200 thermal cycler (Bio-Rad, Hercules, CA, USA) with the following cycling parameters: 25°C for 10 min, 48°C for 30 min, and 95°C for 5 min. The qPCR was then performed using a 20µl reaction volume containing: 1X SYBR Green PCR Master Mix (Thermo-Fisher), 0.4µM forward primer, 0.4µM reverse primer, and 25ng cDNA template. In this study, β-tubulin was used as a housekeeping control, and primer sequences for this and the other genes examined can be found in Table S.D.1. The reactions were carried out using an ABI 7500 platform (Thermo-Fisher) using the following cycles: 50°C for 2 min, 95°C for 10 min, and 40 amplification cycles of 95°C for 15 s, and 60°C for 1 min. Dissociation curves were performed at the end of each cycle to identify possible primer dimerization or off-target amplification. With the obtained threshold cycle (Ct) values, relative gene expression was calculated using a modified Livak method where Relative Expression = $2^{\Delta Ct}$ and $\Delta C_t = C_t$ Housekeeping Gene (β-tubulin) – C_tTarget (Livak and Schmittgen, 2001).

Results

Transcriptome Sequencing

In order to examine the transcriptional responses of aflatoxigenic isolates of *A. flavus* to oxidative stress, we cultured three isolates (AF13, NRRL3357, and Tox4) in aflatoxin production-conducive medium amended with H_2O_2 at different concentrations. Whole transcriptome sequencing of these tissues yielded a total of 1.32 billion raw sequencing reads from 18 cDNA libraries with an average of 73.17 million reads per library. Of the 18 libraries sequenced, one contained a relatively low number reads and was excluded from the analysis. Initial quality filtration resulted in the removal of 9 – 10% of reads followed by further removal of rRNA contamination. Following filtration, a total of 687.33 million filtered reads were obtained with an average of 40.43 million reads per library. For all the libraries, an average of 92.64% of filtered reads mapped to the *A. flavus* NRRL3357 reference genome. For the individual isolates, an average of 91.66%, 94.52%, and 91.58% of filtered reads from AF13, NRRL3357, and Tox4, respectively, mapped to the reference genome.

Of the 13,487 genes annotated in the NRRL3357 genome, 11,144 genes (82.63%) were described in the dataset. Among those described genes, 8,210 genes (73.67%) of the genes had an FPKM $\geq$ 2 in at least one isolate and treatment (Supplementary Dataset 1). Of these genes with an FPKM $\geq$ 2, 338 (4.12%), 62 (0.76%), and 73 (0.89%) genes were exclusively expressed in NRRL3357, AF13, and Tox4, respectively, across all treatments examined in the study (Figure D.1A). For each individual isolate, a relatively low number of genes were exclusively expressed with an FPKM $\geq$ 2 within a specified treatment. For NRRL3357, 73 (0.92%), 187 (2.35%), and 147 (1.85%) of the 7,941 genes expressed were exclusive to the 0 mM, 10 mM, and 20 mM H_2O_2 treatments, respectively (Figure D.1B). For AF13, 104 (1.36%), 45 (0.59%), and

130 (1.69%) of the 7,672 genes expressed were exclusive to the 0 mM, 10 mM, and 20 mM H_2O_2 treatments, respectively (Figure D.1C). For Tox4, 75 (0.97%), 91 (1.18%), and 66 (0.85%) of the 7,728 genes expressed were exclusive to the 0 mM, 10 mM, and 20 mM H_2O_2 treatments, respectively (Figure D.1D). A full list of the uniquely expressed genes in each isolate or treatment can be found in Supplementary Dataset 2.

Differential Expression is correlated with Oxidative Stress Tolerance

Following transcriptome assembly and alignment, differential expression analyses were performed to examine the oxidative stress responses of the isolates. Genes were considered significantly differentially expressed if they exhibited a $|\log_2 (\text{fold change})| \geq 2$ and adjusted $p \leq 0.05$. The Tox4 isolate exhibited 4 and 29 DEGs when comparing the control with 10 mM H_2O_2 and 25 mM H_2O_2 treatments, respectively, and 57 when comparing the two treatments (Table D.1). The AF13 isolate exhibited 6 and 122 DEGs when comparing the control with 10 mM H_2O_2 and 25 mM H_2O_2 treatments, respectively, and 85 when comparing the two treatments (Table D.1). The NRRL3357 isolate exhibited 53 and 117 DEGs when comparing the control with 10 mM H_2O_2 and 20 mM H_2O_2 treatments, respectively, and 112 when comparing the two treatments (Table D.1).

The numbers of significant DEGs for the isolates were then correlated with the previously observed maximum H_2O_2-induced oxidative stress tolerance levels observed for each isolate in our previous study (Fountain et al. 2015). The number of DEGs exhibited a strong, negative correlation with the previously observed tolerance levels (Figure S.D.1) when comparing the control and the 10mM H_2O_2 treatment ($r = -0.979$), and when comparing the two treatment conditions ($r = -0.958$). The correlation was not as strong, however, when comparing

the control and the 20 or 25 mM H_2O_2 treatment (r = -0.658). Interestingly, the isolates which exhibited the lower numbers of differentially expressed genes, especially under 10 mM H_2O_2, also tended to produce higher levels of aflatoxin (Table D.1; Fountain et al. 2015). However, while the isolate with the highest level of H_2O_2 tolerance, Tox4, did exhibit the fewest number of DEGs, it produces similar levels of aflatoxin to AF13 which exhibited slightly lower H_2O_2 tolerance and almost four times the number of DEGs at 25 mM H_2O_2 (Table D.1). In addition, comparison of the overall expression profiles shows a clear segregation by isolate indicative of the differences in isolate-specific gene expression patterns due to background expression differences between isolates and responses to increasing stress (Figure D.2, Table S.D.2).

Secondary Metabolite Gene Expression is regulated in Response to Oxidative Stress

Genes involved in the biosynthesis of aflatoxin were differentially expressed in the toxigenic isolates with distinguished aflatoxin production capabilities in response to increasing levels of oxidative stress (Figure D.3A). The most significant changes in expression mainly came in the isolate with the least tolerance to high levels of H_2O_2 than the other isolates included in this study, NRRL3357, which also produces only a moderate level of aflatoxin under elevated oxidative stress (Fountain et al. 2015). In NRRL3357, the genes encoding O-methyltransferase A (omtA), versicolorin B synthase (vbs), and versicolorin dehydrogenase/ketoreductase (ver-1) were exhibited $\log_2$(fold change) > 3.61 when comparing 0 and 10 mM H_2O_2 treatments, and > 4.85 when comparing 0 and 20 mM H_2O_2 (Supplementary Dataset 3). Additional genes encoding polyketide synthase (pksA), norsolorinic acid ketoreductase (nor-1), and a cytochrome p450 monooxygenase (aflV/cypX) also exhibited $\log_2$(fold change) > 2.32 when comparing the 0 and 20 mM H_2O_2 treatments (Supplementary Dataset 3). In AF13, the *cypX*, *omtA*, and *ver-1* genes

along with the genes encoding the versicolorin B desaturase p450 monooxygenase (verB), and the regulatory transcription factor aflS/aflJ were upregulated when comparing the 0 and 20 mM H_2O_2 treatments (Supplementary Dataset 4). None of these genes were found to be differentially expressed when comparing 0 and 10 mM H_2O_2 (Supplementary Dataset 4).

Surprisingly, in Tox4, no aflatoxin biosynthesis transcripts were found to be differentially expressed in either treatment (Supplementary Dataset 5). Among the aflatoxin biosynthetic genes, the averufin p450 monooxygenase (*avfA*), *hypE* hypothetical protein, O-methyltransferase B (*omtB*), oxidoreductase A (*ordA*), and NADH oxidase (*nadA*) genes were expressed with an FPKM $\geq$ 2 only in NRRL3357 (Supplementary Dataset 2). The aflatoxin genes encoding averantin p450 monooxygenase (avnA), vbs, ver-1, omtA, cypX, the p450 monooxygenase moxY, oxidoreductase B (ordB), and the hypothetical protein hypA were expressed with an FPKM $\geq$ 2 only in AF13 and NRRL3357 (Supplementary Dataset 2). The remaining aflatoxin pathway genes were found to be expressed in AF13, NRRL3357, and Tox4 (Supplementary Dataset 2).

In addition to aflatoxin biosynthesis genes, genes involved in the biosynthesis of two additional secondary metabolites, aflatrem and kojic acid, were found to be differentially expressed in response to increasing oxidative stress (Figure D.3B). In NRRL3357, the aflatrem biosynthesis genes encoding prenyl transferase (atmC) and geranylgeranyl diphosphate synthase (atmG) (Nicholson et al. 2009) were significantly upregulated in when comparing 0 and 10 mM H_2O_2 (Supplementary Dataset 3). The *atmG* gene was however, not upregulated when comparing 0 and 20 mM H_2O_2, though it is significantly reduced when comparing 10 and 20 mM H_2O_2 indicating a dose-dependent response (Supplementary Dataset 3). In contrast, in AF13 the dimethylallyl tryptophan synthase gene (*atmD*), *atmC*, and *atmG* were downregulated when

comparing 0 and 25 mM H_2O_2 while no aflatrem biosynthesis genes were significantly differentially expressed when comparing 0 and 10 mM H_2O_2 (Supplementary Dataset 4). Tox4, however, showed no significant differences in aflatrem biosynthesis gene expression when comparing the control with either treatment, though comparing 10 and 25 mM H_2O_2 did show a significant reduction in atmG expression (Supplementary Dataset 5).

For kojic acid biosynthetic genes (Terabayashi et al. 2010), the *kojA* and *kojR/T* genes were constitutively expressed in all the isolates and did not vary significantly in expression in response to increasing stress (Figure D.3C). The synaptic vesicle transporter SVOP, which is also involved in the biosynthesis of kojic acid (Terabayashi et al. 2010), was found to be differentially expressed in the examined isolates. In NRRL3357, the *SVOP* gene was upregulated by a $\log_2$(fold change) of 3.63 when comparing 0 and 10 mM H_2O_2, but was not significantly different between 0 and 20 mM (Supplementary Dataset 3). For AF13, the *SVOP* gene was also upregulated by a $\log_2$(fold change) of 2.47 when comparing 0 and 25 mM H_2O_2, but was not significantly different between 0 and 10 mM H_2O_2 (Supplementary Dataset 4).For Tox4, the *SVOP* gene was not significantly different between the control and the treatments, but was found to be downregulated when comparing 10 and 25 mM H_2O_2 indicating a slight reduction in response to higher levels of stress (Supplementary Dataset 5). The expression of *kojA* and *SVOP* along with select aflatoxin and aflatrem genes were further confirmed with qPCR which were generally correlated with the FPKM data obtained by RNA sequencing (Figure D.4).

Stress Responsive and Related Biochemical Pathways Regulated by Increasing Stress

In addition to the production mechanisms regulating secondary metabolite biosynthesis, additional stress responsive and associated biochemical pathway genes were also regulated in the

isolates in response to increasing stress (Figure D.5). Among the stress responsive genes, antioxidant and oxidase enzyme-encoding genes were among the most commonly regulated. In the NRRL3357 and AF13, thioredoxin peroxidase and thioredoxin reductase along with several cytochrome p450 monooxygenase genes were upregulated in response to increasing levels of oxidative stress (Supplementary Dataset 3 and 4). Interestingly, in Tox4 there were no antioxidant or oxidase genes regulated by 10 mM H_2O_2, and only one monooxygenase gene was regulated at 20 mM (Supplementary Dataset 5).

In addition to these antioxidant and oxidase genes, genes related to fungal catabolism and antibiosis tolerance were also regulated by stress, particularly in AF13. Comparing 0 and 10 mM H_2O_2, two multiple drug resistance protein-encoding genes were upregulated and expressed at a high level (FPKM's of 1,636.6 and 7,697.7, respectively; Supplementary Dataset 4). These genes were further upregulated when comparing 0 and 25 mM H_2O_2 (FPKMs of 2,627.0 and 15,066.5, respectively), along with a third expressed at a lower level (Supplementary Dataset 4). When comparing 0 and 25 mM H_2O_2, AF13 also exhibited the downregulation of a number of catabolic enzyme-encoding genes including acetyl xylan esterase, alpha-1,3-glucanase, aspergillopepsin 2 and F, class III and V chitinases, chitosanase, and penicillolysin/deuterolysin (Supplementary Dataset 4). NRRL3357 also exhibited a similar downregulation in the chitin catabolic genes encoding beta-N-acetylhexosaminidase (nagA) and beta-N-hexosaminidase when comparing 0 and 20 mM H_2O_2 (Supplementary Dataset 3). Iron metabolic genes were also regulated in NRRL3357 and AF13 in response to increasing stress. In NRRL3357, the siderophore biosynthesis acetylase gene *aceI* was upregulated when comparing 0 and 20 mM H_2O_2, and in AF13, a putative transferrin receptor gene was downregulated when comparing 0 and 25 mM H_2O_2 (Supplementary Dataset 3 and 4). NRRL3357 also exhibited an upregulation in cinnamoyl-

CoA reductase gene expression when comparing 0 and 20 mM H_2O_2 (Supplementary Dataset 3). Tox4 exhibited regulation of two phosphate signaling genes in response to increasing stress, but none of the aforementioned genes (Supplementary Dataset 5).

Fungal Development-Related Genes are regulated by Oxidative Stress

Genes involved in the development of *A. flavus* and other *Aspergillus spp.* were also differentially expressed among the isolates. In NRRL3357, the gene encoding the Cis_2His_2 (C_2H_2) transcription factor flbC was upregulated along with a conidiation-specific family protein gene and a duf221 domain protein gene (Supplementary Dataset 3). AF13 also exhibited an upregulation of a conidial hydrophobin gene in response to increasing stress (Supplementary Dataset 4). In addition, genes involved in benzoate degradation were also regulated in response to stress in the isolates. NRRL3357 and AF13 both exhibited the upregulation of genes involved in benzoate degradation including a multiple inositol polyphosphate phosphatase and a benzoate 4-monooxygenase (Supplementary Dataset 3 and 4). Conversely, Tox4 exhibited a downregulation of an amidohydrolase family protein gene and a multiple inositol polyphosphate phosphatase gene (Supplementary Dataset 5).

bZIP Transcription Factors and Promoter Occurrence among Differentially Expressed Genes

The orthologs of two bZIP transcription factor genes, *atfA* and *atf21*, were previously shown to regulate the expression of genes involved in both the biosynthesis of aflatoxin and sterigmatocystin, and oxidative stress responsive mechanisms (Roze et al. 2011). Here, *atf21* and *atfA* exhibited marginal increases in expression in NRRL3357 and AF13 under high levels of

H_2O_2 stress (Figure S.D.2). The ortholog of atf21 in *A. parasiticus*, atfB, has been well characterized and has been shown to bind a conserved promoter motif, AGCC(G/C)T(G/C)(A/G), upstream of several aflatoxin biosynthetic genes (Roze et al. 2011). Examination of the 1kb upstream regions of the significant DEGs observed in NRRL3357 showed that nine genes possess this predicted atf21 binding domain including a putative cytochrome p450 monooxygenase gene, *aflC*, and the siderophore biosynthesis acetylase *aceI* (Figure S.D.2).

Gene Co-Expression is correlated with Mycelial Dry Weight under Oxidative Stress

In order to identify groups of genes whose expression is directly correlated with isolate oxidative stress tolerance, a co-expression analysis was performed for all isolates and treatments and correlated with previously obtained fungal dry weights (Figure D.6). Co-expressed genes were grouped based on expression profile similarities into color-coded modules, which were further separated by hierarchical clustering. Gene network analysis revealed that the largest modules in terms of gene content were the turquoise, blue, and brown modules (Figure D.6A).

Module-trait association analysis was then performed to correlate fungal dry weights under each treatment. The blue, purple, and turquoise modules were found to be associated with isolate dry weight under oxidative stress (Figure D.6B). Statistical eigengene expression and fungal dry weight were also found to be significantly correlated with the purple ($r = 0.83$, $p = 0.006$) and turquoise ($r = 0.73$, $p = 0.02$) module genes showing a strong positive correlation with isolate dry weight and the blue module genes showing a strong negative correlation ($r = -0.93$, $p = 0.0002$) with isolate dry weight (Figure D.6C). Gene ontology (GO) enrichment analysis of these modules showed that the blue module was enriched for simple sugar

metabolism terms, the purple module for regulation of gene expression and metabolic processes, and the turquoise module for translational mechanisms and additional metabolic processes (Supplementary Dataset 6). The blue and turquoise modules were also found to contain the aflatoxin biosynthetic genes while the purple module contained several MFS transporter and antioxidant genes (Supplementary Dataset 6).

Discussion

The production of secondary metabolites in soil dwelling fungi has been shown to be regulated by a number of factors, particularly environmental stress (Calvo and Cary, 2015). Aflatoxin production by *A. flavus* has been shown to be stimulated by a number of compounds *in vitro*, with reactive oxygen species (ROS) being of particular interest given their prevalence in host plant defense signaling and environmental stress, particularly drought stress, responses (Bhattacharjee, 2005; Jayashree and Subramanyam, 2001; Roze et al. 2013; Yang et al. 2015, 2016). Such ROS have also been shown to be required for the production of aflatoxin with treatment with antioxidant compounds resulting in reduced aflatoxin production and fungal growth (Mahoney et al. 2010; Nesci et al. 2003; Passone et al. 2005). However, the practical role of aflatoxin production in *A. flavus* biology is still not well understood. In order to better understand to biological role of aflatoxin production in *A. flavus*, and its role in oxidative stress responses, we examined the transcriptomes of three aflatoxigenic field isolates exposed to increasing levels of H_2O_2-derived oxidative stress.

The isolates which had previously exhibited greater levels of H_2O_2 tolerance and aflatoxin production (Fountain et al. 2015), Tox4 and AF13, exhibited a fewer numbers of significantly differentially expressed genes in comparison to the isolate with less tolerance,

NRRL3357 (Table D.1). This trend also resulted in strong correlations between previously observed stress tolerance and the numbers of DEGs (Figure S.D.1). Interestingly, the AF13 isolate exhibits both a similar number and composition of DEGs at 25mM H_2O_2 in comparison to NRRL3357 at 10mM (Figure S.D.1; Supplementary Datasets 3 and 4). The requirement of additional stress to elicit a similar response is commensurate with the observed stress tolerance and aflatoxin production capabilities of AF13 and NRRL3357 (Fountain et al. 2015). Tox4, however, may possess stress responsive mechanisms which at more vigorously earlier accounting for the reduced DEG counts observed in this study. Together these results indicate, as has been previously suggested in the literature, that aflatoxin production may contribute to oxidative stress tolerance in *Aspergillus spp.* (Fountain et al. 2014, 2016; Narasaiah et al. 2006; Roze et al. 2013, 2015).

Examining the expression of aflatoxin biosynthetic genes showed that the NRRL3357 isolate exhibited the up-regulation and expression of a greater number of these genes than the other isolates examined in the study (Table D.1, Figure D.3A). An increase in expression, though to a lesser extent, was also observed for AF13 under higher levels of stress, but not for Tox4 (Figure D.3A). This was surprising given that aflatoxin biosynthetic gene expression is typically higher with periods in fungal development *in vitro* that coincide with the highest levels of aflatoxin production, approximately two to six days in conducive media (Davis et al. 1966). The high level of expression of aflatoxin genes in NRRL3357 at seven days under high levels of stress coupled with the reduced fungal biomass and conidiation observed for this isolate and not with AF13 or Tox4 in our preliminary study (Fountain et al. 2015), suggests that a delay in fungal growth and development may contribute to prolonged aflatoxin gene expression in addition to stimulation provided by oxidative stress. In addition, these differential expression

patterns of aflatoxin biosynthetic genes may also be indicative of post-transcriptional regulation of aflatoxin production and oxidative stress responses at either the RNA or protein level. For example, there has been a low degree of correlation observed between gene expression and proteomics data for traits such as temperature stress ($r = 0.14$) suggesting post-transcriptional regulation of protein accumulation in *A. flavus* (Bai et al. 2015). Also, given that aflatoxin biosynthetic gene expression can be detected as early as eight hours in culture, there is ample opportunity for such regulation to have a significant effect on later responses to stress and warrants further investigation (Price et al. 2006).

However, factors in addition to aflatoxin production have been shown to be at play which influence *A. flavus* tolerance to oxidative stress. For example, Reverberi et al. (2012) examined the effects of excessive peroxisome proliferation in a mutant isolate expressing the P33 gene. They found that the P33-containing isolate exhibited elevated ROS and oxylipin accumulation commensurate with excess peroxisomes, and countered this with increased aflatoxin production and higher antioxidant enzyme activity compared to the wildtype isolate. The mutant isolate also exhibited similar fungal growth but reduced conidiation compared to the wildtype. Elevated expression of antioxidant and aflatoxin genes at the time point examined in our study would imply that continued stress is still being experienced by NRRL3357, and not to the same extent in AF13 or Tox4. This suggests that NRRL3357 is less able to sequester ROS and remediate its damage than the other isolates. Our previous observation that culturing these isolates in an aflatoxin production non-conducive medium results only in a slight reduction in stress tolerance also suggests that additional oxidative stress remediation mechanisms are at play in all isolates in addition to aflatoxin production (Fountain et al. 2015, 2016).

Two bZIP transcription factor genes, *atf21* and *atfA*, whose homologs in other *Aspergillus spp*. have been shown to integrate oxidative stress responses and sterigmatocystin/aflatoxin biosynthesis regulation (Hong et al. 2013a, 2013b; Lara-Rojas et al. 2011; Roze et al. 2011, 2013; Sakamoto et al. 2009, 2010), also displayed some marginally significant increases in expression in NRRL3357 and AF13 (Figure S.D.2). Atf21, whose ortholog in *A. parasiticus*, atfB, has been well characterized (Roze et al. 2011), was found to bind a conserved motif in the promoter regions of several aflatoxin biosynthetic genes. This same motif was found in the upstream promoter regions of nine DEGs in NRRL3357 under high levels of stress, and include aflatoxin production, oxidative stress response, and siderophore biosynthetic genes (Figure S.D.2). This suggests that these transcription factors may actively regulate gene expression following aflatoxin production initiation (Roze et al. 2011, 2013) and further supports the case for their involvement in stress tolerance. Also, the co-expression analysis identified several modules of genes exhibiting similar expression profiles which were closely associated with fungal biomass under oxidative stress, including the blue, purple, and turquoise modules (Figure D.6C). These modules contain genes enriched for carbon metabolism and gene expression regulation, but also contain antioxidant enzyme-encoding genes and the aflatoxin biosynthetic genes (Supplementary Dataset 6). This further supports the observed association of aflatoxin production and oxidative stress tolerance in *A. flavus*.

The link between aflatoxin production and fungal development has been widely documented in the literature to involve G-protein mediated signaling along with numerous transcription factors and regulatory proteins (Amaike and Keller, 2011). Here, velvetA (*VeA*), a key developmental regulator influencing sclerotial and conidia formation in response to light levels (Bayram et al. 2008), was constitutively expressed regardless of stress levels while

conidiation-related genes such as *flbC*, a conidiation-specific family protein gene, and a duf221 domain protein gene were also up-regulated under stress conditions (Ben-Ami et al. 2010; Kwon et al. 2010). This suggests as has been previously observed (Fountain et al. 2015, Roze et al. 2015) that oxidative stress can stimulate conidiation in *Aspergillus spp.* Benzoate and amino benzoate degradation genes were also regulated in response to stress (Supplementary Datasets 3-5). These compounds have been shown to reduce aflatoxin production and slow fungal growth and development when applied *in vitro* providing further indication that fungal development may be affected by oxidative stress exposure (Chipley and Uraih, 1980).

Chitin catabolism-related genes tended to be down-regulated under oxidative stress (Supplementary Datasets 3 and 4) which may reduce cell wall degradation and enhance cell well integrity to protect against oxidative stress (Fountain et al. 2016; Fuchs and Mylonakis, 2009; Jain et al. 2011). Also, antibiosis-related genes encoding multiple drug resistance proteins were also upregulated, particularly in AF13, in response to stress. This may provide additional protection for this isolate in competition with other soilborne or plant parasitic microorganisms, especially under environmental stress (Daguerre et al. 2014). NRRL3357 also exhibited an upregulation in cinnamoyl-CoA reductase gene expression in response to stress (Supplementary Dataset 3). This is noteworthy since it was only fairly recently found that phenylpropanoid metabolic genes were present in the genomes of fungi including the Aspergilli (Seshime et al. 2005). Several members of this class of compounds have been found to influence aflatoxin production by *A. flavus in vitro*, and have been shown to function as antioxidants which could enhance stress tolerance and competitive capability of the isolates (Chipley and Uraih, 1980). This may indicate that phenylpropanoids or flavonoids produced in host plants along with ROS during drought stress may also be able to influence the production of aflatoxin by *A. flavus* and

warrants further study (Alvarez et al. 2008; Payton et al. 2009). Genes encoding antioxidant enzymes such as thioredoxin peroxidase and thioredoxin reductase were also significantly regulated in response to increasing stress. In the co-expression analysis, the purple module, which exhibited the highest positive correlation with fungal biomass, also contained antioxidant enzyme encoding genes such as glutathione-S-transferase (Supplementary Dataset 6).

Two additional secondary metabolite biosynthetic gene clusters were also induced by oxidative stress, aflatrem and kojic acid. Aflatrem is a tremerogenic mycotoxin which causes stagger's syndrome in cattle and neurological effects in mammals (Nicholson et al. 2009). Aflatrem is also proposed to function in fungivory prevention for soilborne fungi (TePaske and Gloer, 1992). The biosynthesis of aflatrem is carried out by the indole-diterpenoid (isoprenoid) pathway in *Aspergillus spp*. and shares with aflatoxin biosynthesis the commonality of cytochrome p450 monooxygenase activity (Calvo and Cary, 2015; Nicholson et al. 2009). This along with the activities of various oxidases has led to the proposition that aflatoxin production may function in the alleviation of oxidative stress by promoting antioxidant enzyme production and conidial oxidative stress tolerance through secondary ROS production (Fountain et al. 2016; Roze et al. 2015). We also propose that this process may result in the fixation of excess molecular oxygen (O_2) and detoxified ROS into the aflatoxin molecules which are then secreted from the cell as an indirect means of relieving oxidative stress (Fountain et al. 2016). Alone or in combination, these two proposals would also suggest that isolates which produce higher levels of aflatoxin would exhibit greater oxidative stress tolerance, a trend observed here and in our preliminary study, but which will require further study to confirm (Fountain et al. 2015, 2016). Given the prevalence of cytochrome p450 monooxygenase activity in the aflatrem biosynthetic

mechanism, it is possible that a similar phenomenon may occur which is also in need of further investigation.

Kojic acid is a bi- or tri-dentate iron chelating antioxidant compound produced by several species of Aspergilli including *A. sojae* (Chang et al. 2010). The compound and derivatives of it are useful for the treatment of iron overload in people with thalassemia who accumulate dangerously high levels of iron in their blood stream following multiple transfusions (Nurchi et al. 2016). The iron chelating properties of kojic acid may also, as in the case of cyclopiazonic acid (CPA), may help soil-borne fungi in the remediation of iron starvation under stress conditions by fixing additional iron cations and outcompeting other microbes (Chang et al. 2009). This may also be affected by oxidative stress in *A. flavus* since siderophore biosynthetic genes were also found to be regulated in AF13 and NRRL3357. Also, the chelation of excess iron cations, particularly Fe^{2+}, may prevent Fenton reaction-derived ROS such as hydroxyl radicals (OH^{-}) from forming and resulting in additional cellular damage (Fenton, 1894). Therefore, the production of kojic acid may also supplement *A. flavus* oxidative stress tolerance. Also, these same hydroxyl radicals have also been shown to influence aflatoxin production with treatment of *A. flavus* mycelia with DMSO, a hydroxyl radical scavenger, resulting in significantly reduced aflatoxin production and sclerotial differentiation (Grintzalis et al. 2014).

Together, these results provide an insight into a potentially coordinated secondary metabolite response to oxidative stress in *A. flavus*. While the biological function of the aflatoxin compound in fungal biology remains unclear, it seems possible that the aflatoxin production process may contribute to oxidative stress tolerance. However, in the absence of aflatoxin production capability, the production of other secondary metabolites may compensate for any reduction in stress tolerance, and may be of interest in the biology of atoxigenic biological

control isolates. This role of oxidative stress in stimulating aflatoxin production in *A. flavus* is made all the more interesting by the observed accumulation of ROS in drought stressed host plant tissues (Yang et al. 2015, 2016), and the correlation of elevated antioxidant enzyme and compound accumulation in hosts resistant to aflatoxin contamination (Chitarrini et al. 2014). Together, this may be a contributing factor to the observed correlation between drought stress susceptibility and aflatoxin contamination in host plant species such as maize and peanut (Holbrook et al. 2009; Kebede et al. 2012). The role of oxidative stress in both secondary metabolite production and fungal primary metabolism may also provide a basis for identifying host defense attributes which contribute to reduced aflatoxin contamination in the form of selectable biomarkers and in the selection and characterization of novel resistance genes and genetic markers identified through quantitative trait loci (QTL) studies for marker assisted selection (MAS) and cultivar resistance improvement.

Acknowledgements

We thank Billy Wilson, Hui Wang, Xiaohong Guo, Xiangyun Ji, Gaurav Agarwal, and Hui Song for technical assistance in the laboratory. This work is partially supported by the U.S. Department of Agriculture Agricultural Research Service (USDA-ARS), the Georgia Agricultural Commodity Commission for Corn, the Georgia Peanut Commission, the Peanut Foundation, and AMCOE (Aflatoxin Mitigation Center of Excellence, Chesterfield, MO, USA). This work has also been undertaken as part of the CGIAR Research Program on Grain Legumes and the USAID University Linkages Program between USDA-ARS and ICRISAT. ICRISAT is a member of CGIAR Consortium. Mention of trade names or commercial products in this publication is solely for the purpose of providing specific information and does not imply

recommendation or endorsement by the USDA. The USDA is an equal opportunity provider and employer.

Supplemental Information

Links to supplemental datasets, figures, and tables can be found in Appendix A.

References

1. Alvarez, S., Marsh, E.L., Schroeder, S.G., Schachtman, D.P. (2008). Metabolomic and proteomic changes in the xylem sap of maize under drought. *Plant Cell Environ.* 31, 325-340.
2. Amaike, S., Keller, N.P. (2011). *Aspergillus flavus*. *Ann. Rev. Phytopathol.* 49, 107-133.
3. Andrade, P.D., Caldas, E.D. (2015). Aflatoxins in cereals: worldwide occurrence and dietary risk assessment. *World Mycotoxin J.* 8, 415-431.
4. Bai, Y., Wang, S., Zhong, H., Yang, Q., Zhang, F., Zhuang, Z., et al. (2015). Integrative analyses reveal transcriptome-proteome correlation in biological pathways and secondary metabolism clusters in *A. flavus* in response to temperature. *Sci. Rep*. **5**:15482. doi: 10.1038/srep14582.
5. Baidya, S., Duran, R.M., Lohmar, J.M., Harris-Coward, P.Y., Cary, J.W., Hong, S.Y. (2014). VeA is associated with the response to oxidative stress in the aflatoxin producer *Aspergillus flavus*. *Eukaryotic Cell.* 13, 1095-1103.
6. Bailey, T.L., Boden, M., Buske, F.A., Frith, M., Grant, C.E., Clementi, L., et al. (2009). MEME Suite: tools for motif discovery and searching. *Nuc. Acids Res.* 35, 202-208.

7. Bayram, O., Krappmann, S., Ni, M., Bok, J.W., Helmstaedt, K., Valerius, O. (2008). VelB/VeA/LaeA complex coordinates light signal with fungal development and secondary metabolism. *Science.* 320, 1504-1506.
8. Ben-Ami, R., Varga, J., Lewis, R.E., May, G.S., Nierman, W.C., Kontoyiannis, D.P. (2010). Characterization of a 5-azacytidine-induced developmental *Aspergillus fumigatus* variant. *Virulence.* 1, 164-173.
9. Bhattacharjee, S. (2005). Reactive oxygen species and oxidative burst: roles in stress, senescence and signal. *Curr. Sci. India.* 89, 1113-1121.
10. Calvo, A.M., Cary, J.W. (2015). Association of fungal secondary metabolism and sclerotial biology. *Front. Microbiol.* **6**:62 doi: 10.3389/fmicb.2015.00062.
11. Chanda, A., Roze, L.V., Kang, S., Artymovich, K.A., Hicks, G.R., Raikhel, N.V., et al. (2009). A key role for vesicles in fungal secondary metabolism. *Proc. Nat. Acad. Sci.* 106, 19533-19538.
12. Chanda, A., Roze, L.V., Linz, J.E. (2010). A possible role for exocytosis in aflatoxin export in *Aspergillus parasiticus*. *Eukaryotic Cell.* 9, 1724-1727.
13. Chang, P.K., Ehrlich, K.C., Fujii, I. (2009). Cyclopiazonic acid biosynthesis of *Aspergillus flavus* and *Aspergillus oryzae*. *Toxins.* 1, 74-99.
14. Chang, P.K., Scharfenstein, L.L., Luo, M., Mahoney, N., Molyneux, R.J., Yu, J., et al. (2010). Loss of msnA, a putative stress regulatory gene, in *Aspergillus parasiticus* and *Aspergillus flavus* increased production of conidia, aflatoxins and kojic acid. *Toxins.* 3, 82-104.
15. Chipley, J.R., Uraih, N. (1980). Inhibition of *Aspergillus* growth and aflatoxin release by derivatives of benzoic acid. *App. Environ. Microbiol.* 40, 352-357.

16. Chitarrini, G., Nobili, C., Pinzari, F., Antonini, A., De Rossi, P., Del Fiore, A., et al. (2014). Buckwheat achenes antioxidant profile modulates *Aspergillus flavus* growth and aflatoxin production. *Int. J. Food Microbiol*. 189, 1-10.

17. Daguerre, Y., Siegel, K., Edel-Hermann, V., Steinberg, C. (2014). Fungal proteins and genes associated with biocontrol mechanisms of soil-borne pathogens: a review. *Fungal Biol. Rev.* 28, 97-125.

18. Davis, N.D., Diener, U.L., Eldridge, D.W. (1966). Production of aflatoxins B_1 and G_1 by *Aspergillus flavus* in a semisynthetic medium. *App. Microbiol.* 14, 378-380.

19. Fenton, H.J.H. (1894). Oxidation of tartaric acid in presence of iron. *J. Chem. Soc. Trans.* 65, 899-910.

20. Fountain, J.C., Bajaj, P., Pandey, M., Nayak, S.N., Yang, L., Kumar, V., et al. (2016). Oxidative stress and carbon metabolism influence *Aspergillus flavus* secondary metabolite production and transcriptome composition. *Sci. Rep.* (in press).

21. Fountain, J.C., Scully, B.T., Chen, Z.Y., Gold, S.E., Glenn, A.E., Abbas, H.K., et al. (2015). Effects of hydrogen peroxide on different toxigenic and atoxigenic isolates of *Aspergillus flavus*. *Toxins.* 7, 2985-2999.

22. Fountain, J.C., Scully, B.T., Ni, X., Kemerait, R.C., Lee, R.D., Chen, Z.Y., et al. (2014). Environmental influences on maize-*Aspergillus flavus* interactions and aflatoxin production. *Front. Microbiol.* **5**:40. doi: 10.3389/fmicb.2014.00040.

23. Fuchs, B.B., Mylonakis, E. (2009). Our paths might cross: the role of the fungal cell wall integrity pathway in stress response and cross talk with other stress response pathways. *Eukaryotic Cell.* 8, 1616-1625.

24. Gao, X., Brodhagen, M., Isakeit, T., Brown, S.H., Göbel, C., Betran, J., et al. (2009). Inactivation of the lipoxygenase ZmLOX3 increases susceptibility of maize to *Aspergillus spp*. *Mol. Plant Mic. Interact.* 22, 222-231.

25. Grintzalis, K., Vernardis, S., Klapa, M., Georgiou, C.D. (2014). Role of oxidative stress in sclerotial differentiation and aflatoxin B1 biosynthesis in *Aspergillus flavus*. *App. Environ. Microbiol*. 80, 5561-5571.

26. Guo, B., Chen, Z.Y., Lee, R.D., Scully, B.T. (2008). Drought stress and preharvest aflatoxin contamination in agricultural commodity: genetics, genomics and proteomics. *J. Int. Plant Biol.* 50, 1281-1291.

27. Guo, B., Russin, J.S., Cleveland, T.E., Brown, R.L., Damann, K.E. (1996). Evidence for cutinase production by *Aspergillus flavus* and its possible role in infection of corn kernels. *Phytopathology*. 86, 824-829.

28. Guo, B., Yu, J., Ni, X., Lee, R.D., Kemerait, R.C. and Scully, B.T. (2012). "Crop Stress and Aflatoxin Contamination: Perspectives and Prevention Strategies," in *Crop Stress and its Management: Perspectives and Strategies*, eds. B. Venkateswarlu, A.K. Shankerk, C. Shanker, , M. Makeswari. (New York, NY: Springer), 399-427.

29. Holbrook, C.C., Guo, B., Wilson, D.M., Timper, P. (2009). The US breeding program to develop peanut with drought tolerance and reduced aflatoxin contamination. *Peanut Sci.* 36, 50-53.

30. Hong, S.Y., Roze, L.V., Linz, J.E. (2013a). Oxidative stress-related transcription factors in the regulation of secondary metabolism. *Toxins.* 5, 683-702.

31. Hong, S.Y., Roze, L.V., Wee, J., Linz, J.E. (2013b). Evidence that a transcription factor regulatory network coordinates oxidative stress response and secondary metabolism in aspergilli. *MicrobiologyOpen.* 2, 144-160.

32. Jain, R., Valiante, V., Remme, N., Docimo, T., Heinekamp, T., Hertweck, C., et al. (2011). The MAP kinase MpkA controls cell wall integrity, oxidative stress response, gliotoxin production and iron adaptation in *Aspergillus fumigatus*. *Mol. Microbiol.* 82, 39-53.

33. Jayashree, T., Subramanyam, C. (2000). Oxidative stress as a prerequisite for aflatoxin production by *Aspergillus parasiticus*. *Free Rad. Biol. Med.* 29, 981–985.

34. Jiang, T., Fountain, J.C., Davis, G., Kemerait, R.C., Scully, B.T., Lee, R.D., et al. (2012). Root morphology and gene expression analysis in response to drought stress in maize (*Zea mays*). *Plant Mol. Biol. Rep.* 30, 360-369.

35. Kebede, H., Abbas, H.K., Fisher, D.K., Bellaloui, N. (2012). Relationship between aflatoxin contamination and physiological responses of corn plants under drought and heat stress. *Toxins.* 4, 1385-1403.

36. Kew, M.C. (2013). Aflatoxins as a cause of hepatocellular carcinoma. *J. Gastrointestin. Liver Dis.* 22, 305-310.

37. Kwon, N.J., Garzia, A., Espeso, E.A., Ugalde, U., Yu, J.H. (2010). FlbC is a putative nuclear C_2H_2 transcription factor regulating development in *Aspergillus nidulans*. *Mol. Microbiol.* 77, 1203-1219.

38. Langfelder, P., Horvath, S. (2008). WGCNA: an R package for weighted correlation network analysis. *BMC Bioinform.* **9**:559. doi: 10.1186/1471-2105-9-559.

39. Lara-Rojas, F., Sanchez, O., Kawasaki, L., Aguirre, J. (2011). *Aspergillus nidulans* transcription factor AtfA interacts with the MAPK SakA to regulate general stress responses, development and spore functions. *Mol. Microbiol.* 80, 436-454.

40. Livak, K.J., Schmittgen, T.D. (2001). Analysis of relative gene expression data using real-time quantitative PCR and the $2^{-\Delta\Delta Ct}$ method. *Methods.* 25, 402-408.

41. Mahoney, N., Molyneux, R., Kim, J., Campbell, B., Waiss, A., Hagerman, A. (2010). Aflatoxigenesis induced in *Aspergillus flavus* by oxidative stress and reduction by phenolic antioxidants from tree nuts. *World Mycotoxin J.* 3, 49-57.

42. Matumba, L., Van Poucke, C., Monjerezi, M., Ediage, E.N., De Saeger, S. (2015). Concentrating aflatoxins on the domestic market through groundnut export: A focus on Malawian groundnut value and supply chain. *Food Control.* 51, 236-239.

43. Narasaiah, K.V., Sashidhar, R.B., Subramanyam, C. (2006). Biochemical analysis of oxidative stress in the production of aflatoxin and its precursor intermediates. *Mycopathologia.* 162, 179–189.

44. Nesci, A., Rodriguez, M., Etcheverry, M. (2003). Control of *Aspergillus* growth and aflatoxin production using antioxidants at different conditions of water activity and pH. *J. App. Microbiol*. 95, 279-287.

45. Nicholson, M.J., Koulman, A., Monahan, B.J., Pritchard, B.L., Payne, G.A., Scott, B. (2009). Identification of two aflatrem biosynthesis gene loci in *Aspergillus flavus* and metabolic engineering of *Penicillium paxilli* to elucidate their function. *Appl. Environ. Microbiol.* 75, 7469-7481.

46. Nurchi, V.M., Crisponi, G., Lachowicz, J.I., Medici, S., Peana, M., Zoroddu, M.A. (2016). Chemical features of in use and in progress chelators for iron overload. *J. Trace Elem. Med. Biol.* In press.

47. Pandey, M.K., Monyo, E., Ozias-Akins, P., Liang, X., Guimarães, P., Nigam, S.N., et al. (2012). Advances in *Arachis* genomics for peanut improvement. *Biotech. Adv.* 30, 639-651.

48. Park, H.S., Ni, M., Jeong, K.C., Kim, Y.H., Yu, J.H. (2012). The role, interaction and regulation of the *Velvet* regulator VelB in *Aspergillus nidulans*. *PLoS One.* **7**:e45935. doi: 10.1371/journal.pone.0045935.

49. Passone, M.A., Resnik, S.L., Etcheverry, M.G. (2005). In vitro effect of phenolic antioxidants on germination, growth and aflatoxin B1 accumulation by peanut *Aspergillus* section Flavi. *J. App. Microbiol*. 99, 682-691.

50. Payton, P., Kottapalli, K.R., Rowland, D., Faircloth, W., Guo, B., Burow, M., et al. (2009). Gene expression profiling in peanut using high density oligonucleotide microarrays. *BMC Genomics.* **10**:265. doi: 10.1186/1471-2164-10-265.

51. Price, M.S, Yu, J., Nierman, W.C., Kim, H.S., Pritchard, B., Jacobus, C.A., et al. (2006). The aflatoxin pathway regulator AflR induces gene transcription inside and outside of the aflatoxin biosynthetic cluster. *FEMS Microbiol. Lett*. 255, 275-279.

52. Reverberi, M., Punelli, M., Smith, C.A., Zjalic, S., Scarpari, M., Scala, V., et al. (2012). How peroxisomes affect aflatoxin biosynthesis in *Aspergillus flavus*. *PLoS One*. 7:e48097. doi:10.1371/journal.pone.0048097.

53. Reverberi, M., Zjalic, S., Ricelli, A., Punelli, F., Camera E., Fabbri C., et al. (2008). Modulation of antioxidant defense in *Aspergillus parasiticus* is involved in aflatoxin biosynthesis: a role for the *ApyapA* gene. *Eukaryotic Cell.* 7, 988–1000.

54. Roze, L.V., Chanda, A., Wee, J., Awad, D., Linz, J.E. (2011). Stress-related transcription factor AtfB integrates secondary metabolism with oxidative stress response in Aspergilli. *J. Biol. Chem.* 286, 35137-35148.

55. Roze, L.V., Hong, S.Y., Linz, J.E. (2013). Aflatoxin biosynthesis: current frontiers. *Annu. Rev. Food Sci. Tech.* 4, 293–311.

56. Roze, L.V., Laivenieks, M., Hong, S.Y., Wee, J., Wong, S.S., Vanos, B., et al. (2015). Aflatoxin biosynthesis is a novel source of reactive oxygen species – A potential redox signal to initiate resistance to oxidative stress? *Toxins.* 7, 1411–1430.

57. Sakamoto, K., Arima, T., Iwashita, K., Yamada, O., Gomi, Y., Akita, O. (2008). *Aspergillus oryzae atfB* encodes a transcription factor required for stress tolerance in conidia. *Fungal Genet. Biol.* 45, 922-932.

58. Sakamoto, K., Iwashita, K., Yamada, O., Kobayashi, K., Mizuno, A., Akita, O., et al. (2009). *Aspergillus oryzae atfA* controls conidial germination and stress tolerance. *Fungal Genet. Biol.* 46, 887-897.

59. Seshime, Y., Juvvadi, P.R., Fujii, I., Kitamoto, K. (2005). Genomic evidences for the existence of a phenylpropanoid metabolic pathway in *Aspergillus oryzae*. *Biochem. Biophys. Res. Comm.* 337, 747-751.

60. Stajich, J.E., Harris, T., Brunk, B.P., Brestelli, J., Fischer, S., Harb, O.S., et al. (2012). FungiDB: an integrated functional genomics database for fungi. *Nuc. Acids Res.* 40, 675-681.

61. TePaske, M.R., Gloer, J.B. (1992). Aflavarin and B-aflatrem: New anti-insectan metabolites from the sclerotia of *Aspergillus flavus*. *J. Nat. Prod.* 55, 1080-1086.

62. Terabayashi, Y., Sano, M., Yamane, N., Marui, J., Tamano, K., Sagara, J., et al. (2010). Identification and characterization of genes responsible for biosynthesis of kojic acid, an industrially important compound from *Aspergillus oryzae*. *Fungal Genet. Biol.* 47, 953-961.

63. Torres, A.M., Barros, G.G., Palacios, S.A., Chulze, S.N., Battilani, P. (2014). Review on pre- and post-harvest management of peanuts to minimize aflatoxin contamination. *Food Res. Int.* 62, 11-19.

64. Williams, W.P. (2006). Breeding for resistance to aflatoxin accumulation in maize. *Mycotoxin Res.* 22, 27-32.

65. Williams J.H., Grubb J.A., Davis J.W., Wang J.S., Jolly P.E., Ankrah, N.A., et al. (2010). HIV and hepatocellular and esophageal carcinomas related to consumption of mycotoxin-prone foods in sub-Saharan Africa. *Am. J. Clin. Nutr.* 92, 154–160.

66. Williams, J.H., Phillips, T.D., Jolly, P.E., Stiles, J.K., Jolly, C.M., Aggarwal, D. (2004). Human aflatoxicosis in developing countries: a review of toxicology, exposure, potential consequences, and interventions. *Am. J. Clin. Nutr.* 80, 1106-1122.

67. Wu, F. (2015). Global impacts of aflatoxin in maize: trade and human health. *World Mycotoxin J.* 8, 137-142.

68. Yang, L., Fountain, J.C., Chu, Y., Ni, X., Lee, R.D., Kemerait, R.C., et al. (2016). Differential accumulation of reactive oxygen and nitrogen species in maize lines with contrasting drought tolerance and aflatoxin resistance. *Phytopathology.* 106, S2.16.

69. Yang, L., Fountain, J.C., Wang, H., Ni, X., Ji, P., Lee, R.D., et al. (2015). Stress sensitivity is associated with differential accumulation of reactive oxygen and nitrogen species in maize genotypes with contrasting levels of drought tolerance. *Int. J. Mol. Sci.* 16, 24791-24819.

70. Yu, J., Chang, P.K., Ehrlich, K.C., Cary, J.W., Bhatnagar, D., Cleveland, T.E., et al. (2004). Clustered pathway genes in aflatoxin biosynthesis. *App. Environ. Microbiol.* 70, 1253-1262.

Table D.1. Numbers of significantly, differentially expressed genes.

Isolate	Toxin[a]	H_2O_2[a]	0 v 10 mM[b]	0 v 20/25 mM[b]	10 v 20/25 mM[b]
Tox4	+++	40	4	29	57
AF13	+++	35	6	122	85
NRRL3357	+	20	53	117	112

[a]Aflatoxin production capability (+++, high; +, moderately high) and maximum H_2O_2 tolerance observed in Fountain et al. 2015.

[b]Numbers of DEGs described in Fountain et al. 2016.

Figure D.1. Venn diagrams of genes expressed with an FPKM ≥ 2. Genes exhibiting an FPKM ≥ 2 in at least one isolates and treatment were considered to be expressed. Genes expressed within all isolates and treatments (A), and between treatments within the NRRL3357 (B), AF13 (C), and Tox4 (D) isolates were compared using Venn diagrams generated with Venny 2.1.0.

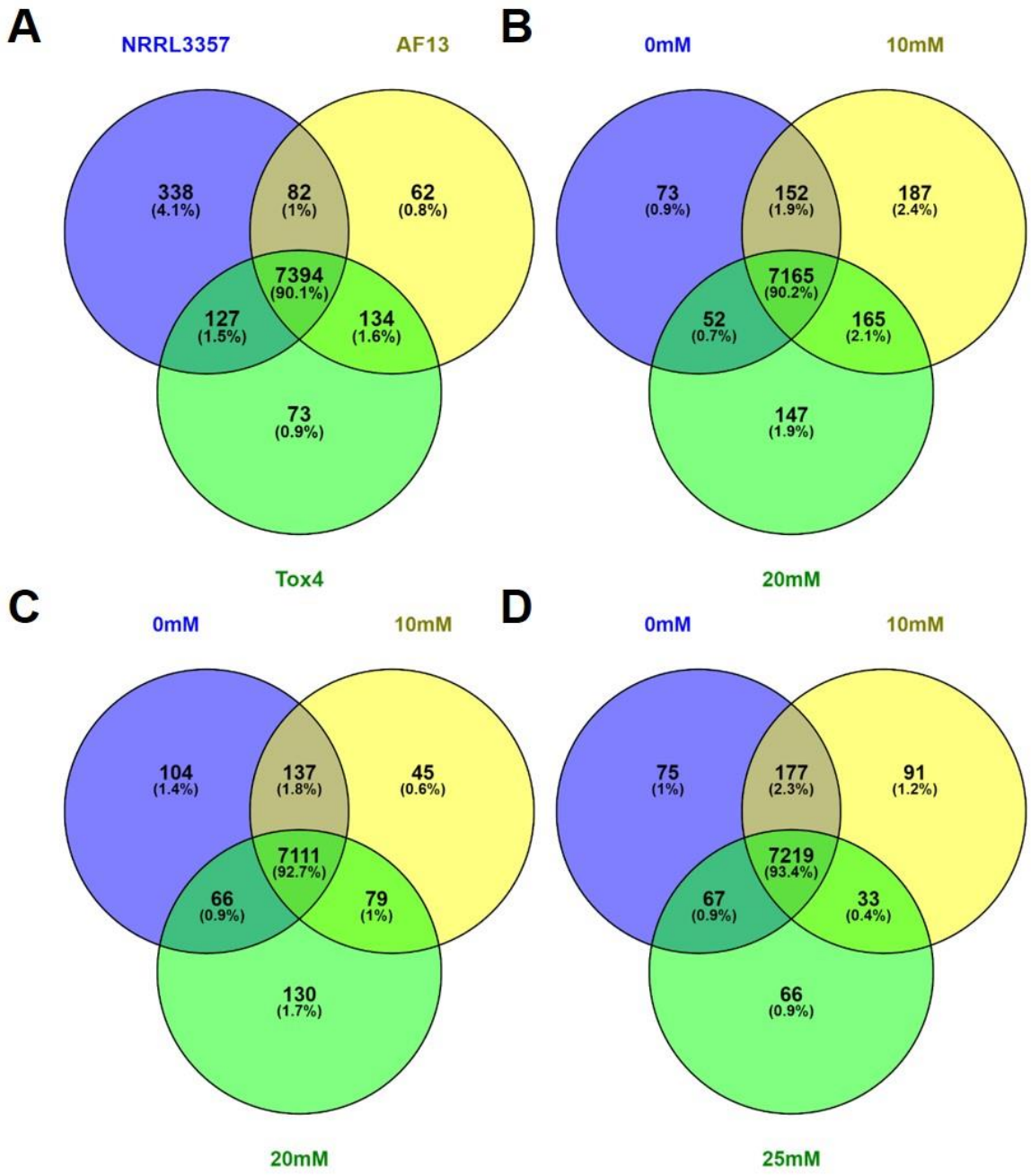
A
NRRL3357
AF13
Tox4
338
(4.1%)
82
(1%)
62
(0.8%)
7394
(90.1%)
127
(1.5%)
134
(1.6%)
73
(0.9%)
B
0mM
10mM
20mM
73
(0.9%)
152
(1.9%)
187
(2.4%)
7165
(90.2%)
52
(0.7%)
165
(2.1%)
147
(1.9%)
C
0mM
10mM
20mM
104
(1.4%)
137
(1.8%)
45
(0.6%)
7111
(92.7%)
66
(0.9%)
79
(1%)
130
(1.7%)
D
0mM
10mM
25mM
75
(1%)
177
(2.3%)
91
(1.2%)
7219
(93.4%)
67
(0.9%)
33
(0.4%)
66
(0.9%)

Figure D.2. Principal component analysis (PCA) and hierarchical clustering analysis (HCA) of the isolate gene expression profiles. A: Principal component analysis (PCA) of the isolate expression patterns with PC1 and PC2 contributing 33.57% and 25.98% of overall variance, respectively. Similar clusters are indicated by the colored circles. B: Hierarchical clustering analysis (HCA) of the isolate expression patterns. Both analyses indicate a similarity in the expression profiles of AF13 and highly stressed Tox4 with NRRL3357 exhibiting a more distinct profile.

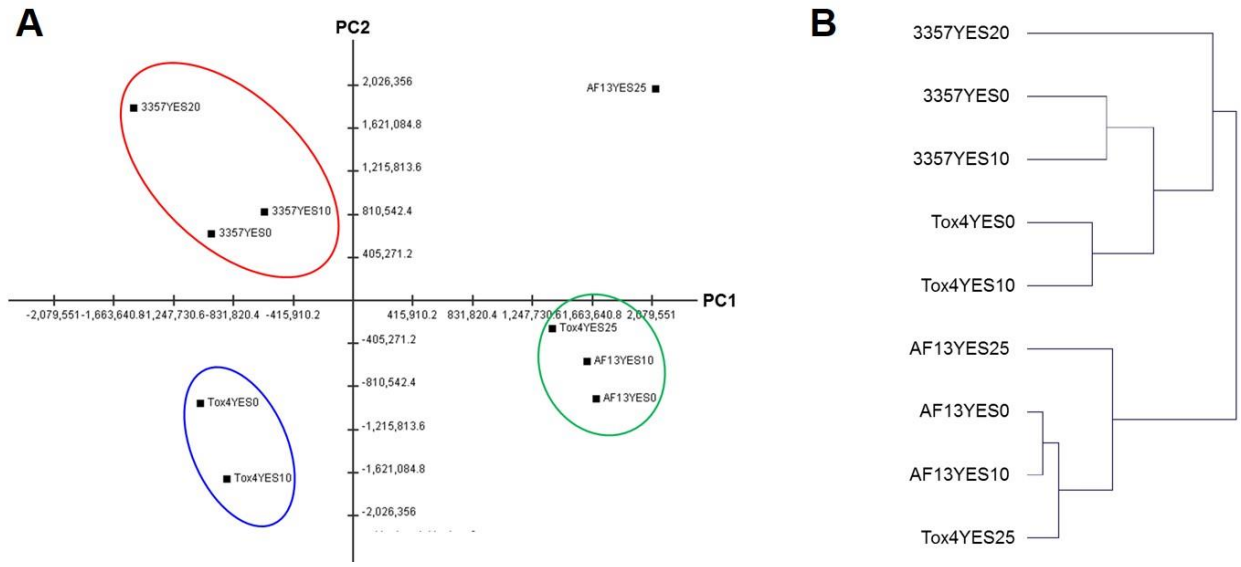
A
PC2
PC1
2,026,356
1,621,084.8
1,215,813.6
810,542.4
405,271.2
-405,271.2
-810,542.4
-1,215,813.6
-1,621,084.8
-2,026,356
-2,079,551
-1,663,640.8
-1,247,730.6
-831,820.4
-415,910.2
415,910.2
831,820.4
1,247,730.6
1,663,640.8
2,079,551
3357YES20
3357YES10
3357YES0
AF13YES25
Tox4YES25
AF13YES10
AF13YES0
Tox4YES0
Tox4YES10
B
3357YES20
3357YES0
3357YES10
Tox4YES0
Tox4YES10
AF13YES25
AF13YES0
AF13YES10
Tox4YES25

Figure D.3. Heatmap of aflatoxin, aflatrem, and kojic acid biosynthetic gene expression with increasing oxidative stress. The expression of aflatoxin (A), aflatrem (B), and kojic acid (C) biosynthetic genes are plotted with colors corresponding to the level of expression of the genes in each condition. Here, FPKM expression values were $\log_{10}$ transformed and plotted based on the color key increasing from blue to red using MeV 4.9. Isolate and treatment combinations for each column are consistent for each heatmap.

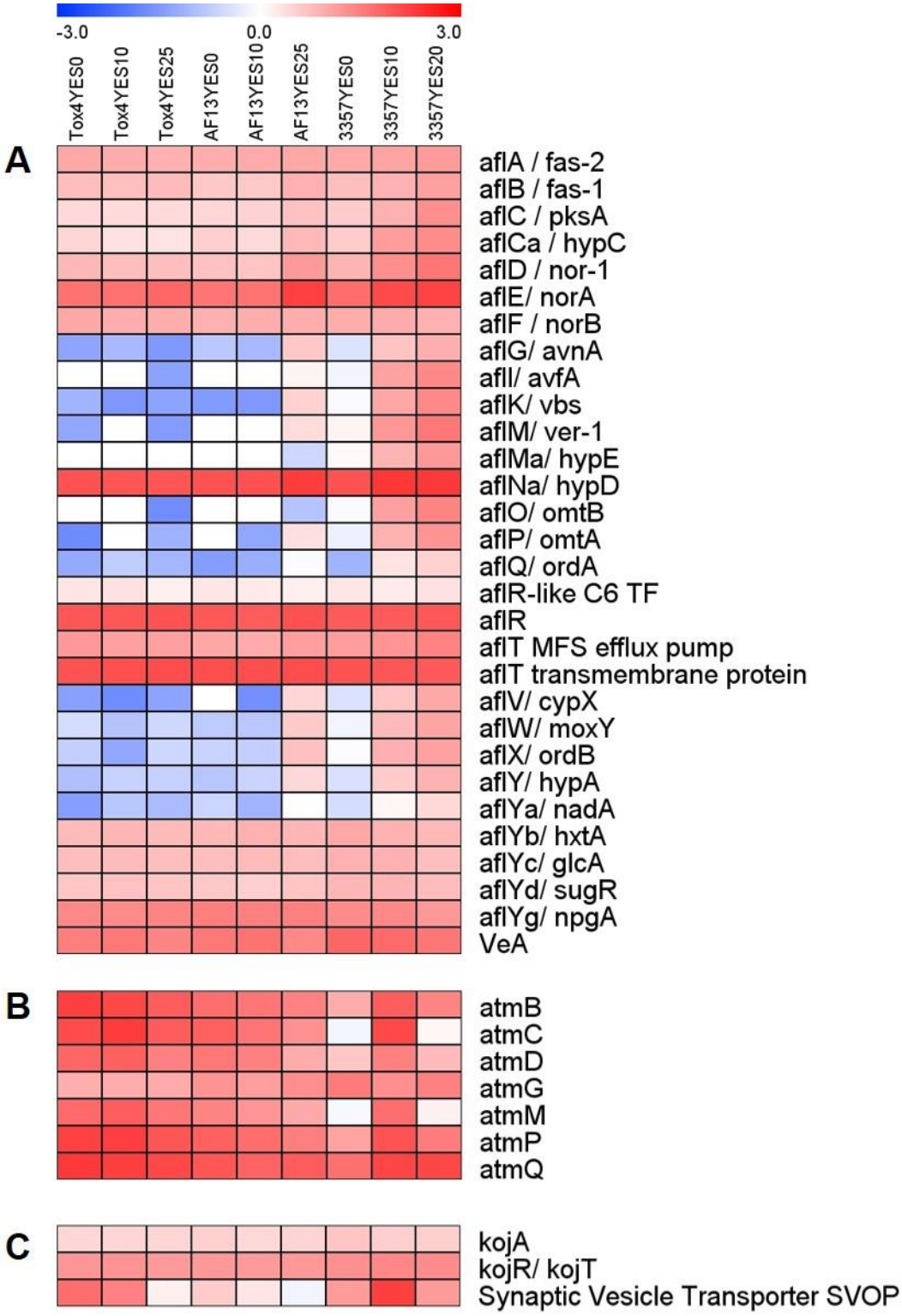
-3.0
0.0
3.0
Tox4YES0
Tox4YES10
Tox4YES25
AF13YES0
AF13YES10
AF13YES25
3357YES0
3357YES10
3357YES20
A
aflA / fas-2
aflB / fas-1
aflC / pksA
aflCa / hypC
aflD / nor-1
aflE/ norA
aflF / norB
aflG/ avnA
aflI/ avfA
aflK/ vbs
aflM/ ver-1
aflMa/ hypE
aflNa/ hypD
aflO/ omtB
aflP/ omtA
aflQ/ ordA
aflR-like C6 TF
aflR
aflT MFS efflux pump
aflT transmembrane protein
aflV/ cypX
aflW/ moxY
aflX/ ordB
aflY/ hypA
aflYa/ nadA
aflYb/ hxtA
aflYc/ glcA
aflYd/ sugR
aflYg/ npgA
VeA
B
atmB
atmC
atmD
atmG
atmM
atmP
atmQ
C
kojA
kojR/ kojT
Synaptic Vesicle Transporter SVOP

Figure D.4. Relative expression and FPKM associations for select secondary metabolite genes. Real-time PCR was used to determine the relative expression of six select secondary metabolite genes: *pksA* and *vbs* (aflatoxin), *atmG* and *atmQ* (aflatrem), and *kojA* and *SVOP* (kojic acid). Relative expression is indicated by the blue bars scaled to the left y-axis. The RNA sequencing-derived FPKM data is indicated by the red line scaled to the right y-axis. The plots are organized into three columns corresponding to data obtained from NRRL3357, AF13, Tox4, respectively, with each plot containing data from the 0, 10, and 20/25 mM H_2O_2 treatments in increasing order.

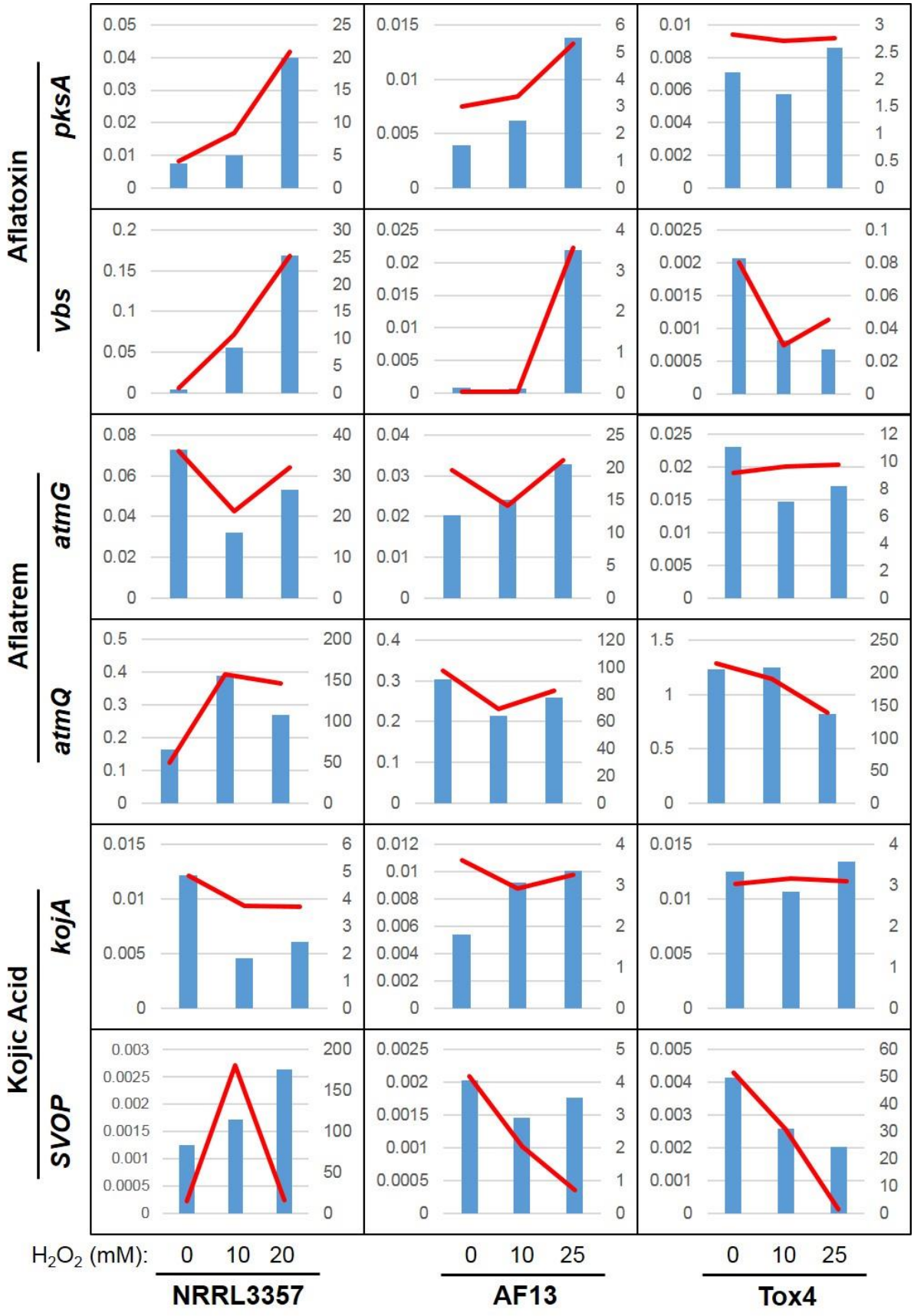
Aflatoxin
pksA
vbs
Aflatrem
atmG
atmQ
Kojic Acid
kojA
SVOP
H2O2 (mM): 0 10 20
0 10 25
0 10 25
NRRL3357
AF13
Tox4

Figure D.5. Gene ontology (GO) analysis of genes differentially expressed between 0 and 20/25mM H_2O_2. Gene ontology (GO) analysis of significant DEGs between 0 and 20/25mM H_2O_2 were determined using Blast2GO. Bars indicate the number of genes differentially expressed within each gene ontology group (biological process). The light blue bar represents Tox4, the gray bar AF13, and the dark blue bar NRRL3357.

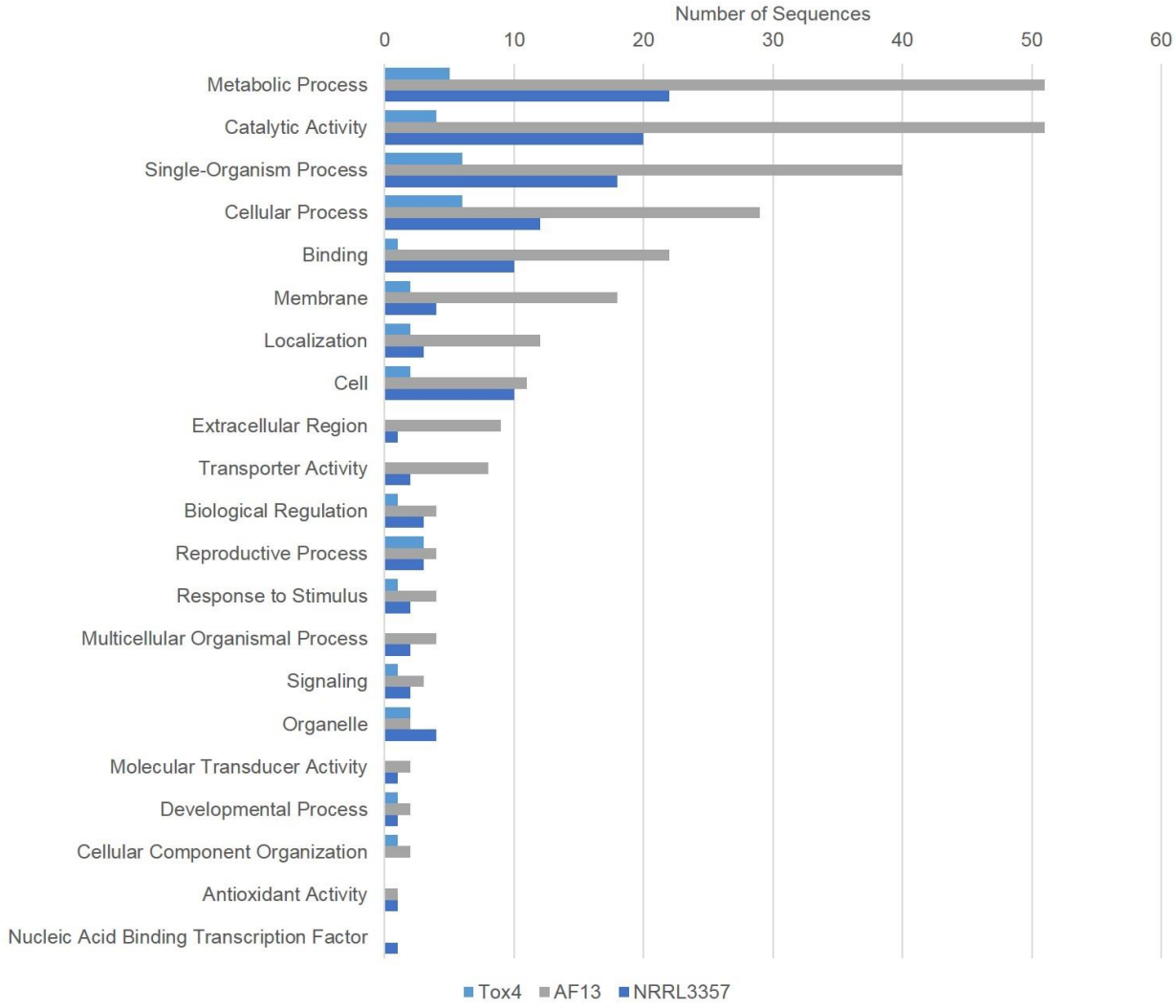
Number of Sequences
0
10
20
30
40
50
60
Metabolic Process
Catalytic Activity
Single-Organism Process
Cellular Process
Binding
Membrane
Localization
Cell
Extracellular Region
Transporter Activity
Biological Regulation
Reproductive Process
Response to Stimulus
Multicellular Organismal Process
Signaling
Organelle
Molecular Transducer Activity
Developmental Process
Cellular Component Organization
Antioxidant Activity
Nucleic Acid Binding Transcription Factor
Tox4
AF13
NRRL3357

Figure D.6. Weighted gene co-expression network analysis of isolate transcriptional responses to oxidative stress. A, Topographical overlap matrix (TOM) of the co-expression network of 500 randomly selected genes in the dataset. Genes are sorted by hierarchical clustering, and represented by the rows and columns with the colors showing the strength of the associations between genes increasing from white to red. Genes clustered tightly together are assigned to color-coded modules shown below the dendrograms. B, Dendrogram produced by hierarchical clustering of the eigengene network showing the relationship of the modules and isolate dry weight under oxidative stress. C, Eigengene adjacency heatmap showing the correlation between the modules and isolate dry weight. Mutual correlations between corresponding modules is higher than most module associations with dry weight, however the purple and turquoise modules exhibit a strong positive correlation with dry weight. In contrast, the blue module shows a strong negative correlation. Eigengene adjacency, which reflects correlation in the heatmap, increases from blue to red in the heatmap.

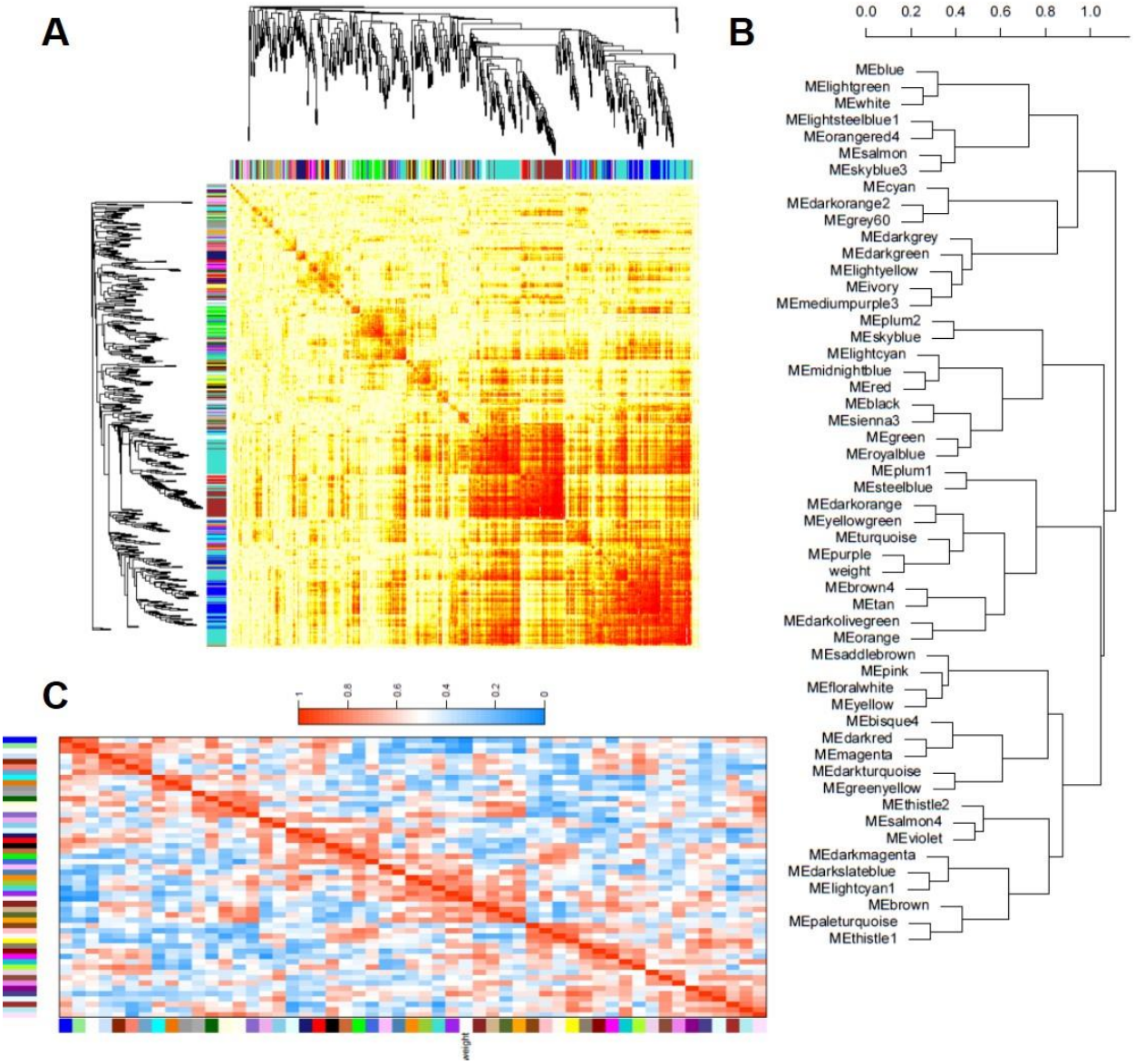
A
B
C
0.0
0.2
0.4
0.6
0.8
1.0
MEblue
MElightgreen
MEwhite
MElightsteelblue1
MEorangered4
MEsalmon
MEskyblue3
MEcyan
MEdarkorange2
MEgrey60
MEdarkgrey
MEdarkgreen
MElightyellow
MEivory
MEmediumpurple3
MEplum2
MEskyblue
MElightcyan
MEmidnightblue
MEred
MEblack
MEsienna3
MEgreen
MEroyalblue
MEplum1
MEsteelblue
MEdarkorange
MEyellowgreen
MEturquoise
MEpurple
weight
MEbrown4
MEtan
MEdarkolivegreen
MEorange
MEsaddlebrown
MEpink
MEfloralwhite
MEyellow
MEbisque4
MEdarkred
MEmagenta
MEdarkturquoise
MEgreenyellow
MEthistle2
MEsalmon4
MEviolet
MEdarkmagenta
MEdarkslateblue
MElightcyan1
MEbrown
MEpaleturquoise
MEthistle1
1
0.8
0.6
0.4
0.2
0
weight